WEST VIRGINIA MINE DRAINAGE TASK FORCE SYMPOSIUM

October 4-5, 2022
Morgantown Marriott Hotel and Conference Center
Morgantown, WV

PROGRAM – PAPERS – ABSTRACTS

West Virginia Mine Drainage Task Force Symposium

October 4-5, 2022
Morgantown Marriott Hotel and Conference Center
Morgantown, WV

CO-SPONSORED BY
WEST VIRGINIA MINE DRAINAGE TASK FORCE
WEST VIRGINIA UNIVERSITY
WEST VIRGINIA COAL ASSOCIATION

2022 PROGRAM
WEST VIRGINIA MINE DRAINAGE TASK FORCE SYMPOSIUM

Marriott Waterfront Hotel
Morgantown, West Virginia
October 4-5, 2022

Tuesday Morning, October 4, 2022

8:00 – 9:00 am Registration

9:00 – 9:05 am Welcome: Ben Faulkner, Chairman of the Task Force, Princeton, WV
Moderator: Randy Maggard, American Consolidated Natural Resources, Monongah, WV

9:05 – 9:30 am **WVDEP Update on Mining, Reclamation, and AMD Treatment**
Jon Rorrer, Acting Director
West Virginia Department of Environmental Protection
Charleston, WV

9:30 – 10:00 am **OSM Update on Mining, Reclamation and AMD**
Tom Shope, Regional Director, Appalachian Region
Office of Surface Mining Reclamation and Enforcement
Pittsburgh, PA

10:00 – 10:30 am BREAK

10:30 – 11:00 am **Strategy for AMD Treatment on Watershed Scales**
Paul Ziemkiewicz
West Virginia Water Research Institute
Morgantown, WV

11:00 – 11:30 am **Beginnings of AMD Passive Treatment in North America**
Bob Kleinmann and Jeff Skousen
Editor-in-Chief of Mine Water and Environment and WVU
Pittsburgh, PA and Morgantown, WV

11:30 – 12:00 pm **Data Needed for Selection and Design of AMD Treatment Systems**
Tim Danehy
Biomost, Inc.
Mars, PA

12:00 – 1:30 pm Lunch

Tuesday Afternoon, October 4, 2022

1:30 – 1:35 pm Regroup
Moderators: Jennie Henthorn, Henthorn Env. Serv., St. Albans, WV
Jamie Gwinn, Arch Resources, Charleston, WV

1:35 – 2:00 pm **2021-22 Legislative Issues on Mining, Reclamation and Water Quality**
Jason Bostic
West Virginia Coal Association
Charleston, WV

2:00 – 2:30 pm **Successful AMD Abatement – Broad Top, PA**
Joe Mills
Skelly and Loy
Morgantown, WV

2:30 – 3:00 pm **A Design and Build Active Treatment Plant for the Globe Mine High Strength Mine Discharge**
Jon Dietz
Iron Oxide Technologies, LLC, & Smith Gardner, Inc.
Ridgway, PA

3:00 – 3:30 pm BREAK

3:30 – 4:00 pm **Two Case Studies of Enhancing Decarbonation by Utilizing Iron Oxidation**
Brent Means and Rich Beam
Office of Surface Mining
New Cumberland, PA

4:00 – 4:30 pm **PHREEQ-N-AMDTreat+REYs Water-Quality Modeling Tools to Evaluate Acid Mine Drainage Treatment Strategies for Recovery of Rare Earth Elements**
Charles Cravotta
US Geological Survey
New Cumberland, PA

4:30 – 5:00 pm **Development of Pilot Plant for Extraction of Rare Earth Elements from AMD Products**
Paul Ziemkiewicz
West Virginia University
Morgantown, WV

5:00 – 5:30 pm **Effectiveness of the T&T AMD Treatment Plant on Muddy Creek**
Ben Fancher
West Virginia Department of Environmental Protection
Philippi, WV

RECEPTION – 5:30 to 7:30 pm

Wednesday Morning, October 5, 2022

8:00 – 8:05 am Moderator: Tiff Hilton, WOPEC, Lewisburg, WV

8:05 – 8:30 am **10+ Year Passive Treatment System Performance Evaluation**
Tim Danehy
Biomost, Inc.
Mars, PA

8:30 – 9:00 am **Large Scale Treatment Plants at Abandoned and Bond Forfeiture Sites**
Rob Rice and Dave McCoy
West Virginia Department of Environmental Protection
Charleston, WV

9:00 – 9:30 am **Anna S Mine: A Century of Mining and Reclamation**
Bob Hedin
Hedin Environmental
Pittsburgh, PA

9:30 – 10:00 am **Co-treating AMD and Municipal Wastewater in Existing Conventional Wastewater Treatment Plants**
Travis Tasker and Ben Roman
St. Francis University
Loretto, PA

10:00 – 10:30 am BREAK

10:30 – 11:00 am **Monitoring Brown Trout Invasion in a Native Brook Trout Stream Post Mine Drainage Remediation – A Cautionary Tale**
Tom Clark and Brianna Hutchison
Susquehanna River Basin Commission
Harrisburg, PA

11:00 – 11:30 am **Mine Pools as a Valuable Municipal and Economic Water Resource in the Central Appalachian Coalfields**

Hannah Patton and Ben Faulkner
Virginia Tech
Blacksburg, VA

11:30 – 12:00 pm **Coagulation and Flocculation Water Treatment**

Jonathan Ceslovnik
Nalco Water
Charleston, WV

12:00 **Adjourn**

1:00 – 3:00 pm **WORKSHOP – PHREEQ-N-AMDTreat Model to Evaluate Water-Quality Effects from Passive and Active Treatment of Mine Drainage**

Charles Cravotta and Brent Means
US Geological Survey and OSMRE
New Cumberland, PA

Instructions for the Workshop

An introduction to the program will be given in the presentation earlier during the conference (see abstract). The workshop will emphasize water-quality modeling using these tools to evaluate various treatment strategies. The workshop begins with a brief Power Point presentation and then will provide demonstrations on how to use the models for examples provided. Participants will use the models so laptop computers will be necessary for them to bring to the workshop. Software will be made available (either via the web ahead of time or on a flash drive for installation during the workshop). The instructors will demonstrate how the information from the models can be used with the currently available version of AMDTreat 5.0. Those already familiar with AMDTreat will be ahead of the learning curve.

WEST VIRGINIA MINE DRAINAGE TASK FORCE SYMPOSIUM

Morgantown Marriott Hotel and Conference Center
Morgantown, West Virginia
October 4-5, 2022

TABLE OF CONTENTS

The Beginnings of Passive Treatment of AMD in North America

Bob Kleinmann[1] and Jeff Skousen[2]

[1]Editor-in-Chief of *Mine Water and the Environment* and [2]WVU
Pittsburgh, PA and Morgantown, WV

Introduction

Only a few of the folks attending this conference are old enough to have been here 40 years ago when the basics of passive treatment were first being discussed here in Morgantown. At the time, we viewed it as a potential way to treat small flows of circumneutral and mildly acidic coal mine drainage that would otherwise flow untreated into streams and creeks. Little did we know that within a decade or so, it would develop into a technology that could be used at both abandoned and active mines, to treat much larger flows than we ever thought possible, and even more contaminated water from metal mines. Jeff thought that some of you younger folks (and that means anyone here is 60 or younger) might want to learn how this pivotal technology was first developed, largely here in northern West Virginia and western Pennsylvania, and how it then continued to evolve.

To be clear, constructed wetlands had been used to treat other wastewater streams, such as municipal wastewater, long before we even considered using the approach to treat MIW (Hammer 1989). In fact, mine water was probably first treated in a constructed wetland system by Seidel (1952), who was working with municipal wastewater that apparently contained some water from the former Grube Ida-Bismarck iron mine (Wolkersdorfer 2021). So, in some ways, we ourselves were guilty of reinventing the wheel when we, unaware of the previous constructed wetlands work, which was quite mature by the 1970s, began to develop the concept of passively treating MIW. Had we known about the earlier work, especially the development of surface and subsurface flow constructed wetlands as well as hybrid systems, our own early work would probably have been more efficient by learning from their results. In addition, we would not have used the term 'constructed wetlands,' since that term had already been enlisted by those treating wastewater that was dominantly contaminated with nutrients and suspended solids. Indeed, many of our old papers from the 1980s and the early 1990s commonly referred to the early passive treatment systems as constructed or engineered wetlands.

Starting with the fundamentals, passive systems sequentially remove metals and/or acidity by using gravity and natural physical, ecological, microbiological and geochemical reactions. Although wetland plants are the most visible aspect of many MIW passive treatment systems, they are only one aspect, and other aspects are often more important. In general, adsorption and ion exchange by the plants and their substrate, abiotic, and bacterial metal oxidation (and associated hydrolysis and precipitation), settling of precipitated metals, acid neutralization through carbonate dissolution and microbial processes, filtration, and sulfate reduction (and associated precipitation of metal sulfides) all contribute, though the relative importance of each varies with the initial water quality, mode of construction, and site-specific conditions; thus, passive treatment systems vary widely in construction details and mode of operation (Ford 2003; Gusek 2009; Kadlec and Wallace 2009; Nairn et al. 2010; Skousen et al. 2000, 2017; URS 2003; Watzlaf et al. 2005; Wieder 1992). Also, since contaminant removal processes in passive treatment systems are slower than conventional chemical treatment, longer retention times and larger areas are often needed to achieve similar results, if they can be achieved at all.

The goal of a passive MIW treatment system is to enhance natural ameliorative processes, so that they occur within the treatment system, not in the receiving water body. Ideally, passive treatment requires no grid energy power and no chemicals after construction and operates effectively for at least a decade with only periodic operation and maintenance activities. Low-maintenance systems that require grid energy power or additions of easily managed amounts of chemicals (e.g. Jenkins and Skousen 1993; Kuyucak and St-

Germain 1994) are generally referred to as semi-passive or enhanced passive treatment techniques.
Given that passive treatment systems are based on natural processes, it should surprise no one that the various components of these systems are generally based on observations of what was occurring naturally at and down-gradient of mine sites as well as what can be observed in the geologic record. Pyrite in coal measures, ferricrete, and manganocrete are some of the obvious examples of iron and/or manganese having been deposited in wetland or open channel flow environments (Browne 1852). Moreover, passive treatment of MIW was a concept whose time had clearly come, due no doubt to the increased environmental awareness and U.S. Clean Water Act regulations associated with the 1970s. It is generally considered to have developed in the eastern USA's Appalachian coalfield (Kleinmann 1985; Kleinmann et al. 1983; Wieder and Lang 1982), though if it hadn't developed here, it likely would have emerged soon elsewhere (Kleinmann et al. 2021).

The Early Years

It appears that the first step on the discovery path occurred in the 1970s when researchers at Wright State University in Ohio, who were investigating whether low pH, metal-laden coal mine drainage flowing into a natural Sphagnum bog in the Powelson Wildlife Area in Ohio was adversely affecting the bog, discovered no adverse effects. Instead, they found that the mine water was apparently being treated very effectively by the combined effects of ion exchange and adsorption of metals onto the Sphagnum moss and neutralization by a limestone outcrop at the down-gradient portion of the bog. The limestone was not being armored because the iron had already been removed by the moss. They speculated in a presentation in 1978 that similar systems could be artificially created. The first author of this paper, who at the time was a new employee of the U.S. Bureau of Mines (USBM), happened to see the published abstract in the Geological Society of America conference proceedings (Huntsman et al. 1978), contacted the authors, and began a collaborative research effort to advance this concept. The intent was fairly modest – to develop a low-cost, low-maintenance technology that could be used to mitigate small flows of acidic mine drainage originating at abandoned coal mines. No one at that time ever imagined that the technology would someday be used at active and abandoned mine sites around the world, or that it would ever be scaled up to effectively treat flows of more than a few liters per minute.

The USBM-Wright State team followed up their work by constructing what we called a "port-a-bog": a plexiglass pilot-scale test apparatus simulating what appeared to be working in the field. They constructed the system on a steel flat-bed trailer, allowing the system to be taken to other sites and tested with that site's MIW (Fig. 1; Kleinmann et al. 1985). The results were very encouraging, and this led to the design and implementation of full-scale field systems. However, we eventually learned that while the Sphagnum moss systems could handle relatively mild coal mine drainage, it was incapable of handling coal mine drainage with high metal loads unless there was large amounts of dilution available (Figure 2a; Girts and Kleinmann 1986; Kleinmann and Girts 1987).

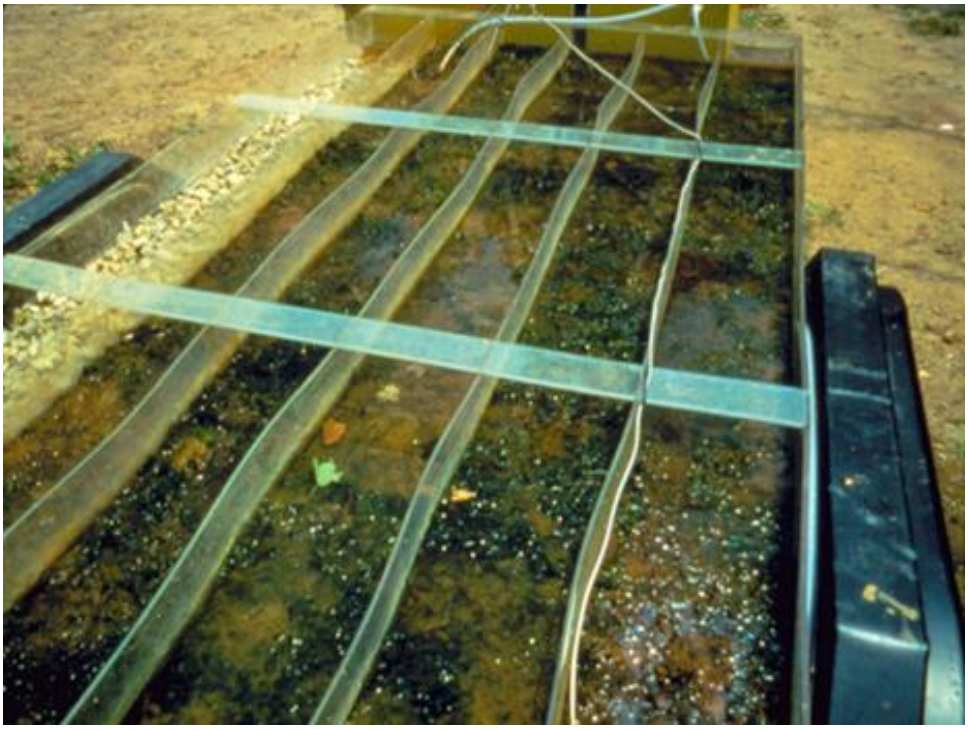

Figure 1. The "port-a-bog" was a pilot-scale wetland constructed on a flat-bed trailer and hauled to sites to test the concept of using Sphagnum moss and limestone to treat MIW.

Independently, another research group here at West Virginia University (WVU) discovered coal mine drainage being treated at Tub Run Bog in northern West Virginia, although their observations included the distinct odors of sulfate reduction occurring there. Indeed, they found that the bog brought the pH of the water from the low 3s to about 6, even though there was no limestone present; the alkalinity was instead being provided by sulfate reduction (Wieder and Lang 1982).

The WVU team followed up their discovery with laboratory tests (Tarleton et al. 1984) and by constructing a pilot-scale (10 m by 27 m) wetland system that they hoped would similarly treat mine water with a pH of 5.6 and iron concentrations of 40 mg/L in a sediment pond at a mine site in western Maryland (Wieder et al. 1985).

Their field tests, like ours, revealed that although the Sphagnum bog concept worked quite well for acidic mine water with low to moderate levels of iron, it could not tolerate iron concentrations above ≈ 100 mg/L, while the ability of the Sphagnum to tolerate a pH of above ≈ 4 varied with the Sphagnum species. The problem with high iron concentrations was that the first meter of Sphagnum moss from the inflow would adsorb so much iron that it essentially petrified; then the next meter of the bog would do the same. This 'advancing wall of death' was a clear indication of the limitations of this approach (Fig. 2b). Other negative aspects were that the Sphagnum proved to be very sensitive to fluctuating water levels and changes in water quality (a common occurrence at and near mine sites). These challenges required replacing old, petrified moss with new moss. This would have mandated the harvesting, transport, and transplanting of Sphagnum from natural wetlands into the constructed system, potentially damaging a natural ecosystem to establish a less ecologically desirable one.

Figure 2A. Attempted recreation of a sphagnum moss bog at the Friendship Hill site by USBM staff; photo shows young versions of Bob Hedin, Michelle Girts, and Trish Erickson. B. Eventual result: the high iron concentrations at the site slowly overwhelmed the moss's adsorptive capacity.

Meanwhile, observations at and near mine sites were suggesting that emergent plants, such as Typha (more commonly known as cattails), were volunteering and thriving in ponds and ditches where acidic coal mine drainage was flowing, and that the water quality was being improved by the process (Kleinmann 1985; Pesavento 1984; Snyder and Aharrah 1984). So, field trials of this approach were soon initiated (Fig. 3). Emergent Typha plants were found to tolerate much higher metal loadings and fluctuating water quality and water levels than Sphagnum. Moreover, although the Typha rhizomes, roots, and leaves did take up significant amounts of iron and manganese when the results were judged by drying and analyzing the plant tissue, the amount actually removed was relatively low when considered by the amount removed over a unit area of the wetland (Sencindiver and Bhumbla 1988). Instead, it appeared that the principal function of the plants was to simply slow down the flow of the MIW, creating an environment in which various bacteria, especially iron-oxidizing bacteria, could be active and the oxidized iron could precipitate. In other words, these wetlands were acting like shallow, abiotic aeration/settling ponds.

Figure 3A. A Typha-based wetland immediately after construction in West Virginia. B. the same site, two months later.

Since iron hydrolysis is actually an acid-generating reaction, at sites where the untreated water or substrate was not alkaline, the pH at the wetland outlet typically decreased as the contaminants, especially the iron, precipitated (e.g. Brodie et al. 1988). At sites where limestone had been incorporated into the wetland's organic substrate, this pH decrease was less of a problem. This limestone is not typically rendered inert because the iron that infiltrated though the organic medium was converted from the ferric form, which would armor the limestone, to the ferrous form, which does not armor it.

Looking back in time, presentations given at conferences held in Pennsylvania, West Virginia, Kentucky, Colorado, and elsewhere, from 1984 onwards, were key to spreading the word about what was being learned. Passive treatment research really accelerated as all the various research groups became aware of each other's work and as other research groups either learned of these developments and began conducting experiments and field tests or had similar discoveries, leading to similar results. These included researchers at the Colorado School of Mines (e.g. Emerick et al. 1988; Wildeman et al. 1993), Pennsylvania State University (e.g. Gerber et al. 1985; McHerron 1986; Stark et al. 1990), Virginia Tech (Duddleston et al. 1992; Hendricks 1991), the Tennessee Valley Authority (TVA; e.g. Brodie et al. 1986, 1988), Montana (Hiel and Kerins 1988), and in Canada (personal communication with Keith Ferguson 1985; Kalin 1988).

As practitioners learned about the research results, more and more began to incorporate wetland systems into their mine plans, first by enhancing wetland vegetation that had volunteered on their mine sites, and then actually constructing wetlands at active and abandoned mine sites. Researchers began to study many of these systems, learning from what worked, what did not work, and from what worked at some sites but not at others. This led to the first of many workshops organized by the U.S. Bureau of Mines and others on how to construct passive treatments systems, sharing the practical aspects of what was being learned empirically (Kleinmann et al. 1986). These continued well into the early 1990s and led to even more wetland systems being constructed by watershed associations, state abandoned mine programs, and mining and consulting companies. Even today, entire sessions at reclamation and water conferences are devoted to passive system application, design, performance, and maintenance, and most importantly innovations and new discoveries.

As these systems were gradually improved, we learned to sequence the passive treatment steps to precipitate the contaminants, generate alkalinity, and correctly size the systems so that they could meet regulatory discharge standards. From the 30 or so such sites that had been constructed in 1984 and 1985 in Pennsylvania (Girts and Kleinmann 1986, 1987; Kleinmann and Girts 1987), the number of such systems more than doubled each year through 1987, and only accelerated after that. The key steps are discussed thematically below. An unintentional outcome of the USBM field trials was that many subsequent applications tended to use the same substrate, spent mushroom compost, that the USBM had used. However, this form of compost was used only because, at the time, it was readily available in Pennsylvania due to the large amount of mushroom farming there. In hindsight, perhaps that should have been clarified.

Alkalinity Generation

As mentioned above, the organic substrate supporting the cattails typically contained limestone or had limestone added to it. Limestone in the anoxic zone could contribute alkalinity without armoring, so it was recognized early on that placing the limestone beneath a layer of soil or compost was beneficial. However, other ways to add alkalinity without having the limestone becoming coated with precipitated iron were soon developed, including sulfate reduction (discussed below), limestone placed up-gradient of the mine discharges, anoxic limestone drains (ALDs), and reducing and alkalinity-producing systems (RAPS), also sometimes referred to as sequential alkalinity producing systems (SAPS) or vertical flow wetlands.
The first of these, introducing the alkalinity up-gradient of the mine discharge was very easy to implement, but very limited in the amount of alkalinity it could provide if the water dissolving the limestone was not already acidic. Limestone placed into neutral pH water with no acidity will generate less than 50 mg/L as CaCO3 alkalinity. However, many mine water discharges from underground mines are acidic with elevated concentrations of metals, allowing the dissolution of the limestone as long as metal precipitates do not armor the limestone or clog the system, preventing flow-through.

Armoring of limestone with iron hydroxides has plagued many passive treatment systems and caused premature failure. Pearson and McDonell (1974, 1975a, b) showed that armored limestone dissolved, but at a rate about 20% that of unarmored limestone. Based on this work, Ziemkiewicz and Skousen conducted laboratory and field experiments and found that armored limestone was between 20 to 50% as effective as unarmored limestone, depending on the thickness of armoring (Ziemkiewicz et al. 1994, 1997). More effective systems were shown to be at sites that had large elevation changes, which prevented the precipitates from forming, removed them from the limestone surfaces, and flushed out void spaces in the channels. This knowledge resulted in hundreds of open limestone channels being designed and built based on these initial studies; open limestone channels are often the default system when no other passive system type is suitable (Fig. 4).

Figure 4. An open limestone channel (1995)

Turner and McCoy (1990) realized that as long as MIW has not yet contacted the atmosphere, the dissolved iron was most likely in the ferrous state. This meant that the limestone would remain unarmored when the mine water contacted it in an anoxic environment. They used this knowledge to construct the first anoxic limestone drain (ALD) in Tennessee. They excavated a trench to intercept the mine discharge before it reached the surface, filled the trench with limestone, and most importantly, covered the limestone to prevent the iron in the mine water from being oxidized, so that it would not armor the limestone. This was then followed by a settling pond to allow the dissolved iron, which rapidly oxidized when released to the surface in the now circumneutral pH water and precipitated in the settling pond (Fig. 5). Independently, Greg Brodie and Cindy Britt of the TVA identified an "accidental" ALD at the IMP-1 site in Alabama, where an abandoned haul road constructed out of limestone rock sub-base was treating subsurface water and adding alkalinity to an aerobic wetland cell receiving seepage from a coal slurry pond. Subsequently, the USBM and TVA developed detailed design criteria for ALDs, which were shared with the passive treatment community (Brodie et al. 1993; Hedin et al. 1994b; Nairn et al. 1991; Watzlaf and Hedin 1994). Performance data for 19 operating ALDs was provided by Faulkner and Skousen (1994).

Figure 5. An anoxic limestone channel being constructed, soon to be covered with plastic sheeting and a soil cover.

An attempt was made in West Virginia to increase the rate of limestone dissolution in ALDs by placing organic matter within the drain. The hay bales were placed on the top of the limestone and the hay bales and limestone were wrapped with plastic so that degradation of the organic matter would consume oxygen and generate CO_2 (Skousen 1991). However, the organic matter encouraged microbial growth, which eventually clogged the ALD.

But what could be done if the MIW already contained dissolved oxygen or significant amounts of dissolved ferric iron? Kepler and McCleary (1994) reasoned that if dissolved oxygen and ferric iron concentrations of the MIW were being reduced by bacterial activity in the wetland substrate, surely a system could be designed where the oxygenated water could be reduced by flowing through substrate to consume the dissolved oxygen, render the water anoxic, and convert the ferric iron to ferrous. The discharge from such a system should be alkaline and contain ferrous iron, would be readily removed by oxidation and hydrolysis after exposure to the atmosphere. They reasoned that given enough space and vertical gradient, pairs of anaerobic and aerobic units could be arranged in sequence and treat highly contaminated MIW. Kepler and McCleary referred to this approach as successive alkalinity-producing systems (SAPS), although the SAPS term soon become synonymous for the vertical flow anaerobic treatment unit, which was the most original aspect of the technology (Fig. 6). Watzlaf et al. (2000) began referring to SAPS units as reducing- and alkalinity-producing systems (RAPS) to describe the process more accurately, and to include systems that did not put more than one unit in sequence. These systems have also been called vertical flow ponds, vertical flow wetlands, vertical flow bioreactors, or simply vertical flow systems. Aluminum, which is not controlled by manipulating redox conditions, is still retained in these systems, so Kepler and McCleary (1997) suggested a simple gravity-powered flushing mechanism to extend their effective life span. Unfortunately, the removal of solids from organic substrate through flushing did not prove practical. But the layered vertical flow approach proved effective for delaying the plugging of the systems with Al and Fe solids and subsequently become a standard passive treatment technique for acidic MIW waters.

Figure 6. Construction of an early SAPS in 1995, which has subsequently also been referred to as RAPS, vertical flow ponds, and vertical flow systems. A. Initial placement of the limestone base layer with underdrain piping. B. Compost layer being placed on top of the limestone. C. The system filled with water.

Passive aluminum removal without any clogging of the organic substrate was first observed in a pilot-scale sulfate-reducing bioreactor system at the Brewer Gold Mine in South Carolina (Gusek 2000). The SRB received low pH (2.0 to 4.7) MIW with aluminum concentrations ranging from 3.6 to 220 mg/L without clogging due to aluminum oxyhydroxide precipitation. Subsequently, Thomas and Romanek (2002) identified aluminum hydroxy-sulfate precipitates in a limestone-buffered organic substrate (LBOS). The aluminum precipitates appeared to replace gypsum (without clogging) in response to exposure to MIW.

In 1990, a passive system was designed for the Douglas Highwall abandoned mine lands (AML) discharge with a flow rate of 13 L/s, a much higher flow rate than previously attempted with passive treatment systems (Skousen 1995). The MIW had a pH of 2.8, and contained 500 mg/L acidity, 50 mg/L total iron (50% ferrous), 40 mg/L aluminum, and 10 mg/L manganese. The limited available space necessitated a long narrow system, which was later called a wetland-ALD (WALD) system. The wetland component of the WALD system was designed to pretreat the partially oxidized water in a 2.1-m wide × 370-m long front section with a 1.3-m deep layer of compost (370 m length) to remove oxygen and convert the ferric iron to ferrous. The ALD portion followed with a 10-m wide × 350-m long section of limestone rock that was 2 m deep. The WALD system did not use pipes in the limestone to induce downward flow because it was thought that the 5- to 10-cm sized limestone rock at the base would allow flow through the system. The system produced net alkaline water for its first four years, but then the outflow water quality slowly degraded until it reached a steady acidity level of 100 mg/L (as $CaCO_3$) for the next 20 years. This site helped demonstrate the challenge of horizontal flow systems and helped explain why the vertical flow approach became preferable over horizontal systems, which often developed hydraulic problems.

Initial evaluations of passive treatment performance were based on simple calculations of concentration efficiency or percent removals (e.g. Girts et al 1987). However, this technique failed to provide reliable evaluations of performance under varied field conditions or at widely different sites. A reliable performance measure was needed that could lead to development of empirical design and sizing criteria by allowing comparison of contaminant removal capabilities for systems of various sizes that received MIW with different flow rates and chemical compositions. Concentration efficiency calculations failed to provide true performance insights for different systems because they did not include influent mass loads or system size. The extensive multi-year, monthly monitoring campaign completed at numerous passive treatment systems by the USBM in western Pennsylvania in the early 1990s developed the data to allow valid system performance evaluations and eventually led to reliable design and sizing criteria. The 18 studied systems were of various designs and surface areas (607 to 8100 m2) and received widely variable flow rates (<1 to 8600 L/min) and influent water chemical compositions (ranging from net acidic to net alkaline; pH 2.6 to 6.2; Fe < 1 to 473 mg/L). Volumetric discharge rates were measured (not estimated) and full elemental analyses were completed. Systems that were not load-limited were intentionally studied so that the capacity or capability of the systems could be determined (Hedin and Nairn 1990, 1992, 1993; Hedin et al. 1991; Nairn and Hedin 1992, Nairn et al. 1992). These findings were all incorporated into a comprehensive USBM publication (Hedin et al. 1994a), which included a design decision tree that separated mine waters into chemical classes based primarily on alkalinity and acidity, and secondarily on the metal contaminants, and identified the passive treatment technologies that were most appropriate for the particular water chemistry conditions. This distinction explained much of the variable performance of existing systems and allowed subsequent researchers and designers to better focus on key geochemical needs (e.g. alkalinity generation, rapid Fe removal, Mn removal). The design decision tree (Fig. 7) has been subsequently adapted and modified by many researchers.

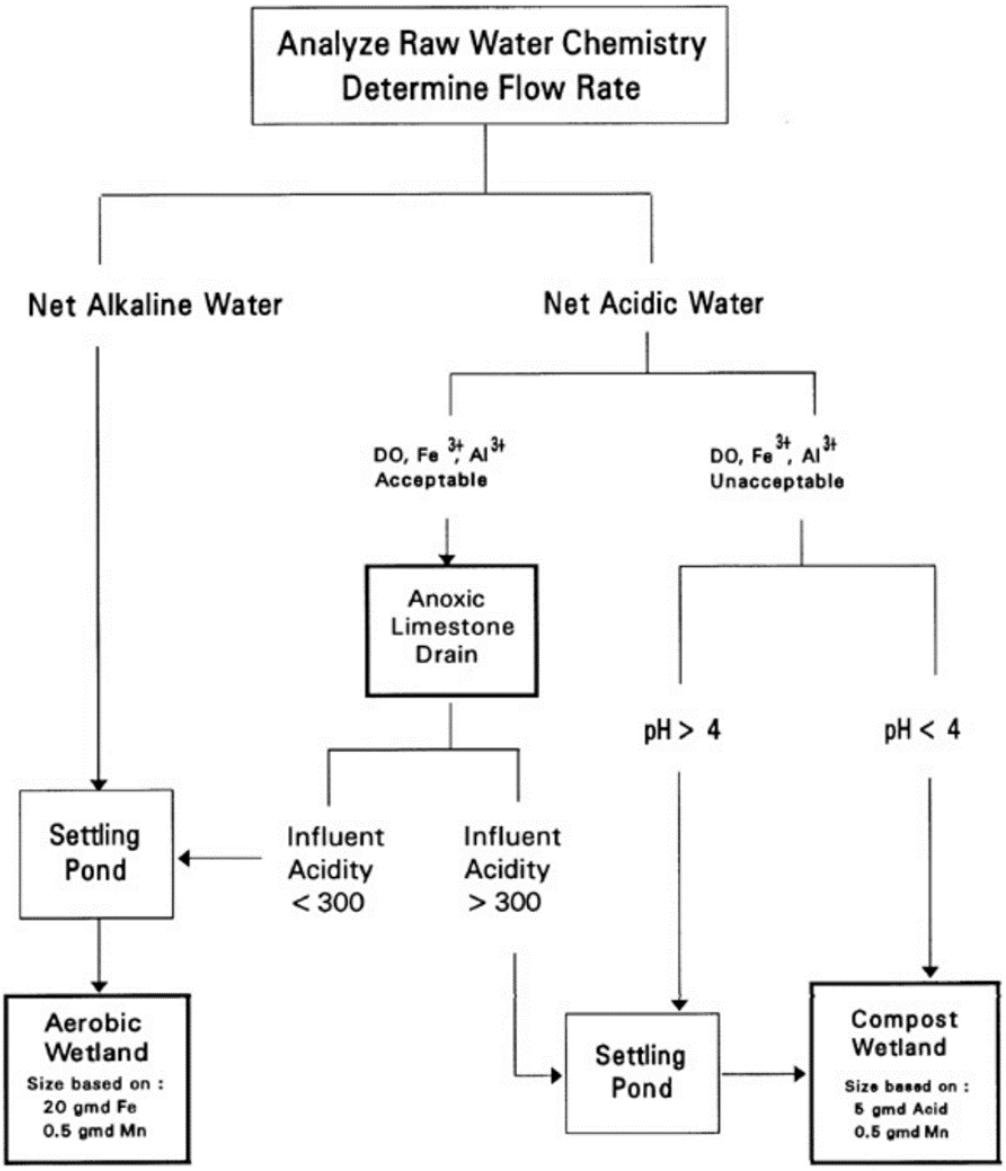

Figure 7. Early decision tree for designing of a passive treatment system for coal mine drainage.

Another contribution of this publication was the development of rate-based sizing criteria for the removal of Fe and Mn. The approach recommended that sizing of passive systems should be based on the contaminant mass load at the site and the expected contaminant removal rate for the proposed technology. The initial report recommended the use of area-adjusted removal rates (gX/day/m^2) because of strikingly consistent area-adjusted Fe removal rates for passive systems treating circumneutral pH alkaline mine water. Subsequently, the rate approach was used to quantify acidity and sulfate removal and modified to reflect volumes and quantities of treatment substrates.

In addition, the use of mass removal rates in the design process allowed estimation of passive treatment system lifetimes. For net alkaline MIW, iron oxide accumulation – the physical filling up of ponds as freeboard is lost over time – led to reasonable system lifetimes of 20-25 years, balancing system surface and volume with practical construction and maintenance constraints. Estimated lifetimes of approximately two decades, for most passive treatment system process units, have become common. However, regular (quarterly to annually), periodic (every two to three years), and rehabilitative (perhaps once per decade)

maintenance are all still necessary; this must be stressed to responsible parties.

In addition to the previously mentioned open limestone channels, Ziemkiewicz and Skousen (1998, 1999) looked for other low-cost alkalinity sources besides limestone and limestone byproducts for passive systems. Experiments showed that steel slag yielded more alkalinity than equal weights of limestone (from 500 to 2,000 mg/L as $CaCO_3$, compared to 60 to 80 mg/L). Slag leach beds were originally designed for freshwater treatment with the now highly alkaline water being introduced into the MIW. Later, installations with coarser slag materials allowed direct contact with the MIW and prolonged system effectiveness.

All of the systems discussed above were focused on passive treatment of MIW at the surface, but other researchers were investigating ways to use similar approaches to treat contaminated groundwater. Permeable reactive barriers (PRBs) are zones of reactive materials installed in aquifers or in unconsolidated waste materials to remove contaminants as the groundwater flows through the reactive material under a natural hydraulic gradient (Blowes et al. 2000). PRBs have been used to treat a range of contaminant sources including MIW.

Sulfate Reduction

U. S. Bureau of Mines researchers, assessing the performance of a cattail-based wetland that had been constructed to treat acidic water, found that in isolated locations, the coal mine water was being neutralized by sulfate-reducing bacteria (SRB) as well as by the limestone and that some of the iron was being precipitated as a sulfide. Apparently, the water was flowing down through the compost/limestone substrate and then back up again, gaining alkalinity in the process as some of the contaminants precipitated as sulfides (Hedin et al. 1988). Although the observation was an important demonstration of the potential utility of bacterial sulfate reduction in mine water treatment systems, it was not an original discovery. In the 1960s, Tuttle et al. (1969) proposed that sulfate reduction might have utility for MIW treatment, but the concept did not advance. However, in the regulatory environment of the 1980s, the idea gained traction. An early review of the natural wetland literature suggested a typical sulfate reduction rate in natural substrates of 0.3 $mol/m^3/day$ (Hedin et al. 1989), a rate that was confirmed by isotope studies (McIntyre and Edenborn 1990). An approach was developed to optimize this effect and was evaluated at bench- and pilot-scale and in the field (Dvorak et al. 1992; Hammack and Hedin 1989; McIntyre and Edenborn 1990; McIntyre et al. 1990; Nawrot and Klimstra 1990); these anaerobic or compost wetlands added alkalinity, but were not very efficient for iron removal, and thus required sequential placement of aerobic and anaerobic steps. Thus, for MIW at coal mining sites, alkalinity generation by limestone dissolution and metal removal by aerobic abiotic and microbial processes was simpler to implement and operate than sulfate reduction systems.

However, sulfate reduction was found to be very useful for treating metal mine drainage, since for most metals other than the iron, manganese, and aluminum that dominate coal mine drainage, sulfides are less soluble than the oxides/hydroxides, allowing the removal of copper, zinc cadmium, lead, and other inorganic constituents typically encountered in MIW at hard rock mines (Wildeman et al. 1990, 1994).

The published research on the use of wetlands to control coal mine drainage led Region VIII of the U.S. EPA in 1987 to assess “constructed wetlands” as a treatment option for metal mine drainage. Funded by a Superfund Innovative Technology Evaluation or “SITE” grant, the Colorado School of Mines (CSM) was chosen to explore sulfate reduction processes and a project was initiated at the Big Five Tunnel in Idaho Springs, Colorado. This project had an important feature. It assembled an interdisciplinary team that included a plant ecologist, environmental engineer, geochemist, and an applied microbiologist, each of whom brought a different perspective to the project. This team relied on civil engineering consultants for building and maintaining the pilot system.

Based on the work of the USBM group (Kleinman and Girts 1987), they decided to build three pilot cells with various mixes of organic substrates and wetland plants. They quickly found that sulfate reduction in the substrate was a major removal process and that designing a system where the water flowed through the organic substrate rather than over it was important. After a few failed attempts, a system where the water was added at the top and flowed through the substrate and out the bottom was found to be the best configuration. In addition, unlike the early versions, which simulated the USBM work, the final big Five pilot-scale facility had no wetland plants.

This primitive SRB led to a number of concepts and practices that are still being used. Since this treatment structure looked nothing like a constructed wetland, the term passive treatment used a decade earlier by Holm and Bischop (1983) was a more appropriate term to describe what was occurring. Also, since bacterial activity, rather than plants, were the critical component, laboratory studies could be used to find the best substrate and inoculum for a given site (Wildeman, et al. 1994a, 1994b).

Because laboratory studies were the logical starting point, standard engineering practices that progressed from laboratory studies to bench-scale tests, to pilot-scale systems, to full-scale systems could be used. This helped convince some mining companies to initiate a program without a large fiscal commitment. This staged design process was also used to address manganese removal (Clayton and Wildeman 1998; Wildeman et al. 1993), and later, other contaminants.

Once it was realized that sulfate reduction catalyzed by bacteria was the important removal mechanism, it became necessary to determine a volume-based sulfide generation rate for a bioreactor. This was especially important for metal-mine drainage because mineral acids could overwhelm the system and destroy the sulfate-reducing bacteria. Like the USBM, the CSM group (Reynolds et al. 1991) conducted an isotopic lab study to determine the rate using substrates from the Big Five pilot system. They found an initial honeymoon period where the sulfate reduction rates were quite high. However, after a month, rates settled down to 0.5 µmol/g/day. Using this result along with the USBM results, it was decided that a volume-based sulfate reduction rate of 0.3 mol/day/m^3 was a reasonable rate (Wildeman et al. 1993). This has turned out to be a basic "rule of thumb" for the design of an SRB. It is imperative that the loading of metals into a volume-based SRB bioreactor is maintained at a level that is below this value. This value presumes that the entire substrate mass participates equally in sulfate reduction. Consequently, sulfate reduction rates within the active microbial zone may be greater than 0.3 mol/day/m^3 as the "reaction front" moves into unreacted substrate over time.

Final Thoughts

Passive treatment technology developed in fits and starts and faced great skepticism from some regulators who saw the tremendous range in the performance and effectiveness of the various passive systems and saw no way to ensure adequate effluent water quality from these systems. Nonetheless, because it was the only affordable option to no treatment at many abandoned mine sites, it found a natural niche there. The subsequent refinement of passive treatment was greatly aided and accelerated by the good working relationships and collaboration that existed at the time between researchers, practitioners, and industry. Gradually, as its high cost effectiveness (compared to active treatment) became obvious, and the performance of passive systems improved and became more predictable, regulators became more open to having them placed on active mine sites, as long as there was a contingency plan in place to implement chemical treatment if water quality requirements were not being met.

As discussed in the beginning of this paper, we wrote this paper to provide the readers with some background

and history of the initial conceptual ideas of passive treatment. Undoubtedly, we have missed the contributions of many additional individuals who contributed to the development of this field. It should also be mentioned that during the time frame that this paper covers, the successful results observed in North America led to many active research teams in other countries retailoring the procedures demonstrated to work here to their local MIW, sources of alkalinity, and sources of suitable organic substrates (e.g. Nuttall and Younger 2000; Sen and Johnson 1999; Younger 1998). In addition, semi-passive systems began to be installed where totally passive treatment proved inadequate (e.g. Jenkins and Skousen 1993; Kuyucak and St-Germain 1994).

One of the more intriguing parts of this story is how the ideas surrounding passive treatment of MIW emerged rather independently to several observant individuals around the late 1970s and early 1980s. Once the researchers and practitioners began discussing their observations and small-scale experiments with others, and collaborating with each other and with industry, a continual expansion of concepts and additional possibilities flourished. When problems appeared, like clogging of wetland substrates or armoring of limestone, new discoveries appeared, such as the development of ALDs, vertical flow wetlands, and open limestone channels. And a variety of substrates have been used to preserve hydraulic conductivity and maintain alkalinity generation, including the use of microorganisms, algae, and other biota to enhance treatment. Today, new ideas are being implemented and we feel fortunate to have provided some of the undergirding of this important field of passive treatment of MIW.

References

Blowes DW, Ptacek CJ, Benner SG, McRae CWT, Bennett TA, Puls RW (2000) Treatment of inorganic contaminants using permeable reactive barriers. J Contam Hydrol 45: 123–137

Brodie GA, Britt CR, Tomaszewski TM, Taylor HN (1993) Anoxic limestone drains to enhance performance of aerobic acid drainage treatment wetlands: experiences of the Tennessee Valley Authority. In: Moshiri GA (Ed), Ch 12, Constructed Wetlands for Water Quality Improvement

Brodie GA, Hammer DA, Tomljanovich (1986) Man-made wetlands for acid drainage control. Proc, 5th Annual National Abandoned Mines Conf

Brodie GA, Hammer DA, Tomljanovich (1988) Constructed wetlands for acid mine drainage control in the Tennessee Valley. Mine Drainage and Surface Mine Reclamation, U.S. Bureau of Mines (USBM) I.C. 9183, Vol 1, pp 325-331

Browne D (1852) The American Muck Book. C.M. Saxton, New York City

Clayton LD, Wildeman TR (1998) Processes contributing to the removal of manganese from mine drainage by an algal mixture. Proc, 15th Annual Meeting of American Soc for Surface Mining and Reclamation, pp 192-201

Duddleston KN, Fritz E, Hendricks AC, Roddenberry K (1992) Anoxic cattail wetland for treatment of water associated with coal mining activities. Proc, 19th Meeting of the American Soc for Surface Mining and Reclamation, pp 249-254

Dvorak DH, Hedin RS, Edenborn HM, McIntyre PE (1992) Treatment of metal-contaminated water using bacterial sulfate reduction: results from pilot-scale reactors. Biotechnol Bioeng 40: 609-616

Emerick JC, Huskie WW, Cooper DJ (1988) Treatment of discharge from a high elevation metal mine in the Colorado Rockies using an existing wetland. Mine Drainage and Surface Mine Reclamation, USBM I.C. 9183, Vol. 1, pp 345-351

Faulkner BB, Skousen JG (1994) Treatment of acid mine drainage by passive treatment systems. Proc, International Land Reclamation and Mine Drainage Conf and 3rd International Conf on the Abatement of Acidic Drainage (ICARD), pp 250-256

Gerber DW, Burris JE, Stone RW (1985) Removal of dissolved iron and manganese ions by a sphagnum moss system. In: Brooks RP, Samuel DE, Hill JB (Eds), Wetlands and Water Management on Mined

Lands, Pennsylvania State Univ, pp 365-372
Girts MA, Kleinmann RLP (1986). Constructed wetlands for treatment of acid mine drainage: a preliminary review. In: Graves DH (Ed), Proc, National Symp on Surface Mining, Hydrology, Sedimentology, and Reclamation, Univ of Kentucky, pp 165–171
Girts MA, Kleinmann RLP, Erickson PM (1987) Performance data on Typha and Sphagnum wetlands constructed to treat coal mine drainage. Proc, 8th Annual Surface Mine Drainage Task Force Symp
Gusek J (2000) Reality check: passive treatment of mine drainage as emerging technology or proven methodology? Proc, SME Annual Meeting, preprint 00-43
Gusek J (2009) A periodic table of passive treatment for mining influenced water. Proc, ASMR Annual Meeting, pp 550-562. DOI: 10.21000/JASMR09010550
Hammack RW, Hedin RS (1989) Microbial sulfate reduction for the treatment of acid mine drainage: a laboratory study. Reclamation – A Global Perspective, Proc, Joint meeting of the Canadian Land Reclamation Assoc and the American Soc for Surface Mining and Reclamation, pp 673-680. DOI: 10.21000/JASMR89010673
Hammer DA (Ed) (1989) Wastewater Treatment: Municipal, Industrial, and Agricultural, CRC Press, Boco Raton, FL
Hedin RS, Dvorak DH, Gustafson SL, Hyman DM, McIntyre PE, Nairn RW, Neupert RC, Woods AC, Edenborn HM (1991) Use of a constructed wetland for the treatment of acid mine drainage at the Friendship Hill National historic site, Fayette County, PA. Interagency Agreement 4000-5-0010
Hedin RS, Hyman DM, Hammack RW (1988) Implications of sulfate-reduction and pyrite formation processes for water quality in a constructed wetland: preliminary observations. Mine Drainage and Surface Mine Reclamation, USBM I.C. 9183, Vol. 1, pp 382-388
Hedin RS, Hammack RW, Hyman DM (1989) Potential importance of sulfate reduction processes in wetlands constructed to treat mine drainage. In: Hammer DA (Ed), Constructed Wetlands for Wastewater Treatment: Municipal, Industrial, and Agricultural, pp 508-514, CRC Press, Boca Raton
Hedin RS, Nairn RW (1990) Sizing and performance of constructed wetlands: case studies. In: Skousen J, Sencindiver J, Samuel D (Eds), Proc, 1990 Mining and Reclamation Conf and Exhibition, pp 385-392
Hedin RS, Nairn RW (1992) Design and sizing of mine drainage treatment systems. Proc, 13th Annual West Virginia Acid Mine Drainage Task Force Symp, pp 111-121. https://wvmdtaskforce.files.wordpress.com/2015/12/92-hedin.pdf
Hedin RS, Nairn RW, Kleinmann RLP (1994a) Passive Treatment of Coal Mine Drainage. US Bureau of Mines IC 9389
Hedin R, Watzlaf GR, Nairn R (1994b) Passive treatment of acid mine drainage with limestone. J Environ Qual 23: 1338-1345. DOI:10.2134/JEQ1994.00472425002300060030X
Hendricks, AC (1991) The use of an artificial wetland to treat acid mine drainage. Proc, International Conf on the Abatement of Acidic Drainage (ICARD).
Hiel MT, Kerins Jr. FJ (1988) The Tracy wetlands: a case study of two passive mine drainage systems in Montana. Mine Drainage and Surface Mine Reclamation, USBM I.C. 9183, Vol. 1, pp 352-358
Holm JD, Bischop MB (1983) Passive mine drainage treatment: selected case studies. In: Medine A, Anderson M (Eds), Proc, National Conf on Environmental Engineering, pp 607-618
Holm JD, Elmore T (1986) Passive mine drainage treatment using artificial and natural wetlands. In: Shuster MA, Zuck RW (Eds), Proc, High Altitude Reclamation Workshop no. 7, pp 41-48
Huntsman BE, Solch JG, Porter MD (1978) Utilization of sphagnum species dominated bog for coal acid mine drainage abatement. Abstracts, 91st Annual Meeting of the Geological Soc of America, Toronto
Jenkins M, Skousen J (1993) Acid mine drainage treatment with the Aquafix system. Proc, West Virginia Acid Mine Drainage Task Force Symp. https://wvmdtaskforce.files.wordpress.com/2015/12/93-jenkins.pdf
Kadlec RH, Wallace SD (2009) Treatment Wetlands. 2nd edit, CRC Press, Boca Raton
Kalin M (1988) Ecological engineering and biological polishing methods to economize waste management.

Proc, 20th Annual Meeting of the Canadian Mineral Processors, pp 302-318
Kepler DA, McCleary EC (1994) Successive alkalinity-producing systems (SAPS) for the treatment of acidic mine drainage. Proc, International Land Reclamation and Mine Drainage Conf, USBM SP 06B-94, Vol 1, pp 195-204
Kepler DA, McCleary EC (1997) Passive aluminum treatment success. Proc, 18th WV Surface Mine Drainage Task Force Symp, Morgantown, WV
Kleinmann B, Skousen J, Wildeman T, Hedin B, Nairn B, Gusek J (2021) The early development of passive treatment systems for mining-influenced water: a North American perspective. Mine Water Environ 40(4):818-830
Kleinmann RLP (1985) Treatment of acid mine water by wetlands. Control of Acid Mine Drainage. USBM IC 9027, pp 48-52
Kleinmann RLP, Erickson PM, Girts MA, Hyman DM (1986) Workshop on passive treatment of mine drainage (unpublished)
Kleinmann RLP, Girts MA (1987) Constructed wetlands for treatment of mine water--successes and failures. Proc, 8th Annual National Abandoned Mine Lands Conf, Montana Dept of State Lands, pp 67-73
Kleinmann RLP, Tiernan TO, Solch JG, Harris RL (1983) A low cost, low maintenance treatment system for acid mine drainage using sphagnum moss and limestone. In: Graves DH (Ed), Proc, Symp on Surface Mining, Hydrology, Sedimentology and Reclamation, Univ of Kentucky, pp. 241-246
Kuyucak N, St-Germain P (1994a) Evaluation of sulphate reducing bacteria and related process parameters for developing a passive treatment method. In: Holmes DS, Smith RW (Eds), Proc, Engineering Foundation Conf, pp 287-302
McHerron LE (1986) Removal of iron and manganese from mine drainage by a wetland: seasonal effects. MS thesis, Pennsylvania State Univ
McIntyre PE, Edenborn HM (1990) The use of bacterial sulfate reduction in the treatment of drainage from coal mines. Proc, Mining and Reclamation Conference and Exhibition, pp 409-416. doi.org/10.21000/JASMR90010409
McIntyre PE, Edenborn HM, Hammack RW (1990) Incorporation of bacterial sulfate reaction into into constructed wetlands for the treatment of acid and metal drainage. In: Graves DH, De Vore (Eds), Proc, 1990 National Symp on Mining, pp 207-213
Nairn RW, Hedin RS (1992) Designing wetlands for the treatment of polluted coal mine drainage. In: Landin MC (Ed.), Wetlands: Proc, 13th Annual Conf of the Society of Wetland Scientists, pp. 224-229
Nairn RW, Hedin RS, Watzlaf GR (1991) A preliminary review of the use of anoxic limestone drains in the passive treatment of acid mine drainage. Proc, 12th Annual West Virginia Surface Mine Drainage Task Force Symp, pp 23-38
Nairn, RW, Hedin RS, Watzlaf GR (1991) A preliminary review of the use of anoxic limestone drains in the passive treatment of acid mine drainage. Proc, 12th Annual WV Surface Mine Drainage Task Force Symp, pp 23-38. https://wvmdtaskforce.files.wordpress.com/2015/12/92-hedin2.pdf
Nairn RW, Hedin RS, Watzlaf GR (1992) Generation of alkalinity in an anoxic limestone drain. Achieving Land Use Potential through Reclamation, Proc, 9th Annual American Soc for Surface Mining and Reclamation Meeting, pp 206-219
Nairn RW, LaBar JA, Strevett KA, Strosnider WH, Morris D, Neely CA, Garrido A, Santamaria B, Oxenford L, Kauk K, Carter S, Furneaux B (2010) A large, multi-cell, ecologically engineered passive treatment system for ferruginous lead-zinc mine waters. Proc, Mine Water and Innovative Thinking, International Mine Water Assoc, pp 255-258
Nawrot JR, Klimstra WB (1990) Biochemical treatment of mine drainage through a reedgrass wetland. In: Skousen J, Sencindiver J, Samuel D (Eds.). Proc, Mining and Reclamation Conf and Exhibition. West Virginia Univ. https://wvmdtaskforce.com/past-symposium-papers/1990-symposium-papers/
Nuttall CA, Younger PL (2000) Zinc removal from hard circum-neutral mine waters using a novel closed-bed limestone reactor. Water Res 34:1262-1268

Pearson FH, McDonell AJ (1974) Chemical kinetics of neutralization of acidic water by crushed limestone. Proc, no. 18, Water Resources Problems Related to Mining, American Water Resources Assoc, Columbus, OH, pp 85-98

Pearson FH, McDonell AJ (1975a) Use of crushed limestone to neutralize acid wastes. J Env Eng Div-ASCE 101:139-158

Pearson FH, McDonell AJ (1975b) Limestone barriers to neutralize acidic streams. J Env Eng Div-ASCE 101: 425-440

Pesavento BG (1984) Factors to be considered when constructing wetlands for utilization as biomass filters tof an innoo remove minerals from solution. In: Burris JE (Ed), Treatment of Mine Drainage by Wetlands, Dept of Biology, Pennsylvania State Univ

Reynolds JS, Machemer SD, Wildeman TR, Updegraff DM, Cohen RR (1991) Determination of the rate of sulfide production in a constructed wetland receiving acid mine drainage. Proc, National Meeting of the American Soc of Surface Mining and Reclamation, pp 175-182

Seidel K (1952) Pflanzungen zwischen Gewässern und Land. Mitteilungen Max-Planck Gesellschaft zur Förderung der Wissenschaften 8:17-21

Sen AM, Johnson DB (1999) Acidophilic sulphate-reducing bacteria: candidates for bioremediation of acid mine drainage. In: Amils R, Ballester A (Eds), Biohydrometallurgy and the Environment: Toward the Mining of the 21st Century, Process Met 9: 709-718. doi.org/10.1016/S1572-4409(99)80073-X

Sencindiver JC, Bhumbla DK (1988) Effects of cattails (Typha) on metal removal from mine drainage. Mine Drainage and Surface Mine Reclamation, USBM I.C. 9183, Vol 1, pp 359-368

Skousen J (1991) Anoxic limestone drains for acid mine drainage treatment. Green Lands 21: 30-35

Skousen J (1995) Douglas abandoned mine land project: description of an innovative acid mine drainage treatment system. Green Lands 25: 29-38

Skousen, J, Zipper C, Rose A, Ziemkiewicz P, Nairn R, McDonald LM, and Kleinmann RLP (2017) Review of passive systems for acid mine drainage treatment. Mine Water Environ. 36:133-153. https://doi.org/10.1007/s10230-016-0417-1

Skousen J, Sexstone A, Ziemkiewicz P (2000) Acid mine drainage control and treatment. Reclamation of Drastically Disturbed Lands, Vol. 41. Agronomy Monographs, Madison, WI.

Snyder C, Aharrah (1984) The influence of the Typha community on mine drainage. Proc, National Symp on Mining, Sedimentology and Reclamation, Univ of Kentucky, Lexington, pp 149-153

Stark LW, Stevens SE, Webster HJ and Wenerick WR (1990) Iron loading, efficiency and sizing in a construction wetland receiving mine drainage. In: Skousen J, Sencindiver J, Samuel D (Eds.). Proc, Mining and Reclamation Conf and Exhibition. West Virginia Univ. https://wvmdtaskforce.com/past-symposium-papers/1990-symposium-papers/

Thomas RC, Romanek C (2002) Passive treatment of low-pH, ferric iron-dominated acid rock drainage in a vertical flow wetland II: metal removal. JASMR, pp 752-775. DOI:10.21000/JASMR02010752

Turner D, McCoy D (1990) Anoxic alkaline drain treatment system, a low-cost acid mine drainage treatment alternative. Proc, National Symp on Mining, Sedimentology and Reclamation, Univ of Kentucky

Tuttle JH, Dugan PR, Randles CI (1969) Microbial sulfate reduction and its potential utility as an acid mine water pollution abatement procedure. Appl Microbiol 17: 297-302

URS (2003) Passive and semi-active treatment of acid rock drainage from metal mines - state of the practice. Prepared for the U.S. Army Corps of Engineers. https://semspub.epa.gov/work/01/43547.pdf

Watzlaf GR, Hedin RS (1994) A Method for predicting the alkalinity generated by anoxic limestone drains. Proc, West Virginia Acid Mine Drainage Task Force. https://wvmdtaskforce.files.wordpress.com/2015/12/93-watzlaf.pdf

Watzlaf GR, Schroeder KT, Kairies C (2000) Long-term performance of alkalinity-producing passive systems for the treatment of mine drainage. Proc, National Meeting of the American Soc for Surface Mining and Reclamation, pp 262-274. DOI: 10.21000/JASMR00010262

Wieder RK (1992) The Kentucky wetlands project: A field study to evaluate man-made wetlands for acid

coal mine drainage treatment. Final Report to the U.S. Office of Surface Mining, Villanova University, Villanova, PA.
Wieder RK, Lang GE (1982) Modification of acid mine drainage in a freshwater wetland. In: McDonald BR (Ed), Proc, Symp on Wetlands of the Unglaciated Appalachian Region, West Virginia Univ, WV
Wieder RK, Lang GE, Whitehouse AE (1985) Metal removal in sphagnum-dominated wetlands: experience with a man-made wetland. In: Brooks RP, Samuel DE, Hill JB (Eds), Wetlands and Water Management on Mined Lands, Pennsylvania State Univ, pp 353-364
Wildeman TR, Machemer SD, Klusman RW, Cohen RRH, Lemke P (1990) Metal removal efficiencies from acid mine drainage in the Big Five constructed wetland. In: Skousen J, Sencindiver J, Samuel D (Eds.). Proc, Mining and Reclamation Conf and Exhibition. West Virginia Univ. https://wvmdtaskforce.com/past-symposium-papers/1990-symposium-papers/
Wildeman TR, Duggan L, Phillips P, Rodriguez-Eaton S, Simms R, Bender J, Taylor N, Britte C, Mehs D, Forse J, Krabacher P, Herron J (1993) Passive treatment methods for manganese: preliminary results from two pilot sites. Proc, National Meeting of the American Soc of Surface Mining and Reclamation, pp 665-677
Wildeman TR, Brodie G, Gusek JJ (1993) Wetland Design for Mining Operations, BiTech Publishers, Richmond, B.C., Canada
Wildeman TR, Filipek LH, Gusek J (1994a). Proof-of-principle studies for passive treatment of acid rock drainage and mill tailing solutions from a gold operation in Nevada. Proc, International Land Reclamation and Mine Drainage Conf, U.S. Bureau of Mines Special Publ 06B-94, Vol. 2, pp 387-394
Wildeman TR, Cevaal J, Whiting K, Gusek JJ, Scheuring J (1994b) Laboratory and pilot-scale studies on the treatment of acid rock drainage at a closed gold-mining operation in California. Proc, International Land Reclamation and Mine Drainage Conf, U.S. Bureau of Mines Special Publ 06B-94, Vol 2, pp 379-386.
Wildeman T, Updegraff D (1998), Passive bioremediation of metals and inorganic contaminants. In: Macalady DL (Ed), Perspectives in Environmental Chemistry, Oxford University Press, New York City, pp 473-495
Wolkersdorfer C (2021) Reinigungsverfahren für Grubenwasser. Springer, Heidelberg
Younger PL (1998) Design, construction and initial operation of full-scale compost-based passive systems for treatment of coal mine drainage and spoil leachate in the UK. Proc, International Mine Water Assoc Symp, Vol 2, pp 413-424
Ziemkiewicz P, Skousen J, Lovett R (1994) Open limestone channels for treating mine drainage: a new look at an old idea. Green Lands 24: 36-41
Ziemkiewicz P, Skousen J, Brant D, Sterner P, Lovett R (1997) Acid mine drainage treatment with armored limestone in open limestone channels. J Environ Qual 26: 560-569
Ziemkiewicz P, Skousen J (1998) The use of steel slag in acid mine drainage treatment and control. Proc, West Virginia Acid Mine Drainage Task Force Symp, pp 651-656. https://wvmdtaskforce.files.wordpress.com/2016/01/98-ziemkiewicz.pdf
Ziemkiewicz P, Skousen J (1999) Steel slag in acid mine drainage treatment and control. Proc, American Soc of Mining and Reclamation. https://www.asrs.us/Portals/0/Documents/Conference-Proceedings/1999/0651-Ziemkiewicz.pdf

Data Needed for Selection and Design of AMD Treatment Systems[1]

Tim Danehy, Kelsea Green[2], and Tiff Hilton[3]

Abstract: Proper characterization of mine drainage is essential to every design process and often begins during initial monitoring associated with permit requirements or stream assessment. It is imperative that a sufficient dataset be developed in order to select the treatment process needed to adequately address the discharge and achieve effluent requirements needed for permit compliance, restoration of aquatic resources, or other project goals. Parameters typically used in the selection and sizing of both active and passive treatment components include flow, pH, acidity (Standard Methods 2310 B, "hot peroxide" method that reports both positive and negative acidity as $CaCO_3$ equivalents), alkalinity, conductivity, iron, aluminum, manganese, sulfates, total suspended solids, and temperature. Depending on the treatment needs and process selected, other parameters may prove critical or otherwise useful. These may include but are not limited to total inorganic carbon, calcium, magnesium, potassium, chloride, sodium, and other metals when known or expected to be of concern such as copper, lead, nickel.

In addition to flow and pH, other field tests may be needed to evaluate alkalinity, dissolved oxygen, and dissolved carbon dioxide. These additional parameters can change dramatically between field collection and laboratory testing even with properly collected and stored samples transported to the laboratory in a timely manner. The location of the sample point is also critical as collecting water samples at the most convenient location can lead to a gross mischaracterization of the drainage and result in an ineffective or otherwise inappropriate design. Care to avoid upstream contamination or interference of the sample point is also vital. It is stressed that flow is the first parameter listed due to the important role that the quantity of water to be treated plays in all aspects of the treatment process including sizing the collection and conveyance systems and calculating component residence time and pollutant load. Evaluating the projected improvements to a receiving stream cannot be done without flow data. In the experience of the authors, absence of sufficient flow information is the most often problematic segment of a dataset. It is hoped that a review of the basics of AMD science will assist all parties involved in working to address the impacts of mine drainage.

---

[1] Presented at the 2022 West Virginia Mine Drainage Task Force Symposium, Morgantown, WV.

[2] Tim Danehy, QEP, Principal, Kelsea Green, Environmental Engineer, BioMost Inc., 434 Spring Street Ext., Mars PA 16046.

[3] Tiff Hilton, Water Treatment Consultant, Working on People's Environmental Concerns, Lewisburg, WV.

Successful Acid Mine Drainage Abatement – Broad Top, PA

Joseph E. Mills
Skelly and Loy
304-590-4300, jmills@skellyloy.com
449 Eisenhower Boulevard, Suite 300
Harrisburg, PA 17111-2302

Abstract

Since 1979, forty-two passive Acid Mine Drainage (AMD) treatment systems have been constructed in the Six Mile, Sandy Run and Longs Run watersheds, Broad Top Township, Bedford County, Pennsylvania.

The first AMD treatment system was funded by the Rural Abandoned Mine Program (RAMP) and constructed in 1979. The success of this project and a growing community interest in AMD abatement prompted a watershed study that was completed in 1981. This study identified illegal garbage dumping, sewage and AMD as the major problems in the study area. Broad Top Township has addressed both the garbage and sewage by making garbage disposal affordable to all its residents and by taking ownership of the sewage management practices within the township.

By the mid-1990's, additional RAMP and Bureau of Abandoned Mine Reclamation (BAMR) projects were completed. In 2005, a Watershed Implementation Plan (WIP) was completed for Longs, Sandy and Six Mile Runs. Since then, over $3.5 million of CWA Section 319 funds and over $0.5 million of Pa. DEP Growing Greener Grant money has been spent on AMD abatement projects in the watersheds.

All of the systems constructed since 2005 have been designed to treat the high flow discharges for a minimum of 20 years. These AMD discharges vary in quantity and quality from site to site. The design goal of all of the AMD treatment systems is to remove 90% of the metal and acid loads entering the streams. Challenging construction conditions were encountered at most of the treatment sites. A variety of passive treatment technologies have been employed. The technology chosen for each site is tailored for that site based on the chemistry and flow at that particular AMD seep location. In 2014, after construction of 13 AMD treatment systems, Longs Run was delisted in the Pennsylvania Integrated Water Quality Monitoring and Assessment Report (Integrated Report).

History and Projects

Since 1979, 42 passive Acid Mine Drainage (AMD) treatment systems have been constructed in the Six Mile, Sandy Run and Longs Run watersheds, Broad Top Township, Bedford County, Pennsylvania, an area of 48.5 square miles. Funding for these systems came mainly from the Environmental Protection Agency's Section 319 Grants and Pennsylvania Department of Environmental Protection's (PA DEP) Growing Greener Grant program.

The PA DEP issues grants for their Nonpoint Source Management Program through the Growing Greener Plus application process, the four programs covered under Growing Greener Plus, are Growing Greener, 319 Nonpoint Source (NPS), Surface Mining Control and Reclamation Act (SMCRA) Bond Forfeiture, and Abandoned Mine Drainage (AMD) Set-Aside grants. There are a number of program-specific criteria regarding the eligibility of projects focused on AMD remediation: projects to address mining-related issues may be funded from bond forfeiture funds if the site is within a bond forfeiture site, by AMD Set-Aside funds if the project is covered by a Qualified Hydrologic Unit Plan (QHUP) or watershed where a QHUP is

being developed; by 319 Nonpoint Source funds if located in areas covered by a 319 Nonpoint Source Watershed Implementation Plan (WIP); and by Growing Greener Watershed Protection funds for a limited number of projects that don't meet the above criteria.

In 1977, under SMCRA, the Rural Abandoned Mine Program (RAMP) was authorized. SMCRA required Abandoned Mine Land Reclamation Funds to be collected through a surcharge placed on each ton of coal mined by either the surface or underground methods. These funds were collected by the Federal Office of Surface Mining. Approximately 50% of the reclamation funds were distributed to the mining states and Tribes with the other 50% being considered the "Secretary's Share". RAMP received approximately 20% of the "Secretary's Share". Funds have not been distributed through the RAMP program since the mid-1990's, and in 2006, SMCRA was amended and the RAMP program was written out of the Act.

In 1979, at an AMD site located near a local church, the first AMD treatment system was constructed in Broad Top Township. This project was constructed using RAMP funding. The high visibility of this project is credited with spurring the interest of the citizens and the township supervisors to explore the recovery of the mine impacted streams in Broad Top Township. Although there was much interest in the success of this AMD treatment project, it took many years for the next AMD treatment project to be constructed.

The growing interest in AMD abatement lead to the development of a watershed study which was completed in 1981. This study was sponsored by the three local conservation districts and relied heavily on community input. The study identified illegal garbage dumping, sewage, and AMD as the major problems in the study area. Unfortunately, it took until the 1990's for the study to gain momentum and concerted efforts to address these problems.

In 1991, a Municipal Solid Waste Landfill began operation in the township and was expanded in 2011. Prior to beginning operation, a Host-Municipality Agreement was signed between the owner of the landfill and Broad Top Township. Under this agreement, the landfill is limited to an average of 700 tons per day with a maximum of 900 tons per day and the landfill is limited as to the type of waste that can be accepted. The Township negotiated numerous clauses into the Agreement that were friendly to the citizens of Broad Top Township. Under the agreement, each landowner is given a $120 annual property tax credit, free weekly curbside garbage pick-up and free semi-annual bulk item disposal. The landfill operator provides to the Township, free roll-off dumpsters and free disposal of the debris for one demolition project each year. The operator of the landfill also provides an annual donation of $5,000 to each of the three volunteer fire companies within the Township. The Township is reimbursed for the hourly wages of their employees during their time on the garbage truck during weekly curbside residential garbage pick-up. The Township receives $3.50 per ton of waste disposed or a minimum of $200,000 annually. The negotiated cost per ton is significantly less than the "going rate" for disposal of waste in most Municipal Solid Waste Landfills, but in return, the Township received the concessions mentioned above, as well as stricter environmental requirements than those mandated by the PA DEP. The agreement has virtually eliminated illegal dumping in the watersheds.

In 1995, a Pennsylvania Sewage Facilities Act 537 Plan was completed. Act 537 requires that all Commonwealth municipalities develop and implement comprehensive official plans that provide for the resolution of existing sewage disposal problems, provide for the future sewage disposal needs of new land development, and provide for the future sewage disposal needs of the municipality. These plans address whole municipalities or groups of municipalities working together. Broad Top Township worked cooperatively with Coaldale Borough to develop and implement the plan which included between 800 and 850 homes. The plan included four cluster systems to treat the sewage from approximately 600 homes with the remaining 200+ homes utilizing on-lot systems. Each on-lot system services two to six homes when

possible. The unique aspect of Broad Top Township's plan is that all of the treatment systems, including the on-lot systems, are owned and maintained by Broad Top Township, therefore there are no repair fees charged to the citizens. Each household is charged a monthly maintenance fee of $20.

This plan has been used as a case study by PA DEP and NANOPDF (an online information dissemination site) as a demonstration to other municipalities as to how an Act 537 Plan can be developed and followed in an economical and effective manner. USCOE Section 313 Program money and other public funding kept the cost low to the residents. Before the implementation of the plan, 75% of the residents had malfunctioning sewage systems. The implementation of this plan has eliminated the nitrate and bacteriological problems in the streams.

After the success of the RAMP project in 1979, three Bureau of Abandoned Mine Reclamation (BAMR) projects were constructed in the upper reaches of Sandy Run. These projects were completed in the mid-1990's. In 2001, Broad Top Township completed an assessment and remediation plan followed by a Watershed Implementation Plan (WIP) in 2005. Since the completion of the WIP, over $3.5 million of CWA Section 319 funds and over $0.5 million of Growing Greener Grant money has been acquired and spent by Broad Top Township in the three watersheds within the township boundaries.

All of the systems constructed since 2005 have been designed to treat the high flow discharges for a minimum of 20 years. These discharges vary from site to site with measured flow rates varying from a low of 3 gallons per minute (gpm) to a high of 300 gpm. The quality of the AMD also varies from site to site, with some sites having dissolved iron concentrations so low as to be non-detectable using standard laboratory equipment, while other sites have concentrations as high as 83.4 mg/l, dissolved aluminum concentrations are in the range between 0.1 mg/l and 33.7 mg/l. Acidity varies from a low of 7.6 mg/l (measured as $CaCO_3$) to a high of 445.0 mg/l. The design goal of each of the AMD treatment systems is to remove 90% of the metal and acid loads entering the streams.

Construction of these projects often present challenges due to constraints caused by the topography of the construction area and/or the proximity of the AMD seep to the stream channel. Most of the projects had to be "squeezed" into spaces between steep hill sides and flood plain boundaries. Occasionally, the seeps required piping or ditching the AMD hundreds of feet from the source to an area suitable for the construction of an adequately sized system that would be capable of accomplishing the goal of 90% contaminant reduction.

A variety of passive treatment technologies have been employed in the three watersheds. The technology chosen for each site is tailored for that site based on the chemistry and flow at that particular AMD seep location. The list of technologies utilized include: limestone channels, low pH iron removal channels, vertical flow limestone ponds, flushable limestone leach beds, aerobic and anaerobic wetlands, oxidation channels, automatic flushing devices (siphons and motor driven valves) and sediment removal basins.

Longs Run

Thirteen (13) AMD treatment systems were installed in Longs Run, a 5.25-mile tributary to Sandy Run. Periodic studies were conducted by PA DEP and in 2007 the first fish were documented in Longs Run. In 2014, based on data collected by PA DEP, Longs Run was delisted in the Pennsylvania Integrated Water Quality Monitoring and Assessment Report (Integrated Report). The Integrated Report is a comprehensive report of the water quality status of surface waters of the Commonwealth of Pennsylvania. The Integrated Report is comprised of the results of assessments for four protected uses of surface waters, recreation, fish consumption, water supply and aquatic life. Longs Run's protected use is aquatic life, which is defined as

maintaining the flora and fauna indigenous to aquatic habitats. Longs Run was delisted with a Freestone Index of Biological Integrity (IBI) score of 78.3. Generally, any IBI score over 60 is considered to have attained cold water fisheries status.

Sandy Run

The Sandy Run watershed drains a significantly impaired portion of abandoned mine lands located in Broad Top Township in Bedford County, Pennsylvania. The main stem of the stream flows approximately 5.25 miles from its headwaters to its mouth near the town of Hopewell, where it enters the Raystown Branch of the Juniata River. Coal mining played a significant role in the industrial development of the region, and many surface and underground mines were operated in the watershed early in the 20th century. Those mines are now abandoned, many are flooded and discharging into Sandy Run, and a few left spoil piles adjacent to the stream contributing to the contamination of Sandy Run and its tributaries. These abandoned mine land features are significant sources of water pollution within the Sandy Run Watershed. Sandy Run is listed as impaired for both pH and metals on the Integrated Report with a Total Maximum Daily Load (TMDL) established for the watershed as part of the Sandy Run Watershed TMDL.

Nine (9) AMD treatment projects have been completed in the main stem of Sandy Run. Another project is currently under design and will go to construction as soon as permits are acquired. Currently there are no other plans for future construction in Sandy Run, although known AMD sources apparently are having sever impacts on the chemistry of the stream. An unnamed tributary flows into Sandy Run near the discharge point of the newest and most downstream AMD treatment system in Sandy Run. This small tributary is severely impacted by AMD.

The three most upstream projects were constructed by and are the responsibility of BAMR. Based on an assessment conducted in the spring and fall of 2019, the three BAMR projects are all in need of maintenance. The project located highest in the watershed has breached and most of the AMD that the system is designed to treat, is flowing directly into Sandy Run, by-passing the AMD treatment system almost entirely. Of course, the location of this input, has a negative impact on the entirety of Sandy Run.

The other two BAMR projects are not very effective in treating their AMD discharges. One of the sites discharges into the other and the final discharge from that system discharges treated AMD at a pH of 6.2 during low flow and 4.4 during high flow.

The next five treatment systems in Sandy Run, have discharge pH's over 7.0, which is an increase of 4.0 or more at each site. The poorest performing of Broad Top Township's systems in Sandy Run is the last project completed in Sandy Run. It was noted that the new system was not being operated as per design, and was discharging at a pH of 6.55, an increase of over 3.0 standard units. After discussing the proper operation of the system with Broad Top Township staff, the discharge is expected to exceed the numbers measured during the fall 2019 sample collection.

The impacts from the upstream most discharges are seen in the water quality analysis and the biological assessment of Sandy Run to its confluence with the Raystown Branch of the Juniata River. Additionally, the upper reaches of Sandy Run are also highly impacted from sediment. These sediments will not be qualified by the chemical samples collected during the spring and fall of 2019, but the impairment will limit the macroinvertebrate community. The biological assessment of Sandy Run, conducted by Trout Unlimited (TU), shows the results of not only the sediment impairment but also the chemical impairment caused by

poorly treated AMD discharges in the upper reaches of the stream. TU's analysis of Sandy Run conclude the benthic macroinvertebrate community and the fish community was found to be impaired due to several potential stressors. TU identified those stressors as AMD impacts, non-point source pollution, and landfill impacts.

Abatement of the impacts of the unnamed tributary and revitalization of the three BAMR systems will remediate the chemical impairments in Sandy Run. An assessment of the sediment and erosion control system at the landfill may identify the source of the high sediment load in Sandy Run which would be the first step in correcting the siltation problem.

Six Mile Run

Twenty (20) AMD treatment systems have been installed in Six Mile Run. The main stem of the stream flows 6.16 miles from its headwaters to its mouth near the town of Defiance, where it enters the Raystown Branch of the Juniata River. Six Mile Run is listed as impaired for both pH and metals on PA DEP's Integrated List with a Total Maximum Daily Load (TMDL) established for the watershed as part of the Six Mile Run Watershed TMDL.

A study conducted by Skelly and Loy, in the spring and fall of 2017, showed all systems were discharging treated water that had a pH of 6.0 or greater with most discharging treated AMD greater than 6.5 pH. One exception was a system that is located in the bottom portion of the stream as it was discharging treated AMD with a pH of 5.1 during the high flow sampling run conducted in March of 2017. The flow into that system on that date was approximately 50% greater than the system's design flow. More data is needed to determine if the flow on that date was an anomaly or if the data collected prior to design was insufficient and did not provide adequate information to design a system capable of treating the AMD.

The study conducted in 2017 indicated that the chemistry of Six Mile Run is not negatively impacted by any of the discharges from the constructed treatment systems. The pH of Six Mile Run was maintained between 6.0 and 7.3 from the headwaters to below the last constructed system. These data indicate that the constructed AMD treatment systems are accomplishing the goal set forth in the Watershed Implementation Plan developed in 2005.

Preliminary plans have been discussed to address the final AMD in the watershed. This discharge is the lowest in Six Mile Run, approximately 300 meters below the last constructed treatment system. Chemical analysis conducted by Broad Top Township and PA DEP indicate that the chemistry of the main stem of Six Mile Run from below the last treatment system to the mouth is adequate to support fish life, and therefore funding for an additional project may be difficult to secure.

The biological assessment of Six Mile Run, conducted by Trout Unlimited (TU) at the same times as the chemical assessment of the stream and treatment systems, indicate improvements throughout the stream but also indicate that biological impairment still exist. Moderate populations of brown trout were located at several locations along the stream, but no brook trout were found at any of TU's test sites. Young of the year brown trout were found at a few of the test sites, indicating the possibility that breeding may be taking place in Six Mile Run.

Benthic measurements were taken at thirteen sites along the main stem of Six Mile Run. Six metrics were used to determine if the stream met the Aquatic Life Use (ALU) threshold for coldwater fishes, warmwater fishes, and trout stocked fishes. At three of the sites, the ALU was met and at two other sites the ALU was very close to the threshold and TU determined that those sites warranted further evaluation. At the remaining

sites, the ALU was not met, nor was it close to the threshold.

Biologic analysis indicated a problem in the area of the system that was found to be discharging treated AMD at a pH below 6.0. The short biological and chemical study and the data collected indicate that the system may be performing below expectations throughout much of the year. This system will be evaluated further in the future to determine if modifications can be made to improve its effectiveness.

In conclusion, much work has been completed in the watersheds within Broad Top Township, but studies indicate that more work is needed if the streams are ever going to approach the condition that existed prior to mining impacts in the watersheds. The studies, especially the studies conducted by TU, direct us to the areas in each stream that are in the most need of attention. Broad Top Township has recently been awarded a grant to fund maintenance on the existing systems. Any maintenance work completed on the existing systems should improve the function of those systems which will improve conditions in the streams allowing for a more robust biologic recovery within the waters of Broad Top Township.

A Design & Build Active Treatment Plant for the Globe Mine High Strength Mine Drainage

Jon Dietz, Ph.D.
Iron Oxide Technologies
Jdietz.IOT@gmail.com

Abstract: The Globe Mine, owned by Vesuvius, U.S., is located on the hillslope of the Ohio River near the town of Newell, West Virginia. The Globe Mine is a closed refractory clay mine with two slope mine discharges, known as Mine 1 and Mine 2. The mine waters are low pH and high acidity (6,000 to 8,000 mg/L) containing high concentrations of dissolved iron (2,000 to 4,000 mg/L) and aluminum (100 to 300 mg/L). This high strength mine water poses a number of treatment challenges including neutralization demand, solids production, and coprecipitation of gypsum. Temporary treatment was installed to address the mine water chemistry. This temporary treatment changed over time in response to operational problems and the high costs of the temporary treatment. The temporary treatment plant was labor intensive, had high chemical requirements and high rental costs, was difficult to operate in cold weather, and produced high volumes of sludge, which was disposed of at an off-site landfill. Iron Oxide Technologies, LLC (IOT) and Joseph Maintenance Services, Inc. (JMS) were contracted to provide a permanent treatment plant to address most of the issues with the temporary treatment. The permanent treatment plant included: 1) modifications and improvements to the two mine entry pump systems: 2) an above ground storage tank into which the mine discharges are pumped and from which raw water is pumped to the treatment plant; 3) a permanent lime slurry storage tank; 4) a pH controlled lime slurry feed system; 5) a reactor system that dissolves the lime and oxidizes the ferrous iron in the mine water to produce a high-density sludge; 6) a flocculation system with polymer addition to form a settleable solid; 7) a lamella clarifier to separate suspended solids from the water and collect settled sludge; 8) a sludge holding tank to store collected sludge; 9) a plate & frame filter press to dewater collected sludge for off-site transport and disposal; and 10) a control system containing remote cellular-based monitoring and alarms for the various treatment plant components. The majority of the treatment components are housed in a pre-fabricated steel building. The presentation provides a description of the treatment approach and treatment plant components.

Enhanced Decarbonation of Mine Drainage using Iron Oxidation

Brent Means, P.G. [1] and Richard L. Beam, P.G. [2]

Abstract: Ferruginous underground coal mine drainage in the Appalachian region contains elevated concentrations of inorganic carbon due to interactions between mine pools and alkaline recharge water. Inorganic carbon species in these waters are predominately either in the form of carbonic acid (H_2CO_3) or bicarbonate alkalinity (HCO_3^-). Alkali chemical costs are increased when mine water enriched in inorganic carbon is treated due to the acidity released when carbonic acid and bicarbonate deprotonate as pH is increased. A common strategy to minimize the deprotonation of carbonic acid is to use an aeration device to decarbonate the mine water before adding alkali chemical. Conversely, the mine drainage treatment community lacks a strategy to minimize the deprotonation of mine water enriched in bicarbonate.

A novel strategy to minimize deprotonation of both carbonic acid and bicarbonate was implemented at two active treatment plants. The strategy consisted of promoting ferrous iron oxidation and precipitation prior to, or in conjunction with, a decarbonation step. The acidity produced by iron hydrolysis serves to deprotonate bicarbonate producing carbonic acid, which then is decarbonated prior to alkali addition. The process aims to decrease the concentrations of bicarbonate and carbonate by transforming these species into carbonic acid before or during decarbonation, prior to pH adjustment.

One site used a 50% by wt. solution of Hydrogen Peroxide (H_2O_2) to promote Ferrous iron oxidization while the other site used mechanical aeration. The strategy increased the removal of inorganic carbon from 26% to 56% and resulted in a net annual cost savings of 50%. Both sites were successfully geochemically modeled proving a cost analysis can be preformed at sites to evaluate whether enhanced decarbonation, decarbonation, or conventional alkali addition is most cost effective.

---

[1] Brent Means is a Hydrologist with the U.S. Department of the Interior, Office of Surface Mining Reclamation and Enforcement (OSMRE) - bmeans@osmre.gov (corresponding author). OSMRE, Harrisburg Office, 215 Limekiln Road, New Cumberland, PA 17070, 814-730-6988

[2] Richard Beam is an Abandoned Mine Lands and Regulatory Program Specialist with the U.S. Department of the Interior, Office of Surface Mining Reclamation and Enforcement (OSMRE) - rbeam@osmre.gov (corresponding author). OSMRE Appalachian Regional Office, 3 Parkway Center, Pittsburgh, PA 15220, 412-495-7324.

PHREEQ-N-AMDTreat+REYs Water-Quality Modeling Tools to Evaluate Acid Mine Drainage Treatment Strategies for Recovery of Rare-Earth Elements

C. A. Cravotta III
U.S. Geological Survey, Pennsylvania Water Science Center
215 Limekiln Rd., New Cumberland, PA 17070, USA cravotta@usgs.gov

ABSTRACT

The PHREEQ-N-AMDTreat+REYs water-quality modeling tools have the fundamental capability to simulate aqueous chemical reactions and predict the formation of metal-rich solids during the treatment of acid mine drainage (AMD). These new user-friendly, publicly available tools were expanded from the PHREEQ-N-AMDTreat tools to include the precipitation of rare-earth elements plus yttrium (REYs) and the adsorption of REYs onto hydrous Fe, Al, and Mn oxides. The tool set consists of a caustic titration model that indicates equilibrium surface and aqueous speciation of REYs as functions of pH and caustic agent, and a kinetics+adsorption model that simulates progressive changes in pH, major ions, and REYs in water and solids during sequential steps through passive and/or active treatment. Each model has a user interface (UI) that facilitates the input of water-quality data and adjustment to geochemical or treatment system variables; for example, retention time and aeration rate are adjustable parameters in the kinetics model. On-screen graphs display results of changes in metals and associated solute concentrations as functions of pH or retention time; details are summarized in output tables.

A goal of such modeling is to identify strategies that could produce a concentrated REYs extract from AMD or mine waste leachate. For example, if REYs could be concentrated after first removing substantial Fe and Al, the final REYs-bearing phase(s) could be more efficiently processed for REYs recovery and, therefore, may represent a more valuable commodity. Preliminary modeling supports the hypothesis that Fe and Al can be removed at pH < 5.5 using conventional sequential oxidation and neutralization treatment processes without removing REYs, and that further increasing pH can promote the adsorption of REYs by hydrous Mn oxides. Alternatively, chemicals such as oxalate or phosphate may be added to precipitate REYs compounds following initial steps to decrease Fe and Al concentrations. The aqueous geochemical model framework is comprehensive and permits evaluation of effects from interactive chemical and physical variables. Field studies that demonstrate REYs attenuation from AMD and corresponding solid-phase formation during specific treatment steps plus laboratory studies of aqueous/solid interactions are helpful to corroborate, refine, and constrain modeling parameters.

Keywords: resource recovery, adsorption, precipitation, equilibrium, kinetics

1.0 INTRODUCTION

Many studies have reported elevated concentrations of rare-earth elements plus yttrium (REYs) plus other critical metals in acid mine drainage (AMD) and in associated solids formed during treatment to remove contaminants from the water (Cravotta, 2008; Vass et al., 2019a, 2019b; Hedin et al., 2020). For example, coal refuse (non-coal material removed during coal cleaning) frequently is pyritic and, consequently, the refuse leachate tends to be acidic and have some of the highest concentrations of REYs and associated metals compared to other types of AMD from coal mines (Cravotta and Brady, 2015). Management of the acidic,

metal-laden leachate and solid waste from coal refuse-disposal facilities is a long-term liability that will persist long after coal mines have closed. An economically sustainable approach for recovery of REYs from such leachate could offset treatment costs.

Routine treatment methods for acid neutralization and metals removal plus various additional steps may be applicable for the recovery of REYs from AMD. Various studies have investigated specific AMD treatment strategies and mechanisms for concentrating REYs by adsorption and/or precipitation with hydroxide, phosphate, or oxalate compounds (Ayora et al., 2018; Zhang and Honaker, 2018; Josso et al., 2018; Edahbi et al., 2018; Royer-Lavallée et al., 2020; Wang et al., 2021; Leon et al., 2021; Mwewa et al., 2022; Hermassi et al., 2022). Appropriate treatment and resource-recovery strategies must also consider the water quality, its volume, and location, plus environmental and economic factors (Fritz et al., 2021). If REYs could be concentrated after first removing substantial Fe and Al, which typically constitute a major fraction of treatment sludge, the final REYs-bearing phase(s) may be more concentrated in a smaller volume of solids formed at later steps. Solids having concentrated REYs may represent a more valuable commodity that can be efficiently transported and processed for REYs recovery, particularly if REYs can be extracted without total digestion of the solids.

Geochemical modeling coupled with cost-analysis software, such as AMDTreat (Office of Surface Mining Reclamation and Enforcement, 2017), may be applied to identify and evaluate treatment strategies for the potential range of variations in influent water quality and to compare costs for construction and operation of different treatment methods that produce the desired effluent quality. The PHREEQ-N-AMDTreat+REYs water-quality modeling tools described in this paper simulate changes in the pH and concentrations of REYs, Fe, Al, Mn, SO_4, and other solutes plus the formation of solids containing REYs in response to changing solution composition, the composition and availability of hydrous-metal-oxide (HMeO) sorbent, and the potential for REYs compounds and other solids to precipitate.

2.0 METHODOLOGY

The PHREEQ-N-AMDTreat+REYs tool set, which is available as a U.S. Geological Survey (USGS) software release (Cravotta, 2022), consists of a caustic titration model that indicates equilibrium aqueous and surface speciation of REYs and other elements as functions of pH and caustic agent, and a kinetics+adsorption model that simulates progressive changes in pH and element concentrations during sequential reaction steps through passive and/or active treatment. The PHREEQ-N-AMDTreat+REYs models were developed with the USGS aqueous speciation program PHREEQC (Parkhurst and Appelo, 2013) and complement the PHREEQ-N-AMDTreat tools (Cravotta, 2020, 2021), which do not consider REYs, other trace elements, fluoride, phosphate, or oxalate. Unlike direct PHREEQC coding, which requires input of values for the solution composition and other model variables, the PHREEQ-N-AMDTreat tools employ a user interface (UI) that facilitates input of initial solute concentrations and adjustment to system variables, such as the potential for precipitation of minerals and/or the availability and properties of HMeO sorbent, without changing the underlying PHREEQC coding. The tools permit mixing of two input solutions, A and B, prior to reactions based on user-specified mixing ratios or flow rates of A and B to compute the volume-weighted concentrations in a 1-L solution, which is the fundamental unit in PHREEQC. The new models utilize the wateq4fREYsKinetics.dat thermodynamics plus kinetics database, which was expanded from wateq4f.dat (Ball and Nordstrom, 1991) provided with PHREEQC to include REYs aqueous and surface species plus relevant REYs solid phases (hydroxide, carbonate, phosphate, and oxalate compounds). Surface species for REYs plus other cations and anions are considered for hydrous ferric oxide (HFO: Dzombak and Morel, 1990; Verplanck et al., 2004; Liu et al., 2017), hydrous aluminum oxide (HAO: Karamilidis and Dzombak, 2010;

Lozano et al., 2019), and hydrous manganese oxide (HMO: Tonkin et al., 2004; Pourret and Davranche, 2013), which together constitute the total HMeO sorbent capacity. Sources of data and values for selected thermodynamic or rate constants are summarized in the software release (Cravotta, 2022). The rate models included in wateq4fREYsKinetics.dat are identical to those in phreeqcAMDTreat.dat previously described by Cravotta (2020, 2021).

The diffuse double layer model of Dzombak and Morel (1990), with an inner surface layer and an outer diffuse layer of counter ions in solution, is used to simulate surface complexation by the HMeO sorbents. Adsorption is computed for freshly precipitated HFO, HAO, and/or HMO plus previously accumulated HMeO that has a specified constant mass and composition. The latter may occur as suspended or recirculated solids or coatings on treatment media. Multiple phases that may precipitate upon reaching equilibrium are considered for the fresh HMeO sorbent: HFO is amorphous $Fe(OH)_3$ plus $Fe(OH)_2$; HAO is amorphous $Al(OH)_3$ plus basaluminite ($Al_4(OH)_{10}SO_4$); and HMO is $Mn(OH)_3$ with solubility of manganite plus $Mn(OH)_2$. Each of the HFO, HAO, and HMO sorbents is considered to have uniform sorbing characteristics indicated by the specific surface area (Asp), site density (n), and surface-binding constants for cations and anions. Based on various literature sources reported by Cravotta (2021, 2022), default values for sorbents and other system parameters are provided automatically in the initial input file. The default Asp and n for each of the sorbents (HFO 600 $m^2\ g^{-1}$ and 1.925 sites nm^{-2}; HAO 68 $m^2\ g^{-1}$ and 4.6 sites nm^{-2}; HMO 746 $m^2\ g^{-1}$ and 1.91 sites nm^{-2}), which may be adjusted in the UI, determine the moles of strong (inner layer) and weak (outer layer) sorption sites with each mole of HFO, HAO, and HMO.

In addition to the precipitation of various Fe, Al, and Mn solids, which may form fresh sorbent, the model also simulates the potential for precipitation of REY-hydroxide, carbonate, phosphate, or oxalate compounds. In general, adsorption and precipitation processes compete with one another. Possible effects from precipitation of REYs and other solids can be evaluated by adjusting the saturation index (SI) value for selected compound(s), as explained by Cravotta (2021). Changing the SI (from the value 0 for equilibrium) is equivalent to changing the equilibrium constant for the precipitation-dissolution reaction. Precipitation of a less soluble phase is simulated by decreasing SI, whereas a relatively soluble phase is simulated by increasing SI. In the extreme case, selecting the SI value of 99 prevents precipitation of the solid. Thus, if one wishes to simulate sorption by HAO consisting of only $Al(OH)_3$, the SI value for basaluminite would be set to 99 and that for $Al(OH)_3$ would be set to 0 (or another value near 0).

Corresponding changes in the equilibrium distribution of REYs and other solutes between aqueous, sorbed, and precipitated fractions are indicated by on-screen graphs and selected output files. Output includes the concentrations of REYs and other solutes in effluent and the accumulated mass of REYs in solids from the combined total REYs adsorbed and precipitated.

2.1 Caustic titration equilibrium-adsorption-precipitation model

The CausticTitrationMix2REYsMoles.exe and CausticTitrationMix2REYs.exe tools consider REYs attenuation from solution by adsorption to HMeO (fresh and/or previously formed) and/or by precipitation as solid compounds (Cravotta, 2022). The aqueous and surface speciation reactions are simulated as equilibrium processes that respond to instantaneous changes in pH and sorbent availability. The pH is increased by 0.25-unit intervals from the initial pH value to a maximum value of 11 by the addition of a selected acid-neutralizing (caustic) agent (NaOH, $Ca(OH)_2$, CaO, Na_2CO_3, or $CaCO_3$). Cravotta et al. (2015) and Cravotta (2021) provided background on AMD neutralization by these caustic agents and offered additional tools for computing estimated caustic quantities to achieve pH targets for "raw" unaerated or aerated AMD.

2.2 Sequential kinetics-adsorption-precipitation model

The TreatTrainMix2REYs.exe tool simulates sequential steps in a passive and/or active AMD treatment system (Cravotta, 2022). Kinetics processes such as CO_2 outgassing, O_2 ingassing, Fe^{II} and Mn^{II} oxidation, SO_4 reduction, and limestone dissolution, all of which affect pH, are coupled with the same equilibrium speciation and precipitation reactions as the CausticTitrationMix2REYs.exe tool. As explained by Cravotta (2021), a total of 11 treatment steps may be considered, with each having a specified reaction (retention) time, CO_2 outgassing rate ($k_{La,CO2}$); availability of limestone (SAcc.cm2/mol), organic matter (SOC.mol), H_2O_2, sorbent (HMeO.mg), and other variables. A target pH may be specified for the addition of a caustic agent (NaOH, $Ca(OH)_2$, CaO, Na_2CO_3, or $CaCO_3$) to begin steps 1 to 5, possibly after aeration (decarbonation) or other pre-treatment steps. Otherwise, the pH may increase or decrease in response to dynamic, kinetically limited processes. The solution composition at the end of each step is passed to the next step.

2.3 Case study datasets

The PHREEQ-N-AMDTreat+REYs tools were used to simulate AMD treatment and formation of REY-bearing solids, including REYs compounds plus REYs adsorbed onto HFO, HAO, and HMO. Data used for demonstration and corroboration of the PHREEQ-N-AMDTreat+REYs models were obtained from previous studies at passive and active AMD treatment facilities in Pennsylvania (Cravotta and Brady, 2015; Ashby, 2017; Cravotta, 2021). Those studies and others in the Appalachian Coalfield of the eastern USA (Cravotta, 2008; Vass et al., 2019) have identified a wide range of concentrations of REYs in AMD and in solids formed in the treatment of these waters, with generally decreasing REYs concentrations with increasing pH. The models were designed with default values for rate constants, sorbent properties, and mineral precipitation potential to be generally applicable to the range of water-quality conditions in coal AMD and commonly used AMD treatment systems.

3.0 RESULTS AND DISCUSSION

3.1 Field AMD Titration Case Study

The CausticTitrationMix2REYs tool was used to simulate pH and solute concentrations observed during field neutralization of AMD at the Nittanny mine (Figs. 1 and 2). The Nittanny AMD, which had low pH (3.0) with elevated concentrations of dissolved (< 0.45 □m) Mg (652 mg L^{-1}), Ca (422 mg L^{-1}), Al (128 mg L^{-1}), Mn (129 mg L^{-1}), Fe (40.7 mg L^{-1}), and REYs (2.0 mg L^{-1}), was titrated in the field with 1.6N NaOH to pH 6.0, 7.5, 9.0, and 10.3 (Cravotta et al., 2015; Cravotta and Brady, 2015). Concentrations of dissolved Fe, Al, Mn, and REYs decreased with increased pH; corresponding precipitated solids and sorbent properties were not characterized.

Simulations with the CausticTitrationMix2REYs tool for the Nittanny AMD generally reproduced trends for measured concentrations of Na, Fe, Al, and Mn with increased pH (Fig. 2). Addition of NaOH accounted for increased Na and pH. Decreased concentrations of Fe, Al, and Mn were simulated by the precipitation of solids that formed fresh HFO, HAO, and HMO sorbent. Although simulations assumed equilibrium with $Al(OH)_3$ or basaluminite would limit dissolved Al concentrations, those phases exhibit increased solubility at pH > 8 that is inconsistent with observed low Al concentrations at pH > 8. Formation of a less soluble phase such as kaolinite could possibly explain low Al concentrations; however, kaolinite is not considered

by the model.

The simulated REYs concentrations, modeled using default Asp values for HFO, HAO, and HMO, were consistent with empirical trends for REYs attenuation (Fig. 2A). For those conditions, adsorption, mainly by HFO with smaller fractions by HMO, accounts for the decreased REYs concentrations between pH 4 and 8. Adsorption by HAO becomes increasingly important at pH > 7. Precipitation of REYs solids may also attenuate REYs, particularly at pH > 9 (Fig. 2B). Although PO_4 was not detected (< 0.02 mg L^{-1} as P), the PO_4 concentration was assumed to be 0.01 mg L^{-1} in the Nittanny influent. Given that PO_4 concentration, $LaPO_4$:$10H_2O$ and several other REY-PO_4 phases are supersaturated. As the pH increased to values > 9, $La_2(CO_3)_3$ and some other REY-CO_3 phases also became supersaturated. Simulated precipitation of REYs compounds limited the REYs concentrations to equilibrium with the REYs solids (SI = 0) and, also, decreased the adsorbed fractions over the pH range where the REYs solids could feasibly form (Figs. 2A and 2B).

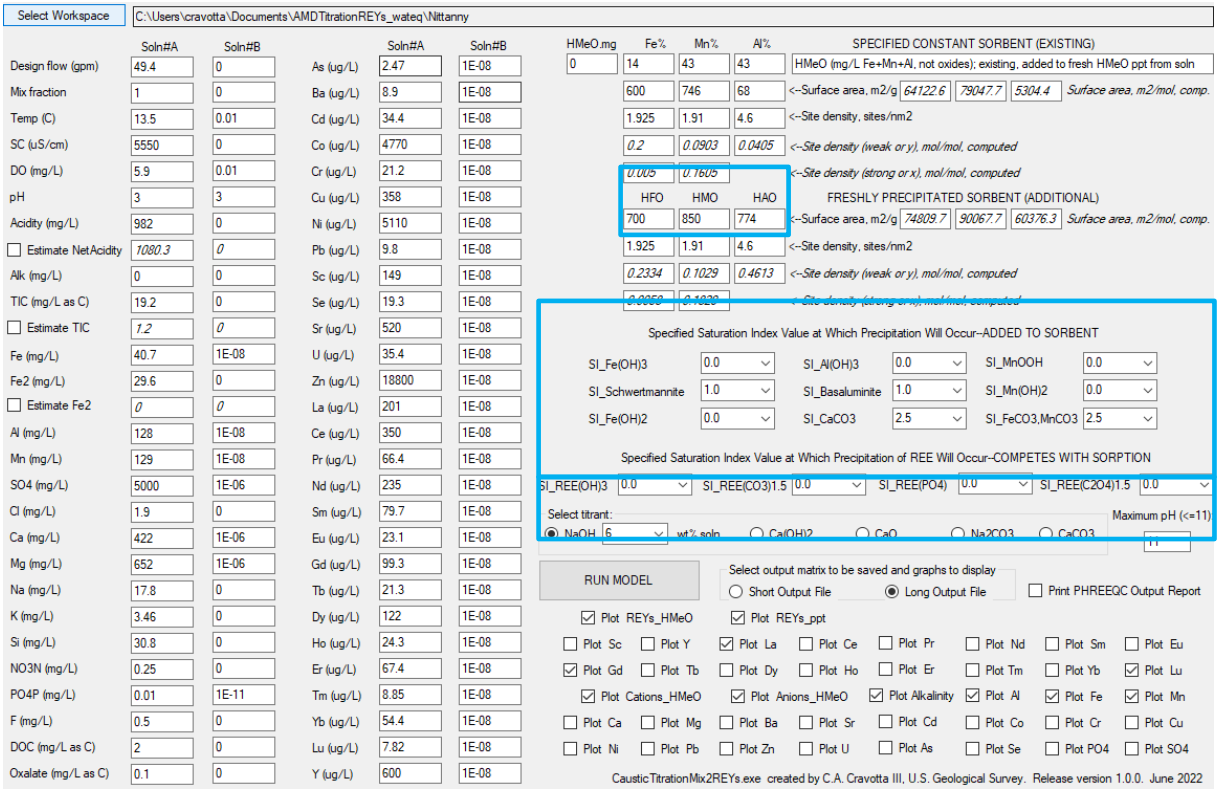

Fig. 1. User interface (UI) for the CausticTitrationMix2REYs tool showing input values for untreated AMD at the Nittanny mine and adjusted parameters for sorption and precipitation of REYs.

A. Default sorbent Asp values: HFO 600 m^2 g^{-1}; HAO 68 m^2 g^{-1}; HMO 746 m^2 g^{-1}; SI_{REY}=99

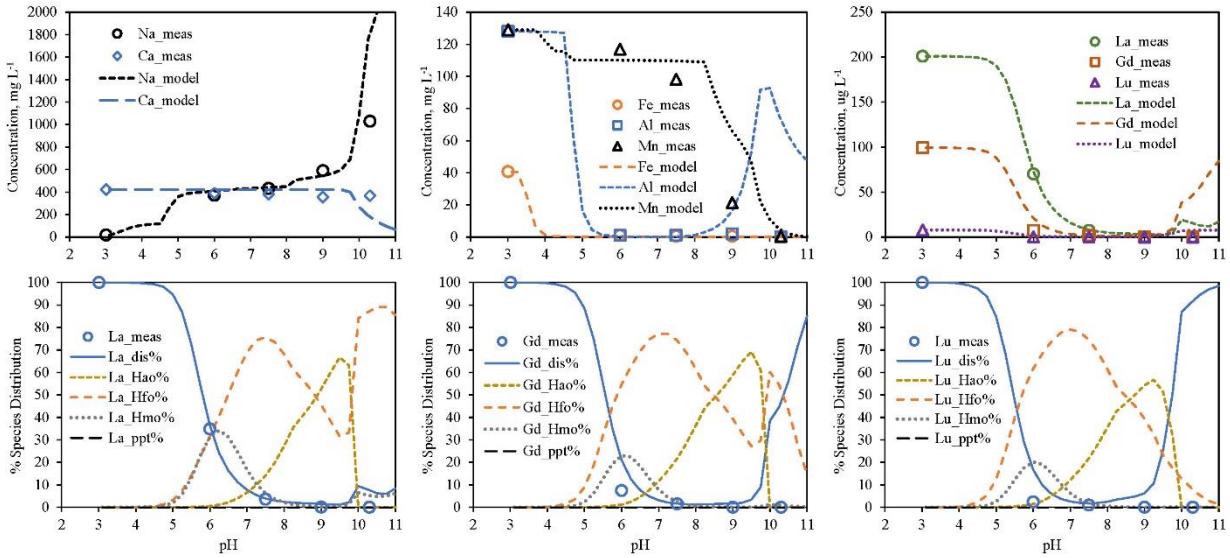

B. Default sorbent Asp values: HFO 600 m^2 g^{-1}; HAO 68 m^2 g^{-1}; HMO 746 m^2 g^{-1}; SI_{REY}=0

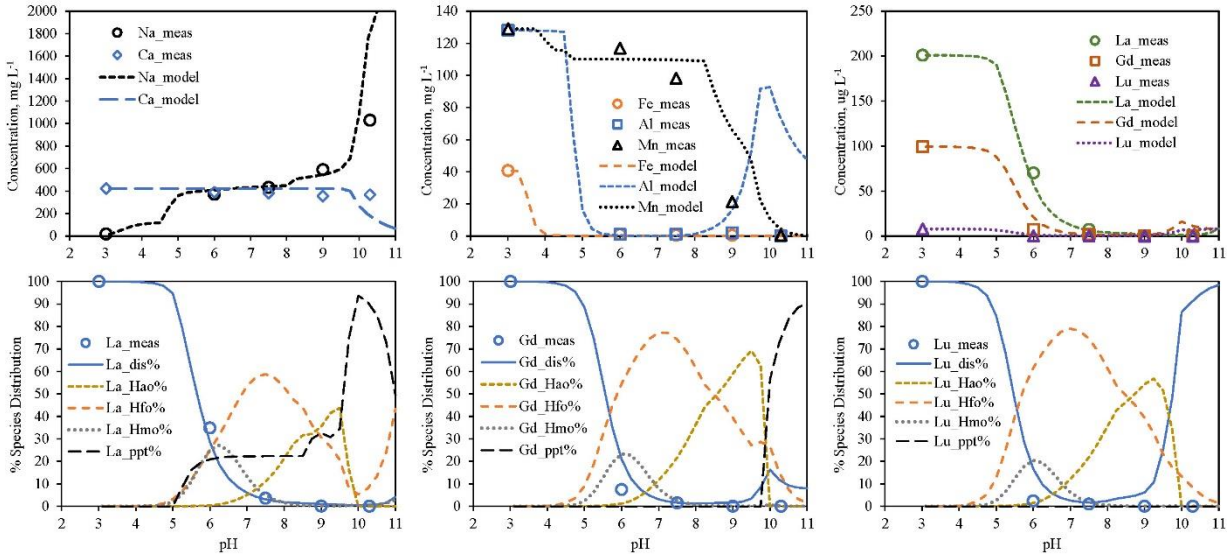

C. Adjusted sorbent Asp values: HFO 700 m^2 g^{-1}; HAO 774 m^2 g^{-1}; HMO 850 m^2 g^{-1}; SI_{REY}=0

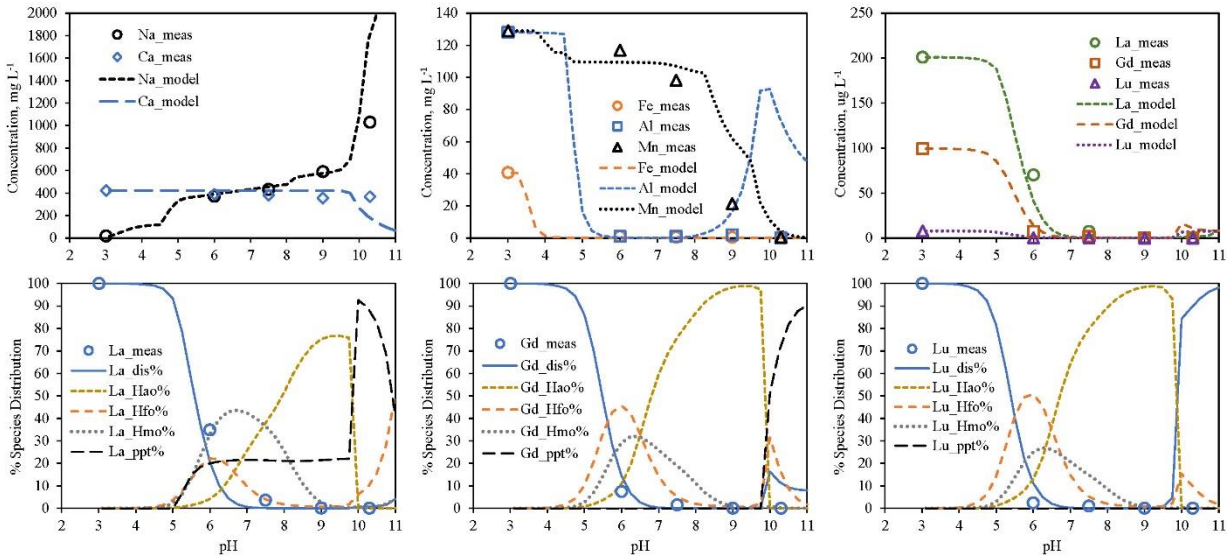

Fig. 2. Results of CausticTitrationMix2REYs model for field titration of Nittanny AMD showing simulation results (curves) compared to measured values (point symbols); measurement errors are roughly the size of symbols. (A) Simulation results for the "fresh" hydrous ferric oxide (HFO), hydrous aluminum oxide (HAO), and hydrous manganese oxide (HMO) sorbent having default values for specific surface area (Asp) and without precipitation of REYs solids; (B) results for same conditions as A *plus* precipitation of REYs; (C) results after increasing Asp to reflect presumed small particle size of the freshly formed sorbent, plus allowing precipitation of REYs.

Alternative fits to observations were obtained by increasing values of Asp for fresh sorbent (Fig. 2C), which may initially precipitate as small particles that have greater Asp than aged, crystalline materials considered for default values. For this scenario, REYs attenuation by all three sorbents is indicated, with HFO predominant at pH ~ 6, HMO at pH ~6.5, and HAO at pH > 7. The modeled Asp of 774 m^2 g^{-1} for HAO, for amorphous $Al(OH)_3$ (Rakotonarivo et al., 1988), is consistent with the Asp used for HFO and HMO. Comparing results shown in the middle and lower sets of graphs (Figs. 2B and 2C) demonstrates that increased Asp causes greater adsorption of La and diminished potential for precipitation of La solids, corresponding to decreased activity of aqueous La^{+3} and decreased saturation index values.

3.2 AMD Treatment Case Studies

To simulate REYs attenuation in a flushable limestone bed, Hedin et al. (2022) applied the CausticTitrationMix2REYs tool with $CaCO_3$ as the titrant and using adjusted Asp values for fresh sorbent. This application of the equilibrium model proved informative, indicating that adsorption on fresh precipitate, alone, could account for observed attenuation of REYs within a limestone bed. However, for complex systems with multiple treatment steps, the TreatTrainMix2REYs model may be appropriate. The TreatTrainMix2REYs sequential model considers the identical equilibrium controls on REYs attenuation in response to variations in pH, solute concentrations, and sorbent properties as the CausticTitrationMix2REYs tool; however, the sequential model simulates disequilibrium conditions with respect to atmospheric exchange, oxidation state of Fe and Mn, dissolution of limestone (instead of $CaCO_3$ titrant), plus other kinetically limited processes that affect pH, redox state, adsorption, and precipitation.

3.2.1 Pine Forest ALD and Aerobic Wetlands

The TreatTrainMix2REYs tool is used to simulate decreasing aqueous concentrations of REYs within a "biofouled" anoxic limestone drain (ALD) at the Pine Forest passive AMD treatment system, previously described by Cravotta (2021). This treatment system consists of an underground, flushable ALD, oxidation/settling pond, and three aerobic wetlands, in series, with aeration steps in between (Figs. 3 and 4). The untreated AMD (43.5 L s^{-1}), sampled during winter 2015, had pH 5.8 with dissolved oxygen (DO) < 0.5 mg L^{-1} and dissolved concentrations of Fe^{II}, Mn^{II}, and Al of 14.0, 3.1, and 0.09 mg L^{-1}, respectively, and total REYs of 5 mg L^{-1}. The treated effluent had pH ~7, Fe and Mn < 2 mg L^{-1}, and total REYs ~0.6 mg L^{-1}. After its first year of operation (2006), the ALD began to clog with gelatinous, Fe-rich precipitate, which was characterized as biogenic in origin (E. Hince, Geovation Engineering, written commun., 2009). Models simulate Fe and Mn oxidation and the attenuation of REYs with the HMeO precipitate.

For the reported simulations, retention time, CO_2 outgassing rate, available limestone, and pre-existing HMeO mass and composition were varied at each step (Figs. 3 and 4). The fractions of Fe, Al, and Mn in the pre-existing HMeO sorbent were estimated from measured sediment composition at the inflow and points downstream of the ALD (Ashby, 2017). HMeO mass of 75 mg L^{-1} specified for the ALD is consistent with a 0.22-□m thick coating on limestone particles (72 cm^2 mol^{-1}) in contact with 1 L water volume, assuming 35 percent bed porosity and sorbent density of 1.92 g cm^{-3}. For subsequent steps, the specified sorbent mass was only 1 to 3 mg, representing suspended particles and/or coatings on rock or plant surfaces. Consistent values for retention time, $k_{La,CO2}$, and sorbent properties were used for different model scenarios whereby the only values varied were the rate factor for iron-oxidizing bacteria (FeOB) and/or potential for REYs solids to precipitate. For the simulated "biofouling" scenario, the FeOB rate factor (factr.kbact) was increased from 1 to 2; for the abiotic scenario, that factor is 0.

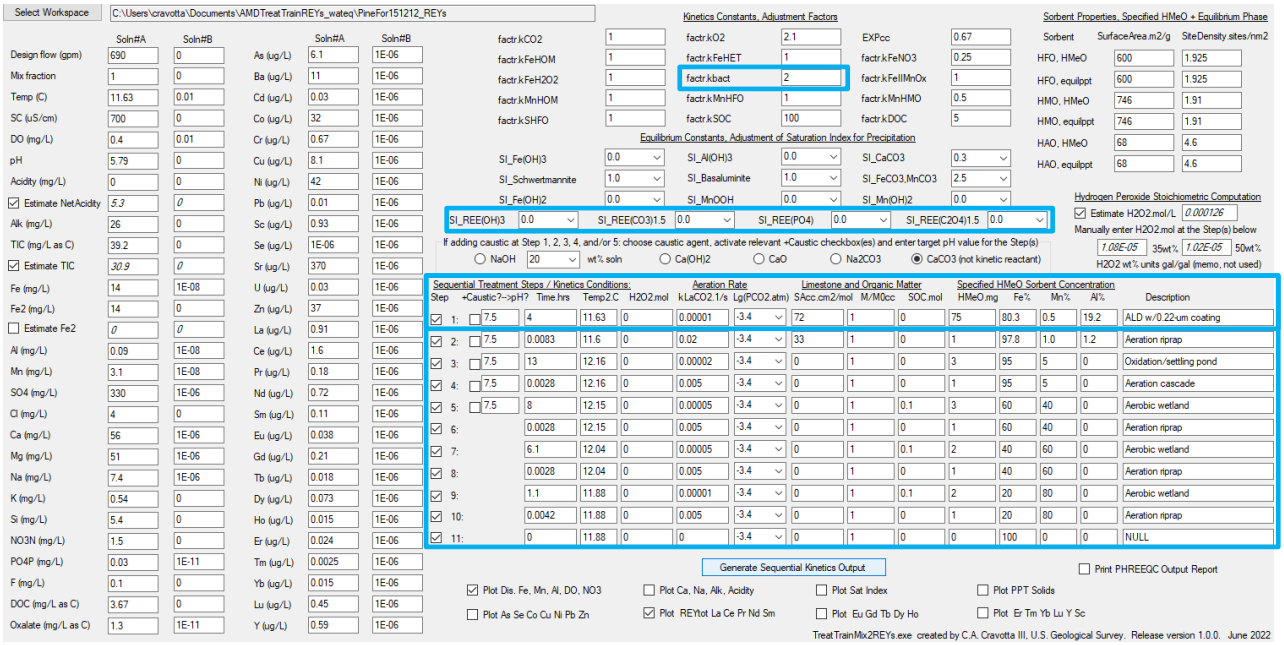

Fig. 3. UI for TreatTrainMix2REYs sequential model showing input values for simulation of water-quality changes through the Pine Forest passive treatment system, December 2015, which consists of a "biofouled" anoxic limestone drain (ALD), oxidation/settling pond, and three aerobic wetlands, with aeration steps in between. The values shown represent enhanced FeOB activity (factr.kbact = 2,

instead of default value of 1) and a specified sorbent mass of 85 mg in the ALD with smaller sorbent mass containing progressively greater Mn content downstream. Results of simulations for this scenario and other conditions where values for factr.kbact = 1 or 0 and for REY saturation index = 99 (no precipitation) are shown in Figure 4.

The TreatTrainMix2REYs model results for pH, DO, Fe, Mn, Al, and total REYs at Pine Forest shown as a function of retention time generally reproduce the longitudinal trends for measured constituent values (Fig. 4). The Fe concentration decreased by 30 percent within the ALD, simulated to result from microbial oxidation combined with Fe^{II} sorption and heterogeneous oxidation, leading to the precipitation and accumulation of HFO on limestone surfaces. Simulated attenuation of REYs took place within the ALD because of adsorption by the accumulated HMeO (HFO with lesser quantities of HAO and HMO). Despite less mass of HMeO specified for wetlands downstream of the ALD, greater Mn content of sorbent and increased pH in wetlands (as observed) promoted further attenuation of dissolved Mn^{II} and remaining REYs. Compared to adsorption, REYs precipitation had only a small effect as indicated by the difference between red-dashed (REY precipitation) and blue-dashed curves (no REY precipitation), both simulating the biofouling scenario where the FeOB rate factor was doubled. Simulation results for the two reference scenarios with default (1X) and nullified (0X) FeOB rate factors (Fig. 4, orange solid or black dotted curves) demonstrate that abiotic, Fe^{II} oxidation does not explain observed Fe removal within the ALD but may explain subsequent trends with increased DO and pH. As explained by Cravotta (2021), neutrophilic FeOB are most active under low DO conditions, whereas acidophilic FeOB require low pH.

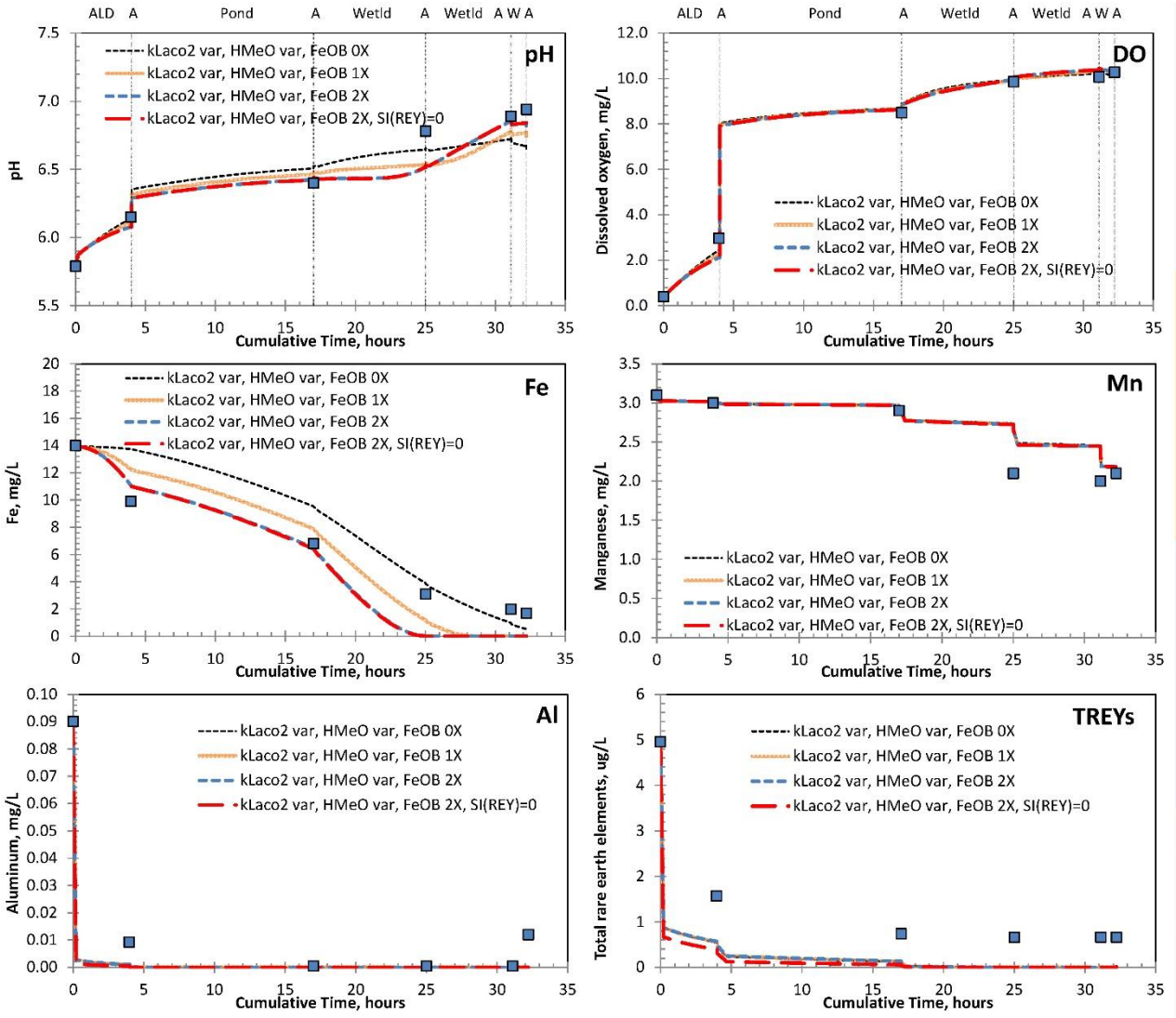

Fig. 4. Comparison of measured (symbols) and simulated (curves) values for pH, Fe, Mn, Al, DO, and total REYs during treatment of AMD at the Pine Forest passive treatment system. Treatment steps are identified at specified times across upper diagrams. Simulations used the TreatTrainMix2REYs sequential model with initial water chemistry for December 2015, specified values for $k_{L,CO2}a$, FeOB rate factor, and sorbent mass and composition (Fig. 3). All models specified sorbent mass in the ALD equivalent to 0.22-□m thick coating on limestone surfaces with smaller sorbent mass having greater Mn content in downstream wetlands. The black dotted curves show results for abiotic conditions (FeOB 0X). The blue or red dashed curves show results for enhanced FeOB activity (FeOB 2X); red curves also simulate REYs minerals precipitation upon reaching saturation (SI(REY)=0).

3.2.2 Silver Creek Aerobic Wetlands

The TreatTrainMix2REYs tool is also used to simulate decreasing aqueous concentrations of REYs within the Silver Creek passive treatment system, described by Cravotta (2021), which consists of a sedimentation pond, two large oxidation/settling ponds, and two aerobic wetlands, in series, with wide, shallow aeration

cascades in between (Figs. 5 and 6). When sampled in 2015 and 2016, the AMD was anoxic with pH 5.9-6.0, concentrations of Fe^{II}, Mn^{II}, and Al of 17.0-20.0, 2.2-2.9, and 0.12-0.17 mg L^{-1}, respectively, and total REYs of 16.5-22.8 mg L^{-1} (Ashby, 2017). Rapid outgassing of CO_2 during aeration steps caused large increases in pH, which facilitated Fe^{II} oxidation in subsequent steps.

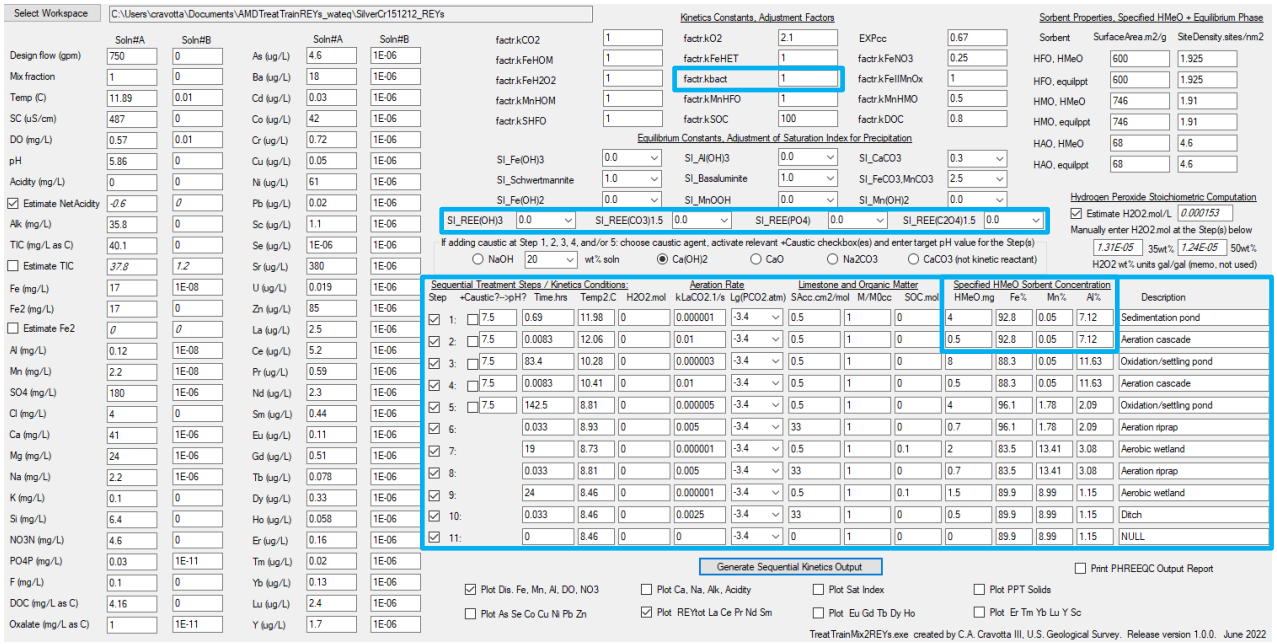

Fig. 5. UI for the TreatTrainMix2REYs sequential model showing input values for simulation of water-quality changes through the Silver Creek treatment system, December 2015, which consists of a small sedimentation pond, two large oxidation/settling ponds, and two aerobic wetlands, with aeration cascades in between. Results of simulations are shown in Fig. 6.

For initial simulations, HMeO composition was based on values reported by Ashby (2017) for sampled sediments at Silver Creek (Fig. 5). The HMeO mass at each step was assumed to be less than or equal to the difference between immediately upstream and downstream samples for the combined mass of Fe, Al, and Mn. Only the CO_2 outgassing rate and sorbent mass and composition (HMeO.mg, Fe%, Mn%, Al%) at each step were adjusted to achieve a reasonable match between empirical and simulated values for longitudinal changes in pH, Fe, Mn, Al, and associated major solute concentrations. Eventual removal of Mn^{II} in the wetland treatment steps were simulated by HMeO sorbent having greater HMO content, as observed for the sampled sediment.

Abiotic oxidation of Fe combined with adsorption and precipitation of solids explains observed attenuation of Fe, Al, Mn, and associated REYs at the Silver Creek treatment system. Microbial Fe oxidation had little effect because of high DO and pH (Fig. 6). Although results for initial simulations effectively reproduced the longitudinal trends for measured pH, DO, Fe, Mn, and Al (Fig. 6, black dashed or orange curves), without REYs mineral precipitation, the corresponding modeled concentrations of total dissolved REYs (and individual REYs, not shown) remaining in solution were at least five times greater than observed values for all but the last steps of the treatment (Fig. 6, black dashed curves). Simulated precipitation of REYs (SI_REEPO4=0) resulted in a substantial decrease in the concentration of total REYs (Fig. 6, blue or red curves), consistent with observations. Nevertheless, many individual REYs remained undersaturated (e.g.

Y, Eu, Gd, Tb, Dy, Ho, Yb, and Lu). As explained by Liu and Byrne (1997), formation of $REEPO_4$ in the environment generally involves co-precipitation of REYs, whereby saturated and undersaturated phases form impure $REEPO_4$ solid solutions.

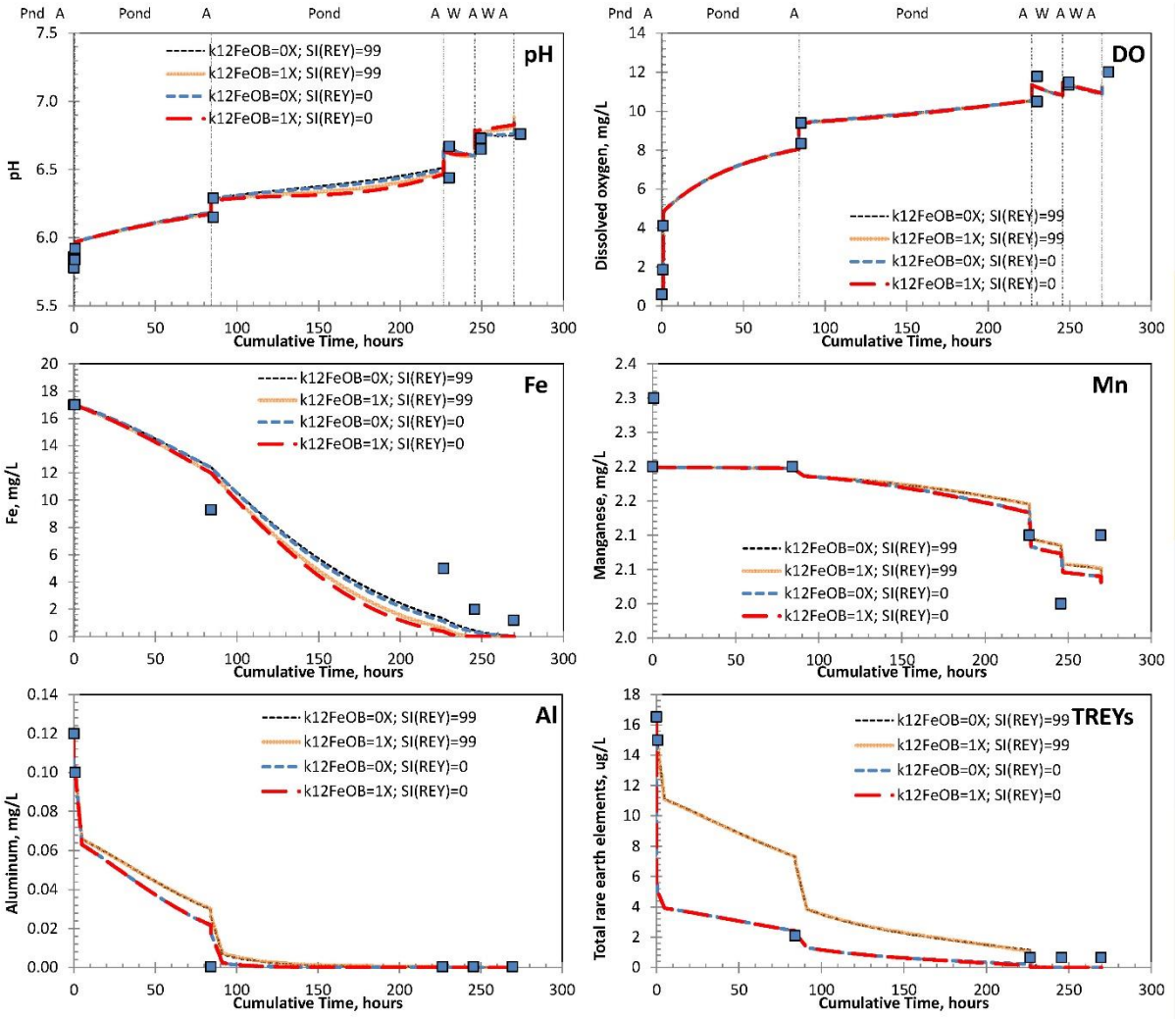

Fig. 6. Comparison of measured (symbols) and simulated (curves) values for pH, DO, Fe, Mn, Al, and total REYs during treatment of AMD at the Silver Creek passive treatment system, December 2015. Treatment steps are identified at specified times across upper diagrams. Simulations used the TreatTrainMix2REYs sequential model with initial water chemistry for December 2015, specified values for $k_{L,CO2}a$, FeOB rate factor, and sorbent mass and composition (Fig. 5). The red dashed curves show results for values in Fig. 5, with specified sorbent having Fe-Mn-Al composition of sediment samples.

3.3 Modeling for Optimization Strategies for REYs Recovery

A goal of modeling with the PHREEQ-N-AMDTreat+REYs tools is to identify strategies that could feasibly produce a concentrated REYs extract from AMD or mine waste leachate that could be valuable. Untreated leachate from a coal-refuse disposal facility in Pennsylvania is considered as a proposed test case for REYs

recovery (Figs. 7 and 8). The untreated effluent (9.7 L s^{-1}), sampled during summer 2011, had pH 3.7 with elevated dissolved concentrations of Fe, Mn, and Al of 3,980, 29.75, and 118 mg L^{-1}, respectively, and total REYs of 1,187 mg L^{-1} (Cravotta and Brady, 2015). Current treatment utilizes neutralization with lime, which causes precipitation of Fe, Al, and associated REYs into a complex sludge mixture. If REYs could be concentrated after first removing substantial Fe and Al, the final REYs-bearing phase(s) may be efficiently processed for REYs recovery.

Three treatments to concentrate REYs from the leachate were simulated with the TreatTrainMix2REYs tool. The active lime treatment to pH 8.5 results in nearly complete removal of REYs with Fe-Al-Ca rich sludge (Fig. 8). REYs are diluted by the major metals and other impurities in the sludge. By comparison, alternative treatment strategies using H_2O_2 to oxidize Fe^{II}, followed by metered addition of Na-caustic agents (NaOH or Na_2CO_3) to achieve a target pH < 5.5 sequentially remove Fe and Al. Subsequent aeration over an extended time results in the oxidation of Mn which adsorbs and concentrates REYs in the final steps. Alternatively, chemicals such as oxalate or phosphate may be added to the effluent at pH 5.5 to precipitate REYs compounds, following initial steps to remove Fe and Al.

A. Conventional treatment with lime to pH 8.5 and sludge disposal

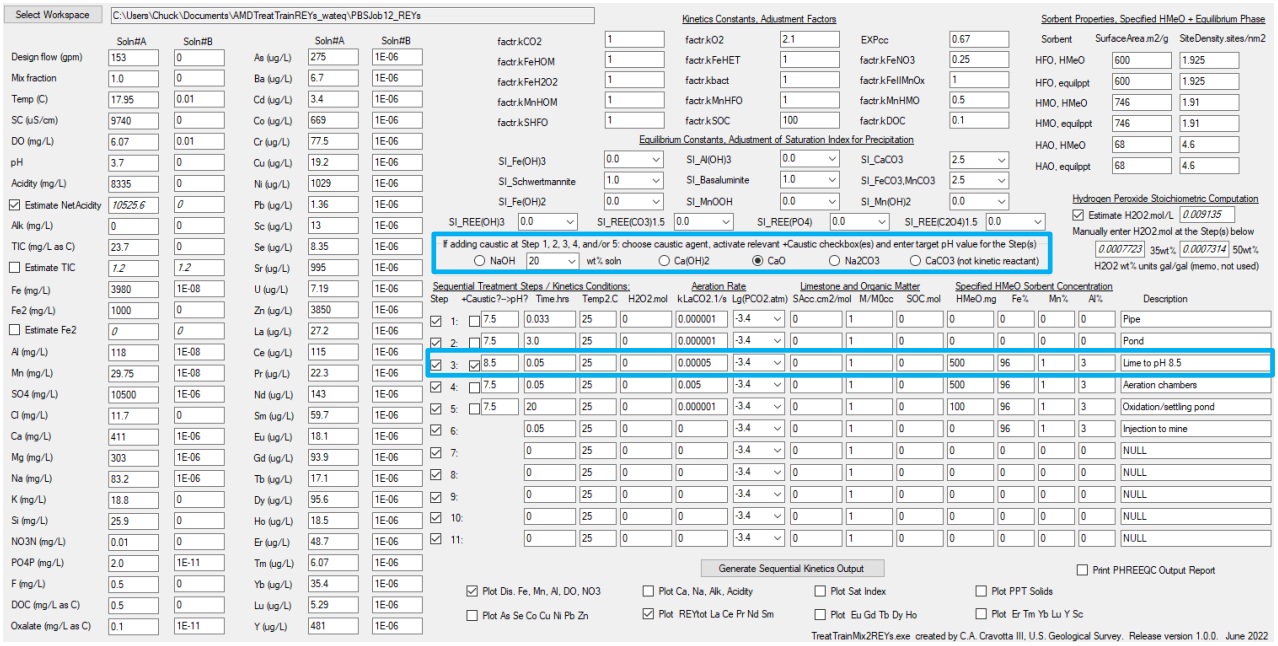

B. Alternative treatment with H_2O_2, then NaOH to pH 5.2, aeration steps, and Mn sorption bed

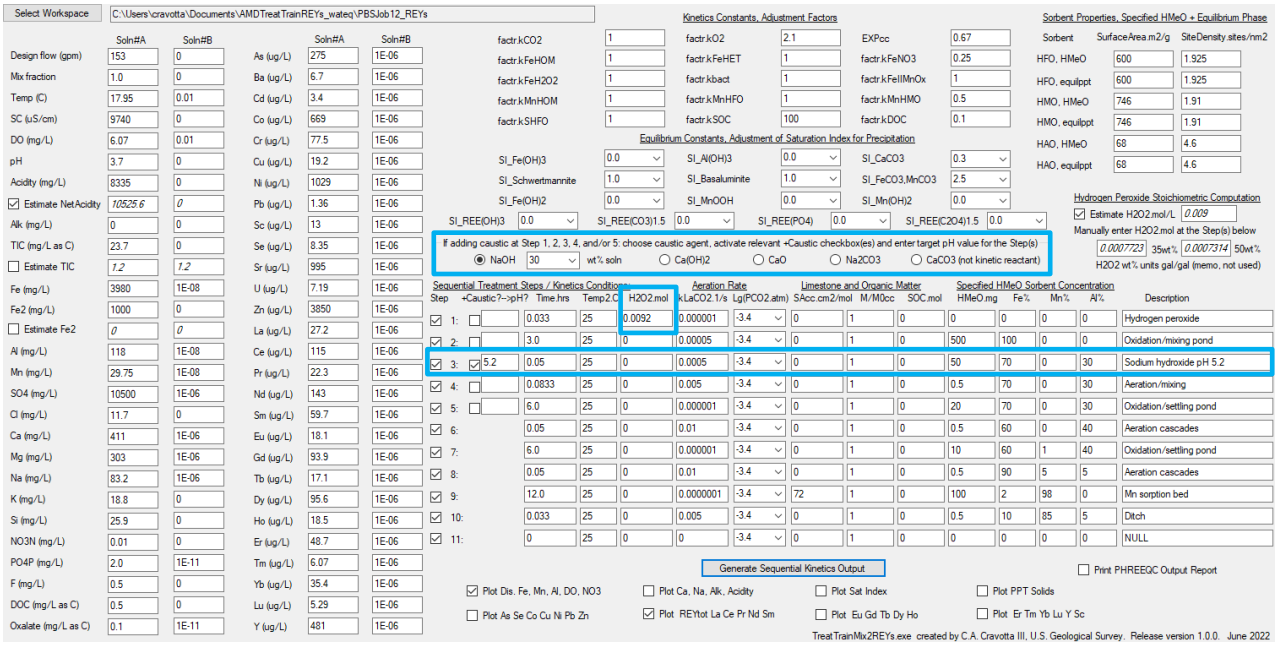

Fig. 7. UI showing the TreatTrainMix2REYs input values for simulation of REYs attenuation from leachate at a coal-refuse disposal facility by conventional and alternative treatment methods.

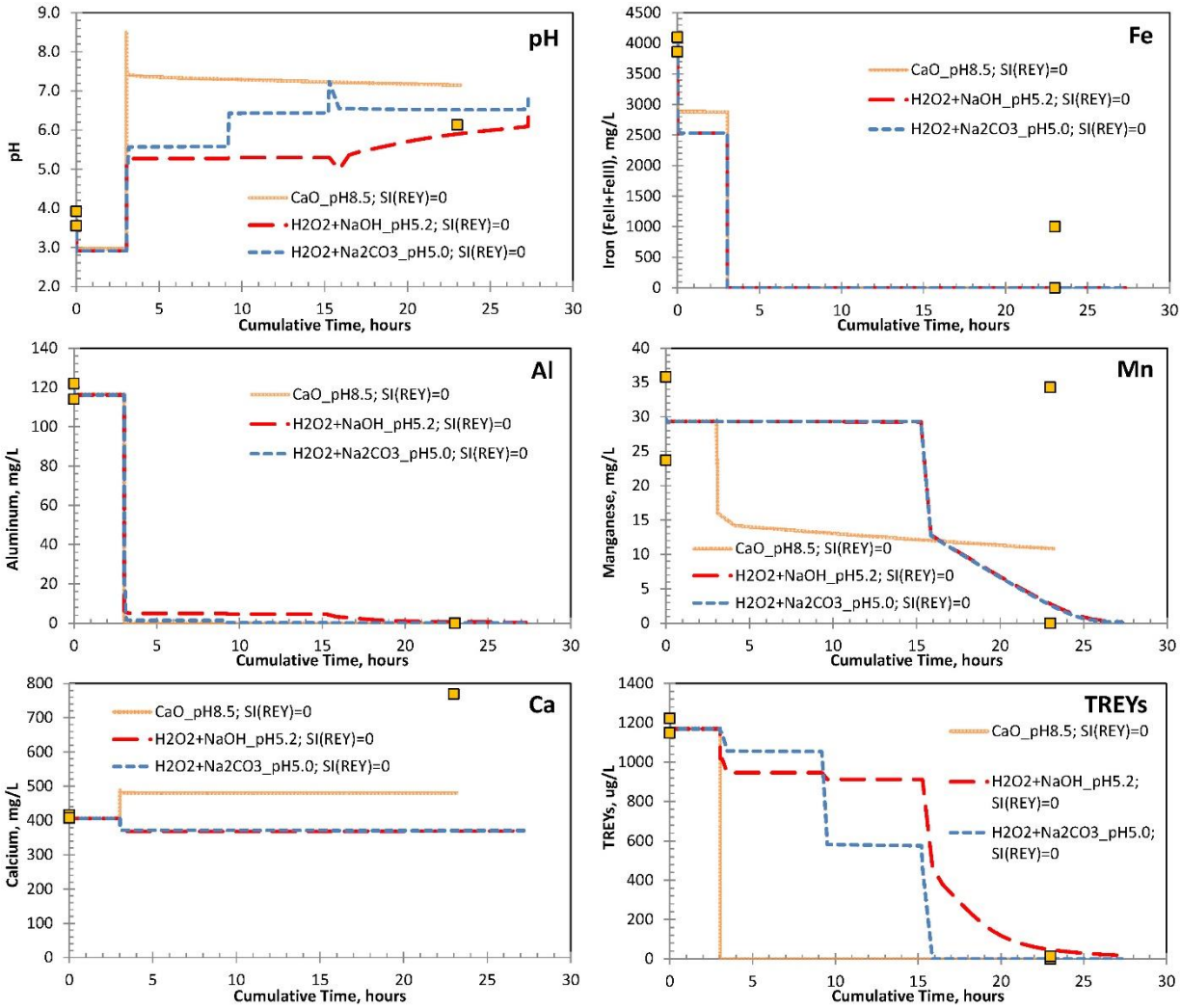

Fig. 8. Comparison of measured (symbols) and TreatTrainMix2REYs simulation results (curves) for pH and dissolved Fe, Al, Mn, Ca, and total REYs concentrations at a coal-refuse disposal facility. Input values for starting water quality and other model variables are shown in Fig. 7. Measured values shown are for lime treatment, sampled on two different dates.

4.0 CONCLUSIONS

The PHREEQ-N-AMDTreat+REYs modeling tools effectively simulate dynamic interactions between Fe, Al, Mn, REYs, and other constituents in complex aqueous systems. Optimization modeling with the TreatTrainMix2REYs tool supports the hypothesis that Fe and Al can be removed from acidic leachate by initial treatment to pH < 5.5 using sequential oxidation and neutralization treatment processes, followed by adsorption and/or precipitation of REYs at higher pH in later steps. The modeling capability of PHREEQC, including aqueous and surface speciation coupled with kinetics of oxidation-reduction and dissolution reactions, provides a quantitative framework for synthesis and application of laboratory equilibrium and rate data to field settings. The UI facilitates adjustment of system variables and the application of the models to evaluate possible design of AMD treatment systems for REYs recovery. Uncertainty in water-quality data, rate data, sorbent quantities and properties, and other system variables can be evaluated by changing values in the UI to identify critical parameters and document potential variations in results. Field studies that

demonstrate REYs attenuation from AMD and corresponding solid-phase formation during specific treatment steps plus laboratory studies of aqueous/solid interactions are helpful to corroborate, refine, and constrain models.

5.0 ACKNOWLEDGMENTS

The Office of Surface Mining Reclamation and Enforcement (OSMRE) and the U.S. Geological Survey (USGS) provided funding and technical support for this work as part of the AMDTreat recoding project. The author is especially grateful to Brent Means of OSMRE, who provided useful data and insights on mine drainage treatment practices and to Benjamin Hedin of Hedin Environmental and Benjamin Roman of Saint Francis University, who provided reviews of the manuscript and software presented herein. Two anonymous reviewers also provided helpful comments on the manuscript. Any use of trade, firm, or product names is for descriptive purposes only and does not imply endorsement by the U.S. Government.

6.0 REFERENCES

Ashby, E.J., 2017. Biogeochemical mechanisms of rare earth element enrichment in mining-affected aqueous environments. University of Ottawa, Canada, M.S. thesis, 133 p.

Ayora, C., Macías, F., Torres, E., Lozano, A., Carrero, S., Nieto, J.M., Pérez-López, R., Fernández-Martínez, A., and Castillo-Michel, H., 2016, Recovery of rare earth elements and yttrium from passive-remediation systems of acid mine drainage. Environ. Sci. Tech.50, 8255-62.

Ball, J.W., and Nordstrom, D.K., 1991. User's manual for WATEQ4F, with revised thermodynamic data base and test cases for calculating speciation of major, trace, and redox elements in natural waters. U.S. Geol. Surv. Open-File Report 91-183.

Cravotta, C.A. III, 2008. Dissolved metals and associated constituents in abandoned coal-mine discharges, Pennsylvania, USA -- 1. Constituent concentrations and correlations. Appl. Geochem. 23, 166-202.

Cravotta, C.A. III, 2020. Interactive PHREEQ-N-AMDTreat water-quality modeling tools to evaluate performance and design of treatment systems for acid mine drainage (software download). U.S. Geol. Surv. Software Release https://doi.org/10.5066/P9QEE3D5

Cravotta, C.A. III, 2021. Interactive PHREEQ-N-AMDTreat water-quality modeling tools to evaluate performance and design of treatment systems for acid mine drainage. Appl. Geoch., 126, 104845. https://doi.org/10.1016/j.apgeochem.2020.104845.

Cravotta, C.A. III, 2022. Interactive PHREEQ-N-AMDTreat+REYs water-quality modeling tools to evaluate potential attenuation of rare-earth elements and associated dissolved constituents by aqueous-solid equilibrium processes (software download). U.S. Geol. Surv. Software Release https://doi.org/10.5066/P9M5QVK0

Cravotta, C.A. III, and Brady, K.B.C., 2015. Priority pollutants and associated constituents in untreated and treated discharges from coal mines in Pennsylvania, U.S.A.: Appl. Geoch. 62, 108-130.

Cravotta, C.A. III, Means, B., Arthur, W., McKenzie, R., and Parkhurst, D.L., 2015. AMDTreat 5.0+ with PHREEQC titration module to compute caustic chemical quantity, effluent quality, and sludge volume. Mine Wat. Environ. 34, 136-152.

Dzombak, D.A., and Morel, F.M.M., 1990. Surface complexation modeling: Hydrous ferric oxide. John Wiley and Sons, New York, NY, USA.

Edahbi, E., Plante, B., Benzaazoua, M., Ward, M., and Pelletier, M., 2018. Mobility of rare earth elements in mine drainage Influence of iron oxides, carbonates, and phosphates. Chemosphere 199, 647-654.

Fritz, A.G., Tarka, T.J., and Mauter, M.S., 2021. Technoeconomic assessment of a sequential step-leaching process for rare earth element extraction from acid mine drainage precipitates. ACS Sustainable Chemistry and Engineering 9, 9308-9316.

Hedin, B.C., Hedin, R.S., Capo, R.C, and Stewart, B.W., 2020. Critical metal recovery potential of Appalachian acid mine drainage treatment solids. Int. J. Coal Geol. 231, 103610.

Hedin, B.C., Cravotta, C.A. III, Stuckman, M.Y., Lopano, C.L., Capo, R.C, and Hedin, R.S., 2022. Determination and prediction of rare earth element geochemical associations in acid mine drainage treatment wastes. 12th International Conference on Acid Rock Drainage.

Hermassi, M., Granados, M., Valderrama, C., Ayora, C., and Cortina, J.L., 2022. Recovery of rare earth elements from acidic mine waters: An unknown secondary resource. Sci. Tot. Environ. 810, 152258.

Josso, P., Roberts, S., Teagle, D.A.H., Pourret, O., Herrington, R., and Ponce de Leon Albarran, C., 2018. Extraction and separation of rare earth elements from hydrothermal metalliferous sediments. Min. Eng. 118, 106-121.

Karamalidis, A.K., and Dzombak, D.A., 2010. Surface complexation modeling: Gibbsite. John Wiley & Sons, Inc., Hoboken, NJ, USA.

Leon, R., Macias, F., Canovas, C.R., Perez-Lopez, R., Ayora, C., Nieto, J.M., and Olias, M., 2021. Mine waters as a secondary source of rare earth elements worldwide: The case of the Iberian Pyrite Belt. J. Geoch. Explor. 224, 106742.

Liu, X., and Byrne, R.H., 1997. Rare earth and yttrium phosphate solubilities in aqueous solution. Geochim. Cosmochim. Acta 61, 1625-1633.

Liu, H., Pourret, O., Guo, H., and Bonhoure, J., 2017. Rare earth elements sorption to iron oxyhydroxide: Model development and application to groundwater. Appl. Geoch. 87, 158-166.

Lozano, A., Ayora, C., and Fernández-Martínez, A., 2019. Sorption of rare earth elements onto basaluminite: The role of sulfate and pH. Geochim. Cosmochim. Acta 258, 50-62.

Mwewa, B., Tadie, M., Ndlovu, S., Simate, G.S., and Mitinde, E., 2022. Recovery of rare earth elements from acid mine drainage: A review of the extraction methods. J. Environ. Chem. Eng. 10, 107704.

Office of Surface Mining Reclamation and Enforcement, 2017. AMDTreat. https://amd.osmre.gov/

Parkhurst, D.L., and Appelo, C.A.J., 2013. Description of input and examples for PHREEQC version 3—A computer program for speciation, batch-reaction, one-dimensional transport, and inverse geochemical calculations. U.S. Geol. Surv. Techniques Methods 6-A43.

Pourret, O., and Davranche, M., 2013. Rare earth element sorption onto hydrous manganese oxide: a modeling study. J. Colloid Interface Sci. 395, 18-23).

Rakotonarivo, E., Bottero, J.Y., Thomas, F., Poirier, J.E., and Cases, J.M., 1988. Electrochemical modeling of freshly precipitated aluminum hydroxide-electrolyte interface. Colloids and Surfaces 33, 199-207.

Royer-Lavallée, A., Neculita, C.M., and Coudert, L., 2020. Removal and potential recovery of rare earth elements from mine water. J. Indust. Chem. Eng. 89, 47-57.

Tonkin, J.W., Balistrieri, L.S., and Murray, J.W., 2004. Modeling sorption of divalent metal cations on hydrous manganese oxide using the diffuse double layer model. Appl. Geoch., 19, 29-53.

Vass, C.R., Noble, A., and Ziekiewicz, P., 2019. The occurrence and concentration of rare earth elements in acid mine drainage and treatment byproducts. Part 2: regional survey of northern and central Appalachian coal basins. Mining Metal. Explor. 36, 917-929.

Verplanck, P.L., Nordstrom, D.K., Taylor, H.E., and Kimball, B.A., 2004. Rare earth element partitioning between hydrous ferric oxides and acid mine water during iron oxidation. Appl. Geoch. 19, 1339-1354.

Wang, Y., Ziemkiewicz, P., and Noble, A., 2021. A hybrid experimental and theoretical approach to optimize recovery of rare earth elements from acid mine drainage precipitates by oxalic acid precipitation. Minerals 12, 236.

Zhang, W., and Honaker, R.Q., 2018. Rare earth elements recovery using staged precipitation from a leachate generated from coarse coal refuse. Int. J. Coal Geol. 195, 189-199.

Recovery of Rare Earth Elements from Coal Mine Drainage

Paul Ziemkiewicz and Jeff Skousen
West Virginia University

Rare earth elements (REEs) are critical in today's technology-driven world. These elements are used in electronics such as smart phones, magnets, computers, televisions, and most notably in national defense technologies. The REEs are located at the bottom of the periodic table (Figure 1) and include 17 different elements (Table 1). The elements listed as REEs are not really "rare," but they rarely occur in concentrations that make them economically attractive to mine and process.

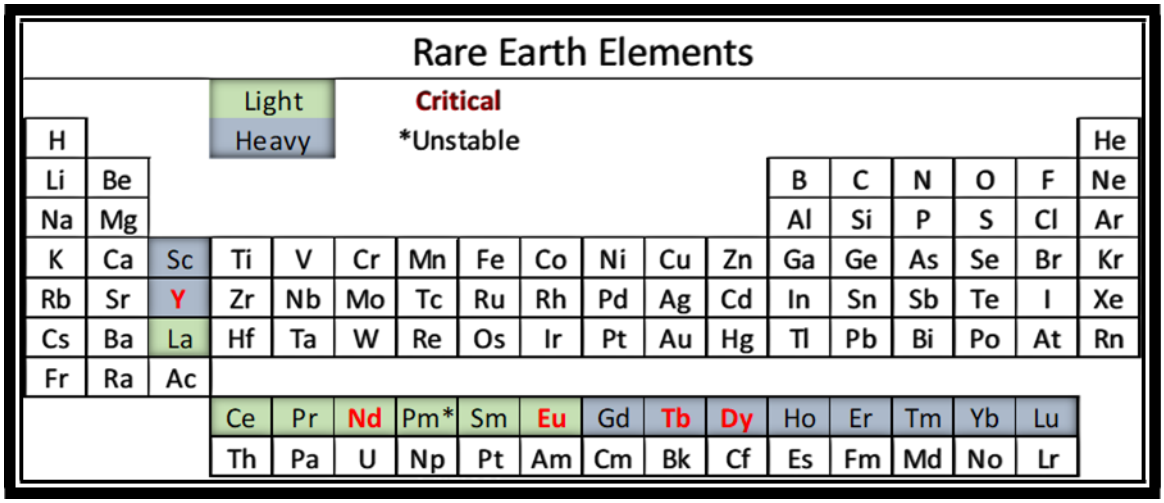

Figure 1. The rare earth elements typically include the 15 lanthanides plus Yttrium and Scandium. They are further classified as light, heavy, and critical (See Tables 1 and 2). Promethium* does not occur naturally.

Table 1. List of 17 Rare Earth Elements (REE) with their atomic number and symbol. Table from Thermofisher.com. *Promethium is unstable and does not occur naturally. ** Scandium and Yttrium are classified as rare earths although not lanthanides.

Atomic Number	Element	Symbol
21	Scandium**	Sc
39	Yttrium	Y
57	Lanthanum	La
58	Cerium	Ce
59	Praseodymium	Pr
60	Neodymium	Nd
61	Promethium*	Pm
62	Samarium	Sm
63	Europium	Eu
64	Gadolinium	Gd
65	Terbium	Tb
66	Dysprosium	Dy
67	Holmium	Ho
68	Erbium	Er
69	Thulium	Tm
70	Ytterbium	Yb
71	Lutetium	Lu

These elements occur in a wide variety of geologic formations but are rarely found in concentrations to facilitate extraction and refinement. Where they are found in significant concentrations, the ore body is often contaminated with radioactive thorium and uranium, which causes problems with handling and disposal of ores and processing wastes. As such, the U.S. currently imports 90% of its REEs from China. With increasing demand for REEs for technology and defense uses, U.S. mining companies have invested time and capital to discover and secure REE resources outside of China. Unfortunately, many of these companies entered bankruptcy or lost interest due to unpredictability in demand and shifting prices.

Only two REE mines started production outside of China in response to this demand. The Mount Weld deposit in Australia began production in 2013. The ore from Mount Weld is processed in Malaysia, whose operating permit has come under scrutiny because of unsafe practices for disposing of radioactive waste, and hence their production of REEs has ceased. The second mining operation, Mountain Pass located in the U.S., has experienced instability in reaching full scale production due to lower REE prices and uneven distribution of light- vs heavy-REEs in the ore body.

There continues to be a strong need to find domestic, predictable supplies of these critical elements, regardless of their pricing. Many industrial processes rely on REEs for their products including catalysts, metallurgy, petroleum refining, catalytic converters, ceramics, phosphors, and electronics. The availability of heavy REEs are of particular concern because identifying geologic sources of these elements in the U.S. have been unsuccessful. Of the 15,000 tons of REEs used by the U.S. every year, approximately 800 tons (5%) are required for the defense industry. To develop secure, predictable, domestic supplies, the U.S. Department of Energy's National Energy Technology Laboratory (USDOE NETL) initiated a national competition in 2015 to develop economical and environmentally safe methods for extracting REEs from domestic material sources.

The presence of REEs in coal was known as early as 1964. In 2014, the USDOE analyzed the economic feasibility of recovering REEs from coal, coal refuse and coal fly ash as material sources. In 2015, with a small startup grant from USDOE, researchers at West Virginia University sampled AMD precipitates from nine sites and found significant concentrations of REEs in these precipitates formed during acid mine drainage (AMD) treatment (Ziemkiewicz et al., 2016).

A detailed study of REE occurrence in the northern and central Appalachian Coal Basin was developed by Dr. Paul Ziemkiewicz, director of West Virginia University's Water Research Institute (WRI). He and his team at WVU collected AMD from both surface and underground mines and collected precipitates formed during AMD treatment with alkaline chemicals at these sites (Figure 2). The aqueous samples were acidified in 2% nitric acid and analyzed using ICP-MS by certified laboratories. The precipitate samples were digested using sodium peroxide and re-dissolved in hydrochloric acid and analyzed by ICP-MS.

Figure 2. Typical AMD treatment pond were precipitates are captured and allowed to settle from treated AMD.

Ziemkiewicz and his team found an average total REE concentration of 258 ug/L (or ppb) with a range of 8 to 1,139 ug/L in aqueous samples of AMD (Table 2). The REE concentration from AMD precipitates averaged 517 mg/kg (or ppm) with a range of 29 to 1,286 mg/kg, a concentration factor of more than 2 ,000 over aqueous AMD samples (Table 2). The AMD precipitates contain almost 10 times more REE concentrations than U.S. coal (66 mg/kg) (Vass et al., 2016). Another important finding was that REE concentrations were much higher in aqueous AMD samples with a solution pH of 5.0 or less (Figure 3).

Table 2. The concentrations of individual REEs in samples of untreated AMD and samples of AMD precipitates formed during AMD treatment. Elements highlighted in green are "light," those highlighted in blue are "heavy," and those with red lettering are termed "critical" elements. *Note: mg/kg (ppm) is 1000 times greater than the unit ug/L (ppb). Therefore, the concentration of REEs in precipitates is more than 1000 times greater than in raw, untreated AMD.

Element	Untreated AMD (ug/L)*	Precipitates (mg/kg)*
Sc	13	16
Y	**70**	**125**
La	11	62
Ce	42	108
Pr	7	15
Nd	**39**	**74**
Sm	14	21
Eu	**4**	**5**
Gd	19	28
Tb	**3**	**5**
Dy	**17**	**26**
Ho	3	5
Er	8	13
Tm	1	2
Yb	6	10
Lu	1	2
Total REEs	258	517

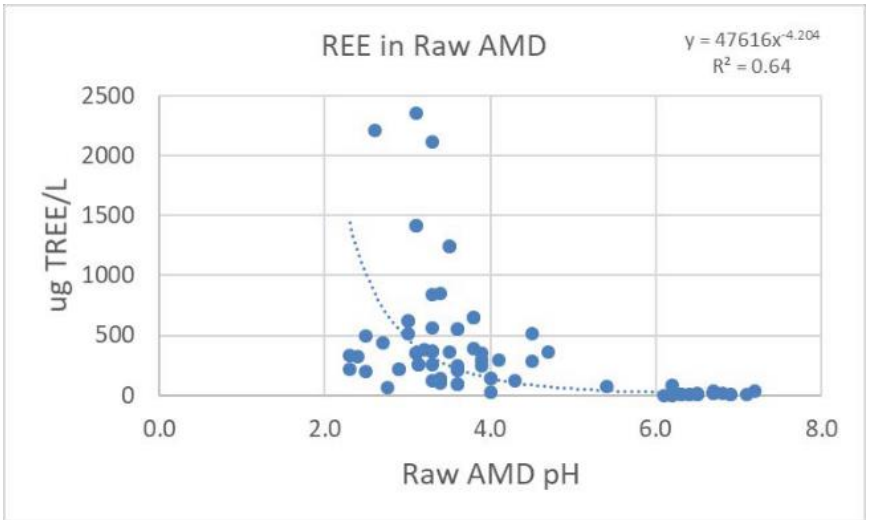

Figure 3. The relationship between the pH of raw AMD and the concentration of Total REEs (TREE) in the aqueous phase. Clearly, higher concentrations of TREEs occur in AMD at less than 5.0 pH.

Given the high REE concentrations extracted from AMD precipitates, estimates of REE production from AMD treatment plants could produce from 800 to 2,200 metric tons (Mg) of REEs per year

(Ziemkiewicz et al., 2016). The high concentrations of REEs in AMD sludge and their processing and sale on the market provide an opportunity to recover some of the costs of treating AMD. This financial recovery would encourage companies to maintain AMD treatment which would improve the quality of streams and rivers in the region. AMD treatment is an environmental and costly obligation for mining companies; therefore, collecting and processing the REEs from these AMD treatment precipitates could create a revenue stream and provide a financial return from a costly treatment and disposal process. This process would promote a new industry for economic development and generate a secure, domestic supply of REEs.

To evaluate the monetary value of REEs in AMD, the average prices of REEs were compiled for the lanthanide series plus Yttrium from 2008 to 2015. Using a detailed pricing structure and analysis (see Vass et al., 2016), a value of $89 per kg of total REEs was identified. (More information on the assumptions used for pricing is available from the authors and in the two cited papers). Using this value, a minimum estimate of the value of REEs in AMD precipitates is $3 million per year.

Now that REEs were identified and quantified in AMD precipitates and a monetary value placed on the precipitates if all the REEs could be extracted, additional work was needed to separate REEs from the other elements in AMD treatment precipitates (Fe, Al, Mn, Ca, Mg). Therefore, a procedure for economically recovering REEs from AMD precipitates was needed to realize this estimate of tonnage and monetary potential, and whether the process of recovery was economically viable at a production scale.

Separation technologies such as ion exchange, solvent extraction, or selective precipitation can be used to recover REEs in an oxide form. Once separated, the REE oxides could be packaged and sold to refiners with advanced capabilities to turn the oxides into metals (Figure 4). These processes utilize smelting or electrolysis to isolate REE metals that can then be sold on the open market.

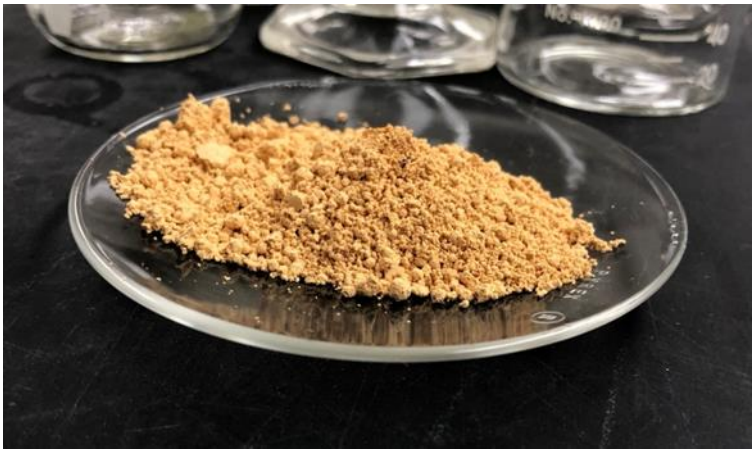

Figure 4. West Virginia University's REE Extraction Facility produces highly concentrated Rare Earth products from AMD precipitates. This sample is 87% rare earth oxide.

In 2018 with NETL funding, a bench scale pilot plant was opened through a joint venture among WVU, Rockwell Automation and Shonk Investments LLC on West Virginia University's campus to test the technical and economic feasibility of scaling-up their extraction and refining technology with plans to rapidly commercialize the process.

In 2019, this project was successful in identifying economically-attractive recovery of REEs from

AMD such that USDOE Secretary Rick Perry announced the award of $5 million to the WVU team to expand their process to a full-scale field facility to be built into a new AMD treatment plant near Mt. Storm, in northern WV. Figure 5 shows a conventional AMD treatment plant operated by the West Virginia Department of Environmental Protection where AMD precipitates will be generated and collected.

Figure 2. The West Virginia Department of Environmental Protection's Muddy Creek AMD treatment plant near Albright, WV, showing the lime silo and system control building in the lower left, two clarifiers and Geotubes across the creek for collection and dewatering of AMD precipitates.

This phase of the project will be achieved by collaborating with the West Virginia Department of Environmental Protection's Office of Special Reclamation to design and build the treatment plant, Rockwell Automation to provide the sensor and control technology, and TenCate Corporation to engineer materials to further concentrate REE-extracted materials. The onsite processing plant will reduce costs of operation significantly and pave the way for a new industry in Appalachia.

These collaborations are vital to the success and implementation of this pilot facility. Support of West Virginia's congressional leaders has been key. Senator Joe Manchin said, "These projects allow continued use of our domestic resources in an environmentally friendly way and will help reduce our vulnerability to foreign sources of rare earth elements." Senator Shelley Moore Capito added, "REEs are essential to modern advanced manufacturing, and WVU's technology will help provide a domestic source of this material while cleaning up legacy mine waste. This is a win-win-win for our economy, our national security, and the environment." Representative David McKinley stated, "WVU's work to develop a domestic REE source is critical and this funding will help to build an American supply chain and ensure

that we are not dependent on other nations for our supply."

With this new funding, the WVU team will scale up and demonstrate how AMD treatment and watershed restoration can operate hand in hand with REE recovery. Success will generate a revenue stream that will offset stream restoration costs and point the way toward a new way of thinking about environmental cleanup – one that engages market forces while fulfilling a critical national need.

In conclusion, this is a great opportunity to demonstrate the economics and environmental benefits of combining AMD treatment, watershed restoration and critical mineral recovery. The team at WVU has worked together for the past several years and are poised to move rapidly toward commercial development.

References:

Vass, C., A. Noble, P. Ziemkiewicz. 2016. The occurrence and concentration of rare earth elements in acid mine drainage and treatment byproducts. Mining, Metallurgy & Exploration. https://www.osti.gov/servlets/purl/1577094

Ziemkiewicz, P., T. He, A. Noble, X. Liu. 2016. Recover of rare earth elements (REEs) from coal mine drainage. In: 2016 West Virginia Mine Drainage Task Force Symposium, March 29-30, 2016, Morgantown, WV. https://wvmdtaskforce.files.wordpress.com/2016/04/2016-ziemkiewicz-etd30-amdtf-29mar16-a.pdf

Effectiveness of the T&T AMD Treatment Plant on Muddy Creek

Ben Fancher
West Virginia Department of Environmental Protection
Philippi, WV

Abstract: The West Virginia Department of Environmental Protection (WVDEP) Office of Special Reclamation's T&T Fuels Treatment Facility treats acid mine drainage (AMD) from above ground and below ground sources throughout the Muddy Creek Watershed. The treatment facility began operations at the end of 2017 and has been operating within the watershed for nearly five years. Within this period, there have been increases in fish and benthic populations in the impaired portion of Muddy Creek helping to connect the headwaters of Muddy Creek with the Cheat River. The environmental gains within Muddy Creek are due to the effective operation of the T&T Fuels Treatment Facility and its components such as the Glade Run In-Stream Doser, the Viking Lift Station and Force Main system, and T&T Fuels 3 Sludge Injection Borehole. Throughout the five years of AMD treatment, there have been several lessons learned which will be discussed to assist with design and operations of similar treatment facilities.

10+ Year Passive Treatment System Performance Evaluation[1]

Tim Danehy, R.M. Mahony, C.A. Neely, C.F. Denholm, D.A. Guy, K.J. Green, L.V. Hauck[2]

Abstract: The North Fork Montour Run Passive Treatment System[3] was installed in two phases to treat acidic, iron- and aluminum-bearing coal mine drainage. The anoxic limestone drain constructed in 2004 as part of the mine drainage collection and conveyance system situated underneath Pennsylvania Turnpike Route 576 continues to produce alkalinity despite the presence of aluminum. Six additional treatment components were installed in 2008 that include two parallel Jennings-type vertical flow ponds (JVFPs) and were designed to last 15 years. The JVFPs were designed to treat a maximum/average 110/68 gal m^{-1} flow and 353/100 lb d^{-1} acid load. After 12 years the system was overwhelmed during the record-setting rainfall experienced in 2018 when the 58-inch average annual precipitation was 19.7 inches (51%) above normal. The JVFPs experienced inflow up to 228 gal m^{-1} and an acid load of at least 778 lb d^{-1}, and the final treated system outflow was measured in April 2018 to be acidic for the first time. Despite these extreme flow conditions, the entire system was able to neutralize over 602 lb d^{-1} of acid. Alkaline system effluent was restored in June 2018 even though the inflow to the JVFPs was 149 gal m^{-1} and contained 395 lb d^{-1} of acid. As the system was overwhelmed both chemically and hydraulically, the maximum performance that can be expected from this seasoned passive treatment system was quantified. Additional data was collected in subsequent years including April 2020 and March 2022. With one year remaining until the system will reach the 15-year design life, sampling conducted in March 2022 documented a flow of about 180 gal m^{-1} (63% over maximum design) and an acid load entering the JVFPS of 239 lb d^{-1} (77% of maximum design). Despite these above maximum flow conditions, the effluent of the system was alkaline (-87 mg/L acidity as $CaCO_3$) and contained total and dissolved iron and aluminum concentrations below 1 mg/L.

---

[1] Presented at the 2022 West Virginia Mine Drainage Task Force Symposium, Morgantown, WV.

[2] Tim Danehy, QEP (presenter); Ryan M. Mahony, Environmental Scientist; Cody A. Neely, PE, Sr. Environmental Engineer; Clifford F. Denholm III, Sr. Environmental Scientist; and Daniel A. Guy, PG, Geologist, Kelsea Green and Logan Hauck, Environmental Engineers – BioMost Inc., 434 Spring Street Ext., Mars PA 16046.

[3] Work reported here was conducted near 40.474444, -80.277778 information available at: https://www.datashed.org/index.php/project-north-fork-montour-run

Anna S Mine: A Century of Mining, Acid Mine Drainage, and Remediation

Robert Hedin, Neil Wolfe, Ted Weaver
Hedin Environmental
195 Castle Shannon Blvd, Pittsburgh PA 15228
412 571 2204
Bhedin@hedinenv.com

Abstract: The Anna S Mine (Tioga County, Pennsylvania) has supported underground and surface coal mining activities in the Bloss coal seam since the 1890s. The mining is in poorly buffered net acidic strata located above the regional drainage. The mine drainage is low pH with elevated concentrations of Al, Fe, and Mn. In the 1970's surface mining along the crop daylighted portions of the underground workings. Daylighting activities significantly worsened the chemistry of the mine drainage, caused severe water quality problems in Babb Creek, and degraded water quality downstream in Pine Creek, a nationally recognized cold-water fishery. The degradation prompted the formation of the Babb Creek Watershed Association (BCWA) who lobbied aggressively for remediation actions. In 2003/04 two passive treatment systems were installed to treat mine water discharging from the Anna S mine at a total cost of $2.5 million. The systems utilize vertical flow ponds and constructed wetlands and are the largest passive treatment project ever undertaken by a non-profit organization in Pennsylvania. The systems have continuously produced net alkaline effluents which has contributed to restoration of good water quality in Babb Creek. In 2010 Babb Creek and Pine Creek were removed from the degraded stream list and reclassified as high quality cold-water fisheries. The BCWA has managed the operation of the systems since their installation. This responsibility includes sampling, routine maintenance, and major maintenance projects in 2014 and 2016 when the organic substrates in the VFPs were replaced.

The presentation will present the 45-year record of chemical and hydrologic characteristics of mine water discharges from the Anna S mine. The presentation will highlight the degradation caused by the daylighting operations, natural improvements in water chemistry in decades since completion of mining, benefits realized by the passive treatment, and the full cost of the passive systems.

Long-term Performance and Costs for the Anna S Mine Passive Treatment Systems

Robert S Hedin, Neil Wolfe and Ted Weaver[1]

[1]Hedin Environmental, 195 Castle Shannon Blvd, Pittsburgh Pennsylvania, USA, bhedin@hedinenv.com,

Abstract

Acid mine drainage from the Anna S coal mine in Pennsylvania (USA) has been treated successfully since 2004 in the Anna and HD passive systems. The systems, which consist of vertical flow ponds and constructed wetlands, are the largest and most costly mine water treatment project installed by a non-profit group in the United States, to date. Fifteen years of monitoring data show that the systems effectively treated 1,910 L/min of flow with pH 2.8-3.1 containing 121-330 mg/L acidity (as $CaCO_3$), 11-31 mg/L Al, 6-33 mg/L Fe and 6 mg/L Mn. The systems produced effluents with pH 7.5, 134-140 mg/L alkalinity, <1 mg/L Al, 1 mg/L Fe, and 2-3 mg/L Mn and never discharged water with less than 60 mg/L alkalinity (106 samples). In 15 years of operation the systems generated a combined 5,600 tonnes of net alkalinity. Unit treatment costs were converted to 2018 dollars and compared to active treatment systems. Over a 20-year period, passive systems generate alkalinity at a cost of $1,168/tonne $CaCO_3$ which is 50% lower than unit costs realized for lime treatment plants currently operated in Pennsylvania.

Keywords: passive mine drainage treatment, vertical flow ponds, coal mine drainage, unit cost of passive mine drainage treatment

Introduction

Passive mine drainage treatment systems utilize natural materials and biogeochemical processes to generate alkalinity, neutralize acidity, and remove metal contaminants while making full use of gravity to transfer water to and through the systems (Hedin et al. 1994; Younger et al. 2002). Passive treatment technologies are a primary tool for the restoration of streams polluted by legacy coal mines in Pennsylvania (USA). As of 2015, approximately 275 passive mine water treatment systems have been installed in Pennsylvania at a total cost of approximately $93 million (Stream Restoration Inc 2019). Eighty percent of the systems were installed by non-profit citizen groups, while the balance were installed by the PA Department of Environmental Protection.

The passive treatment approach is often preferred over conventional active treatment due to cost savings arising from the avoidance of routine maintenance activities and reduced energy requirements. Conventional systems require the continuous addition of chemical reagents, the management of large volumes of low-solids sludge, and the perpetual input of electricity (Younger et al. 2002). Through its use of natural substrates as a source of chemical modification and gravity as a source of energy, passive treatment avoids these routine costs. The neutralization of acidity is achieved through limestone dissolution or through a biologically active organic substrate. The limited solubility and kinetics of these processes allow the initial installation of enough reactive substrates to supply years of treatment. Passive treatment processes produce a low volume of high-solids sludge and it is feasible to design systems with years of storage capacity.

The sustained effective treatment of passive systems requires long-term maintenance which can be divided into minor and major categories. Minor maintenance events generally occur on quarterly or semi-annual schedule and include tasks that can be performed by hand and do not involve the management or replacement of treatment components. Minor maintenance also includes inspections and monitoring efforts that identify developing problems.

Major maintenance tasks are scheduled activities that are too large to be accomplished as a routine action. Examples include the removal of metal sludge deposits and the replacement of reactive substrates. These actions are typically performed on multi-year intervals and involve heavy equipment to replace treatment system components and/or replenish treatment materials. Though infrequent, major maintenance tasks can be costly

because they deal with years of sludge accumulation or large-scale substrate replacement. The need for major maintenance actions must be recognized in the operation of passive treatment systems and included in cost comparisons of the treatment approaches. Because passive systems are often designed with 10-20 years of substrate and sludge storage capacity, considerations of major maintenance are typically theoretical (Hedin 2008). A more meaningful analysis utilizes realized maintenance costs from installed functional passive treatment systems.

This paper presents performance and cost data for two passive systems that were installed in 2004 to treat acidic mine water discharging from the Anna S Mine in Tioga County, Pennsylvania. The systems are among the largest and most costly passive treatment projects undertaken by a nonprofit citizen group in the U.S to date. The installation and first five years of treatment performance were described in Hedin et al (2010). This paper provides ten more years of monitoring information and an accounting of the realized minor and major maintenance costs. The data are used to develop unit treatment costs that are compared to similar calculations made for three systems that utilize conventional chemical treatment technologies.

Background

Mining History and Pollution History

Table 1 shows a timeline of the mining, monitoring and remediation activities at the site. The Anna S underground mine is in the Bloss coal seam and was operated by the Fall Brook Coal Company between the 1890s and the 1930s. The mine is above drainage, so the workings are largely unflooded. The coal and associated strata are acidic, while the overlying sandstone geology is largely inert. Mining in these geologic conditions without alkaline addition results in acidic metal-contaminated drainage. The Anna S mine was also subjected to several surface mining activities that were focused on the extraction of shallow crop coal and the overlying Cushing coal. Between 1977 and 1986 surface mining methods known as "daylighting" were used to remove stumps and pillars from the previously abandoned deep mine as well as the Cushing coal seam. The surface mining avoided disturbance to the primary mine portal and a drainage tunnel, which combined produced most of the mine drainage flow. Areas surface mined after 1977 were regraded and successfully revegetated with standard herbaceous reclamation species.

The mine discharges flow to Wilson Creek, a tributary of Babb Creek which is a major tributary to Pine Creek, a world-renowned cold-water trout fishery. Prior to the daylighting activities in the watershed, Pine Creek was able to assimilate pollution from Babb Creek without degradation. In the 1980s, the quality of Pine Creek below Babb Creek deteriorated substantially, causing the stream to be placed on the EPA's 303(d) list of degraded streams. The cause was attributed to increased contamination of acid discharges from mines in the Babb Creek watershed. In 1990 the Pennsylvania Fish and Boat Commission surveyed Babb Creek and found native trout in its headwaters but no fish downstream of Wilson Creek. Soon after the survey the Babb Creek Watershed Association (BCWA) was formed with a goal to promote the restoration of Babb Creek. Over the next 30 years, the BCWA implemented three reclamation projects and installed ten treatment systems. The two largest treatment projects are a lime treatment plant and the Anna S Mine passive treatment systems. The BCWA supports a small staff that operates the lime plant and maintains its passive treatment systems.

Anna S Mine Passive Treatment Systems

Two passive treatment systems were installed in 2003-04 to treat three discharges from the Anna S Mine. (Figure 1). The HD system treats water flowing from the Hunters Drift drainage tunnel with four parallel vertical flow ponds (VFPs) followed by a series of three constructed wetlands. The Anna system treats water flowing from the S1 and S2 mine portals with four parallel VFPs followed by a single polishing pond.

Due to topographical and geologic constraints, a limited area was suitable for construction of gravity-driven treatment systems. The available sites required long pipelines to transfer the discharges from their collection to treatment. The pipelines for the HD, S1, and S2 discharges are 730 m, 267 m, and 318 m long, respectively. The pipelines flow into structures that distribute water into the VFPs. The structures facilitate maintenance activities by

allowing restriction of flow to the VFP units undergoing maintenance while maintaining treatment through the other VFPs.

In both the HD and Anna systems, each individual VFP consists of 0.9 m of limestone aggregate overlain with 0.3 m of alkaline organic substrate overlain with 0.6 – 0.9 m feet of standing water (Figure 2). An underdrain system constructed with perforated plastic pipe is located at the bottom of the limestone aggregate. Mine water flows into each VFP through a piped inlet at the surface, down through the organic substrate and limestone aggregate to the underdrain collection system. Water discharges through a structure that controls the water elevation in each VFP. In each system the effluents from the VFPs are collected into a single flow that is discharged to a series of ponds and constructed wetlands for polishing via aerobic reactions. Details of the designs, including quantities, volumes, and surface areas are available in Hedin et al. (2010).

The alkaline organic substrate in each VFP is a mixture of spent mushroom compost and limestone fines that is intended to both treat the mine drainage and protect the integrity of the limestone underdrain. Calcite dissolution and microbial activity in the substrate generate alkalinity which raises pH and promotes the hydrolysis of dissolved Al and Fe^{3+} to hydroxide solids. The fertile organic substrate supports microbial activity that removes dissolved oxygen, reduces ferric iron (Fe^{3+}) to ferrous iron (Fe^{2+}), and generates dissolved carbon dioxide. As water flows through the limestone aggregate, calcite dissolution generates additional bicarbonate alkalinity. Fe^{2+} and Mn^{2+}, which are highly soluble at circumneutral pH, pass through the limestone aggregate and are discharged from the VFP. Both metals are subject to removal by oxidizing reactions in the aerobic ponds and wetlands.

The systems contain flow restriction mechanisms that limit the maximum treated flow and bypasses excess flow. The Anna system was designed to accept up to 1635 L/min, approximately the 90^{th} percentile flow rate for the combined S1 and S2 discharges. The Hunters Drift was designed to accept up to 1211 L/min, approximately the 75^{th} percentile flow rate.

Methods

Historic water chemistry and flow data for the discharges were obtained from various sources. In 1975-1976, discharges from the Anna S Mine were monitored through Pennsylvania's Operation Scarlift program (Boyer Kantz and Associates1976). Between 1977 and 1984, the discharges were monitored by the United States Geological Survey (USGS) as part of a project intended to measure the effect of daylighting operations on mine drainage quality (Reed 1980). During this period, weirs were installed and monitored continuously for flow, while water samples were collected monthly and analyzed for mine drainage parameters using procedures reported in Reed (1980). Between 1985 and 1989, the discharges were monitored by Antrim Mining company as part of mining permit requirements. Data from this period was obtained from permit files available from the Pennsylvania Department of Environmental Protection (PADEP) District Mining Operations. Between 1996 and 2000, the discharges were monitored by PADEP and Babb Creek Watershed Association as a prelude to development of treatment plans.

The passive treatment systems were installed in 2004. Monitoring has occurred regularly at influent and effluent locations and irregularly at internal points. pH and temperature were measured using a calibrated electronic pH meter and field alkalinity was measured within 4 hours of sample collection by titration with 1.6 N sulfuric acid to pH 4.5 (American Public Health Association 1999). A raw sample was analyzed in a PADEP-certified laboratory for pH, alkalinity, hot hydrogen peroxide acidity, sulfate, and total suspended solids by standard methods. When available, field measurements of pH and alkalinity were used in preference to laboratory values. An acidified sample (pH <2 with nitric acid) was analyzed for total concentrations of Fe, Al, and Mn by inductively coupled plasma spectrometry (American Public Health Association 1999). Metals and sulfate are reported as mg/L. Acidity and alkalinity are reported as mg/L $CaCO_3$ equivalents. In 2004 and 2005, laboratory analyses were conducted by the Pennsylvania State Laboratory. Since 2006, laboratory analyses have been conducted by G&C Coal Analysis Laboratory (Summerville, PA).

The quality of field and laboratory analyses was evaluated by comparing measured and calculated acidities for samples of mine water that did not have visible particulates when collected and acidified following the method described by Hedin (2006). The acid balance error was calculated in a manner analogous to a charge balance error calculation as follows.

$$\text{Acid balance error} = (\text{Acid}^{meas} - \text{Acid}^{calc}) / (\text{Acid}^{meas} + \text{Acid}^{calc})$$

The measured and calculated acidity values showed good correspondence. The influent and effluent sampling points had, on average, imbalances between -2% and -7%. The reason for the negative imbalances (calculated acidities slightly larger than measured acidities) is not known.

Flow was measured at the piped influents to treatment systems by the timed-volume method and is reported as liters per minute (L/min). Load (kg/day) was calculated using the product of flow and chemistry with appropriate unit adjustments.

Costs for the installation of the Anna S passive systems and two recent major maintenance events were obtained from PADEP Growing Greener grant documents. Costs for the annual operation and maintenance of the Anna S systems were obtained from audited financial reports provided by BCWA. Treatment information and costs for the installation and operation of the lime treatment systems were obtained from the PADEP Bureau of Abandoned Mine Reclamation (PADEP 2019b) and from the PADEP Bureau of District Mining Operations (PADEP 2017). Costs were adjusted to 2018 dollars using the US Bureau of Reclamation Construction Cost Trends composite cost index (US Bureau of Reclamation 2019). Future costs were estimated assuming a 20 year straight line depreciation and a 5% interest rate.

Results

Mine Drainage Characteristics

Table 2 shows the average flow, chemistry and acidity loads for the discharges pre-daylighting (1975-78), during daylighting (1979-89), during the passive treatment system design (1995-98), and since installation of the system in 2004. Individual flow and acidity measurements are shown in Figures S-1 and S-2 (supplemental information). All three discharges are acidic with elevated concentrations of Fe, Al, and Mn. The HD and S1 discharges are the primary sources of flow and contamination. The S2 discharge always produced less flow with lower contaminant concentrations.

Pre-daylighting flows were higher than during and after daylighting. The combined pre-daylighting average flow was 3,457 L/min while the combined daylighting flow averaged 2,009 L/min, and the pre-treatment-system period averaged 2,451 L/min. The differences in flow were not attributable to differences in precipitation as a review of local weather records (Williamsport Municipal Airport, 53 km south) did not identify unusual precipitation during the pre-daylighting period. The difference in flow was likely a consequence of the daylighting activities. The remining and reclamation of abandoned mines can lessen mine water flow due to the more effective exclusion of surface water from the underground workings (Hawkins 1998).

Daylighting significantly increased the release of contaminants. Concentrations of acidity and metals increased up to five fold during the daylighting period (Figure S2). Figure 3 shows combined loadings for the HD and S1 discharges between 1974 and 1999. During the daylighting period several very high loading events were observed and low loading events were less common. The increased contaminant loading coincided with the observed degradation of Pine Creek downstream of Babb Creek.

Since cessation of mining activities and reclamation of the site, concentrations of acidity and metals have decreased. Contaminant concentrations at HD have returned to levels observed before the daylighting operations; concentrations at S1 and S2 are 30% lower than pre-daylighting levels.

Major Maintenance

The parallel VFP design allows individual VFP units to be isolated for inspection or maintenance while maintaining treatment by the other units. The organic substrates in the VFPs have been periodically inspected to assess their reactivity. The alkaline organic substrates have a limited capacity for supporting beneficial chemical and microbial processes. When the capacity is exhausted, low pH metal-contaminated water will enter the underlying limestone aggregate and compromise its effectiveness. Because of the very large investment in the limestone aggregate (33,000 tonnes of limestone with installed cost of approximately $1 million), a primary goal of operation and maintenance activities is to protect the integrity of the limestone aggregate. This goal is accomplished by replacing the organic substrate before its failure results in degradation of the underlying aggregate.

All organic substrates in the VFPs were recently replaced using similar methodology. Flow into the VFP targeted for rehabilitation was diverted to other VFPs using the distribution infrastructure. Each targeted VFP was drained empty and the existing substrate was stripped off and set aside. The exposed underlying limestone aggregate was scarified by raking with an excavator. Approximately one foot of new alkaline organic substrate was placed on top of the limestone aggregate and the old substrate, which was not entirely exhausted, was placed on top of the new substrate. The new substrate was a 2:1 volume mixture of fresh spent mushroom compost and limestone fines. The substrate replacement process was developed in 2012 on one VFP and then used to rehabilitate the remaining three HD VFPs in 2013 and all four Anna VFPs in 2016. Effective treatment of the mine drainage was maintained during substrate replacement by assuring that all flows passed through functional VFPs. During the substrate replacement projects, general repairs were made to the systems including cleanout of channels, repairs to water level control structures, and rehabilitation of the S2 and HD collection systems.

Treatment Effectiveness

Table 3 shows the average chemistry of the system influents, VFP effluents, and final effluents of the two passive treatment systems. The effluents from the VFPs had circumneutral pH and were strongly net alkaline. The VFPs in both systems decreased Al to less than 1 mg/L, had marginal impact on Mn, and had variable impact on Fe. The Anna VFPs did not markedly decrease Fe, while the HD VFPs decreased Fe concentrations by approximately 50%. Additionally, the Fe removal by all the VFPs was variable with respect to flow rate (Figure 4). Under many low flow conditions, the VFPs released Fe. Under all high flow conditions, the VFPs removed Fe.

The VFPs had little effect on sulfate. If the changes in sulfate were attributable to the bacterial sulfate reduction, then the alkalinity generation attributable to sulfate reduction (100 mg/L $CaCO_3$ generation per 96 mg/L SO_4 removal) only accounted for 3% of the net alkalinity generation by the Anna VFPs and 6% of the alkalinity net generation of the HD VFPs. Calcite dissolution was the dominant source of alkalinity in both systems.

The VFPs discharge to aerobic wetlands and ponds that were intended to remove residual Fe and Mn by oxidative processes. The aerobic units were effective. Fe was decreased to 1.1 mg/L at the final effluent of the Anna system and to 0.5 mg/L at the final effluent of the HD system. The passive removal of Mn requires alkaline aerobic conditions and low concentrations of ferrous iron (Hedin et al. 1994). This was accomplished in both systems, but was more effective in the HD system, which has a larger aerobic wetland.

The oxidative removal of Fe and Mn in the wetlands consumes alkalinity, yet the effluents of both systems are still strongly net alkaline. The average net generation of alkalinity, calculated from the difference of acidity between the influent and effluent, was 229 mg/L $CaCO_3$ for the Anna system and 444 mg/L $CaCO_3$ for the HD system. The average generation of net alkalinity by the systems, calculated from the net alkalinity generation and the influent flow rates, was 266 kg/day $CaCO_3$ for the Anna system and 642 kg/day $CaCO_3$ for the HD system. On average, the

combined systems generated 332 tonne/year $CaCO_3$. Over the 5,598 days of operations (Jan 1, 2004 – Apr 30, 2019), the systems generated a combined 5,033 tonnes alkalinity as $CaCO_3$.

The treatment was reliable. Figure 5 shows effluent concentrations of alkalinity and net acidity over the 15-year monitoring period for both systems. The lowest concentration of alkalinity was 60 mg/L $CaCO_3$ and the highest concentration of acidity was -50 mg/L $CaCO_3$. Effluent pH was always greater than 6.5.

The replacement of organic substrate resulted in short-term changes in water chemistry. Figure 4 notes two samples with elevated Fe that were collected from the effluents of two VFPs within a month of their organic substrate replacement. These temporary changes in chemistry were not detected when the systems were sampled several months later.

Costs

Table 4 shows the costs to construct, operate and maintain the Anna and HD systems. In 2003, the construction cost was $2,215,699 and the cost for design, engineering, permitting, and project management was $301,000. For this analysis, operation and maintenance (O&M) cost is divided into routine activities and major maintenance events. Routine O&M is conducted by BCWA and includes monthly inspections, semi-annual sampling, and simple maintenance activities. BCWA maintains nine passive treatment systems located at six sites. In 2018, the total cost to maintain all nine sites was $64,267, of which $10,711 was allocated to the Anna S passive treatment systems. Major maintenance includes tasks that require the hiring of engineering support, contractors, mobilization of heavy equipment, and major materials purchases. Two major maintenance events have occurred that addressed the replacement of organic substrates in the HD VFPs in 2012 ($210,008) and in the Anna VFPs in 2016 ($201,706). As noted previously these budgets included general and site-specific system improvements.

Costs to install and operate the Anna S passive systems were realized at different times throughout the 15-year operational period. All costs were adjusted to 2018 dollars using the US Bureau of Reclamation Construction Cost Trends composite cost index (US Bureau of Reclamation 2019). Between 2003 and 2018, construction costs increased by 66% or 3.45% per year (compounded basis). Table 4 shows all costs converted to 2018 values. The cost to design, permit and install the Anna S Mine passive treatment complex systems in 2018 is estimated at $4,200,000.

Discussion

The HD and Anna passive treatment systems effectively treated acidic coal mine drainage contaminated with Al, Fe and Mn for 15 years. Every effluent water sample collected from the system (114 samples) had pH above 6.5 and at least 60 mg/L alkalinity. Based on influent flows and differences in influent and effluent chemistry, the two systems removed approximately 3,100 tonnes acidity (as $CaCO_3$), 310 tonnes Al, 290 tonnes Fe, and 60 tonnes Mn from the influent waters.

The success of the treatment systems contrasts with current policies regarding the use of passive treatment for coal mine waters in the United States. In West Virginia, passive treatment is considered only appropriate for mine water with less than 100 mg/L acidity (Mack et al. 2010). The US Office of Surface Mining Reclamation and Enforcement (OSMRE) and PADEP have developed criteria for evaluating proposed passive treatment projects (PADEP 2019a). The guidance, shown in Table 5, assigns “risk of failure” to proposed projects based on influent chemistry (summed concentrations of Fe plus Al) and hydrologic loading (flow per treatment cell). The Anna system was designed to treat up to 409 L/min per VFP containing 26 mg/L Fe+Al while the HD system was designed to treat up to 303 L/min per VFP containing 79 mg/L Fe+Al. Both systems would have been classified as high risk of failure.

As noted previously, the influent chemistry of both systems improved between their design and the construction, resulting in lower influent metal concentrations and loads. An evaluation was made of the actual chemical and hydraulic conditions received by each system. The Anna system was classified as having a medium risk of failure 30 times and as having a low risk 7 times. The HD system was classified as having a high risk of failure 45 times

and as having a medium risk 10 times. Based on these evaluations and the high cost of the projects, neither would be fundable under current PADEP and OSMRE project evaluation criteria. As a result, the recommended remedial action would be more expensive and energy intensive chemical treatment. The success of the Anna and Hunters Drift passive treatment systems suggests reconsideration of these criteria.

The 15-year effectiveness of the Anna and HD passive treatment systems can be attributed to several factors. The primary reason for success is the conservative system sizing and design. The Anna and HD systems were designed for 90^{th} and 75^{th} percentile acidity loads, respectively. This feature ensures that under most operating conditions the VFPs are oversized. The VFPs were designed with raised berms and upslope diversion channels that protect them from stormwater damage during extreme precipitation events. Both systems contain functional bypasses that prevent spikes in flow that could damage the VFPs. The systems receive influent flows through adjustable distribution structures that deliver water to multiple treatment units in parallel. This feature allows individual VFPs to be taken off-line for inspection and O&M activities, while maintaining treatment through the other VFPs. By scheduling O&M activities for low flow periods when there is excessive treatment capacity, no degradation of the final effluent quality occurs.

Another factor related to this success is the ongoing operation and maintenance provided by BCWA. The systems are inspected and sampled regularly, and minor maintenance is conducted as a routine operation. BCWA is able to support its O&M activities through funding received from a dedicated tipping fee at a local landfill. Major maintenance, such as replacement of the organic substrates, cleanout of ditches and channels, and repairs to collection systems and hydrologic controls, is conducted as necessary. The latter activities require the BCWA to obtain funding to support these activities. The organization has successfully met these objectives.

Finally, the chemistry of the influent mine water has improved since the systems were designed. Influent concentrations of acidity and metals to the HD and Anna systems have averaged 30% and 50% lower, respectively, then those assumed in the design. These changes resulted in lower contaminant loading to the systems. Gradual improvement in mine water chemistry is a common characteristic of mine drainage discharges from abandoned coal mines in Appalachia (Demchak et al. 2004; Mack et al. 2010; Burrows et al. 2015). Passive treatment systems are intended to provide decades of treatment and the natural amelioration of contaminant concentrations in the water collected for treatment can be a component of their long-term success.

Reliability is an important aspect of mine water treatment, especially when the treatment system is essential to maintaining ecosystem function in the receiving stream. Short-term failures of chemical treatment systems can create large and rapid changes in effluent chemistry that have long-lasting impacts on the receiving stream ecology (Kruse et al. 2012). Except under catastrophic events, the failure of a passive treatment system is a gradual process that, with proper monitoring, can be recognized and corrected before the receiving stream has been seriously degraded. In the case of the Anna S passive systems, the declining VFP performance was recognized and corrected through planned major maintenance actions.

The generation of excess alkalinity at the effluents is an important benefit of the Anna S treatment systems. Many streams degraded by legacy mining receive flows of acidic water that cannot be cost-effectively collected and treated. The in-stream treatment of these flows is achieved through inputs of excess alkalinity from treatment systems. Approximately 40% of the alkalinity generated by the Anna S systems is realized as alkalinity in the system effluents which provide valuable neutralization and buffering capacity for Babb Creek.

The reliable treatment and net alkalinity generation provided by the Anna S systems has contributed significantly to the restoration of improved water quality in Babb Creek and downstream in Pine Creek. A native brook trout fishery has reestablished in Babb Creek below Wilson Creek and both Babb Creek and Pine Creek have been removed from EPA's 303(d) list of degraded streams (PADEP 2012).

Comparative Cost Evaluations

The high cost of the conservative design and ongoing maintenance raises the question: Are the Anna S passive treatment systems cost-effective? The conventional method for active treatment of acidic mine water is lime. Current costs and performance data were obtained for three lime treatment plants constructed and operated by the PADEP. Like the Anna S systems, these three treatment plants discharge circumneutral pH water with net alkalinity and low concentrations of metals. Table 6 shows costs realized at the time of expenditure and adjusted to 2018 dollars. These costs are used to calculate the annual cost of the treatment assuming that 2018 construction and engineering costs are depreciated over 20 years at 5% interest rate. The total annualized cost of treatment is compared to the annual alkalinity generation (ton/yr $CaCO_3$) to calculate the cost per ton $CaCO_3$. The Anna and HD systems, combined, generate 327 tonne/year alkalinity at a unit cost of $1,168/tonne.

The Hollywood hydrated lime plant treats multiple low pH mine discharges with aeration, lime neutralization and clarification. The discharges are collected by an extensive gravity flow system and the sludge is pumped into a nearby abandoned underground mine. The plant was installed in 2013 at a cost of approximately $16,800,000 and had an operating cost in 2017 of $670,248 (PADEP 2019b). The plant generates 911 tonne/year alkalinity (as $CaCO_3$) at a 20-year cost of $2,491/tonne $CaCO_3$.

The Smail-Orcutt system treats two flows of high-Fe acidic water with lime slurry in reaction tanks followed by earthen settling ponds. The plant was installed in 2015 at a cost of $682,000 and had an operational cost in 2016 of $77,000 (PADEP 2017). The sludge is periodically removed and buried on-site. The plant generates 52 tonne/yr alkalinity at a unit cost of $2,707/tonne $CaCO_3$.

The Brandy Camp system was originally installed as a hydrated lime plant to treat a high-Fe acidic discharge. The plant has been retrofitted several times over the last 20 years at a total cost of approximately $2,400,000. The plant was recently redesigned for treatment with lime slurry and hydrogen peroxide (H_2O_2) and had an operating cost in 2017 of $263,499 (PADEP 2019b). The plant generates 264 tonne/yr alkalinity at a unit cost of $2,278/tonne $CaCO_3$.

The Anna S passive systems are generating alkalinity and removing metals over a 20-year period at a cost that is 49-57% less than lime systems. Extending the analysis to a longer time frame increases the savings because the annual costs of passive treatment are so much lower than lime treatment. The differential is an underestimate because the long-term major maintenance costs of the Anna S systems are known and accounted for in its costs. The lime systems are all relatively new construction with unknown major maintenance needs. It is likely that expensive repairs or equipment replacement will be required in the next 10-15 years which will increase the unit treatment costs.

A common reason for excluding passive treatment from consideration is the difficulty of finding a suitable site that is accessible by gravity. Pumping of mine water to a passive system is common practice in the United Kingdom (Coal Authority 2012), but it is rarely considered in the U.S. By disregarding pumping, many feasible passive treatment projects are not installed. If the Anna S passive systems included pump stations to raise the mine water 30 m, the capital costs would increase by approximately $100,000 and the annual costs would increase by approximately $26,500 (calculated with AMDTreat (U.S. Office of Surface Mining and Enforcement 2019) assuming 1,910 L/min flow, 30 m lift, 75% pump efficiency, 85% motor efficiency, $0.10/kwh, and 18%/yr pump maintenance). The addition of these costs increases the unit cost to $1,274/tonne $CaCO_3$. Even with pumping costs included, the passive option is still 49% less than the cost of lime treatment.

Conclusion

The Anna S Mine passive treatment complex has provided 15 years of reliable treatment of low pH coal mine drainage containing elevated Al, Fe and Mn. The effectiveness of the treatment systems has contributed to the reestablishment of cold-water fisheries in Babb Creek and Pine Creek. The success of the systems is attributable to

conservative design, diligent maintenance by the Babb Creek Watershed Association, and natural attenuation of the mine drainage chemistry. The unit cost of alkalinity generation in the passive systems is 50% the cost of comparable conventional lime treatment operations in Pennsylvania. The analysis presented in this paper speaks to the need for reconsideration of the current regulatory understanding of passive treatment's reliability and cost-effectiveness in the United States.

Acknowledgements

Babb Creek Watershed Association provided water sampling data, system information, and has been a continuous steward of the Anna S passive treatment systems. Michael Smith, Neil Wolfe, Naomi Anderson and an anonymous reviewer provided valuable feedback about draft versions of the paper.

Literature Cited

American Public Health Association (1999) Standard Methods for the Examination of Water and Wastewater. Clesceri LS, Greenberg AE, Eaton AD (eds), (20th Edit), American Public Health Assoc, American Water Works Assoc, and the Water Environment Federation, Washington, DC, USA

Boyer Kantz and Associates (1976) Operation Scarlift, Babb Creek Mine Drainage Abatement Project. Abandoned Mine Reclamation Clearinghouse. http://amrclearinghouse.org/Sub/SCARLIFTReports/ Accessed 2019-06-22

Burrows, J.E., Peters, S.C, Cravotta, C.A (2015) Temporal geochemical variations in above- and below-drainage coal mine discharge. Appl. Geochem. 62:84-95

Coal Authority (2012) Mine Water Treatment Schemes, Code of Practice. https://assets.publishing.service.gov.uk/government/uploads/system/uploads/attachment_data/file/356529/pos-tca-mine-water-treatment-schemes_codeofpractice_2012.pdf Accessed 2019-06-18

Demchak J, Skousen J, McDonald LM (2004) Longevity of acid discharges from underground mines located above the regional water table. J. Environ. Qual. 33:356-668

Hawkins JW (1998) Remining. In Brady K, Smith M, Schueck J. (eds) Coal Mine Drainage Prediction and Pollution Prevention in Pennsylvania. PA Department of Environmental Protection, Harrisburg

Hedin RS, Nairn RW, Kleinmann RLP (1994) Passive treatment of polluted coal mine drainage. Bureau of Mines Information Circular 9389. United States Department of Interior, Washington DC

Hedin RS (2006) The use of measured and calculated acidity values to improve the quality of mine drainage datasets. Mine Water Env. 25: 146-152

Hedin RS (2008) Iron removal by a passive system treating alkaline coal mine drainage. Mine Water Env. 27:200-209

Hedin RS, Weaver T, Wolfe N, Weaver K. (2010) Passive treatment of acid mine drainage: the Anna S Mine passive Treatment complex. Mine Water Env, 29:165-175

Kruse NA, Bowman JR, Mackey AL, McCament B, Johnson KS (2012) The lasting impacts of offline periods in lime doses streams: A case study in Racoon Creek, Ohio. Mine Water Environ. 31: 266-272

Mack B, McDonald LM, Skousen J (2010) Acidity decay of above-drainage underground mines in West Virginia. J Environ. Qual. 39: 1-8

Pennsylvania Department of Environmental Protection (2012) Pennsylvania Nonpoint Source Management Program FFFY2011 Annual Report. Commonwealth of Pennsylvania, Department of Environmental Protection, Harrisburg PA

Pennsylvania Department of Environmental Protection (2017) Mining and Reclamation Advisory Board April 2017 meeting, Chris Yeakle Presentation. https://www.dep.pa.gov/PublicParticipation/AdvisoryCommittees/Mining/MiningReclamation/Pages/2017.aspx Accessed 2019-05-03

Pennsylvania Department of Environmental Protection (2019a) Acid Mine Drainage (AMD) Set-Aside Program, Acid Mine Drainage Set-Aside Program Implementation Guidelines.

https://www.dep.pa.gov/Business/Land/Mining/AbandonedMineReclamation/Pages/AMD-Set-Aside-Program.aspx Accessed 2019-06-22

Pennsylvania Department of Environmental Protection (2019b) Acid Mine Drainage (AMD) Set-aside Program, Summary of BAMR's Active Mine Drainage Treatment Plants
https://www.dep.pa.gov/Business/Land/Mining/AbandonedMineReclamation/Pages/AMD-Set-Aside-Program.aspx Accessed 2019-06-22

Reed LA (1980) Effects of strip mining the abandoned deep Anna S Mine on the hydrology of Babb Creek, Tioga County, Pennsylvania. USGS-WRI-80-53

Stream Restoration Inc (2019) Datashed. https://www.datashed.org/ Accessed 2015-08-15

U.S. Bureau of Reclamation (2019) Construction Cost Trends. https://www.usbr.gov/tsc/techreferences/mands/cct.html Accessed 2019-06-22

U.S. Office of Surface Mining and Enforcement (2019) AMD Treat. https://amd.osmre.gov/default.htm Accessed 2019-06-22

Younger PL, Banwart SA, Hedin RS (2002) Mine Water: Hydrology, Pollution, Remediation. Springer, New York

Table 1. Mining, monitoring and treatment activities at Anna S Mine.

Years	Activity
1890s – 1930s	Underground mining
1975-76	Monitoring, Operation Scarlift
1977-1986	Daylighting and surface mining
1976-1984	Monitoring, USGS
1985-1989	Monitoring, Antrim Mining Company
1996-2000	Monitoring, PADEP and BCWA
2003-2004	Construction of treatment system
2004-present	Operation and monitoring of system, BCWA and HE
2012-2013	Hunters Drift organic substrate replacement
2016	Anna organic substrate replacement

Table 2. Average flow, chemistry and acidity load for S1, S2, and HD pre-daylighting (DL), during DL, and pre and post passive treatment system (PTS) installation. "na" indicates not available.
[1] Influent flow rates for the PTS are limited by the bypass structure.

Period	type	Flow	pH	Acid	Fe	Mn	Al	SO4	Acid
		L/min		mg/L	mg/L	mg/L	mg/L	mg/L	kg/d
S1 Discharge									
1975-78	Pre DL	1651	3.0	218	12.5	4.1	na	340	516
1979-89	DL	828	2.9	480	37.7	18.0	33.4	704	583
1995-98	Pre PTS	1054	3.0	271	12.1	14.4	16.1	542	425
2004-19	PTS	713[1]	3.0	133	6.5	7.5	11.8	332	134
S2 Discharge									
1975-76	Pre DL	147	3.8	39	0.2	na	na	96	8
1980-91	DL	108	3.0	294	20.0	20.6	15.0	639	47
1995-98	Pre PTS	221	3.2	140	2.2	8.4	7.4	286	60
2004-18	PTS	92[1]	3.8	28	1.2	5.3	1.7	121	4
HD Discharge									
1975-78	Pre DL	1659	2.8	358	38.4	4.1	na	475	794
1979-89	DL	1073	2.7	1000	112.3	24.1	74.3	715	1361
1995-98	Pre PTS	1176	2.8	491	43.9	9.9	35.5	715	845
2004-18	PTS	1006[1]	2.8	330	32.6	6.0	30.7	535	409

Table 3. Average flow and chemistry for Anna and HD treatment systems, 2004 – 2018. "N" is the sample size. "na" indicates not available. [A] Chemical values are flow weighted average of S1 and S2; [B] chemical values are flow weighted average of effluent of VFPs 1-4; [C] chemical values are the flow weighted average of effluent of VFPs 5-8.

Point	Flow L/min	Flow N	pH	Alk mg/L	Acid $CaCO_3$	Fe mg/L	Mn mg/L	Al mg/L	SO4 mg/L	Chem N
Anna System										
S1 influent	713	47	3.0	0	133	6.5	7.5	11.8	332	44
S2 influent	92	41	3.8	0	28	1.2	5.3	1.7	121	38
S1&S2 influent[A]	804		3.1	0	121	5.9	7.2	10.7	308	
VFPs effluent[B]	na		7.0	157	-124	5.3	6.2	0.4	300	28
Final effluent	na		7.5	134	-108	1.1	3.3	0.3	294	46
HD System										
HD influent	1006	54	2.8	0	330	32.6	6.0	30.7	535	59
VFPs effluent[C]	na		6.8	191	-129	17.3	5.0	0.5	507	29
Final effluent	na		7.5	140	-114	0.5	1.9	0.2	468	60

Table 4. Costs to install, operate and maintain the Anna S passive treatment systems. Costs are provided for the year realized and adjusted to 2018 using the US Bureau of Reclamation Construction Cost Trends composite cost index.

Item	Cost periodicity	Cost (year)	Cost, 2018
Construction	One-time	$2,215,699 (2003)	$3,668,910
Engineering	One-time	$301,000 (2003)	$498,417
Routine O&M	Annual	$10,711 (2018)	$10,711
HD OS Replacement	Every 12 years	$210,008 (2013)	$246,070
Anna OS Replacement	Every 12 years	$201,706 (2016)	$216,057

Table 5. Risk Analysis Matrix used by US Office of Surface Mining Reclamation and Enforcement, and Pennsylvania Department of Environmental Protection to evaluate feasibility of passive treatment proposals (PADEP 2019a).

	Design Flow Rate for Each Treatment Cell, L/min			
Fe + Al, mg/L	< 95	≥ 95 and < 189	≥ 189 and < 379	≥ 379
< 5	Low	Low	Low	Low
≥ 5 and < 15	Low	Medium	Medium	Medium
≥ 15 and < 25	Low	Medium	Medium	Medium
≥ 25 and < 50	Medium	Medium	Medium	High
≥ 50	High	High	High	High

Table. 6. Treatment costs and alkalinity generation for Anna S passive systems and three lime treatment systems. Costs are adjusted to 2018 dollars using the US Bureau of Reclamation Construction Cost Trends composite cost index. [A] engineering cost assumed at 15% of construction cost. [B] annual cost assuming straight depreciation over 20 years at 5% interest rate

	Anna S (Anna and HD) passive		Hollywood hydrated lime		Smail Orcutt lime slurry		Brandy Camp lime slurry and H_2O_2	
	realized	2018	realized	2018	realized	2018	realized	2018
Construction	$2,215,699 (2003)	$3,668,910	$14,608,912 (2013)	$17,117,532	$600,000 (2015)	$644,094	$2,419,038 (2001-16)	$3,577,484
Engineering	$301,000 (2003)	$498,417	$2,207,060[A] (2013)	$2,708,325	$82,000 (2015)	$$88,026	$362,856[A] (2001-16)	$536,623
Major Maintenance	$411,714 (2013-16)	$462,127	Unknown		Unknown		Unknown	
Annual (Routine)	$10,711 (2018)	$10,711	$670,248 (2017)	$689,733	$77,000 (2016)	$82,442	$263,499 (2017)	$273,531
	Annualized cost		Annualized cost		Annualized cost		Annualized cost	
Construction, $/yr[B]	$294,403		$1,373,555		$51,684		$287,067	
Engineering, $/yr[B]	$39,994		$206,033		$7,063		$43,060	
Major Maint., $/yr	$37,187		unknown		unknown		unknown	
Annual, $/yr	$10,711		$689,733		$82,442		$273,531	
Total, $/yr	$382,295		$2,269,321		$141,190		$603,657	
	Treatment and unit cost		Treatment and unit cost		Treatment and unit cost		Treatment and unit cost	
Flow, L/min	1,779		7,241		208		3,785	
Acid in, mg/L	238		224		439		43	
Acid out, mg/L	-112		-15		-37		-90	
Alk gen, mg/L	350		239		476		133	
Alk gen, tonne /yr	327		911		52		264	
$/tonne $CaCO_3$	$1,168		$2,491		$2,707		$2,278	

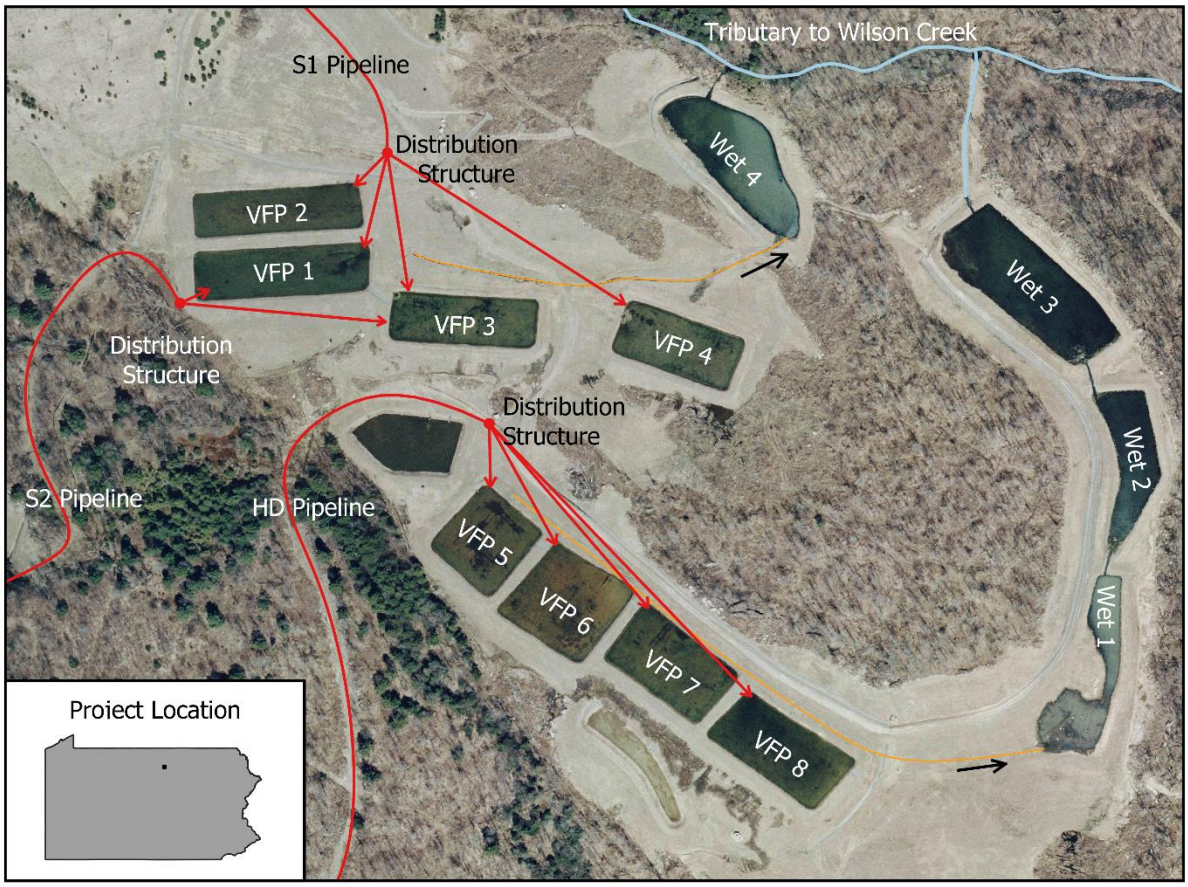

Figure 1. Layout of Anna and HD passive treatment systems and location in Tioga County, Pennsylvania. "VFP" indicates vertical flow ponds. "Wet" are constructed wetlands.

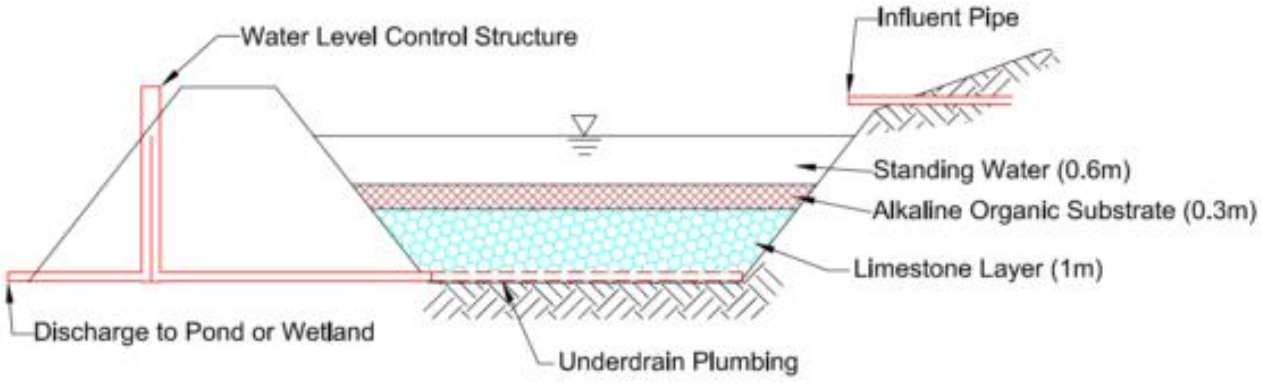

Figure 2. Cross section of vertical flow pond

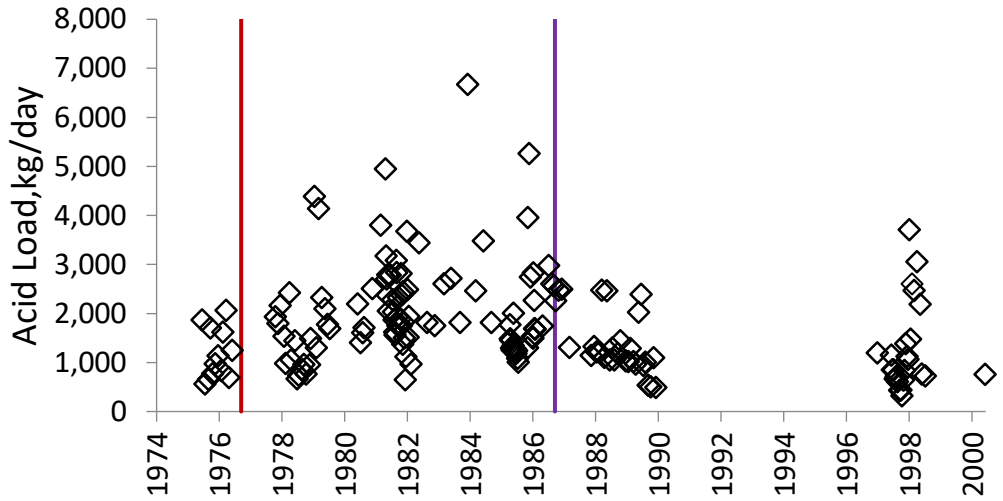

Figure 3. Summed acidity loadings for HD and S1 prior to treatment system installation. Red line is the start of daylighting. Purple line is end of daylighting.

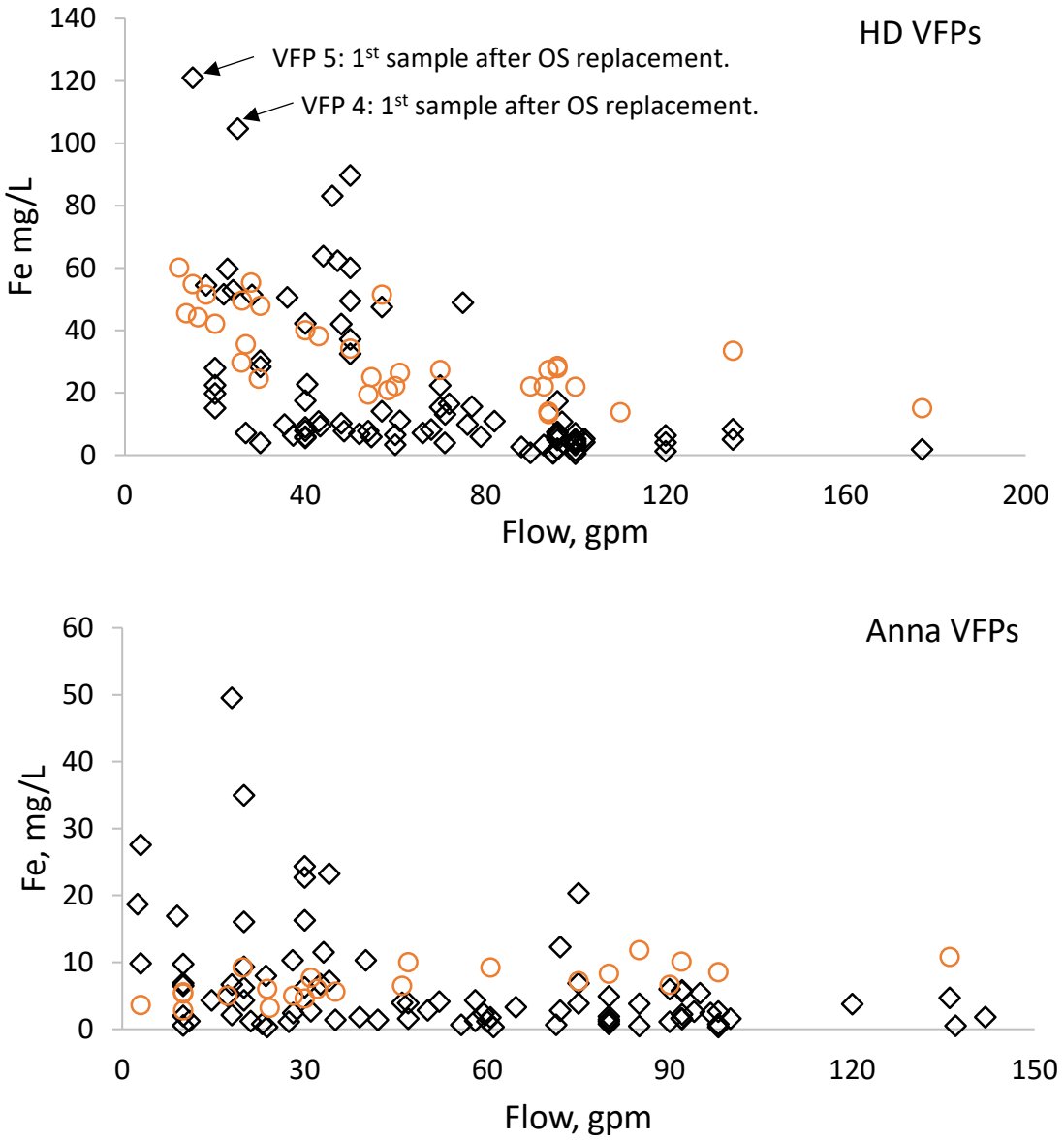

Figure 4. VFP influent (○) and effluent (◇) concentrations of Fe plotted against influent flow rate for the HD and Anna VFPs. "OS" is organic substrate.

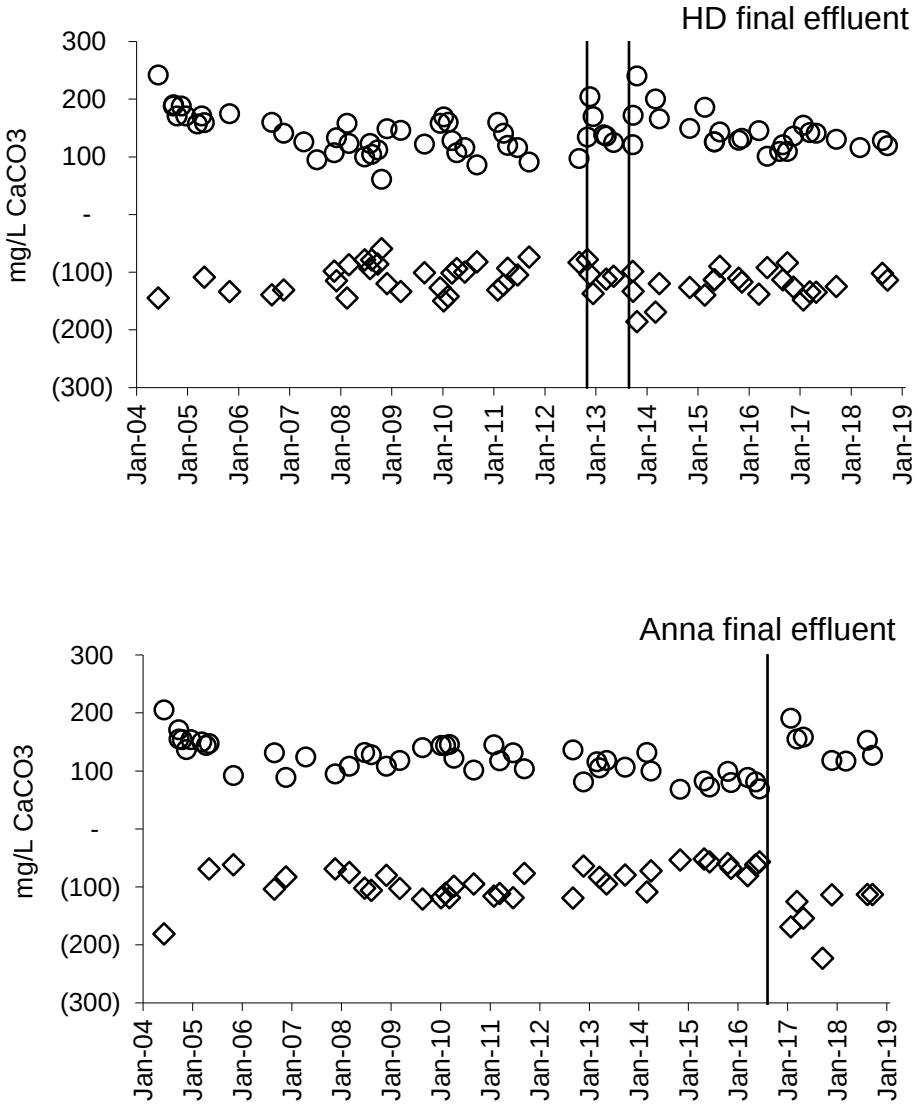

Figure 5. Effluent concentrations of alkalinity (○) and net acidity (◇) for the HD and Anna systems. The vertical lines indicate the substrate replacement events. A measurement of -505 mg/L acidity for the Anna system immediately after the substrate replacement is not shown.

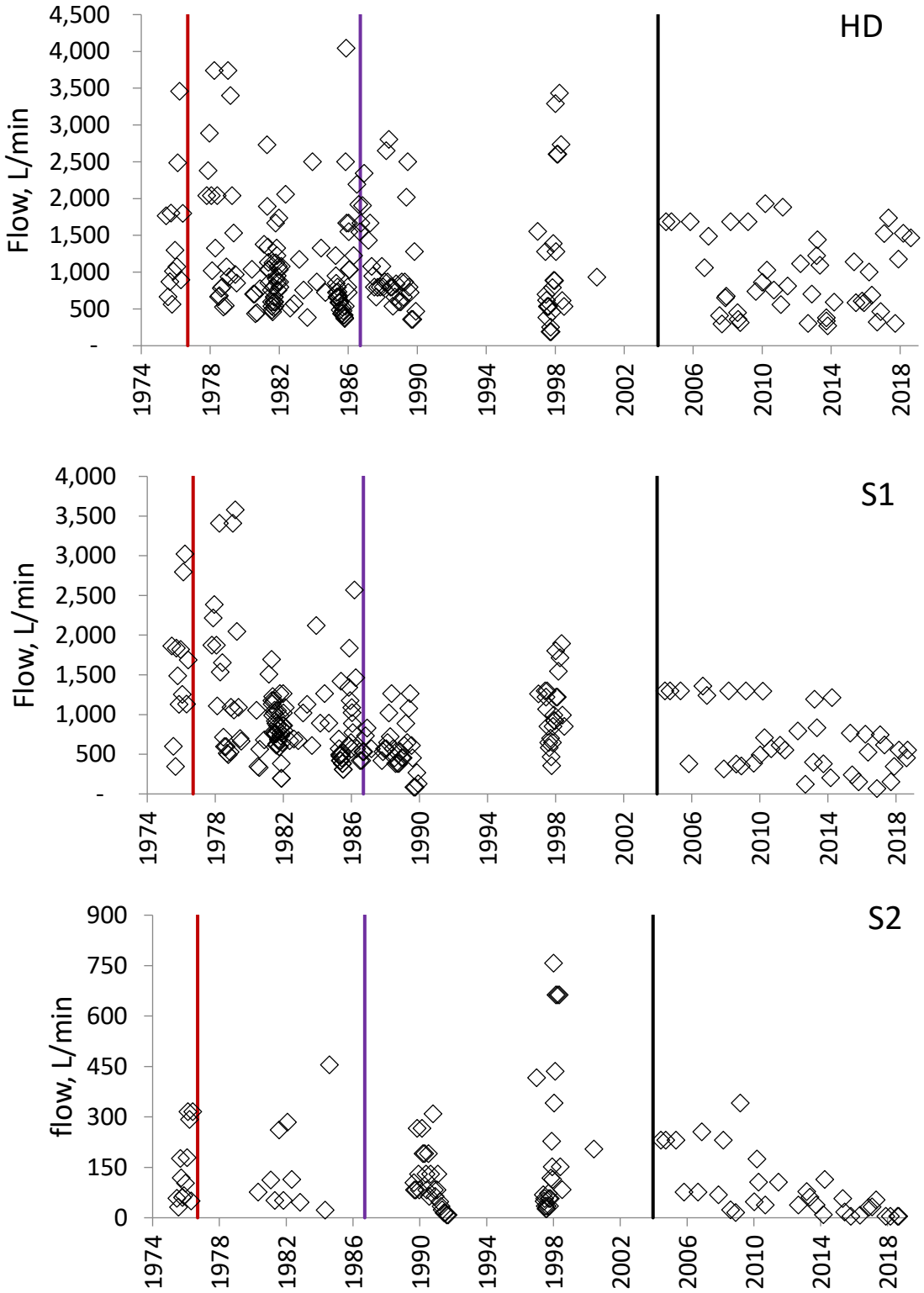

Figure S1. Flow rates for the three discharges. Red line is the start of daylighting. Purple line is the end of daylighting. Black line is installation of treatment system. Flow rates measured since 2004 are at the influent to the treatment systems and are limited by the distribution structures.

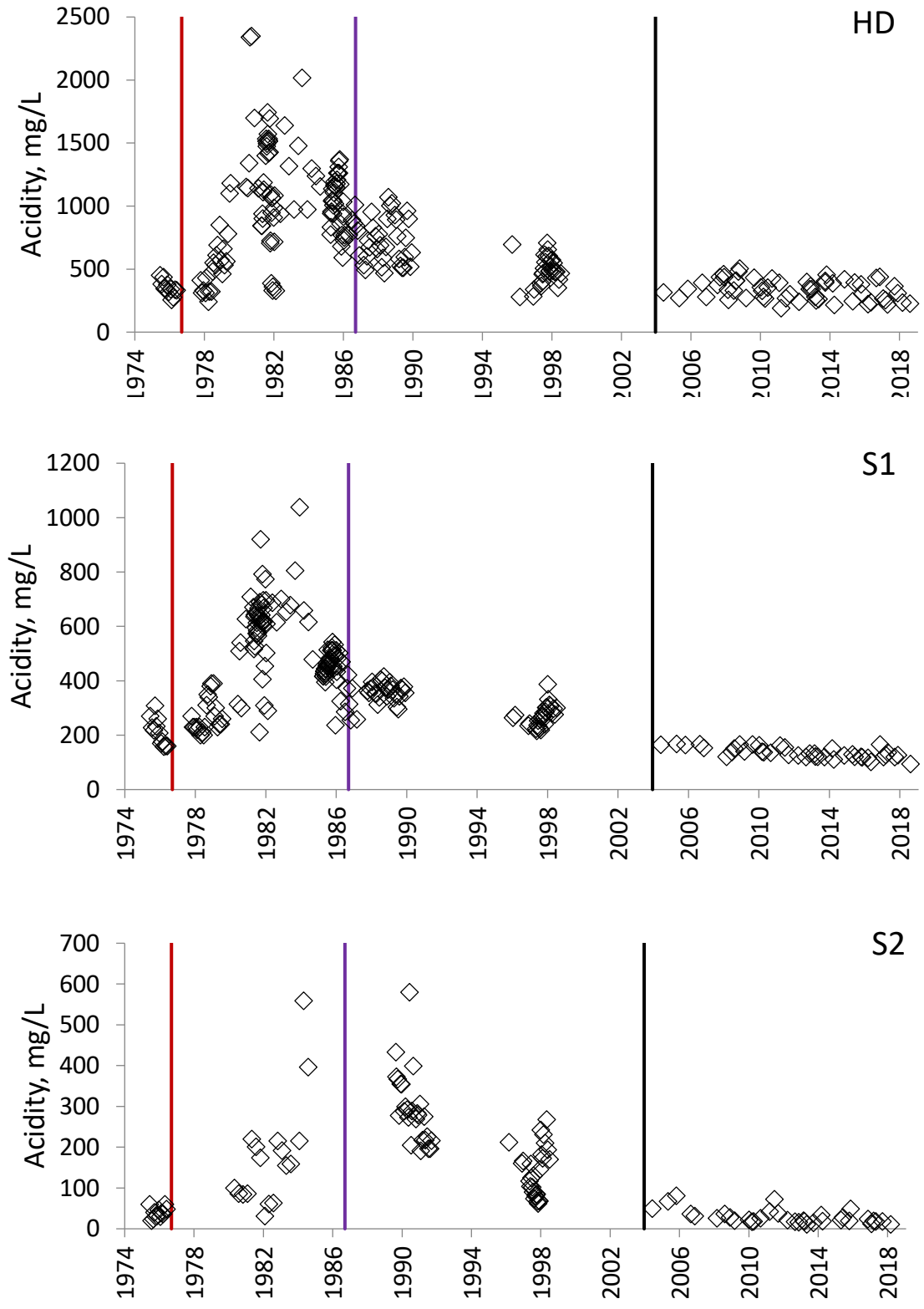

Figure S2. Concentrations of acidity for the three discharges. Red line is the start of daylighting. Purple line is the end of daylighting. Black line is installation of treatment system.

Evaluation of cotreatment of bituminous coal mine drainage in the primary clarifier of municipal wastewater treatment facilities

Travis Tasker and Ben Roman
St. Francis University
Loretto, PA

Abstract: Mine drainage (MD) is a persistent source of pollution throughout the world. While effective at raising the pH and removing dissolved metals from solution via oxidation, sorption, and/or precipitation, both passive and active MD treatment entail significant economic and environmental costs. Another option for MD treatment is utilizing existing municipal wastewater (MWW) treatment facilities to process MD. This approach provides potential benefits for the treatment of both waste streams: 1) the alkalinity present in MWW can raise the pH of MD, allowing dissolved metals to precipitate; and 2) the metals present in MD will react with PO_4 in wastewater by forming metal-PO_4 minerals or by adsorption of PO_4 to metal-hydroxides. However, there are concerns that adding MD to a MWW treatment system could impact the microbial metabolic rates in the aeration basins responsible for removing organics and nutrients from MWW.

In this study, MD from three sites with varying Fe and Al concentrations were mixed with raw MWW in 10% and 40% MD ratios and allowed to settle for two hours (simulating primary clarification in MWW treatment facilities), after which samples were taken from the supernatant and analyzed for pH, metals, PO_4, and BOD consumption. Control reactors using 10% and 40% distilled water were also evaluated. The pH after mixing and settling for two hours remained circumneutral for both 10% and 40% MD solutions. Fe and Al removals were substantial in both 10% and 40% AMD reactors, with dissolved Fe < 5 mg/L and dissolved Al < 1 mg/L in all reactors after mixing and settling for two hours. PO_4 removal from MWW was controlled by the molar ratio of ([Fe]+ [Al])/[PO_4-P] in the initial mixed solution, where PO_4-P removal increased with increasing [Fe] + [Al], and ≥95% PO_4 removal was consistently observed at ([Fe]+[Al])/[PO_4-P] > 2.0. The first-order kinetic rate of BOD removal was not significantly different between the raw MWW, MD reactors, and distilled water reactors used to observe dilution effects, indicating that the addition of bituminous coal MD to MWW treatment facilities will have little-to-no impact on BOD removal rates, given that the pH of the resulting solution remains circumneutral. Additionally, sweep floc coagulation was observed in the 40% Fe+Al MD reactor, which resulted in a ~30% decrease in the ultimate BOD (UBOD) in comparison to the 40% DI reactor. The decreased aeration requirements from removing oxygen demand in the primary clarifier could have substantial impacts on the operational costs of wastewater treatment facilities, where aeration typically accounts for over 50% of the total energy requirements in conventional activated sludge systems. Incorporating AMD treatment in existing WWTP could be an economically viable way to treat AMD while decreasing PO_4 loading in WWTP effluent. However, the alkalinity of MWW and acidity of AMD must be considered to determine appropriate mixing ratios that do impact the microbial metabolisms responsible for MWW treatment.

Monitoring Brown Trout Invasion in a Native Brook Trout Stream Post Mine Drainage Remediation – A Cautionary Tale

Tom Clark and Brianna Hutchison
Susquehanna River Basin Commission
Harrisburg, PA

Abstract: Over the past several decades, there has been a push in Pennsylvania to reclaim abandoned mine lands and remediate acid discharges, thereby mitigating water quality impacts and restoring connectivity to previously fragmented watersheds. Although these restoration activities have obvious benefits to the overall ecosystem, removing the chemical barrier that prevents brown trout from colonizing areas where brook trout have been thriving in isolation could prove detrimental to the latter species. This situation poses a conundrum for natural resource managers as it represents a significant trade-off between ecosystem function and conservation of a declining native species. However, information regarding pre- and post-remediation distributions of brook and brown trout in AMD impacted watersheds is currently lacking.

The Kratzer Run watershed near Curwensville in Clearfield County, Pennsylvania, provides the ideal setting for monitoring distributions, abundance, and movement of brook and brown trout before and after AMD remediation. Previous surveys conducted by the Pennsylvania Fish and Boat Commission (PFBC) in 2015 documented a brook trout-only salmonid population in Bilger Run, a Kratzer Run tributary heavily impacted by acidic discharges. The mainstem of Kratzer Run hosted a mixed population dominated by brown trout. SRBC, starting in 2017, has begun to remediate the four main AMD pollution sources impacting Bilger/Kratzer. Implementation may improve water quality in Bilger Run to the point that the stream can be removed from the list of impaired streams. However, this improvement could also allow brown trout to invade Bilger Run, which could potentially overpower the resident brook trout population.

The Commission, is conducting a long-term study to document the effects of AMD remediation on the distribution and abundance of brook trout in Kratzer Run and the Bilger Run subwatershed and is focused on the following objectives:

1. Documenting pre/post-remediation water quality conditions (water temperature, dissolved oxygen, pH, specific conductance, and turbidity) using YSI sondes;
2. Documenting current distribution and abundance of brook and brown trout populations through electrofishing surveys;
3. Tracking pre/post-remediation movements of brook and brown trout throughout the watershed using Passive Integrated Transponder (PIT) tags.

We hypothesize that low pH caused by untreated discharges is acting as a chemical barrier to brown trout colonization of Bilger Run, and that movement of fish between Bilger Run and Kratzer Run is currently limited.

Mine Pools as a Valuable Municipal and Economic Water Resource in the Central Appalachian Coalfields

Hannah Patton[1] and Ben B. Faulkner[2]

Presented at the 2022 West Virginia Mine Drainage Task Force Symposium. Morgantown, WV October 4-5, 2022.

Abstract: Underground mine pools represent a substantial water resource when water quality is acceptable for the intended use and pool storage and recharge provides a reliable quantity of gravity discharge or pumped flow. In 1981, 72 cities and communities in West Virginia depended solely on mine pools for public water supply. Currently, 30 cities and communities provide safe drinking water from mine pools. While many publicly owned water treatment systems in West Virginia have abandoned their mine water sources, others have included them in the last 40 years. Simultaneously, water line extensions, often funded through the Abandoned Mine Lands Program, have increased the number of households served by public water systems. Many individuals in Appalachia are still not served by a PSD and rely on private water systems, such as roadside "springs" (often mine pool gravity discharges). Examination of water quality at some of these water sources indicates that they may represent a health risk due to bacterial contamination or metal contaminants. A simple point-of-use chlorine disinfection method was evaluated and then shared with spring users. As clean, dependable water sources become increasingly scarce and valuable across the United States and the world, agencies and several entrepreneurs are utilizing mine pools, not only as public drinking water sources, but for aquaculture projects.

---

[1]Hannah Patton, MS, MPH, EIT, CPH, PhD Candidate, Biological Systems Engineering, Virginia Polytechnic Institute & State University. hpatton@vt.edu
[2]Ben B. Faulkner, Field Supervisor - Virginia Tech, Sr. Consultant – Civil & Environmental Consultants, Inc., Environmental Consultant at Bratton Farm. BenBFaulkner@gmail.com

WORKSHOP--PHREEQ-N-AMDTreat model to evaluate water-quality effects from passive and active treatment of mine drainage

Chuck Cravotta, Research Hydrologist, USGS Pennsylvania Water Science Center; cravotta@usgs.gov
Brent Means, Hydrologist, OSMRE Pittsburgh Field Office; bmeans@osmre.gov
Brad Shultz, Mining Engineer, OSMRE Pittsburgh Field Office; bshultz@osmre.gov

Agenda for Workshop (October 5, 2022, 1 - 3:00 pm):

12:00 pm	Box lunch provided to registered participants
1:00 pm	Overview of PHREEQ-N-AMDTreat water-quality modeling tools (Power Point)
1:40 pm	Overview of AMDTreat 6.0 Beta cost-analysis software (Power Point or YouTube video)
2:00 pm	Break
2:10 pm	Live demonstrations of corresponding cost and water-quality models for example passive and active treatment systems
2:30 pm	Group Q&A
2:40 pm	Hands-on participant trials for provided case studies or their own AMD case
3:00 pm	Adjourn

Abstract for Workshop:

AMDTreat 6.0 Beta (2022) is a newly updated computer application for estimating costs and sizing of facilities to abate acid mine drainage (AMD) through application of passive or active treatment technologies. The software has comprehensive cost-analysis modules for passive systems, including vertical flow pond, oxic or anoxic limestone drains, manganese removal bed, aerobic or anaerobic wetlands, and bioreactors, plus active systems, including caustic soda, soda ash, lime products, hydrogen peroxide, permanganate, polymer, and ancillary components such as decarbonation (aeration), conveyance channels, ponds, and clarifiers. The software provides over 400 user modifiable variables for excavation, construction, revegetation, piping, road construction, land acquisition, system maintenance, labor, water sampling, design, surveying, pumping, sludge removal, chemical consumption, and other functions. The default cost data can be modified to adjust for inflation or site-specific requirements. AMDTreat 6.0 also contains several financial and scientific tools to help select and plan treatment systems. These tools include a long-term financial forecasting module, an acidity calculator, a sulfate reduction calculator, a Langelier saturation index calculator, a mass-balance calculator, and iron oxidation tools, plus an integrated version of the PHREEQ-N-AMDTreat "TreatTrainMix2" water-quality modeling tool (Cravotta, 2020, 2021). The integrated PHREEQ-N-AMDTreat tool incorporates all the other scientific tools into a single program to evaluate potential changes in pH, dissolved metals, and associated solute concentrations resulting through sequential steps of passive and active treatment of AMD.

The integrated PHREEQ-N-AMDTreat (TreatTrainMix2) tool and stand-alone PHREEQ-N-AMDTreat tool sets (CausticTitration.exe, ParallelTreatment.exe, and TreatTrainMix2.exe) utilize PHREEQC equilibrium (aqueous and surface speciation) and kinetics models for gas exchange, iron and manganese oxidation and precipitation, limestone dissolution, and organic carbon oxidation combined with reduction of nitrate, sulfate, and ferric iron. Reactions with caustic chemicals (CaO, $Ca(OH)_2$, NaOH, Na_2CO_3) or oxidizing agents (H_2O_2) also may be simulated separately or combined with sequential kinetic steps. A user interface for each stand-alone tool facilitates input of water chemistry and flow data for one or two influent solutions and adjustment of system variables, such as gas-exchange kinetics, abiotic and biological contributions to iron oxidation kinetics, and limestone kinetic properties, without changing the

basic PHREEQC coding. Similar adjustments to key variables can be made with the integrated tool. Graphical and tabular output indicates the changes in pH, specific conductance, total dissolved solids, alkalinity, net acidity, metals, and other solute concentrations of treated effluent plus the cumulative quantity of precipitated solids as a function of retention time or the amount of caustic agent added. By adjusting kinetic variables or chemical dosing, the effects of independent or sequential treatment steps that have different retention times (volume/flow rate), aeration rates, quantities of reactive solids, and temperatures can be simulated for the specified influent quality. The size (land area) of a treatment system can be estimated using reaction time estimates for each of the treatment system components considered in the PHREEQ-N-AMDTreat model. Volume for a corresponding treatment step is computed as the product of reaction time and flow rate; area is computed as the volume divided by depth. Alternatively, given the estimated reaction time to achieve the desired effluent quality, the AMDTreat cost-analysis model may be used to compute the size for each system component and the corresponding costs for installation (capital) and annual operations and maintenance (O&M), with summary results for the net present value of the treatment system as a whole. Thus, various passive and/or active treatment strategies can be identified that could potentially achieve the desired effluent quality, but could require different land areas, equipment, and costs for construction and O&M.

References:

AMDTreat 6.0 Beta (2022) https://www.osmre.gov/programs/reclaiming-abandoned-mine-lands/amdtreat

Cravotta, C.A. III (2020) Interactive PHREEQ-N-AMDTreat water-quality modeling tools to evaluate performance and design of treatment systems for acid mine drainage (software download): U.S. Geological Survey Software Release (https://doi.org/10.5066/P9QEE3D5)

Cravotta, C.A. III (2021) Interactive PHREEQ-N-AMDTreat water-quality modeling tools to evaluate performance and design of treatment systems for acid mine drainage: Applied Geochemistry, v 126, 10845 (https://doi.org/10.1016/j.apgeochem.2020.104845)

AMDTreat 6.0 Beta and PHREEQ-N-AMDTreat Software Access and Installation:

AMDTreat 6.0 Official Web page:

The official web page for AMDTreat 6.0 has links for download of the AMDTreat software, help files, tutorial videos, bug list, and other relevant information.
AMDTreat | Office of Surface Mining Reclamation and Enforcement (osmre.gov)
https://www.osmre.gov/programs/reclaiming-abandoned-mine-lands/amdtreat

AMDTreat 6.0 tutorials, YouTube by AMDTreat team members available online.
https://www.youtube.com/playlist?list=PL-UVrc-RbMgT-Le9ITND0kenZG2muGvFl

Important:

Prior to installing and running AMDTreat Beta 6.0 or PHREEQ-N-AMDTreat software packages, the following prerequisites must be installed:

- Microsoft .NET Framework 4.8 (x86 and x64) Download here
- Install both 32- and 64-bit versions of IPhreeqcCOM Modules:
  IPhreeqcCOM-3.7.3-15968-win32.msi
  IPhreeqcCOM-3.7.3-15968-x64.msi

Administrative privileges may be required to install the above pre-requisites.

Next, the zip files, below, that include the AMDTreat 6.0 Beta and PHREEQ-N-AMDTreat software need to be downloaded and extracted to your computer.

PHREEQ-N-AMDTreat and AMDTreat 6.0 Software for download:

AMDTreat 6.0 Beta and the stand-alone PHREEQ-N-AMDTreat software packages that complement the integrated tool in AMDTreat 6.0 are available at the ftp link below:
ftp://ftpext.usgs.gov/pub/er/pa/new.cumberland/cravotta/

PHREEQ-N-AMDTreatFiles_2021_v1.4.5.zip	*TreatTrainMix2.exe, ParallelTreatment.exe, and CausticTitration.exe tools.*
PHREEQ-N-AMDTreat+REYsFiles_2022_v1.0.1.zip	*TreatTrainMix2REYs.exe and CausticTitrationMix2REYs.exe tools include rare-earth and selected trace elements.*
AMDTreat 6.0 Beta Release_cac.zip	*Same as AMDTreat 6.0 Beta at OSMRE web page but includes all currently available help files in pdf.*

To access any of the above zip files on ftp: Use Windows Explorer to open any folder (e.g. Documents) on your computer. Copy the above ftp link and paste it into the Documents folder address bar, then hit return. Contents of the ftp folder should now show. Copy the selected files and paste on your computer. Administrative privileges should not be needed.

Once downloaded, users should unzip or copy contents of the AMDTreat 6.0 Beta.zip to a user directory on their local computer, and then find the file called **AMDTreat 6.0 Beta.exe** and double click on it to run. The screenshot below shows the directory tree that will be created and the location of the executable file.

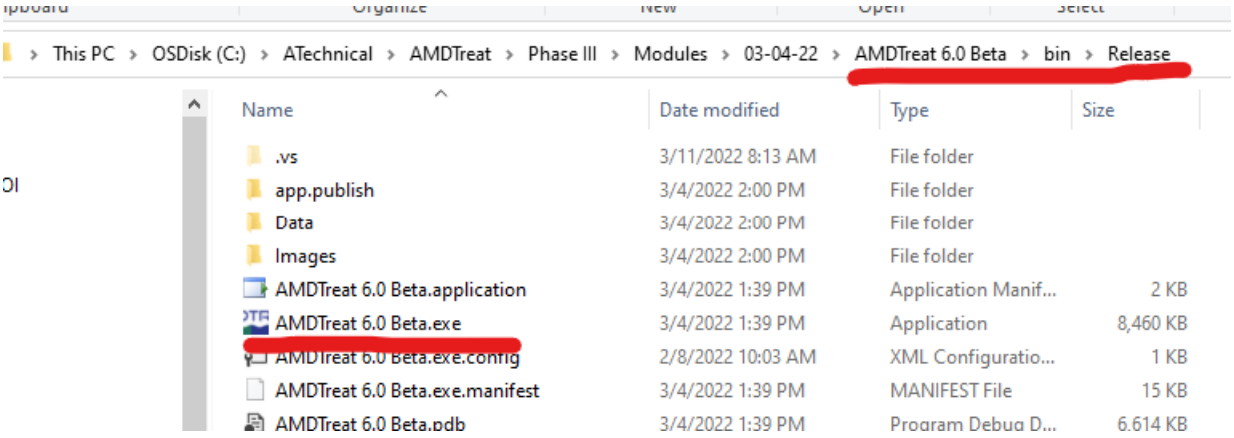

Optional – create a shortcut to the executable program on your desktop:

Navigate to the directory where installed and find the file named AMDTreat 6.0 Beta.exe. Right click on the file and select “send to” from the menu and choose “Desktop”. You can now run the program from this icon that has been created on your desktop.

2022 WV Mine Drainage Task Force Attendee List				
Last Name	**First Name**	**Email**	**Company**	**Work Phone**
Akers	Mark	mark.akers@enviromineusa.com	Chemstream	304-539-1958
Akers	Robert	Robert.Akers@wvhouse.gov	WV House of Delegates	304-673-3616
Andrew	Kelli	kandrew@mail.wvu	WV Water Research Institute	304-677-8495
Ashby	Jim	ashbyjim@msn.com	Ashby Environmental Consulting	301-334-8508
Atkins	Meredith	meredith.atkins@coronadous.com	Greenbrier Minerals, LLC	304-545-7026
Bailey	Clairene	cbailey@osmre.gov	OSMRE	304-347-7158
Ball	Steve	sball@osmre.gov	OSMRE	412-937-2166
Ball	Madison	madison@cheat.org	Friends of the Cheat	304-329-3621
Beam	Richard	rbeam@osmre.gov	OSMRE	814-289-5432
Beckford	Omar	Obeckford@osmre.gov	OSMRE	412-937-2118
Bess	Danny	dbess@SomersetInternational.com	SI	412-475-1727
Bolyard	Russell	rbolyard@lpmineral.com	LP Mineral LLC	304-296-7531
Bonner	Josh	joshua.t.bonner@wv.gov	WVDEP	304-457-3219
Bostic	Jason	jbostic@wvcoal.com	West Virginia Coal Association	304-610-1343
Bowen	Cheryl	Cheryl.E.Bowen@wv.gov	WVDEP	304-239-8338
Brown	Kristin	kbrown2@osmre.gov	US Dept of the Interior - OSMRE	303-236-3410
Brown	Kristin	kbrown2@osmre.gov	US Dept of the Interior - OSMRE	303-236-3410
Buchanan	Steve	sbuchanan@thethrashergroup.com	The Thrasher Group	304-844-8315
Butler	Matthew	matthew.c.butler@wv.gov	WV DEP	304-574-4465
Caccese	Matthew	mcaccese@pa.gov	PA DEP, BAMR	570-826-2371
Calhoun	Roger	calhounroger60@yahoo.com	Retired from OSM	304-895-3149
Campbell	James	isaac_24938@yahoo.com	Spring Creek Contract & Consult	304-646-0290
Carey	John	john.carey@maryland.gov	MDE	301-689-1442
Carey	John	john.carey@maryland.gov	MDE	301-689-1442
Carico	Mike	mike0carico@gmail.com	WVDEP-Retired	304-777-9841
Carpenter	Mike	mrc26288@gmail.com	Retired	304-880-0678

Castle	Michael	mcastle@osmre.gov	OSMRE	859-260-3900
Castro	Nathalia	ncastro@solmax.com	TenCate Geosynthetics	813-928-9991
Cavazza	Eric	eric.cavazza@tetratech.com	Tetra Tech, Inc.	412-522-9764
Ceslovnik	Jonathan	jfceslovnik@ecolab.com	Nalco Water	304-610-2195
Christ	Martin	Martin.J.Christ@wv.gov	WVDEP	304-932-5741
Chverchko	Daniel	dchverchko@pa.gov	PA DEP - DMO	814-242-6581
Clark	Tom	tclark@srbc.net	Susquehanna River Basin Com.	717-238-0423
Constant	James	james.constant@mail.wvu.edu	WVWRI	304-293-7009
Cook	Bobby	bcook@saulsseismic.com	Sauls Seismic, LLC	304-752-2499
Cook	Thomas	tcook@navigatortechnical.com	Navigator Envn & Technical Serv	304-586-6280
Cravotta	Charles	cravotta@usgs.gov	U.S. Geological Survey	484-650-5327
Crisst	James	Jamescriss@snf.com	SNF Mining	681-208-3161
Cruz	Shauntelle	scruz@osmre.gov	OSMRE	412-937-3001
Culver	William	william@innoh2osolutions.com	InnoH2O Solutions LLC	814-445-4491
Dailey	Brian	Bdailey@osmre.gov	OSMRE	412-937-2122
Danehy	Tim	timdanehy@biomost.com	BioMost, Inc.	724-776-0161
DeFranco	John	john@amdindustriesinc.com	AMD Industries, Inc.	724-938-2657
Derberry	Dalton	dderberry@neosolutionsinc.com	Neo Solutions Inc.	724-480-9509
Dietz	Jon	jdietz.iot@gmail.com	Iron Oxide Technologies	814-404-3227
Doss	Barry	bdoss@dei-wv.com	Doss Engineering, Inc	304-595-2845
DuBois	Deborah	deborah.dubois@mail.wvu.edu	WVU Research Corp., WRI	304-293-7083
DuBois	Gary	gary.dubois@frontier.com	GMD Consultants, LLC	724-833-7779
Fancher	Ben	benjamin.fancher@wv.gov	WV DEP	
Faulkner	Ben	benbfaulkner@gmail.com	Bratton Farm	304-920-0627
Feltner	Jacob	Jacob@KirkEnvironmental.US	Kirk Environmental, LLP	304-222-0522
Ferguson	Malcolm	mferguson@somersetenvironmental.com	SES	412-475-1727
Fillhart	Jason	jason.fillhart@mail.wvu.edu	WV Water Research Institute	304-293-7066
Flippin	Jennifer	jennifer_flippin@nps.gov	National Park Service	304-465-6513
Fox	Jason	jason.d.fox@wv.gov	WV DEP	304-574-4465
Fulton	Robbie	rfulton@osmre.gov	OSMRE	412-510-1611
Gehlhar	Mark	mgehlhar@osmre.gov	OSMRE	202-208-2716

Gibson	Scott	sgibson@mepcollc.net	Mepco, LLC	304-296-9701
Gillian	Martin	marting@chemtreat.com	Chemtreat Virginia	540-676-4455
Glascock	Caitlin	caitlin.glascock@mail.wvu.edu	WVWRI	304-293-7006
Gray	Bryan	bryan.c.gray@wv.gov	WV DEP	304-574-4465
Green	Kelsea	kelsea@biomost.com	BioMost, Inc.	814-771-4868
Green	John	jodgree@pa.gov	PA DEP, BAMR	570-830-3134
Green	Kelsea	kelsea@biomost.com	BioMost, Inc.	724-776-0161
Greenfield	Lauren	lauren.greenfield@mbakerintl.com	Michael Baker International	412-269-2939
Greenfield	Gregory	grgreenfie@pa.gov	PA DEP BAMR	717-787-3174
Gump	Katarina	kgump@ironsenergy.com	Iron Senergy	724-825-3806
Guy	Daniel	dan@biomost.com	BioMost, Inc.	724-776-0161
Gwinn	Jami	jgwinn@archrsc.com	Arch Resources	304-549-4823
Hajas	Mark	mark.hajas@maryland.gov	MDE	301-689-1445
Halstead	Lewis	lhalstead@cumberlandsurety.com	Indemnity National Insurance Co	304-550-1104
Hammond	Scott	scotthammo@pa.gov	PA DEP - Moshannon District Off	814-505-3252
Hamric	Ron	rlhamric@icloud.com	Task Force Member	304-288-0479
Hardin	Scott	shardin@snf.com	SNF Mining	304-860-8849
Hauck	Logan	logan@biomost.com	Biomost Inc.	814-979-6808
Hedin	Bob	bhedin@hedinenv.com	Hedin Environmental	412-977-4234
Heflin	William	mou10eer@hotmail.com	Quinwood Coal Company	304-846-6600
Henkes	Colin	colin.a.henkes@wv.gov	WVDEP	304-574-4465
Henthorn	Jennie	jennie@henvtl.com	Henthorn Environmental	304-727-1445
Hilton	Tiff	wopec@suddenlink.net	WOPEC	304-645-7633
Hilton	Tiff	ghilton@osmre.gov	OSMRE	618-463-6460
Hoadley	Charles	choadley@greerindustries.com	Greer Industries, Inc.	304-216-6099
Hoffman	David	david.hoffman@mail.wvu.edu	WVWRI	304-293-7006
Hynes	Greg	greg.hynes@tetratech.com	Eng.Proj Mgr II Civil PM.	330-286-3683
Iman	Craig	ciman@neosolutionsinc.com	Neo Solutions	724-728-1847
Jansure	Eric	ejansure@pa.gov	PA DEP, BAMR	814-472-1800
Jenkins	Michael	mjj@aquafix.com	Aquafix Systems, Inc.	304-282-1801
Johnson	Ken	kej5867@yahoo.com	Golden Eagle	304-742-5867
Jones	Derick	djones@osmre.gov	OSMRE	618-463-6460

Joseph	Bill	bjoseph@osmre.gov	OSMRE	618-463-6460
Kearns	Mike	mike.kearns@tetratech.com	Tetra Tech, Inc.	740-298-9066
Kirk	Ed	Ed@KirkEnvironmental.US	Kirk Environmental, LLP	540-570-3149
Kisner	Scott	skisner@greerindustries.com	Greer Industries, Inc.	304-276-5263
Kitchen	Tracie	tracie.a.kitchen@wv.gov	WVDEP	304-239-8337
Kleinmann	Bob	robert.kleinmann@gmail.com	Mine Water and the Environment	412-973-4341
Knepper	Jeffrey	jeffk@ascentconsultigengineers.com	Ascent Consulting & Engineering	304-931-9870
Kortas	John	jkortas@frontier.com	New Allegheny, Inc.	304-457-9899
Koury	Daniel	dkoury@pa.gov	PA DEP, Bureau of Mining	570-640-8879
Kreitzer	Sarah	skreitzer@osmre.gov	OSMRE	412-937-2874
Kreps	Jared	jkreps@snf.com	SNF Mining	304-860-8849
Lambert	Russ	rlambert@alphametresources.com	Alpha Metallurgical Resources	304-369-3689
Lavender	Leslie	llavender@coronadoglobal.com	Coronado Coal LLC	304-206-8363
Lavender	Nathaniel	nllavender8@gmail.com	Spring Creek Contract & Consult	304-932-1626
Lilly	Ron	rlammonia@yahoo.com	Mallard Environmental Services	304-787-5550
Logan	Marisa	mlogan@cecinc.com	Civil & Environ Consultants, Inc.	412-429-2324
Maggard	Randall	randallmaggard@acnrinc.com	ACNR Resources, Inc.	304-544-4956
Mann	Richard	rmann@osmre.gov	OSMRE	865-545-4103
Marino	Nick	jmarino@snf.com	SNF Mining	304-641-1757
Martin	Rock	rmartin@osmre.gov	OSMRE	717-919-3756
Martin	Hunter	hunterm@chemtreat.com	ChemTreat	434-258-6635
Martinez	Daniel	dmartinez@cecinc.com	Civil & Environ Consultants, Inc.	304-203-8655
Mastrorocco	Tom	tmastrorocco@osmre.gov	OSMRE	412-937-2939
Matthews	Doug	doug.k.matthews@wv.gov	WV DEP/Div. Land Restoration	304-926-0440
McCluskey	Mike	mike@innoh2osolutions.com	InnoH2O Solutions LLC	814-445-4491
McCoy	David	david.b.mccoy@wv.gov	WV DEP	304-203-2921
McElwayne	Scott	scott.mcelwayne@wv.gov	WV DEP	304-314-6158
McPeek	Jamie	jamie.mcpeek@coronadous.com	Greenbrier Minerals, LLC	304-946-5356
Means	Brent	bmeans@osmre.gov	OSMRE	717-919-3982
Meck	Angela	Angela.Meck@tetratech.com	Tetra Tech, Inc.	570-449-4054
Meeks	Teresa	tmeeks@solmax.com	TenCate	304-409-8704
Miller	Tim	tim.miller@maryland.gov	MDE	301-689-1465

Miller	Corey	ctmiller@osmre.gov	OSMRE	859-260-3900
Mills	Joe	jmills@skellyloy.com	Skelly and Loy	304-590-4300
Morgan	Justin	Jmorgan@osmre.gov	OSMRE	606-657-4115
Morgan	John	john.morgan@respec.com	Respec	859 361 8392
Morosetti	Matt	j.servick@wkmerriman.com	W. K. Merriman Inc.	412-262-7024
Morris	Jacob	jam0172@mail.wvu.edu	WVU Water Research Institute	304-293-6968
Morris	Mark	mmorris@blackhawkmining.com	Blackhawk Mining LLC	304-550-8331
Mulheren	Bill	bill.mulheren@resfuel.com	Robindale Energy Services	724-388-4654
Neely	Buck	buck@biomost.com	BioMost, Inc.	724-776-0161
Neider	William	wneider@mbakerintl.com	Michael Baker International	724-495-4225
Ntumngia	Rose	rntumngia@osmre.gov	OSMRE	202-208-2867
O'Dell	Sam	sam.odell@enviromineusa.com	Chemstream	304-552-2543
O'Neal	Melissa	melissa.oneal@mail.wvu.edu	WV Water Research Institute	304-2937006
Owens	Ben	bowens@osmre.gov	OSMRE	412-512-7369
Pachol	Stephen	stevepachol@yahoo.com	Retired	304-290-4248
Parks	Nathan	nathan.l.parks@wv.gov	WV DEP	304-574-4465
Parsons	Travis	travis.g.parsons@wv.gov	WV DEP/Div. Mining/Reclam	304-926-0499
Patton	Hannah	hpatton@vt.edu	Virginia Tech	240-812-2976
Peacock-Jones	Kristina	kpeacockjo@pa.gov	PA DEP, BAMR	717-329-1186
Pehur	Joe	birdmine@gmail.com	AMD Industries, Inc.	724-938-2657
Perry	Mark	mark.perry@tetratech.com	Tetra Tech, Inc.	412-921-7217
Petry	David	david.w.petry@wv.gov	WV DEP	304-842-1900
Phillips	Gregory	gregory.r.phillips@wv.gov	WV DEP	304-314-6163
Pino	Richard	richard.l.pino@wv.gov	WV DEP	304-574-4465
Pitzer	Amanda	amanda@cheat.org	Friends of the Cheat	304-329-3621
Polce	Terry	terry.polce@mail.wvu.edu	WV Water Research Institute	304-293-7041
Polenik	Jeff	jeff.polenik@resfuel.com	Robindale Energy Services, Inc.	814-525-1373
Poljak	Paul	ppoljak@somersetenvironmental.com	SES	412-475-1727
Pontzer	Aaron	apontzer@pa.gov	DEP - Moshannon District Mining	814-923-9502
Pugh	Katie	katie.pugh@tetratech.com	Tetra Tech, Inc.	412-921-8868
Quinlan	Scott	SCOTT.QUINLAN@tetratech.com	Tetra Tech	412-584-4508

Ramsey	Adam	aramsey@osmre.gov	OSMRE	865-545-4103
Revetta	Nick	revettanp@cdmsmith.com	CDM Smith	614-847-6817
Reynolds	Justin	just_inn90@yahoo.com	Amer Consolidated Natural Res.	304-288-9004
Rice	Robert	robert.rice@wv.gov	WV DEP	
Roberts	Doug	douglas.d.roberts@wv.gov	WV DEP/Div. Land Restoration	304-926-0499
Rockwell	Josh	jrockwell@osmre.gov	OSMRE	412-937-3004
Roddy	David	davidroddy@acnrinc.com	Amer Consolidated Natural Res.	304-410-8403
Roman	Benjamin	broman@francis.edu	Saint Francis University	724-678-3414
Rorrer	Jon	jonathan.rorrer@wv.gov	WV DEP	
Rowley	Matt	matthew.rowley@maryland.gov	MDE	301-689-1444
Schaer	Andrew	aschaer@osmre.gov	OSMRE	304-347-7158
Schafer	Erik	erik.schafer@maryland.gov	MDE	301-689-1462
Schmidt	Terry	tschmidt@earthres.com	EARTHRES GROUP, INC.	267-446-9145
Schmidt	Terry	tschmidt@earthres.com	EARTHRES GROUP, INC.	267-446-9145
Seckman	Jimmie	jseckman@3wlogic.net	WVDEP	304-613-4521
Seckman	Dian	dmitchelle@3wlogic.net	WVDEP	304-613-4520
Self	Stefanie	SSelf@osmre.gov	OSMRE	412-937-2105
Servick	Joe	j.servick@wkmerriman.com	W.K. Merriman, Inc.	412-262-7024
Shafer	Jamie	jamie.m.shafer@wv.gov	WV DEP/Div. Land Restoration	304-848-2111
Sheehan	Mike	mike.sheehan@tetratech.com	Tetra Tech, Inc.	304-212-3600
Shope	Thomas	tshope@osmre.gov	OSMRE	412-512-7369
Shultz	Bradley	bshultz@osmre.gov	OSMRE	717-576-2950
Siefert	Eliza	eliza.siefert@mail.wvu.edu	WV Water Research Institute	304-615-6862
Simmons	Walter	walter.g.simmons@wv.gov	WV DEP	304-926-0499
Sisson	Mike	msisson@navigatortechnical.com	Navigator Environmental	304-389-0943
Skousen	Jeff	jskousen@wvu.edu	West Virginia University	304-293-2667
Snyder	Jeff	jeff.snyder@maryland.gov	MDE	301-689-1443
Spirnak	Rachel	rachel.pell@mail.wvu.edu	WV Water Research Institute	304-293-6968
Stephens	Tom	tstephens@solmax.com	TenCate	404-660-2317
Stone	Steve	sstone@navigatorenvironmental.com	Navigator Environmental	304-222-9291
Stuart	Robert	robert.s.stuart@wv.gov	WV DEP	304-848-2073

Surles	Shelley	shelleyd212@yahoo.com	Alpha Metallurgical Resources	276-608-3434
Tasker	Travis	ttasker@francis.edu	Saint Francis University	724-822-6163
Taylor	Darrell "Jason"	dtaylor@osmre.gov	OSMRE	606-657-4108
Tichinel	Rodney	rtichinel@archrsc.com	Arch Resources	304-813-7993
Toler	Chris	ctoler@archrsc.com	Arch Resources	304-226-2116
Tracey	Adam	adam.s.tracey@wv.gov	WV DEP	304-314-6182
Trump	Jeffrey	jtrump@osmre.gov	OSMRE	412-937-2918
Uranowski	Lois	loisbutter@yahoo.com	Retired	412-759-8469
Vanhouten	Lisa	Lisa@FullCircleMushroomCompost.com	Full Circle Mushroom Compost	610-331-1849
Vilseck	Keith	KeithVIlseck@acnrinc.com	ACNR Coal Services Group, Inc.	937-776-6614
Vukovich	Sheila	sheila.m.vukovich@wv.gov	WV DEP/Div. Land Restoration	304-848-2117
Wagner	Richard	rwagner@musserengineering.com	Musser Engineering, Inc.	814-754-8477
Wigal	Mark	mwigal@greerindustries.com	Greer Industries, Inc.	304-413-3503
Williams	Laurence	laurence.b.williams@wv.gov	WV DEP	304-314-6186
Williams	Kenny	Kwilliams@alphametresources.com	Alpha Met Resources	304-854-3054
Winters	Marybeth	marybeth.winters@mma1.com	Marshall Miller & Associates, Inc.	304-250-4753
Wood	Todd	twood@pa.gov	PA DEP, BAMR	570-826-2371
Worley	P. Andy	Pworley@alphametresources.com	Alpha Met Resources	304-854-3007
Wright	Chester	chester.k.wright@wv.gov	WV DEP	304-457-4588
Yoho	Seth	SYOHO@wfatrees.com	Williams Forestry & Associates	304-244-9380
Ziemkiewicz	Paul	paul.ziemkiewicz@mail.wvu.edu	WV Water Research Institute	304-293-6958
Zirkle	Amaris	amaris.k.zirkle@wv.gov	WVDEP	304-314-6191

West Virginia coal...

...Firing the furnaces that forge a better world.

WV COAL Friends of Coal

Proudly representing those who mine the world's fuel of choice.

Visit www.wvcoal.com and follow us online!
@friendsofcoalwv www.facebook.com/friendsofcoal/

Practical, Efficient, Cost-Effective AMD Treatment

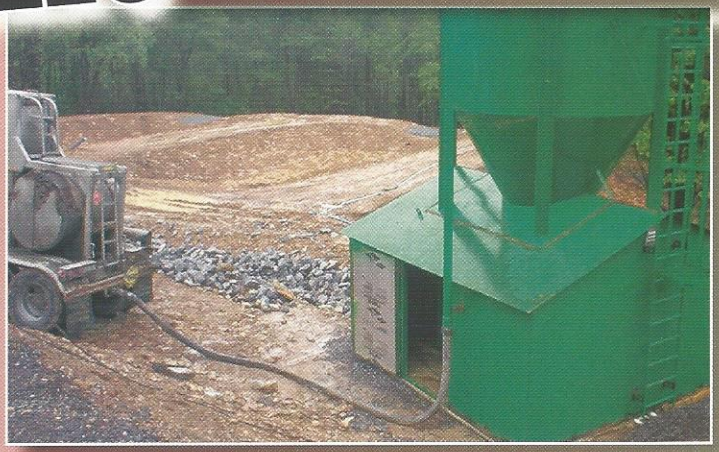

The Proven System

AQUAFIX

301 Maple Lane, Kingwood, WV 26537
Phone (304) 329-1056
www.aquafix.com

Protecting people. For decades

The effects upon the environment

The protective solution

Fox River, Wisconsin, USA

TENCATE
Geotube®

The proven dewatering solution

TenCate Geotube® technology has proven to be exceptionally valuable as a dewatering solution. This proven and cost effective containment technology is applied worldwide in marine remediation, mining and mineral processing, power and utility, contaminated sludge processing, municipal applications, industrial processing, agriculture and aquaculture. Our high strength woven fabric and systems are protecting people. In past decades and decades to come.

ECONOMICAL

- Shortened total project time
- On-site containment and consolidation
- Reduced overall cost

ECOLOGICAL

- Consolidates solids in to manageable form
- Low CO_2 footprint
- Provides flexible, green solutions

SOCIAL

- Protection from airborne contamination
- Minimal noise and odor
- Cleaner waterways

www.tencategeo.com
www.geotube.com

TENCATE GEOSYNTHETICS

Applied Geochemistry 126 (2021) 104845

Contents lists available at ScienceDirect

Applied Geochemistry

journal homepage: http://www.elsevier.com/locate/apgeochem

Interactive PHREEQ-N-AMDTreat water-quality modeling tools to evaluate performance and design of treatment systems for acid mine drainage

Charles A. Cravotta III

Research Hydrologist, U.S. Geological Survey, Pennsylvania Water Science Center, 215 Limekiln Rd, New Cumberland, PA, 17070, USA

ARTICLE INFO

Editorial handling by Dr. Z Zimeng Wang

Keywords:
Acid mine drainage
Metals
Treatment
Water quality model
Kinetics
Adsorption
PHREEQC

ABSTRACT

The PHREEQ-N-AMDTreat aqueous geochemical modeling tools described herein simulate changes in pH and solute concentrations resulting from passive and active treatment of acidic or alkaline mine drainage (AMD). The "user-friendly" interactive tools, which are publicly available software, utilize PHREEQC equilibrium aqueous and surface speciation models and kinetics models for O_2 ingassing and CO_2 outgassing, iron and manganese oxidation and precipitation, limestone dissolution, and organic carbon oxidation combined with reduction of nitrate, sulfate, and ferric iron. Reactions with synthetic caustic chemicals (CaO, $Ca(OH)_2$, NaOH, Na_2CO_3) or oxidizing agents (H_2O_2) also may be simulated separately or combined with sequential kinetic steps. A user interface facilitates input of water chemistry data for one or two (mixed) influent AMD solutions and adjustment of kinetic variables. Graphical and tabular output indicates the changes in pH, metals and other solute concentrations, total dissolved solids, and specific conductance of treated effluent plus the cumulative quantity of precipitated solids as a function of retention time or the amount of caustic agent added. By adjusting kinetic variables or chemical dosing, the effects of independent or sequential treatment steps that have different retention time (volume/flow rate), aeration rate, quantities of reactive solids, and temperature can be simulated for the specified influent quality. The size (land area) of a treatment system can then be estimated using reaction time estimates (volume for a corresponding treatment step is the product of reaction time and flow rate; area is volume divided by depth). Given the estimated system size, the AMDTreat cost-analysis model may be used to compute approximate costs for installation (capital) and annual operations and maintenance. Thus, various passive and/or active treatment strategies can be identified that could potentially achieve the desired effluent quality, but require different land area, equipment, and costs for construction and operation.

1. Introduction

Contaminated drainage and associated metal-rich precipitates from abandoned coal and metal mines degrade aquatic habitats and affect the potential utilization of water resources in mining regions worldwide. The mine effluents can have a wide range of pH values (2–8) along with elevated concentrations of SO_4, Fe, Al, Mn, and other constituents (Blowes et al., 2014; Cravotta, 2008a; Feng et al., 2014; Gombert et al., 2018; Li, 2018; Nordstrom, 2011a, 2011b). Although various trace elements, such as Zn, Cd, Co, Cu, Pb, Ni, As, Se, and others, can be present at concentrations that approach or exceed aquatic toxicity thresholds, dissolved concentrations of Fe, Al, and Mn account for most metals loading from coal mines (Cravotta, 2008a; Cravotta and Brady, 2015; Feng et al., 2014; Gombert et al., 2018). Metal-mine drainage generally overlaps the composition of coal-mine drainage and produces similar precipitates but can have more extreme values for pH, sulfate, and trace-element concentrations (Nordstrom, 2011a). After exposure to atmospheric conditions, dissolved Fe, Al, and Mn tend to precipitate as ochreous encrustations composed of amorphous to poorly crystalline Fe^{III}- and Al-hydroxide and hydroxysulfate compounds, including ferrihydrite ($Fe(OH)_3$), schwertmannite ($Fe_8O_8(OH)_6SO_4$), goethite (FeOOH), boehmite (AlOOH), gibbsite ($Al(OH)_3$), and basaluminite ($Al_4(OH)_{10}SO_4$) (Bigham et al., 1996; Bigham and Nordstrom, 2000; Cravotta, 2005, 2008a, 2008b; Kairies et al., 2005; Lozano et al., 2020; Robbins et al., 1999a; Sánchez-España et al., 2016; Winland et al., 1991), plus locally important $Mn^{III\text{-}IV}$ hydroxides and oxides (Cravotta and Trahan, 1999; Cravotta and Watzlaf, 2003; Kairies et al., 2005; Santelli et al., 2010; Tan et al., 2010).

Treatment of acidic or alkaline mine drainage (AMD) to attenuate dissolved metals can decrease acidity (Kirby and Cravotta, 2005) and contaminant loadings to streams, potentially mitigating aquatic impacts. At active mining operations, aggressive aeration and/or the addition of

E-mail address: cravotta@usgs.gov.

https://doi.org/10.1016/j.apgeochem.2020.104845
Received 2 September 2020; Received in revised form 24 November 2020; Accepted 27 November 2020
Available online 1 December 2020

alkaline (caustic) chemicals (NaOH, CaO, $Ca(OH)_2$) or oxidizing agents (H_2O_2) may be used along with polymers to facilitate the precipitation and settling of metal-rich (Al, Fe, Mn) solids (Cravotta and Brady, 2015; Cravotta et al., 2015; Skousen et al., 2017, 2019; U.S. Environmental Protection Agency, 1983). At abandoned mines, passive treatment using natural substrates, such as limestone and organic-rich compost, may be combined with aeration cascades to increase alkalinity, pH, and O_2 with associated attenuation of metals concentrations (Geroni et al., 2012; Hedin et al., 1994; Johnson and Hallberg, 2005; Watzlaf et al., 2004). Decreased concentrations of trace metals concomitant with increased pH during mine-water treatment are consistent with their attenuation by coprecipitation or adsorption with hydrous Fe^{III} oxides (HFO), hydrous Al oxides (HAO), and hydrous Mn^{III-IV} oxides (HMO) (Burrows et al., 2017; Cravotta et al., 2015; Cravotta and Brady, 2015; Cravotta and Trahan, 1999; Cravotta and Watzlaf, 2003; Kairies et al., 2005). These hydrous metal oxides (HMeO) in AMD treatment systems and associated aquatic environments may be present as discrete phases or combined with other sorbent materials as components of particulate matter, sediments, and biofilms (e.g. Ashby, 2017; Burgos et al., 2012; Chen and Thompson, 2018; Coston et al., 1995; Hedin et al., 2019; Kairies et al., 2005; Lofts and Tipping, 1998; Munk et al., 2002; Tipping et al., 2011; Webster et al., 1998; Winland et al., 1991).

A specific water-treatment strategy may be appropriate for a mine effluent depending on variations in its flow rate and chemistry, site characteristics, funding, and operational logistics plus the chemical and biological characteristics of the receiving water body (Pennsylvania Department of Environmental Protection, 2016). Empirical testing of aeration rate, chemical dosing, and/or contact time with limestone or other substrates can (1) demonstrate the potential effectiveness of a treatment method to meet criteria for discharge and the protection of aquatic life and (2) be useful to indicate system sizing and estimate associated costs (e.g. Cravotta, 2003; 2007; 2008; 2015; Cravotta and Watzlaf, 2003; Cravotta et al., 2008; 2015; Means and Hilton, 2004; Watzlaf and Hedin, 1993; Watzlaf et al., 2004). However, the empirical data, if available, may not demonstrate variations in treatment resulting from changes in the flow rate, water quality, temperature, and other environmental conditions. Geochemical modeling coupled with cost-analysis software, such as AMDTreat (Office of Surface Mining Reclamation and Enforcement, 2017; Cravotta et al., 2015), may be applied to identify and evaluate treatment strategies for the potential range of variations in influent water quality and to compare costs for construction and operation of different treatment methods that produce the desired effluent quality.

In this paper, a novel geochemical tool set is presented that couples aqueous and surface complexation equilibrium with kinetics models to simulate potential changes in water quality during passive and active treatment of AMD. The reactions considered may occur in various environmental settings and affect a wide range of major and trace elements; however, the current scope of modeling and this paper are limited to those constituents (acidity, Al, Fe, Mn, and SO_4, plus total dissolved solids and specific conductance) that are the focus of pollutant discharge regulations at coal mines in the USA. Although the geochemical tool set can be used independently, it was developed for eventual incorporation with AMDTreat, which is currently (2018–2020) being recoded from FoxPro to C++ (Cravotta, 2018). This paper provides background on the software development, describes relevant rate expressions and associated sources of information, explains some of the options for adjusting variables, and provides examples for the potential application and interpretation of modeling results.

2. Materials and methods

The PHREEQ-N-AMDTreat water-quality modeling tools, accessible in the U.S. Geological Survey software release (Cravotta, 2020) and with supplemental data, were developed by building on previous PHREEQC (Parkhurst and Appelo, 2013) geochemical codes reported by Cravotta (2015) and Burrows et al. (2017). The modified PHREEQC code was adapted to run using IPhreeqcCOM (Charlton and Parkhurst, 2011) with an expanded thermodynamic database and a user interface (UI) for input and adjustment of the modeled variables. The code combines equilibrium aqueous and surface speciation and kinetics equations for gas exchange, aqueous Fe^{II} and Mn^{II} oxidation, limestone dissolution, and organic carbon oxidation coupled with reduction of NO_3, SO_4, and Fe^{III}. Other reported models considered Fe^{II} and Mn^{II} oxidation kinetics and may also have considered adsorption and neutralization processes that are important for AMD treatment (Antoniou et al., 2013; Vries et al., 2017; Burrows et al., 2017). Nevertheless, the executable PHREEQ-N-AMDTreat tools were specifically designed to facilitate simulations of water-quality effects from AMD treatment processes.

Modeled variables include initial solution chemistry and important physical and chemical parameters that may affect the water quality during treatment (Table 1 and S1). For the current effort, the phreeqc.dat database (provided with Phreeqc Interactive 3.6.2.15100 January 2020), which includes diffusivity coefficients for computation of specific conductance (SC), was supplemented with thermodynamic data for solubilities of Fe, Al, Mn, or SO_4 solids (Table S2), surface speciation involving HFO, HMO, and HAO sorbents (Tables S3 and S4), and rate models for kinetic reactants (Table S5). To prevent unrealistic instantaneous equilibration to oxidized or reduced species, relevant equilibrium expressions were replicated for "decoupled" redox species of Fe (+2, +3), Mn (+2, +3), N (−3, +5), and S (−2, +6), which are involved in kinetic (disequilibrium) reactions (e.g. Antoniou et al., 2013; Bethke, 2008; Parkhurst and Appelo, 2013; Vries et al., 2017). Oxidation or reduction reactions for the decoupled species occur only through the rate models. All the rate models included in phreeqc.dat (provided with Phreeqc Interactive 3.6.2.15100 January 2020) were modified; the modified rate models plus additional rate models, described below, include adjustment factors that are multiplied by the rate constants. Hereinafter, the expanded thermodynamic database including the rate models, which are used by the PHREEQ-N-AMDTreat modeling tools, is identified as phreeqcAMDTreat.dat.

The UI, which was generated with Visual Studio (2019), is illustrated for each of the PHREEQ-N-AMDTreat tools with different case-study examples in the Results and Discussion and in the supplementary data. The UI facilitates the input, adjustment, and saving of values for water-quality and kinetic variables and permits selection of on-screen graphical displays of results as well as output reports. Instead of "hard-coded" numeric values within the PHREEQC code, which would require modification of the code each time a value is changed, the IPhreeqcCOM code that is linked to the UI incorporates text variables. Numeric values for these text variables, which are displayed in the UI and saved in xml files, are specified for input solution chemistry, kinetics parameters, and sorbent characteristics.

2.1. Kinetics

The PHREEQ-N-AMDTreat modeling tools consider time-dependent chemical reactions that are affected by variations in the temperature, pH, concentrations of dissolved gases and solutes, the availability of sorbent surfaces or reactive substrates, and/or catalysis by iron-oxidizing bacteria (FeOB). All the rate expressions and rate constants for the kinetics models were adapted from the literature. The literature rate constants are automatically corrected for temperature effects and may be further adjusted by user-selected multiplication factors, explained below.

2.1.1. Atmospheric exchange

Because aeration affects the aqueous concentrations of O_2 and CO_2 and, consequently, pH and aqueous ion activities (e.g. Cravotta, 2015; Geroni et al., 2012; Kirby et al., 2009), the kinetics of gas exchange can affect numerous equilibrium and kinetics processes. A generalized first-order asymptotic expression is used to estimate the rates of CO_2

Table 1
Abbreviated description of variables used in PHREEQ-N-AMDTreat modeling tools.

Variable description	Variable on User Interface
Solutions A and B[a]	
Design flow	Design flow (gpm)[a]
Mix fraction	Mix Fraction
Water temperature, Celsius	Temp (C)
Specific conductance at 25°C	SC (uS/cm)
Dissolved oxygen	DO (mg/L)
pH	pH
Acidity	Acidity (mg/L)
Net acidity, calculated	Estimate NetAcidity
Alkalinity	Alk (mg/L)
Total inorganic carbon	TIC (mg/L as C)
Total inorganic carbon, calculated	Estimate TIC
Total iron	Fe (mg/L)
Ferrous iron	Fe2 (mg/L)
Ferrous iron, calculated	Estimate Fe2
Aluminum	Al (mg/L)
Manganese	Mn (mg/L)
Sulfate	SO4 (mg/L)
Chloride	Cl (mg/L)
Calcium	Ca (mg/L)
Magnesium	Mg (mg/L)
Sodium	Na (mg/L)
Potassium	K (mg/L)
Silicon	Si (mg/L)
Nitrate	NO3N (mg/L)
Total dissolved solids	TDS (mg/L)
Dissolved organic carbon	DOC (mg/L as C)
Humate	Humate (mg/L as C)
Hydrogen peroxide, calculated (after conservative mixing of A and B)	Estimate H2O2.mol/L
Kinetic adjustment factor (multiplied by rate constant) applied equally to all steps of ParallelTreatment or TreatTrainMix2 tools	
Factor kCO2, multiplied by CO2 outgassing rate constant (kLaCO2)	factr.kCO2
Factor kO2, multiplied by CO2 outgassing rate constant to estimate O2 ingassing rate constant	factr.kO2
Factor kFeHOM, multiplied by homogeneous Fe2 oxidation rate constant	factr.kFeHOM
Factor kFeHET, multiplied by heterogeneous Fe2 oxidation rate constant	factr.kFeHET
Factor kFeIIMnOx, multiplied by heterogeneous Fe2 oxidation rate constant	factr.kFeIIMnOx
Factor kbact, multiplied by microbial rate constant (assumes Fe oxidizing bacteria MPN = 5.3e11 cells/L)	factr.kbact
Factor kFeNO3, multiplied by homogeneous Fe2 oxidation rate constant	factr.kFeNO3
Factor kMnHOM, multiplied by homogeneous Mn2 oxidation rate constant	factr.kMnHOM
Factor kMnHFO, multiplied by heterogeneous Mn2_HFO oxidation rate constant	factr.kMnHFO
Factor kMnHMO, multiplied by heterogeneous Mn2_HMO oxidation rate constant	factr.kMnHMO
Factor kSHFO, multiplied by FeIII reduction-sulfide oxidation rate constant	factr.kSHFO
Factor kSOC, multiplied by sedimentary organic carbon oxidation rate constant	factr.kSOC
Factor kDOC, multiplied by dissolved organic carbon oxidation rate constant	factr.kDOC
Factor kH2O2, peroxide Fe2 oxidation rate constant	factr.kFeH2O2
Exponential factor for calcite dissolution rate model	EXPcc
Kinetic adjustment and equilibrium variables used in CausticTitration tool	
Time, in seconds, for pre-aeration step	Time0
kCO2, CO2 mass-transfer rate for pre-aeration step; see Table S6	kLaCO2.1/s
Steady-state log PCO2, used with kCO2 in CO2 mass-transfer rate expression	Steady-state logPCO2
Concentration of caustic soda (NaOH) solution in weight percent	NaOH wt%soln
Equilibrium value (solid-phase precipitation limit) for all steps in CausticTitration, ParallelTreatment, or TreatTrainMix2 tools	
Saturation index for calcite precipitation as equilibrium phase	SI_CaCO3
Saturation index for siderite precipitation as equilibrium phase	SI_FeCO3
Saturation index for Fe(OH)3 precipitation as equilibrium phase; see Table S2	SI_Fe(OH)3
Saturation index for schwertmannite precipitation as equilibrium phase; see Table S2	SI_Schwertmannite
Saturation index for Al(OH)3 precipitation as equilibrium phase; see Table S2	SI_Al(OH)3
Saturation index for basaluminite precipitation as equilibrium phase; see Table S2	SI_Basaluminite
Kinetic adjustment factor applied differently to each step of ParallelTreatment or TreatTrainMix2 tools, i = (1:11)	
Target pH specified for caustic addition at steps 1-5	– > pH
Hours total for step (1:11)	Time.hrs
Water temperature at end of step (1:11)	Temp2.C
Hydrogen peroxide at beginning of step (1:11)	H2O2.mol
kCO2, CO2 mass-transfer rate at beginning of step (1:11); see Table S6	kLaCO2.1/s
Steady-state log PCO2, used with kCO2 in CO2 mass-transfer rate expression for each step (1:11)	Lg(PCO2.atm)
Calcite unit surface area at beginning of step (1:11); see Table S7	SAcc.cm2/mol
Calcite mass fraction in limestone at beginning of step (1:11)	M/M0cc
Sedimentary organic carbon mass at beginning of step (1:11)	SOC.mol
Sorbent mass at beginning of step (1:11)	HMeO.mg
Sorbent content as percent iron at beginning of step (1:11)	Fe%
Sorbent content as percent manganese at beginning of step (1:11)	Mn%
Sorbent content as percent aluminum at beginning of step (1:11)	Al%
Description of step (1:11)	Description

[a] Input values for two different solutions, A and B, may be entered. Suffix "B" applies to variable names for solution B.

outgassing and O_2 ingassing:

$$d[C]/dt = -k_{L,C}a \cdot K_C \cdot (Pc - Pc_S) = -k_{L,C}a \cdot ([C] - [C]_S) \quad (1)$$

where C is either CO_2 or O_2, [C] is the molar concentration of the dissolved gas, $k_{L,C}a$ is the mass-transfer coefficient in units of inverse time, K_C is the temperature-adjusted Henry's Law solubility constant, P_C is the gas partial pressure, and P_{CS} is the steady-state partial-pressure value at equilibrium with the ambient atmosphere ($[C]_S = Kc \times Pc_S$), typically assuming Pco_{2S} is $10^{-3.4}$ atm and Po_{2S} is $10^{-0.67}$ atm. The gas mass-transfer rate is adjusted for variations in temperature relative to a reference temperature of 20 °C (Dempsey et al., 2001; Rathbun, 1998).

$$k_{L,C}a_T = k_{L,C}a \cdot (1.0241)^{T-20} \quad (2)$$

where T is degrees Celsius.

For generalized application of the gas-exchange kinetics, empirical data were collected on the rates of O_2 ingassing and CO_2 outgassing during an aeration experiment at one AMD site described by Cravotta (2015) and at several active or passive treatment AMD sites in Pennsylvania that employed various aeration or other treatment technologies (Means et al., 2015; this paper). Values for $k_{L,}co_2$ and $k_{L,}o_2$ were estimated from the linear slope of $Ln(C_0\text{-}C_S)/(C_t\text{-}C_S)]$ versus t, where t is elapsed time during the aeration experiment or travel time between measurement points. For aeration cascades and ditches, travel time for intentionally dislodged HMeO sediment was measured for the distance traveled. For a pond, wetland, or limestone bed, the travel time

(residence time) was computed by dividing the estimated water volume by the measured flow rate on the date of sampling. No attempt was made to explicitly consider the effects of water depth, wind, and other hydrodynamic parameters on the gas exchange rates or solute transport (e.g. Rathbun, 1998; Zappa et al., 2003). The empirical values corrected to 20 °C for $k_{L,CO2}$ ranged from 0.000001 s^{-1} to 0.05 s^{-1} (Table S6); values of $k_{L,O2}$ were a factor of approximately 2.1 times those of $k_{L,CO2}$ on average, which corresponds to a $k_{L,}co_2$: $k_{L,}o_2$ ratio of 0.48 and indicates CO_2 outgassing is approximately half the rate of O_2 ingassing. Dempsey et al. (2001) reported $k_{L,}co_2$: $k_{L,}o_2$ ratios for passive mine water treatment ponds and channels they investigated ranged from 0.30 to 0.65.

2.1.2. Kinetics of iron oxidation

The iron oxidation rate models directly consider the effects of pH and concentrations of dissolved oxygen (DO), nitrate, and aqueous Fe^{2+} (homogeneous oxidation) plus catalysis by adsorption of Fe^{2+} to HFO and HMO surfaces (heterogeneous oxidation) and/or microbial activity (biotic oxidation).

The homogeneous Fe^{II} oxidation rate law of Stumm and Lee (1961), expressed in terms of $[O_2]$ and $\{H^+\}$ ($=10^{-pH}$) by Stumm and Morgan (1996, p. 683–685), describes the abiotic oxidation of aqueous Fe^{2+}:

$$d[Fe^{II}]/dt = -k_{HOM}\cdot[O_2]\cdot\{H^+\}^{-2}\cdot[Fe^{2+}] \quad (3)$$

where { } indicates aqueous activity, [ ] indicates aqueous concentration in mol/L, and at pH 5 to 8 and 20 °C, the homogeneous rate constant k_{HOM} = 5.0 (±1.56) x 10^{-14} mol L^{-1} s^{-1} (Singer and Stumm, 1970; Stumm and Morgan, 1996). The uncertainty range corresponds to 0.7 to 1.3 times the reported reference value of k_{HOM}. Oxidation of Fe^{II} by nitrate $[NO_3^-]$, which has been reported to be one-fourth the rate by $[O_2]$ (Appelo and Postma, 2005), was computed by replacing $[O_2]$ in Eq. (3) with 0.25 × $[NO_3^-]$. The homogeneous Fe^{II} oxidation rate model, shown as Eq. (3), is commonly expressed in terms of Po_2 and $\{OH^-\}$:

$$d[Fe^{II}]/dt = -k_{HOM\text{-}OH}\cdot Po_2\cdot\{OH^-\}^2\cdot[Fe^{2+}] \quad (4)$$

with a corresponding rate constant of 1.33 × 10^{12} $(mol/L)^{-2}$ atm^{-1} s^{-1} ($= k_1\cdot Ko_2/Kw^2$) at 20 °C, which includes factors for the hydrolysis of water ($Kw = 10^{-14.168} = \{OH^-\}\cdot\{H^+\}$) and the Henry's Law constant for O_2 solubility in water ($Ko_2 = 10^{-2.854} = [O_2]/Po_2$ adjusted from 25 °C to 20 °C using polynomial expressions in phreeqc.dat and phreeqcAMD-Treat.dat). The rate expressions given in Eqs. (3) and (4) are interchangeable in PHREEQC and provide the same results, provided the relevant rate constants and the temperature corrections for Kw and Ko_2 are applied.

By using the reported activation energy of 96.2 kJ mol^{-1} (23 kcal mol^{-1}) for Eq. (3) (Stumm and Morgan, 1996, p. 684) with the Arrhenius equation (Appelo and Postma, 2005), the rate constant is automatically adjusted in the PHREEQ-N-AMDTreat model from the reference temperature to lower or higher temperatures:

$$k_{HOM\text{-}T2} = k_{HOM\text{-}T1} / \exp\{E_a/(R)\cdot(1/TK_2 - 1/TK_1)\} \quad (5)$$

where TK_1 is the reference temperature of 20 °C expressed in absolute temperature (degrees Kelvin, 293.15 K), TK_2 is the modeled temperature, $k_{HOM\text{-}T2}$ is the temperature-adjusted value of the rate constant, $k_{HOM\text{-}T1}$ is the reference value of the rate constant, E_a is the activation energy, and R is the ideal gas constant.

The heterogeneous oxidation rate model for Fe^{II} is expressed in terms of the concentrations of adsorbed Fe^{II} and dissolved oxygen (Tamura et al., 1976):

$$d[Fe^{II}ads]/dt = -k_{HET}\cdot[O_2]\cdot[Fe^{II}ads] \quad (6)$$

where the rate constant k_{HET} has a value of 73 $(mol/L)^{-1}$ s^{-1} at 25 °C and the activation energy is 179 kJ mol^{-1} (Dempsey et al., 2001; Sung and Morgan, 1980). The amount of adsorbed Fe^{II}, which is computed as a function of the pH, explained later, is the sum of Fe^{II} on strong and weak adsorption sites of HFO (Dzombak et al., 1990) plus analogous x- and y-adsorption sites of HMO (Tonkin et al., 2004). Increasing the available mass of sorbent, for example by recirculating HFO solids or by accumulation of HFO on submerged surfaces, increases the corresponding surface area and potential for adsorption of the dissolved Fe^{2+} and other ions at a given pH, with corresponding heterogeneous oxidation (e.g. Davison and Seed, 1983; Dempsey et al., 2001; Jones et al., 2014; Dietz and Dempsey, 2017).

Although Eq. (6) does not distinguish between HFO and HMO as the sorbent, the catalytic oxidation of Fe^{II} by HMO may, in fact, be coupled with the reductive dissolution of the sorbent $Mn^{III,IV}$ oxide (Postma and Appelo, 2000). Through this process, Mn^{2+} is released into solution and HMO is replaced by HFO, with the net result, if any, being a minor change in the total sorbent and sorbed-Fe^{II} and a corresponding increase in dissolved Mn^{II}. The "pyrolusite" reduction rate model in PHREEQ-N-AMDTreat uses the rate constant, k_P of value of 6.98 × 10^{-5} $(mol/L)^{-1}$ s^{-1} at 25 °C (Parkhurst and Appelo, 2013; Postma and Appelo, 2000, Eq. (12)), with the computed mass of HMO as MnOOH instead of pyrolusite; temperature correction is not applied.

Microbial catalysis of Fe^{II} oxidation is computed as a function of the concentration of FeOB (microbes), pH, DO, and temperature. Acidophilic and neutrophilic FeOB contributions are considered separately. The acidophilic FeOB rate increases as pH decreases from 5 to 2.8 and generally exceeds the abiotic Fe^{II} oxidation rate at these low pH values (Kirby et al., 1999; Kirby and Elder-Brady, 1998; Pesic et al., 1989). In the PHREEQ-N-AMDTreat model, the acidophilic FeOB oxidation rate is added to the homogeneous rate:

$$d[Fe^{II}]/dt = -k_{bio}\cdot C_{bact}\cdot[Fe^{2+}]\cdot[O_2]\cdot\{H^+\} \quad (7)$$

In Eq. (7) the rate constant k_{bio} is 5.15 × 10^{-2} L^3 mol^{-2} mg^{-1} s^{-1} at 25 °C (given the pre-exponential factor of 1.02 × 10^{-2} and activation energy of 58,770 J mol^{-1} reported by Kirby et al., 1999), C_{bact} is the concentration of iron-oxidizing bacteria in mg L^{-1} (dry weight) (Kirby et al., 1999; Pesic et al., 1989), and other variables are as previously defined. Because the most-probable number (MPN) method is traditionally used for enumeration of FeOB (Alexander, 1982; Greenberg et al., 1982), the MPN value of 5.3 × 10^{11} cells per liter, which equals Cbact of 150 mg L^{-1} (= MPN × 2.8 × 10^{-10} mg $cell^{-1}$), is the default, constant value used in PHREEQ-N-AMDTreat. Increasing the FeOB adjustment factor (factr. kbact) from the default of 1 implies greater FeOB activity than predicted by Eq. (7), whereas decreasing this factor to 0 results in the abiotic homogeneous rate. For rate computations, the same MPN value and factr.kbact are assumed without distinction for the acidophilic or neutrophilic FeOB rate models.

Catalysis by neutrophilic FeOB generally involves adsorption of Fe^{II} by HFO and increases with the amount of HFO-sorbed Fe^{II} (van Beek et al., 2012). Thus, the neutrophilic FeOB contribution is added to the heterogeneous rate in the PHREEQ-N-AMDTreat model. The neutrophilic FeOB rate generally does not exceed the abiotic oxidation rate, except at optimum pH and DO conditions. Eggerichs et al. (2014) showed that at optimum conditions of near-neutral pH (6.5–7.5) and low DO (1.9–2.2 mg L^{-1}), the neutrophilic FeOB rate was approximately a factor of 20 times the abiotic heterogeneous Fe^{II} oxidation rate of Davies and Morgan (1989). Thus, based on the data distributions of Eggerichs et al. (2014, Figs. 4 and 8 therein), an estimate of the overall rate contribution by neutrophilic FeOB is obtained herein by combining adjustment factors for pH and DO.

The combined effects of pH and DO on the neutrophilic FeOB rate are computed as the product of two rate adjustment factors, which yields a value of approximately 20 under optimum conditions (e.g. 4.6 × 4.5 = 20.7) that is then multiplied by the temperature-adjusted heterogeneous rate constant, k_{HET} (Eq. (6)). The neutrophilic FeOB adjustment factor for pH is:

$$pH\_factor = -1.605(pH)^2 + 22.383(pH) - 73.351 \quad (8)$$

at 5.25 < pH < 8.5; the pH_factor is null for pH values outside this range.

Eq. (8) indicates that the pH rate factor is greatest, ~4.6, at pH 6.8 to 7.2. The neutrophilic FeOB adjustment factor for DO is:

$$DO\_factor = 4.22 \times 10^{12}[O_2]^3 - 1.59 \times 10^{9}[O_2]^2 + 1.50 \times 10^{5}[O_2] + 0.282 \quad (9)$$

at $[O_2] < 1.9 \times 10^{-4}$ mol L^{-1} (6.1 mg L^{-1}); the DO_factor is 0.3 for greater DO values. Eq. (9) indicates the greatest DO factor, ~4.5, at $[O_2]$ of 6.0×10^{-5} mol L^{-1} (1.9 mg L^{-1}) to 6.9×10^{-5} mol L^{-1} (2.2 mg L^{-1}).

In addition to the above models for Fe^{II} oxidation by oxygen or nitrate, an additional kinetic expression for the oxidation of Fe^{II} by hydrogen peroxide (H_2O_2) is included in the PHREEQ-N-AMDTreat model. The rate expression is first order with respect to molar concentrations of H_2O_2 and total aqueous Fe^{II} (Hardwick, 1957; Millero et al., 1987; Millero and Sontolongo, 1989):

$$d[H_2O_2]/dt = -k_{H2O2} \cdot [H_2O_2]\ [Fe^{II}] \quad (10)$$

The total $[Fe^{II}]$ oxidized is computed as $0.5 \times [H_2O_2]$ on the basis of the following stoichiometry:

$$Fe^{2+} + 0.5\ H_2O_2 + H^+ = Fe^{3+} + H_2O \quad (11)$$

Empirical tests on near-neutral mine drainage indicate that upon the addition of H_2O_2, Fe^{II} oxidation and subsequent Fe^{III} hydrolysis are practically instantaneous, occurring within seconds, while Mn^{II} is unaffected (Cole et al., 1977; Burrows et al., 2017; Cravotta, 2015; Means et al., 2013). Although Mn^{II} is not oxidized by H_2O_2 (Sato, 1960), H_2O_2 can oxidize dissolved sulfide and organic carbon (Hoffman, 1977; Millero and Sotolongo, 1989). PHREEQ-N-AMDTreat computes the quantity of $[H_2O_2]$ needed to oxidize only the aqueous concentration of Fe^{II} on the basis of the stoichiometry of Eq. (11); this computed value may be deficient for actual treatment where sulfide and/or organic carbon compounds are present in the water or where the pH is very low.

Millero and Sontolongo (1989) reported the rate constant for Eq. (10) increases dramatically with pH from 3.5 to 8.5 but is independent of pH at values less than 3.5. The value of k_{H2O2} as a function of pH is estimated herein using a linear regression equation for log(k) versus pH for freshwater at 5 °C based on Figure 13 of Millero and Sotolongo (1989):

$$\log k_{H2O2} = 0.72\ pH - 1.02 \quad (12)$$

The corresponding rate constant is automatically adjusted to higher or lower temperature using the Arrhenius equation with an activation energy of 56 kJ mol^{-1} (Millero and Sotolongo 1989). Eq. (12) yields values of k_{H2O2} at 5 °C of 109,650 (mol/L) $^{-1}$ s^{-1} at pH 7 and 31.6 (mol/L) $^{-1}$ s^{-1} at pH ≤ 3.5. The latter value corrected to 20 °C is 109.2 (mol/L) $^{-1}$ s^{-1}, which is similar in magnitude to the rate of 42.6 (mol/L) $^{-1}$ s^{-1} for dilute sulfuric acid solution at 20 °C reported by Hardwick (1957).

2.1.3. Kinetics of manganese oxidation

The oxidation rate models for Mn^{II} in PHREEQ-N-AMDTreat consider homogeneous and heterogeneous contributions such as those for Fe^{II}; however, the applicable Mn^{II} oxidation rate expressions do not explicitly consider biological catalysis. The kinetics equation for the homogeneous Mn^{II} oxidation rate law is adopted from Davies and Morgan (1989) with Po_2:

$$d[Mn^{II}]/dt = -k_{1Mn} \cdot Po_2 \cdot \{OH^-\}^{2.56} \cdot [Mn^{2+}] \quad (13)$$

Davies and Morgan (1989) reported the rate model for Po_2 of 1 atm with the rate constant k_{1Mn} value of 2.08×10^{-2} $(mol/L)^{-2.56}$ s^{-1} atm^{-1} at 25 °C and activation energy of 272 kJ mol^{-1}; they used the homogeneous rate model given in Eq. (13) to correct the rate constant values for the much faster heterogeneous Mn^{II} oxidation rate.

The heterogeneous Mn^{II} oxidation rate model incorporates pH-dependent adsorption of Mn^{2+} by HFO (Davies and Morgan, 1989) and/or HMO (Morgan, 2005):

$$d[Mn^{II}ads]/dt = -k_{2Mn} \cdot Po_2 \cdot [Mn^{II}ads] \quad (14)$$

where the rate constant k_{2Mn} has a value of 2.1×10^{-4} s^{-1} atm^{-1} and the activation energy is approximately 100 kJ mol^{-1} as reported by Davies and Morgan (1989). The amount of adsorbed Mn^{II} ·(Mn^{II}ads), which is computed in PHREEQ-N-AMDTreat as a function of the pH and the composition and mass of sorbent, is the sum of that sorbed on strong and weak sites of HFO (Dzombak and Morel, 1990) and on analogous x- and y-adsorption sites of HMO (Tonkin et al., 2004). The default Mn^{II}-HMO heterogeneous oxidation rate constant is estimated as 0.5 that reported for Mn^{II} on HFO by Davies and Morgan (1989). This Mn^{II}-HMO rate estimate accounts for the spontaneous disproportionation of MnOOH to yield 0.5 MnO_2 and 0.5 aqueous Mn^{II} (Bricker, 1965). Despite the slower heterogeneous oxidation rate for Mn^{II}-HMO, half of that for Mn^{II}–HFO, Mn^{II} adsorption on HMO greatly exceeds that by HFO of equivalent mass at moderately acidic to near-neutral pH (see Tables S3 and S4).

Increasing the available surface area of HFO or HMO, for example by accumulation of HMO coatings on limestone particles in a Mn-removal bed (e.g. Means and Rose, 2005), increases potential for attenuation of dissolved Mn at a given pH. Eventually, the adsorbed Mn may oxidize in place, adding to the HMO sorbent. Although microbial catalysis is not modeled explicitly, increasing the available HFO and/or HMO surface area (mass of sorbent) or increasing the respective multiplication factors for the heterogeneous Mn^{II} oxidation rate (factr.kMnHFO, factr. kMnHMO) may be applied to account for the enhanced biological catalysis of Mn oxidation in passive AMD treatment (Cravotta and Trahan, 1999; Means and Rose, 2005; Robbins et al., 1999b; Santelli et al., 2010; Tan et al., 2010; Vail and Riley, 2000).

2.1.4. Kinetics of limestone dissolution

The calcite dissolution kinetics model in PHREEQ-N-AMDTreat is adapted from the oft-cited Plummer, Wigley, and Parkhurst ("PWP") calcite-dissolution rate model, which considers pH, partial pressure of CO_2, and proximity of solution to calcite equilibrium (Plummer et al., 1978). The PWP model indicates the rate of calcite dissolution is a function of three dissolution reactions (forward; k_1, k_2, k_3) and the precipitation reaction (backward; k_4).

$$r = (k_1 \cdot a_{H+} + k_2 \cdot a_{H2CO3*} + k_3 \cdot a_{H2O}) - k_4 \cdot a_{Ca2+} \cdot a_{HCO3-} \quad (15)$$

At equilibrium, the backward and combined forward reactions occur at an equal rate. For the above expression, Plummer et al. (1978) reported the forward rate constants in millimoles calcite per centimeter squared per second (mmol cm^{-2} s^{-1}) as a function of temperature (T, in K):

$$\log k_1 = 0.198 - 444 / T; \quad (16)$$

$$\log k_2 = 2.84 - 2177 / T; \quad (17)$$

$$\log k_3 = -5.86 - 317 / T \text{ for } T \leq 298;\ \log k_3 = -1.10 - 1737 / T \text{ for } T > 298 \quad (18)$$

Appelo et al. (1998) and Appelo and Postma (2005) adapted the PWP model to consider physical characteristics of the system as well as solution chemistry:

$$R_{CC} = k \cdot (A / V) \cdot (1 - \Omega)^n \quad (19)$$

where A is calcite surface area, V is volume of solution, Ω is saturation ratio ($IAP/K = 10^{SIcc}$; where SIcc is the saturation index for calcite) and n is an empirical coefficient (typically set to 0.67) that accounts for variations in particle shape. For the PWP model applied to 1-L solution, the overall rate of calcite dissolution becomes:

$$R_{CC} = (k_1 \cdot a_{H+} + k_2 \cdot a_{H2CO3*} + k_3 \cdot a_{H2O}) \cdot (A) \cdot (1 - 10^{(n \bullet SIcc)}) \quad (20)$$

Generally, the dissolution rate increases with increased values of A (decreased particle size) and/or decreased values of SIcc (distance from equilibrium). For the PHREEQ-N-AMDTreat model, limestone particle

surface area and corresponding particle volume are estimated for standard dimensions of various aggregate sizes assuming an ellipsoid shape (e.g. Cravotta et al., 2008; Pennsylvania Department of Environmental Protection, 2012; Santomartino and Webb, 2007). Using the same dimension and shape information, the approximate volume and mass of HMeO surface coating per liter of water in a limestone bed (void volume) can be estimated given the thickness and density of the coating and the porosity of the limestone bed. Table S7 in the supplementary data is provided for the computations of limestone particle surface area and coating thickness.

Although the rate model does not consider the effects of hydrodynamics or surface coatings on limestone dissolution (e.g. Cravotta, 2008c; Huminicki and Rimstidt, 2008; Palomino-Ore et al., 2019; Rose, 1999; Santomartino and Webb, 2007), the model includes an adjustment factor, M/M_0, that can account for inefficiency of dissolution or impurity of the limestone (Tables 1 and S1). A value of 1 for M/M_{0CC} implies efficient dissolution of pure calcite; values less than 1 indicate decreased availability of $CaCO_3$ for reaction. Likewise, the M/M_{0CC} factor can be used to define the mass fraction of limestone in a mixture with organic matter. For example, a value of 0.25 for M/M_{0CC} indicates the compost mix contains 25% limestone, with the remainder being solid organic carbon (examples are given in Results and Discussion and in supplementary data).

2.1.5. Organic carbon oxidation

Solid organic matter and dissolved organic carbon are essential microbial substrates in bioreactors, anaerobic wetlands, and reducing and alkalinity producing systems. The compositions of organic materials used in such systems vary widely, but frequently include compost mixtures containing 20–25% dispersed limestone fines, bivalve shells, or other calcareous material. Dissolution of the calcareous materials within the compost layer helps (1) to maintain a pH environment favorable to biological sulfate reduction (McCauley et al., 2009; Neculita et al., 2011; Reeder et al., 2010) and (2) to facilitate the precipitation of HAO and HFO solids within the organic-rich layer (Carballo et al., 2011; Rose, 2004; Skousen et al., 2017; Thomas and Romanek, 2002a, 2002b).

Solid organic carbon (SOC) of the compost mixture, represented as CH_2O, may be oxidized by aqueous oxygen, nitrate, and/or sulfate:

$$CH_2O + O_2 = CO_2 + H_2O \quad (21)$$

$$CH_2O + 0.8NO_3^- + 0.8H^+ = CO_2 + 0.4N_2 + 1.4\ H_2O \quad (22)$$

$$CH_2O + 0.5SO_4^{2-} + H^+ = CO_2 + 0.5H_2S \quad (23)$$

Considering the above reactions, the overall rate model for solid organic carbon oxidation is:

$$d[SOC]/dt = -\ k_{SOC}\cdot[SOC]\cdot R_{OX} \quad (24)$$

where [SOC] is the concentration (mol/kg), k_{SOC} is the first-order decay constant with a value of 1.57×10^{-9} s^{-1}, and R_{OX} is the oxidant multiplier in the form of an additive Monod kinetics expression modified from Appelo and Postma (2005):

$$R_{OX} = 1.0[O_2]/(2.94\times10^{-4}+[O_2]) + 0.01\,[NO_3^-]/(1.55\times10^{-4}+NO_3^-]) + 6.4\times10^{-5}[SO_4^{2-}]/(1\times10^{-4}+[SO_4^{2-}])\,(\arctan(0.42\,(pH\ -4.75))+5) \quad (25)$$

The factor 1.0, 0.01, or 6.4×10^{-5} in the numerator for the O_2, NO_3^-, or SO_4^{2-} contribution, respectively, indicates the maximum rate (s^{-1}) when multiplied by k_{SOC}. The value in the respective denominators is the half-saturation constant, $K_{1/2}$, which is the concentration (mol L^{-1}) where the rate is half the maximum value. The arctan term in Eq. (25) accounts for the inhibition of sulfate reduction at low pH (Peiffer, 2016).

The Monod parameters in Eq. (25) are empirical values for the oxidation of natural organic carbon in soils by the specified oxidants (Eckert and Appelo, 2002). Appelo and Postma (2005) explained that the overall oxidation rate may be decreased to account for slower decay of recalcitrant organic carbon in sedimentary rock aquifers, or increased, if appropriate. For example, Eckert and Appelo (2002) found the rate of degradation of dissolved organic carbon (DOC) in a contaminated aquifer was 10^7 faster than that for natural organic matter in soil. Likewise, the rate of oxidation is expected to be higher for relatively labile SOC sources, such as fresh or composted manure, compared to sedimentary organic carbon. Thus, in PHREEQ-N-AMDTreat, the default adjustment factor for k_{SOC} is set to 100, which results in a value of k_{OC} equal to 1.57×10^{-7} s^{-1} that is 100 times faster than that for soil organic carbon. The default adjustment factor for k_{DOC} is set to 1, to reproduce the relatively rapid DOC degradation rate of Eckert and Appelo (2002).

Degradation of SOC and DOC mainly affects the availability of oxidants in the PHREEQ-N-AMDTreat model; aqueous and surface complexation by the uncharacterized SOC and DOC are not considered. Although concentrations of DOC are not routinely measured for AMD samples, untreated AMD may contain ~1 mg L^{-1} (0.5–3.2 mg L^{-1}) of uncharacterized DOC (Cravotta and Brady, 2015), which could decrease or increase through a treatment system depending on microbial CH_2O degradation rates and input from algae, aquatic plants, and leaf litter. Humate is included in the PHREEQ-N-AMDTreat model as a surrogate for natural organic matter (NOM) and other uncharacterized aqueous components of DOC that have varying capacities to form metal-organic complexes. As reported by Burté et al. (2019), aqueous complexation of Fe^{II} and Fe^{III} by humate has the potential effect of decreasing the activity (availability) of Fe^{2+} and slowing the rate of Fe^{II} oxidation. The concentration of humate specified for influent is assumed to be non-degradable; the initial concentration of humate is assumed to be 10% of the initial concentration of DOC unless a non-zero value for humate is specified.

2.1.6. Reduction of Fe^{III} and oxidation of sulfide

In a reducing and alkalinity producing system, also known as a vertical flow wetland (VFW) or vertical flow pond (VFP), water transports solutes down through the organic-rich layer before reaching the underlying bed of limestone aggregate (Rose, 2004; Skousen et al., 2017; Watzlaf et al., 2000, 2004). Reduction of solid or aqueous Fe^{III} to Fe^{II} within the anoxic organic-rich layer of the VFP decreases potential for HFO accumulation within the underlying limestone bed, which otherwise could coat limestone particles or decrease porosity and flow through the bed. In the PHREEQ-N-AMDTreat model, the reductive dissolution of HFO by surface-adsorbed sulfide is included as the relevant kinetic process for the conversion of Fe^{III} to Fe^{II} (dos Santos Alfonso and Stumm, 1992; Peiffer et al., 1992; Poulton, 2003). The rate of Fe^{III} reduction coupled with the oxidation of adsorbed sulfide is faster than that for the microbial reduction of Fe^{III} oxyhydroxides coupled with organic carbon oxidation (e.g. Bonneville et al., 2009; Lovley et al., 1991). In the model, aqueous sulfide, which is produced by sulfate reduction coupled with organic carbon oxidation (Eq. (23)), may adsorb to HFO, if present, or precipitate as mackinawite (FeS). The concentrations of HFO-adsorbed sulfide species on weak and strong sorption sites (HFO_wOH and HFO_sOH, respectively) are computed as a function of pH (Peiffer et al., 1992; Poulton, 2003):

$$HFO\_wOH + HS^- = HFO\_wS^- + H_2O\ (\log K = 5.3) \quad (26)$$

$$HFO\_wOH + HS^- + H^+ = HFO\_wHS + H_2O\ (\log K = 10.82) \quad (27)$$

$$HFO\_wHS = HFO\_wS^- + H^+\ (\log K = -5.5) \quad (28)$$

The adsorbed sulfide then chemically reduces solid Fe^{III} to aqueous Fe^{II}, which is represented by the rate model below, adapted from dos Santos Alfonso and Stumm (1992):

$$d[HS^-]/dt = -\ (k_{e1}\cdot[HFO\_wS^-] + k_{e2}\cdot[HFO\_wHS])\ /\ A_{HFO} \quad (29)$$

where the rate constant k_{e1} is 30 m^2 h^{-1} (8.33×10^{-3} m^2 s^{-1}) for the

oxidation of HS^- on the neutral surface (HFO_wS^-) (mol L^{-1}), the rate constant k_{e2} is 400 $m^2\ h^{-1}$ ($1.11 \times 10^{-1}\ m^2\ s^{-1}$) for the oxidation of HS^- on the protonated surface (HFO_wHS) (mol L^{-1}), and A_{HFO} is the surface area of HFO per liter of solution ($m^2\ L^{-1}$). Peiffer et al. (1992) reported the rate of oxidation of adsorbed sulfide is approximately 15 times faster than the rate of Fe^{II} dissolution. Thus, [Fe^{II}] released is computed as 1/15 (0.0667) of total [H_2S] oxidized.

2.2. Adsorption by hydrous metal oxides

The PHREEQ-N-AMDTreat model accounts for surface-catalyzed oxidation kinetics as functions of adsorbed Fe^{2+} and Mn^{2+} on HFO and HMO surfaces (e.g. Chen and Thompson, 2018; Davies and Morgan, 1989; Stumm and Morgan, 1996; Tamura et al., 1976) and HS^- on HFO (dos Santos Alfonso and Stumm, 1992; Peiffer et al., 1992; Poulton, 2003). Thus, surface-complexation equilibria for cations and anions are included in phreeqcAMDTreat.dat (Tables S3 and S4) to model the potential interactions among Fe^{2+}, Mn^{2+}, and other aqueous ions with HMeO surfaces. The inclusion of a broad array of surface speciation reactions is important to indicate potential competition among major and trace ions for available surface sites. The PHREEQ-N-AMDTreat model does not consider sorption of Fe^{3+} and Mn^{3+} or the oxidation of Mn^{3+}. Instead, the concentrations of Fe^{3+} and Mn^{3+} are controlled only by their kinetic production and the consequent precipitation of amorphous $Fe(OH)_3$ or schwertmannite and MnOOH. In addition to all the published HFO, HMO, and HAO equilibrium equations and associated binding constants from the primary works, equilibrium expressions for the adsorption of Fe^{2+} by HFO (Appelo et al., 2002), Al^{3+} by HFO (Burrows et al., 2017; Hiemstra and van Riemsdijk, 2007), HS^- by HFO (Peiffer et al., 1992; Poulton, 2003), and Fe^{2+} by HMO (computed from reported linear free energy (LFER) relations reported by Tonkin et al., 2004) also are included in phreeqcAMDTreat.dat. Other potential mineral sorbents, including various oxides, carbonates, or clay minerals or solid organic matter, which are considered with the Windermere Humic Aqueous Model (Lofts and Tipping, 1998; Tipping et al., 2011) and Visual MINTEQ (Gustafsson, 2013) equilibrium models, were not included in the PHREEQ-N-AMDTreat model.

The adsorption expressions for HFO and HMO employ the diffuse double-layer concept, which considers a monoprotic sorbent with a small number of strong binding sites and a larger number of weak binding sites (Appelo and Postma, 2005; Dzombak and Morel, 1990; Tonkin et al., 2004; Parkhurst and Appelo, 2013). A single binding site is considered for monoprotic HAO (Karamalidis and Dzombak, 2010). Instead of goethite (FeOOH), birnessite (MnO_2), and gibbsite ($Al(OH)_3$), for which the original binding constants were developed, the PHREEQ-N-AMDTreat model defines amorphous ferric hydroxide ($Fe(OH)_3$), manganite (MnOOH), and amorphous $Al(OH)_3$ as the HFO, HMO, and HAO phases, respectively, which are presumed to have the same number of sorption sites per mole and unit surface areas as the original solids, but have different molar mass. In aqueous systems where pH and other conditions change rapidly, the modeled sorbent compounds tend to precipitate readily upon reaching equilibrium (saturation), removing Fe^{3+}, Mn^{3+}, and Al^{3+} from solution and forming fresh surface coatings (e.g. Bigham and Nordstrom, 2000; Chen and Thompson, 2018). For example, Nordstrom (2020) modeled effects of variations in solubility of Fe^{III} and Al phases on the attenuation of the dissolved metals in neutralized AMD and concluded that precipitation of amorphous Fe^{III} and Al compounds controlled the aqueous concentrations. Because the modeled sorbents are more soluble than the crystalline reference compounds, the default equilibrium condition determined by the PHREEQ-N-AMDTreat model results in supersaturation with respect to goethite, birnessite, and/or gibbsite. To consider different precipitates that may limit Fe or Al concentrations, the PHREEQ-N-AMDTreat models permit a user to specify the saturation index at which relevant phases precipitate, which is equivalent to adjusting the solubility constant (Table S2).

Total sorbent mass in the PHREEQ-N-AMDTreat model includes contributions from (1) the precipitation of amorphous $Fe(OH)_3$, MnOOH, and $Al(OH)_3$ to maintain equilibrium (autocatalytic fraction) upon reaching saturation, plus (2) an optional specified mass of previously formed HFO, HMO, and HAO that may be present as surface coatings (previously accumulated fraction) or suspended particles (recirculated sludge). For the autocatalytic fraction, the mass of sorbent will increase to a maximum concentration equal to the initial dissolved metal concentration, following kinetic oxidation of dissolved Fe^{2+} and Mn^{2+}. For the specified additional sorbent fraction, the PHREEQ-N-AMDTreat model requires input on the quantity and composition of the solids expressed as the metal mass per liter of solution (HMeO.mg, Fe %, Mn%, Al%). The model uses these input data with literature values for specific surface area, site densities, and formula weights for the respective sorbents (Table S3) to compute the moles of combined autocatalytic and previously formed sorption sites on HFO, HMO, and HAO for surface-speciation computations.

Surface-equilibrium computations consider the mass of sorbent plus the effects of protons and complexing ligands on the surface charge and the consequent distribution of surface and aqueous species. For example, the distribution of aqueous and adsorbed Fe^{2+} on HFO is determined by the pH and the availability of sorbent with corresponding equilibrium expressions:

$$HFO\_sOH + Fe^{2+} = HFO\_sOFe^{+} + H^{+} \quad (30)$$

$$HFO\_wOH + Fe^{2+} = HFO\_wOFe^{+} + H^{+} \quad (31)$$

$$HFO\_wOH + Fe^{2+} + H_2O = HFO\_wOFeOH + 2H^{+} \quad (32)$$

where HFO_s indicates strong sites, and HFO_w indicates weak sites, consistent with Eqs. 26–28. The binding constant for Eq. (30) is $10^{-0.95}$ (Appelo et al., 2002) and those for Eqs. (31) and (32) are $10^{-2.98}$ and $10^{-11.55}$, respectively (Liger et al., 1999; Parkhurst and Appelo, 2013). Although the equilibrium constants to compute activities of aqueous species are corrected for temperature, the binding constants for HFO, HMO, and HAO used in the PHREEQ-N-AMDTreat models are not adjusted for temperature variations.

2.3. Empirical data for model development and calibration

Available data from case studies were used to develop and calibrate simulations using the PHREEQ-N-AMDTreat models. The empirical data had been collected during prior studies to evaluate the attenuation of AMD contaminants (e.g. Ashby, 2017; Burrows et al., 2017; Cravotta, 2015; Cravotta and Brady, 2015; Cravotta and Trahan, 1999; Cravotta et al., 2014; R. Beam, 2020, Pennsylvania Department of Environmental Protection, written commun.). In general, grab samples representing increased reaction time or travel time were collected at points along flow paths in locations where flow was concentrated; integrated depth or width sampling was not attempted. Water temperature, SC, DO, redox potential (Eh), pH, and alkalinity were measured in the field. Field-filtered (0.20 or 0.45-μm) samples were analyzed in the laboratory for dissolved concentrations of major and trace elements. In a few instances, travel times between sample points were measured directly, in order to estimate the CO_2 outgassing rate for aeration steps (Eq. (1)). However, in most cases, travel times or retention times corresponding to the empirical data were computed later using volume estimated from engineering designs divided by the inflow or outflow rate on the date of sampling. Given the retention time for a treatment step (which ranged from seconds to days), other variables in the model, such as CO_2 outgassing rate, limestone particle size, and/or sorbent mass and composition, were adjusted to "calibrate" simulation results to measured water-quality values. Model fit was visually evaluated for multiple variables including pH, Pco_2, Po_2, and concentrations of Fe, Al, Mn, SO_4, and other solutes and was considered acceptable if simulation results were within a factor of ~2 of most measured values (which commonly

varied over an order of magnitude to the end of a flow path).

3. Results and Discussion—Simulation of observed changes in chemistry of AMD

Input variable values and model results for the three complementary PHREEQ-N-AMDTreat tools (CausticTitration, ParallelTreatment, and TreatTrainMix2) are presented below and in supplementary data for multiple case studies. The simulation results are compared to empirical observations in order to calibrate and "validate" the PHREEQ-N-AMDTreat models. Subsequently, the models are used to evaluate potential water-quality effects from different hypothetical treatment strategies.

3.1. Caustic titration case

The "CausticTitration" tool simulates the incremental addition of a caustic chemical (NaOH, $Ca(OH)_2$, CaO, or Na_2CO_3) to net-acidic or net-alkaline AMD (Fig. 1). The results include the quantity of the selected caustic titrant required to increase pH by 0.25 unit up to 11.0; the concentrations of dissolved Fe, Mn, Al, and other solutes plus net acidity, total dissolved solids (TDS), and SC; the mass of solids precipitated; and saturation indices for relevant solid phases. Although caustic agents may be added without prior treatment steps, aeration of AMD to outgas CO_2 before the addition of caustic chemicals has been reported to decrease chemical usage, sludge volume, and treatment costs (Jageman et al., 1988; Means et al., 2015). Thus, the PHREEQ-N-AMDTreat caustic titration model was expanded from the equilibrium titration tool in AMDTreat 5.0 (Cravotta et al., 2015) to include the option for pre-aeration ("decarbonation") before addition of caustic chemicals. For the no-aeration and equilibrium-aeration options, all reactions are assumed instantaneous equilibrium processes, whereas for the pre-aeration simulation, CO_2 outgassing, O_2 ingassing, and redox reactions are simulated as kinetics processes.

Figs. 1 and 2 show input data and simulation results for caustic titration of the St. Michael AMD with CaO (pebble quick lime) considering scenarios without aeration and with pre-aeration. According to data collected August 2020 (R. Beam, 2020, Pennsylvania Department of Environmental Protection, written commun.), the St. Michael AMD is characterized as a large volume (19,684 L min^{-1}, 5200 gal min^{-1}), anoxic, net-acidic coal-mine discharge (net acidity 223 mg L^{-1} as $CaCO_3$; alkalinity 50.8 mg L^{-1} as $CaCO_3$) that has pH 5.7 with elevated concentrations of dissolved CO_2 (Pco_2 $10^{-1.0}$ atm) and Fe^{II} (148 mg L^{-1}) and lower concentrations of Mn^{II} (3.6 mg L^{-1}) and Al (0.34 mg L^{-1}). Cravotta (2008a) reported similar composition of the AMD in 1999. In 2014, Means et al. (2015) evaluated the potential benefits of pre-aeration to outgas CO_2 before addition of lime to the AMD: The original lime treatment plant, which began operations in 2013, was

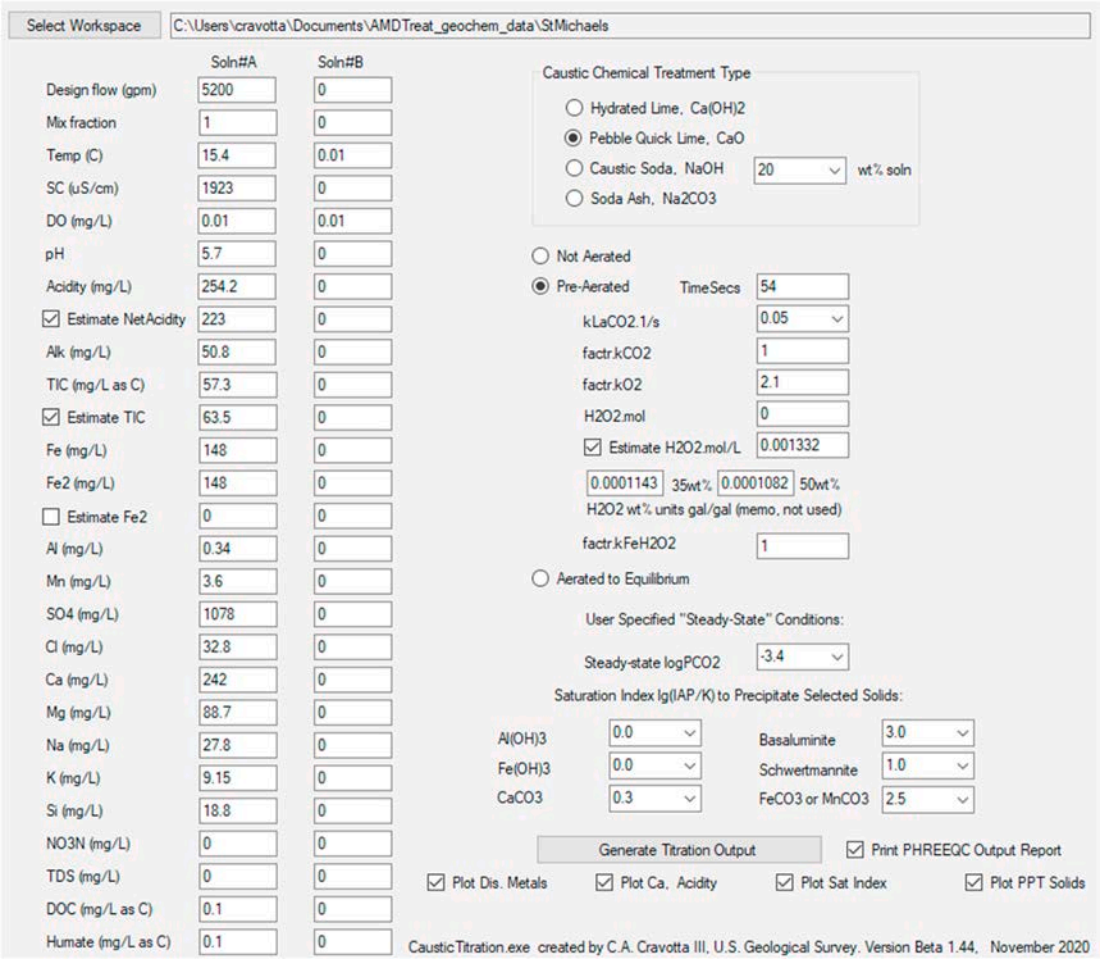

Fig. 1. User interface (UI) for PHREEQ-N-AMDTreat "CausticTitration" modeling tool. Input values for one initial solution (A) or two solutions (A and B mixture) may be entered. Data shown are for simulated pre-aeration before caustic addition at the St. Michael AMD, August 2020 (R. Beam, 2020, Pennsylvania Department of Environmental Protection, written commun.). Selected output results are displayed as a pH matrix in Fig. 2. Detailed descriptions of the model variables are given in Table S1 of supplementary data. Although solution B has zero flow, non-zero values must always be entered for temperature and dissolved oxygen (DO) and values for all other parameters must be provided (blanks are not acceptable).

A. CausticTitration.exe: Not aerated (**CaO** reacted to achieve pH 8.5 is **675** mg/L as $CaCO_3$)

pH	Caustic asCaCO3mg	Fe_mg	Fe2_mg	Al_mg	Mn_mg	TDS_mg	NetAcidity_mg	SolidsPPT_mg	CO2_mg	O2_mg
5.699391	0.000000	148.253946	148.184017	0.340583	3.606177	1,844.993285	219.160655	0.000000	184.696702	0.000000
5.698863	0.000000	148.192824	148.184017	0.340589	3.606188	1,844.843522	219.051235	0.116997	184.743198	0.000000
6.000000	36.694286	148.189513	148.184989	0.340591	3.606212	1,881.558706	182.288486	0.125192	152.974763	0.000000
6.500000	112.570987	148.188619	148.186989	0.125352	3.606260	1,956.151328	106.359043	0.753005	87.623936	0.000000
7.000000	171.880310	148.189212	148.188493	0.204352	3.606297	2,016.003903	47.027779	0.526362	37.108986	0.000000
7.500000	304.913856	148.187159	148.186724	0.340595	3.606254	1,955.324734	108.502893	194.644240	8.208932	0.000000
8.000000	420.943189	148.184464	148.184105	0.340589	3.606190	1,859.127523	204.623649	406.792768	0.939037	0.000000
8.500000	674.529768	31.972639	31.972263	0.340599	3.606297	1,671.810545	44.644131	687.418049	0.074199	0.000000
9.000000	737.552245	3.319670	3.319157	0.340602	3.606323	1,629.448665	1.378623	753.285879	0.007021	0.000000
9.500000	752.060641	0.379644	0.378671	0.340601	3.606321	1,629.762183	-7.720410	763.426508	0.000694	0.000000
10.000000	767.704290	0.055916	0.053479	0.340601	2.441687	1,639.455711	-21.535525	767.660752	0.000068	0.000000
10.500000	1,067.563230	0.018483	0.011410	0.340618	0.266277	1,695.835449	-39.623063	935.930409	0.000005	0.000000
11.000000	1,171.884112	0.027497	0.005748	0.055888	0.034796	1,729.690739	-65.761207	987.130878	0.000000	0.000000

B. CausticTitration.exe: Pre-aerated, CO_2 decreased almost 90% (**CaO** reacted to achieve pH 8.5 is **290** mg/L as $CaCO_3$)

pH	Caustic asCaCO3mg	Fe_mg	Fe2_mg	Al_mg	Mn_mg	TDS_mg	NetAcidity_mg	SolidsPPT_mg	CO2_mg	O2_mg
5.700000	0.000000	148.253944	148.253944	0.340583	3.606177	1,796.954955	218.906769	0.000000	184.683994	0.010018
6.697709	0.000000	148.153294	148.152157	0.131429	3.606182	1,795.523678	218.803412	0.797321	17.796470	10.215814
6.000000	-28.616060	148.152569	148.151421	0.131434	3.606169	1,766.883972	247.467641	0.000009	42.257085	10.215762
6.500000	-7.568373	148.153121	148.151973	0.122499	3.606183	1,787.899450	226.379052	0.025841	24.223205	10.215800
7.000000	9.055535	148.153108	148.152391	0.131435	3.606193	1,804.585382	209.741323	0.000836	10.263163	10.215829
7.500000	18.349692	148.152996	148.152562	0.131435	3.606197	1,813.885563	200.442332	0.001376	3.580427	10.215841
8.000000	35.672893	148.152651	148.152292	0.131435	3.606191	1,810.601897	203.719540	20.603783	0.958068	10.215822
8.500000	289.472888	32.288226	32.287850	0.131439	3.606297	1,660.197303	45.284262	302.427612	0.075796	10.216122
9.000000	352.483745	3.743785	3.743272	0.131440	3.606322	1,626.972166	2.424687	368.515322	0.007173	10.216195
9.500000	367.272893	0.673854	0.672881	0.131440	3.606321	1,628.061164	-6.846925	378.974003	0.000709	10.216191
10.000000	383.349079	0.123433	0.122284	0.131440	2.431956	1,637.645626	-21.058240	383.628171	0.000070	10.216184
10.500000	683.966927	0.020465	0.019316	0.131446	0.264708	1,694.073381	-39.188404	552.424752	0.000005	10.216705
11.000000	786.717176	0.007691	0.006542	0.060071	0.034620	1,730.957523	-65.661659	598.666335	0.000000	10.216884

Fig. 2. Matrix output display (cropped and highlighted) for CausticTitration tool. Results are shown for simulated treatment of St. Michael discharge with CaO, (A) without and (B) with pre-aeration to drive off CO_2 (input data values are given in Fig. 1). For this example, the dissolved CO_2 concentration is decreased by 90% and the caustic requirement to attain a pH 8.5 is decreased by 57% through aggressive aeration for 54 s with a Maelstrom Oxidizer® ($k_{L,CO2} = 0.05\ s^{-1}$) prior to lime addition. For A and B, CaO reacted to achieve pH 8.5 is 675 mg/L as $CaCO_3$ and 290 mg/L as $CaCO_3$, respectively. Empirical treatment evaluation by Means et al. (2015) indicated similar results.

retrofitted with a Maelstrom Oxidizer® (plug-flow, coarse-bubble diffuser), and aggressive aeration was conducted for 46 s prior to the lime dosing. The pre-aeration step decreased dissolved CO_2 from 189 mg L^{-1} to 18 mg L^{-1} and the pebble lime dose from 10.1 tons/day to 3.8 tons/day (63% decrease). Using the water chemistry data from August 2020 and assuming $k_{L,CO2} = 0.05\ s^{-1}$, which is the highest value of aeration technologies evaluated in this study (Table S6), the PHREEQ-N-AMDTreat simulations indicate a result consistent with empirical data—pre-aeration decreased CO_2 from 185 mg L^{-1} to 18 mg L^{-1} and decreased the theoretical caustic requirement for treatment to pH 8.5 by 57%. Additional treatment steps, including recirculation of solids, which improved performance, are evaluated later in this paper using the TreatTrainMix2 tool.

An additional caustic titration case study at the Nittanny mine discharge where NaOH was added to strongly acidic, metal-laden AMD without aeration is included in the supplementary data (Figs. S1-S3). The Nittanny treatment case, previously reported by Cravotta et al. (2015) and Cravotta and Brady (2015), demonstrates consistency among changes in pH and associated solute concentrations between the empirical titration measurements and simulation results.

3.2. Parallel treatment case

The "ParallelTreatment" tool simulates simultaneous treatment of the same starting water composition and is useful to evaluate effects on treatment resulting from different values for "system" variables. Relevant variables include temperature, caustic or H_2O_2 addition, and kinetics variables such as CO_2 mass-transfer (outgassing/ingassing) rate, limestone particle size, and/or sorbent availability. The tool is used herein to simulate complex interactions among CO_2 outgassing, pH, Fe^{II} oxidation, and the attenuation of associated metals, which were observed during aeration of net-alkaline AMD at the Oak Hill boreholes (Burrows et al., 2017; Cravotta, 2015; Henry, 2015). Such vertical boreholes, installed from a low-elevation surface location into underlying mine workings to prevent AMD discharging at higher elevation into buildings and other infrastructure, are a challenge to remediate because of their anoxic character and proximity to streams (e.g. Cravotta et al., 2014). The untreated AMD had pH 6.4 with concentrations of DO < 0.5 mg L^{-1} and dissolved Fe^{II}, Mn^{II}, and Al of 19.7, 3.6, and 0.056 mg L^{-1}, respectively. The side-by-side batch tests, which were conducted for 5–5.5 h duration, evaluated a control (Aer0), three progressively higher aeration rates (Aer1, Aer2, Aer3), and an initial dose of H_2O_2 without aeration (Figs. 3 and 4). As explained by Cravotta (2015) and Burrows et al. (2017), the field experiments demonstrated higher rates of aeration promoted CO_2 outgassing, thereby increasing pH and the rate of Fe^{II} oxidation; the results of field aeration experiments were consistent with in-stream changes. In contrast, H_2O_2 added without aeration instantaneously oxidized Fe^{II} and caused a precipitous decline in pH; thereafter pH remained relatively stable and paralleled that of the control (Fig. 4). The concentrations of dissolved Al, which were initially at equilibrium with amorphous $Al(OH)_3$, decreased to values below equilibrium for the H_2O_2 treatment at pH 6.2 and for the aeration treatments as the pH increased to ~7 and newly formed (autocatalytic) suspended HFO particles accumulated. Burrows et al. (2017) modeled the Al trends by adsorption to HFO; the same Al–HFO binding constant is assumed in phreeqcAMDTreat.dat. Concentrations of Mn^{II} were unaffected by H_2O_2 and decreased slightly with aeration. The trends in Mn also could be explained by adsorption to suspended HFO particles, with a higher pH required for binding than that for Al.

The parallel kinetics simulations of the pH, Fe^{II}, Mn^{II}, Al, alkalinity, DO, Pco_2, and Po_2 (curves in Fig. 4) generally reproduced the non-linear trends for the measured values (point symbols in Fig. 4). Note that error bars (not shown) are approximately twice the size of point symbols shown in Fig. 4; details are given by Burrows et al. (2017). Except for adjusting values of $k_{L,}co_2$ and H_2O_2 for the simulations, default values were used for all the kinetic parameters. The model results are consistent with abiotic, homogeneous oxidation of Fe^{II}, whereas the attenuation of a small fraction of the dissolved Mn^{II} concentration is consistent with its

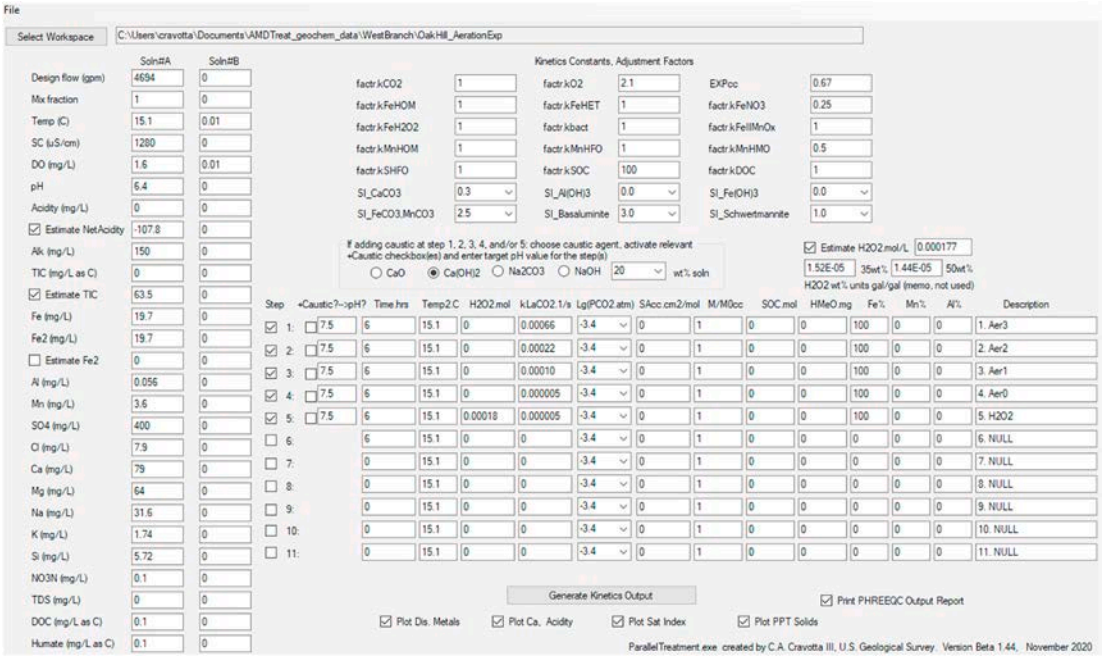

Fig. 3. UI for PHREEQ-N-AMDTreat "ParallelTreatment" modeling tool exhibiting input values for simulations of batch aeration experiments at the Oak Hill Boreholes. Results of simulations are shown in Fig. 4; kinetic adjustment parameters and other input variables in the model are described in Tables 1 and S1.

adsorption by suspended particles of HFO (produced by Fe^{II} oxidation) and, possibly, heterogeneous Mn^{II} oxidation. Although other model scenarios are not shown, setting the rate adjustment factor to 0 (e.g. Fig. 3) for FeOB (factr.kbact) or heterogeneous (factr.kHET) contributions to Fe^{II} oxidation or homogeneous oxidation of Mn^{II} (factr. kMnHOM) did not affect simulation results.

An additional case study, using the ParallelTreatment tool for simulations, is given in supplemental data (Figs. S4 and S5). For that case, the tool was used to evaluate effects of different limestone particle sizes and quantities of HMeO sorbent on water quality during AMD treatment in an oxic limestone drain (OLD) with retention time less than 6 h. As previously reported by Cravotta and Trahan (1999) and Cravotta and Watzlaf (2003), influent pH of 3.5 increased to 5.5 within 1.5 h and to 6.5 within 6 h; Fe^{III} and Al precipitated at pH < 5.5 near the inflow while dissolved Fe^{II} and Mn^{II} were transported relatively conservatively through the OLD during the first 6 months of operation (<6 mos in Figs. S4 and S5). After approximately 6 months of operation, HMeO had accumulated in the downflow part of the OLD where elevated pH (>6) promoted sorption and coprecipitation of dissolved Mn, Cu, Co, Ni, and Zn as indicated by decreased concentrations of the metals in effluent and their enrichment relative to Fe in HMeO suspended solids and coatings on limestone. Simulation results demonstrate the importance of particle size on limestone dissolution rate and of HMeO and pH on the attenuation of Mn (Fig. S5).

3.3. Sequential treatment cases

The "TreatTrainMix2" modeling tool, which combines the capabilities of the CausticTitration and ParallelTreatment tools, simulates progressive changes in water quality resulting from sequential passive or active treatment steps that typically involve neutralization, oxidation, and solids precipitation processes. To demonstrate model validity, empirical data for case studies, where field and laboratory water-quality measurements were obtained at multiple points through passive and active treatment systems, are presented with simulation results as a function of retention time (computed as the void volume of the treatment component divided by the flow rate).

3.3.1. Passive treatment case

The Pine Forest passive AMD treatment system consists of an anoxic limestone drain (ALD), oxidation/settling pond, and three aerobic wetlands, in series, with aeration steps in between (Figs. 5 and 6). The untreated AMD (690 gal min^{-1}, 43.5 L s^{-1}), sampled during winter 2015 (Ashby, 2017), had pH 5.8 with DO < 0.5 mg L^{-1} and dissolved concentrations of Fe^{II}, Mn^{II}, and Al of 14.0, 3.1, and 0.09 mg L^{-1}, respectively. The treated effluent had pH ~7 with Fe and Mn < 2 mg L^{-1}. After its first year of operation (2006), the ALD began to clog with gelatinous, Fe-rich precipitate. Although equipped with flushing pipes, manual activation of flushing was not attempted during the first year.

For the simulated "biofouling" scenario, the FeOB rate factor was increased from 1 to 2 and a pre-existing (accumulated) sorbent mass (HMeO.mg) of 116 mg was specified for the ALD (Fig. 5). This sorbent mass in the ALD is consistent with a 0.5-μm thick coating on the limestone particles (72 cm^2/mol) in contact with 1 L water volume, assuming 35% bed porosity and sorbent density of 1.25 g/cm^3 (Table S7). The assumed bed porosity, which represents partial clogging by accumulated sludge, is less than values of 42–53% for well-sorted limestone fragments (e.g. Cravotta and Watzlaf, 2003; Cravotta et al., 2008). For subsequent steps, the specified sorbent mass was only 1–3 mg, representing suspended particles or coatings on rock or plant surfaces.

The sequential model results for pH, Fe^{II}, Mn^{II}, Al, Pco_2, and Po_2, shown as a function of the retention time for the biofouling simulation, generally reproduce the longitudinal trends for measured constituent values (Fig. 6, red dashed curves). The simulated Fe^{II} concentration decreased by 30% within the ALD because of microbial oxidation combined with sorption and heterogeneous oxidation. Despite less mass of sorbent indicated for wetlands, progressively increased pH and greater Mn content of sorbent promoted attenuation of dissolved Mn^{II} in wetlands. Simulation results for a reference scenario (Fig. 6, black dotted curves) demonstrate abiotic, homogeneous processes are not adequate to explain observations at the Pine Forest ALD. The reference simulation uses the same aeration coefficients and retention times as the biofouling simulation, but the existing sorbent and FeOB rate factor were set to 0, equivalent to the abiotic homogeneous Fe^{II} oxidation rate model. This reference scenario underpredicts removal of Fe, Mn, and Al in the upper stages of the system where most chemical changes occur

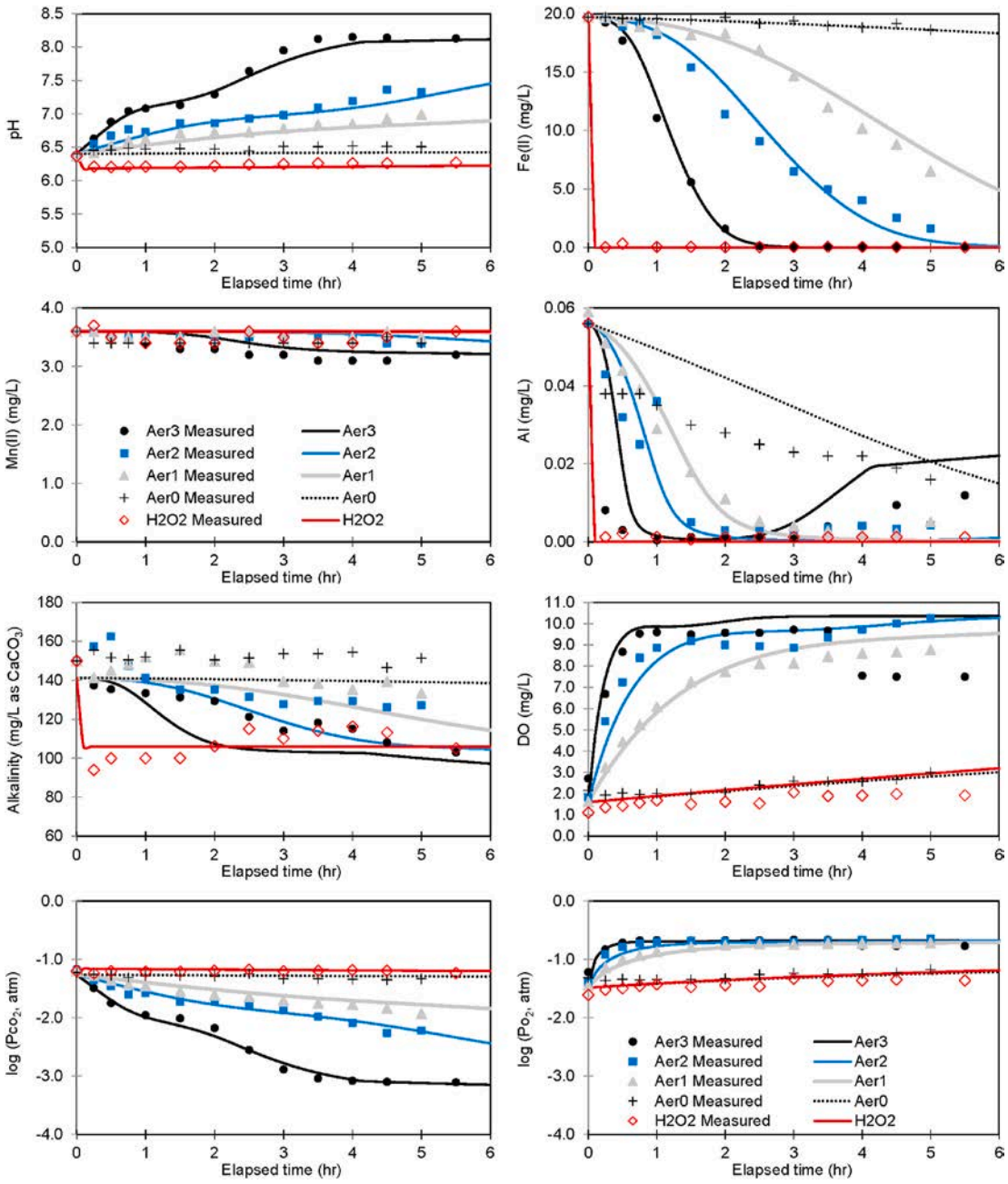

Fig. 4. Comparison of measured (symbols) and simulated (curves) values for pH, Fe^{II}, Mn^{II}, Al, alkalinity, DO, Pco_2, and Po_2 during batch aeration experiments on AMD from the Oak Hill Boreholes. Simulations used the ParallelTreatment tool with the same initial water chemistry and default values for kinetic adjustment factors, and different values for $k_{L,CO2}$ and $[H_2O_2]$, given in Fig. 3.

and does not indicate observed Mn^{II} attenuation. Thus, a combination of abiotic, microbial, and surface processes account for the attenuation of Fe within the limestone bed. Considering the reference model results, one may hypothesize that frequent flushing of the limestone bed immediately after construction may be effective to avoid sludge accumulation and associated biofouling (e.g. Wolfe et al., 2010).

In supplemental data, the TreatTrainMix2 tool is also used to simulate effects of passive treatment at the Silver Creek aerobic wetlands using data collected by Ashby (2017) and Cravotta (this study) under high-flow (December 2015) and low-flow (August 2016) conditions (Figs. S8-S11). In addition to data on water temperature, DO, pH, alkalinity, and solute concentrations used to calibrate these models, sediment chemistry data at the outflow of each treatment step at the Silver Creek system were available to estimate the sorbent composition (Ashby, 2017). For the Silver Creek models, the CO_2 outgassing rate ($k_{La,CO2}$) and sorbent mass and composition (HMeO.mg, Fe%, Mn%, Al%) at each step were the only kinetics variables adjusted to achieve a reasonable match between empirical and simulated values for dynamic changes in pH, Fe, Mn, Al, and associated solute concentrations. Shallow, wide aeration cascades and long riprap runs were highly effective at facilitating gas exchange and rapid increases in pH, followed by Fe^{II} oxidation in large ponds with long retention times where gas exchange was limited by minimal advection. Greater mass and/or Mn content of sorbent increased Fe^{II} and Mn^{II} attenuation; most Mn was attenuated in wetlands at later treatment steps.

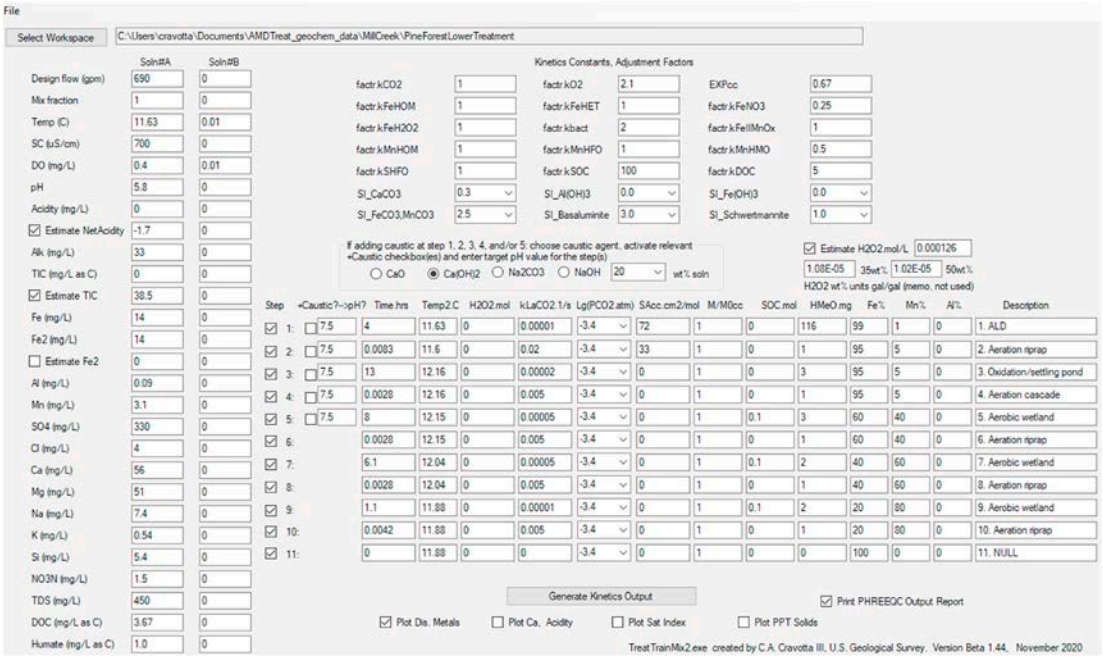

Fig. 5. UI for TreatTrainMix2 sequential model exhibiting input values for simulation of water-quality changes through the Pine Forest treatment system, December 2015, which consists of a "biofouled" anoxic limestone drain (ALD), oxidation/settling pond, and three aerobic wetlands, with aeration steps in between. The values shown represent enhanced FeOB activity (factr.kbact = 2, instead of default value of 1) and a specified sorbent mass of 116 mg in the ALD and smaller sorbent mass with progressively greater Mn content downstream. Results of simulations are shown in Fig. 6.

3.3.2. *Active treatment case*

The active treatment of St. Michael AMD, described previously, involves pre-aeration and lime dosing (Fig. 1) plus, importantly, the recirculation of high-density sludge (9.5 L s^{-1}, 150 gal min^{-1}), which consists of HMeO precipitate and unreacted lime, followed by settling of solids in a clarifier before discharge. Using August 2020 data on dissolved and total concentrations of metals and associated constituents in the untreated AMD and at points through the treatment process, the TreatTrainMix2 tool was set up and calibrated to simulate observed changes in pH, alkalinity, and dissolved metals concentrations (Figs. 7 and 8). During the first simulation step, (1) pre-aeration with the Maelstrom Oxidizer® for 54 s increased the pH from 5.7 to 6.7 and decreased aqueous CO_2 by 90 percent (as described previously). Next, the target pH of approximately 8.5 in the mix tank (continuously receiving slaked lime) was maintained for a duration of ~15 min by the addition of CaO over *three simulation steps* to (2) instantaneously precipitate $Fe(OH)_2$ and $Al(OH)_3$ as equilibrium phases, (3) sorb and heterogeneously oxidize Fe^{II} and Mn^{II} with the consequent precipitation of $Fe(OH)_3$ and MnOOH, and (4) adjust the pH of effluent exiting the caustic mix tank. Although the clarifier step (5) that followed involved more than 14 h for settling the solids precipitated during prior steps, the solute concentrations were relatively unchanged in the clarifier; nearly all oxidation and precipitation reactions had taken place during the 15 min of retention in prior steps.

The previous examples and others in supplemental data demonstrate that the PHREEQ-N-AMDTreat water-quality modeling tools can be used to quantify effects of factors that could increase or decrease the rates of Fe^{II} oxidation and Fe^{III} hydrolysis. Factors that can increase Fe-attenuation rates include increased temperature, increased pH, increased availability of sorbent HMeO, and increased FeOB activity. On the other hand, Rose and Waite (2003) reported that natural organic-matter-Fe^{II}-complex formation occurs on a similar time scale as Fe^{II} oxidation, and the formation of stable aqueous complexes (e.g. Fe^{II}-humate) can decrease Fe^{II} attenuation. To evaluate potential effects of NOM complexes on Fe attenuation, initial DOC and humate values may be adjusted from zero to non-zero values. Effects of other variables may also be evaluated by changing their initial values to represent temporal variability in AMD flow rates, chemistry, and system characteristics (e.g. Cravotta et al., 2010; 2014; Gammons et al., 2015).

General agreement between simulated and measured values and the ability to adjust input variables to simulate site-specific conditions support the use of the PHREEQ-N-AMDTreat modeling tools for the evaluation of hypothetical AMD treatment strategies. An expansive supplemental data (section S4) is provided that continues the demonstration of the TreatTrainMix2 tool for the conceptual design and preliminary economic assessment of potential passive and active treatment strategies for AMD. In that section, Figures S12 and S13 show the input data and output results for passive treatment simulation using the TreatTrainMix2 tool to evaluate progressive changes in water quality along the generalized flow sequence through a vertical flow system containing layers of compost and limestone, followed by an aerobic pond, wetland, and finally a manganese removal bed, with aeration steps in between. For the same initial water quality, Figures S14 and S15 show the simulation of active lime treatment, with the "+Caustic?" check box active for a target pH value of 8.5 at step 3, with $Ca(OH)_2$ as the caustic agent. In addition to the water-quality simulations, corresponding system sizing and summary cost estimates are given (Table S8) for evaluation of the cost-effectiveness of the hypothetical passive and active treatments.

4. Conclusions

Three complementary user-friendly geochemical models simulate the treatment of AMD to neutralize acidity and attenuate dissolved metals. The interactive UI for each of the PHREEQ-N-AMDTreat tools facilitates input of initial water chemistry data and adjustment of model variables while avoiding manual revisions to the variable values within the linked PHREEQC code. Graphical and tabular output indicates the changes in pH, solute concentrations, total dissolved solids, and specific conductance of treated effluent plus the cumulative quantity of precipitated solids as a function of retention time or the amount of caustic or oxidizing agent added. By adjusting chemical dosing or kinetic

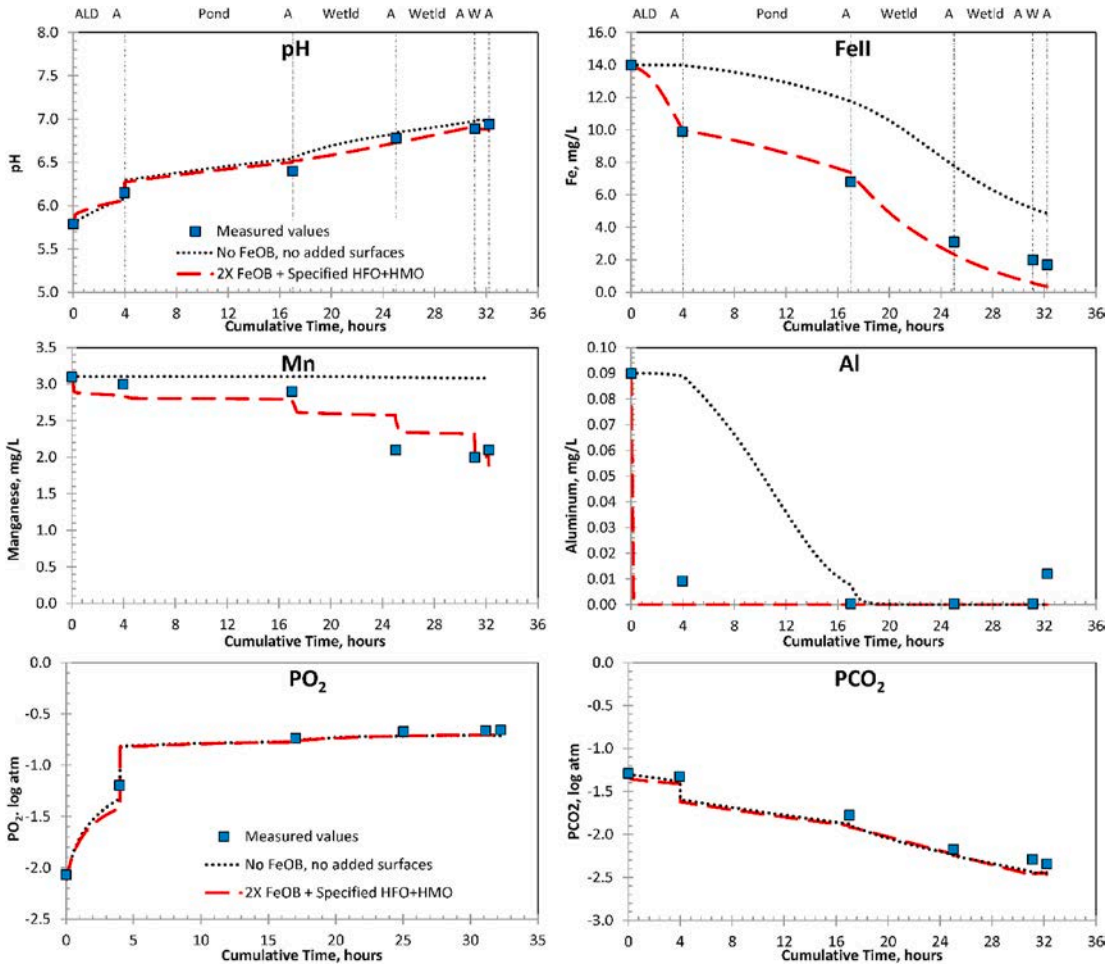

Fig. 6. Comparison of measured (symbols) and simulated (curves) values for pH, Fe^{II}, Mn^{II}, Al, Pco_2, and Po_2 during treatment of AMD at the Pine Forest passive treatment system, December 2015. Simulations used the TreatTrainMix2 sequential model with initial water chemistry, specified values for $k_{L,CO2}a$, FeOB rate factor, and sorbent mass and composition (Fig. 5). The black dotted curves show results for abiotic conditions without specified sorbent. The red dashed curves show results for enhanced FeOB activity (2X default FeOB rate) and specified sorbent mass in the ALD equivalent to 0.5-μm thick coating on limestone surfaces and smaller sorbent mass with progressively greater Mn content in downstream wetlands. Simulation results for additional parameters (alkalinity, net acidity, temperature, specific conductance, accumulated solids, mass of limestone and SOC dissolved, DO, nitrate, DOC, sulfate, and TDS) are included in the supplementary data (Figs. S6-S7). (For interpretation of the references to colour in this figure legend, the reader is referred to the Web version of this article.)

variables, the effects of independent or sequential treatment steps that have different retention time, aeration rate, quantities of reactive solids, and temperature can be simulated. Interactions among different variables and corresponding water-quality effects can be readily evaluated.

The model results indicate that effluent quality can be affected by the interactions of several independent and dependent variables. The key independent variable is the time specified for kinetic steps; this variable is essentially the travel time or retention time (volume/flow rate) for individual treatment steps. For most rate models, increased time generally results in greater reaction progress. However, forward reactions may be limited by atmospheric or solubility equilibrium, with diminished benefit from increased time for reaction as the system approaches equilibrium. One of the key dependent variables is pH, which affects aqueous and surface speciation and the rates of kinetic reactions. Importantly, the PHREEQ-N-AMDTreat models account for processes that may increase or decrease the pH. For example, the pH of treated effluent varies in response to atmospheric exchange (CO_2 outgassing), limestone dissolution, oxidation Fe^{II} and hydrolysis of Fe^{III}, and oxidation of organic carbon and can be modified through the addition of caustic agents or sorptive capacity. The geochemical models indicate potential for solids to precipitate or dissolve, but do not consider physical processes that could affect treatment performance such as particle settling, clogging of voids, or consumption of reactive substrates.

This paper demonstrates the models (1) to gain an understanding of the relative effects and importance of certain water-quality and system variables affecting AMD treatment and (2) to evaluate potential treatment strategies for cost-effective mitigation of Fe, Al, Mn, and associated contaminants from AMD. First, the CausticTitration tool quantifies the effects of commonly used caustic chemicals to increase pH and precipitate solids. Using this tool, preliminary treatment scenarios may be considered for caustic addition before or after aeration to drive off CO_2. Second, the ParallelTreatment tool considers the same starting water composition but with different possible values for kinetics variables such as CO_2 outgassing rate, limestone particle size, and/or sorbent availability. Field experiments that evaluated the effects of aeration or H_2O_2 treatment on the pH and Fe^{II} oxidation rate were accurately simulated with the parallel reactions tool. Third, the TreatTrainMix2 sequential treatment tool, which combines the capabilities of the caustic titration and parallel kinetics tools, simulates progressive changes in water quality resulting from passive or active treatment steps that typically involve neutralization, oxidation, and solids precipitation processes. The TreatTrainMix2 tool was applied to indicate observed changes in pH, dissolved O_2, metals, and associated solute concentrations in passive and active AMD treatment systems that had a range of retention times, aeration rates, and system components. Using this sequential treatment

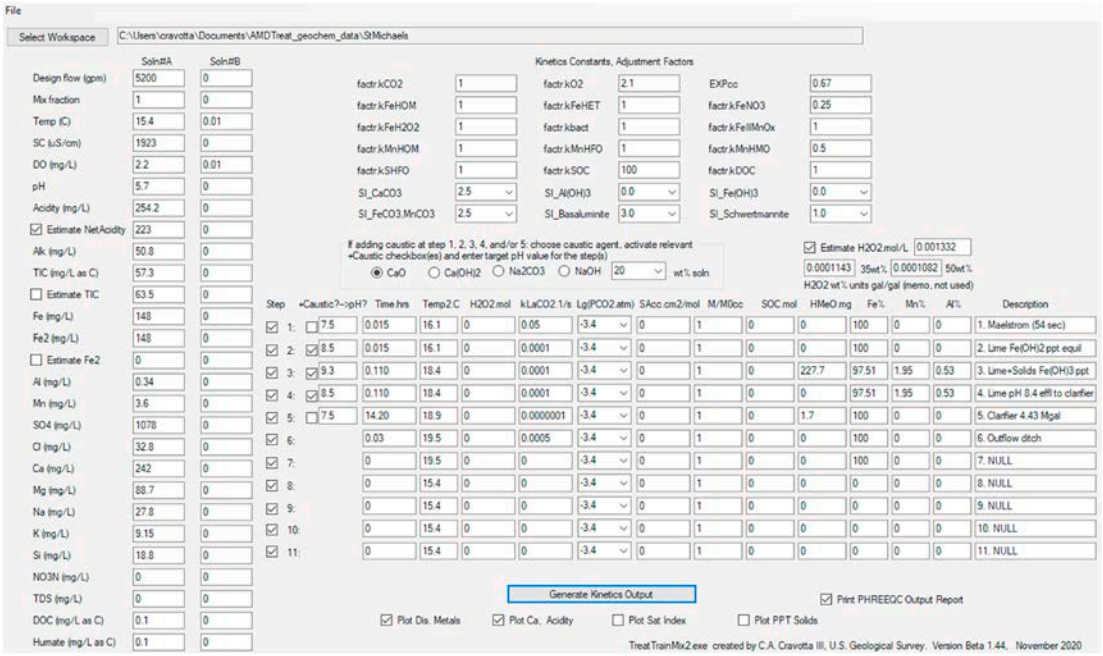

Fig. 7. TreatTrainMix2 input values for simulation of St. Michael active treatment system, which involves pre-aeration, continuous lime dosing with high-density sludge recirculation, and sludge settling steps. Results of simulations are shown in Fig. 8. Note the concentration and composition of HMeO sorbent specified for step (3) were computed as the sum of suspended Fe + Mn + Al concentrations (measured total minus dissolved concentration) exiting the mix tank (step 4). To prevent calcite precipitation and improve alkalinity simulation, the modeled calcite saturation index was increased from the default of 0.3–2.5; calcite was not detected (precipitated solids did not effervesce on reaction with HCl).

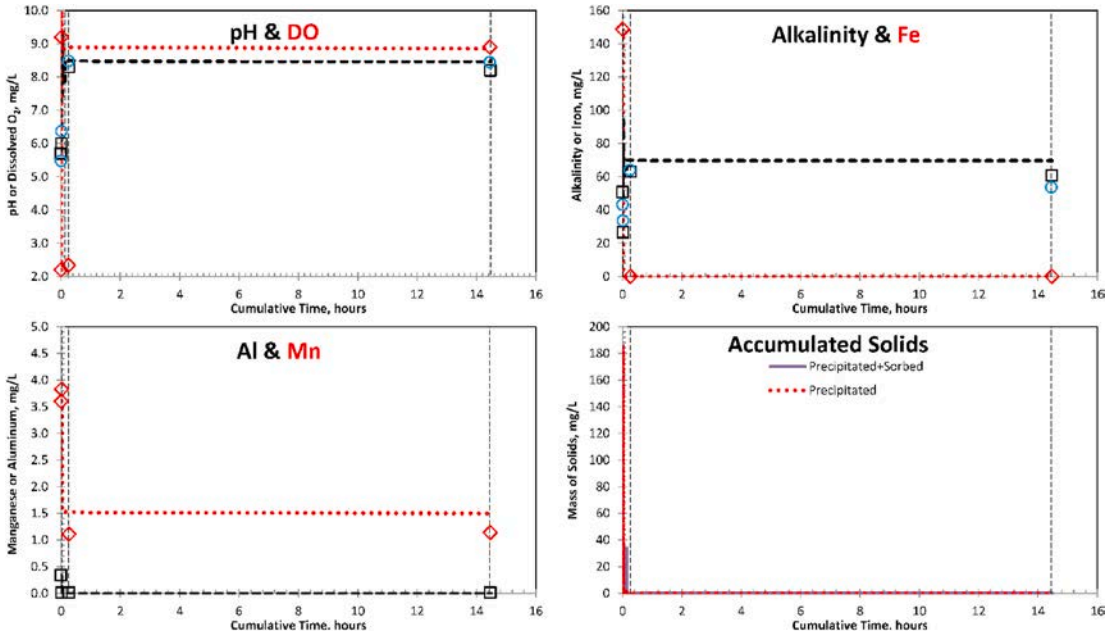

Fig. 8. Comparison of measured (symbols) and TreatTrainMix2 simulation results (curves) for pH, alkalinity, dissolved O_2, Fe, Al, and Mn, plus estimated concentration of accumulated solids at the St. Michael active treatment system. Input values for starting water quality and other model variables are shown in Fig. 7.

tool with chemistry and flow data for one or two AMD sources plus user-specified retention time and other system characteristics, various passive and/or active treatment strategies can be identified that achieve the desired effluent quality. Thus, considering land area and other requirements for installation, operation, and maintenance of the alternatives, potentially cost-effective, feasible treatment methods can be identified.

In conclusion, the PHREEQ-N-AMDTreat modeling tools effectively simulate dynamic interactions between dissolved Fe, Al, Mn, and other solutes in complex aqueous environments that exhibit gradients in pH, redox, and solute concentrations. The modeling capability of PHREEQC, including aqueous and surface speciation coupled with kinetics of oxidation-reduction and dissolution reactions, provides a quantitative framework for synthesis and application of laboratory rate data to field settings. The PHREEQ-N-AMDTreat UI facilitates application of the models to evaluate the performance and design of a wide variety AMD

treatment systems. Uncertainty in water-quality data, rate data, sorbent quantities and properties, and other system variables can be evaluated by changing values in the UI to identify critical parameters and document potential variations in results. Although publicly available, the models are not "smart," and practitioners may lack experience in water-quality analysis or engineering concepts. A user must choose appropriate values for system variables and treatment steps in the models. Site-specific information is essential for feasibility analysis and design.

Nordstrom and Campbell (2014) offered several relevant conclusions and recommendations on the sort of modeling presented herein: "Expert judgment, developed over long time periods and involving many mistakes, along with carefully acquired empirical observations in the field and in the laboratory, will ultimately guide our models from possibility to probability." They added, "Future efforts should be directed toward developing standardized test cases for a wide variety of processes against which code performance can be compared and tested." To this end, additional data collection is underway at several active and passive treatment facilities. The data collection is targeted to improve our knowledge of important variables or processes and associated effects on effluent quality at those facilities. Accordingly, revisions to improve the software may be anticipated. Additionally, efforts are underway to integrate the PHREEQ-N-AMDTreat water-quality modeling tools with the AMDTreat cost analysis model. The integrated models will facilitate feasibility and cost analysis.

Declaration of competing interest

The authors declare that they have no known competing financial interests or personal relationships that could have appeared to influence the work reported in this paper.

Acknowledgments

The Office of Surface Mining Reclamation and Enforcement (OSMRE) and the U.S. Geological Survey (USGS) provided funding and technical support for this work as part of the AMDTreat recoding project. Interaction with Brent Means and Bradley Schultz of OSMRE and Jeremiah Lant of USGS was crucial for the development and testing of the modeling applications for the treatment of coal-mine drainage. The author is especially grateful to Brent Means, who provided useful data and insights on mine drainage treatment practices and also provided reviews of the software presented herein. Helpful reviews of an early draft of the manuscript were provided by Robert Seal of USGS. Additional interaction with Jill (Burrows) Henry at Lehigh University, Mary (Rogers) McWilliams at Towson University, Luc Burté at Université de Rennes 1 and Centre National de la Recherche Scientifique, and Elizabeth J. Ashby at University of Ottawa, while they were graduate students, provided the author with the opportunity to explain, refine, and demonstrate the modeling methods to evaluate dissolved iron and aluminum attenuation along a stream flow path, well clogging by the adsorption and precipitation of iron and manganese, and the associations of trace metals and rare-earth elements with iron, aluminum, and manganese in passive treatment wetlands. Finally, the author wishes to express his appreciation to David Parkhurst for developing and providing guidance on the use of PHREEQC and to Kirk Nordstrom for sharing his knowledge of geochemical modeling, particularly with application to AMD systems. Any use of trade, firm, or product names is for descriptive purposes only and does not imply endorsement by the U. S. Government.

Appendix A. Supplementary data

Supplementary data to this article can be found online at https://doi.org/10.1016/j.apgeochem.2020.104845.

References

Alexander, M., 1982. Most probable number method for microbial populations. In: Page, A.L., Miller, R.H., Keeney, D.R. (Eds.), Methods of Soil Analysis, Part 2. Chemical and Microbiological Properties (2nd): Madison, Wis, vol. 9. American Society of Agronomy Monograph, pp. 815–820.

Antoniou, E.A., Stuyfzand, P.J., van Breukelen, B.M., 2013. Reactive transport modeling of an aquifer storage and recovery (ASR) pilot to assess long-term water quality improvements and potential solutions. Appl. Geochem. 35, 173–186. https://doi.org/10.1016/j.apgeochem.2013.04.009.

Appelo, C.A.J., Postma, D., 2005. Geochemistry, Groundwater and Pollution (2nd). Balkema, Leiden, p. 678.

Appelo, C.A.J., Van Der Weiden, M.J.J., Tournassat, C., Charlet, L., 2002. Surface complexation of ferrous iron and carbonate on ferrihydrite and the mobilization of arsenic. Environ. Sci. Technol. 36, 3096–3103.

Appelo, C.A.J., Verweij, E., Schäfer, H., 1998. A hydrogeochemical transport model for an oxidation experiment with pyrite/calcite/exchangers/organic matter containing sand. Appl. Geochem. 13, 257–268.

Ashby, E.J., 2017. Biogeochemical Mechanisms of Rare Earth Element Enrichment in Mining-Affected Aqueous Environments. University of Ottawa, Canada, M.S. thesis, p. 133.

Bethke, C.M., 2008. Geochemical and Biogeochemical Reaction Modeling, 2nd. Cambridge University Press, p. 543.

Bigham, J.M., Nordstrom, D.K., 2000. Iron and aluminum hydroxysulfates from acid sulfate waters. In: Alpers, C.N., Jambor, J.L., Nordstrom, D.K. (Eds.), Sulfate Minerals – Crystallography, Geochemistry, and Environmental Significance. Mineral. Soc. Amer. 40, Washington, DC, pp. 351–403.

Bigham, J.M., Schwertmann, U., Traina, S.J., Winland, R.L., Wolf, M., 1996. Schwertmannite and the chemical modeling of iron in acid sulfate waters. Geochem. Cosmochim. Acta 60, 2111–2121. https://doi.org/10.1016/0016-7037(96)00091-9.

Blowes, D.W., Ptacek, C.J., Jambor, J.L., Weisener, C.G., Paktunc, D., Gould, W.D., Johnson, D.B., 2014. The geochemistry of acid mine drainage. In: Holland, H.D., Turekian, K.K. (Eds.), Treatise on Geochemistry (2nd) 9. Elsevier, Oxford, pp. 131–190.

Bonneville, S., Behrends, T., Van Cappellen, P., 2009. Solubility and dissimilatory reduction kinetics of iron(III) oxyhydroxides: a linear free energy relationship. Geochem. Cosmochim. Acta 73, 5273–5282.

Bricker, O.P., 1965. Some stability relations in the system $Mn\text{-}O_2\text{-}H_2O$ at 25 °C and one atmosphere total pressure. Am. Mineral. 50, 1296–1354.

Burgos, W.D., Borch, T., Troyer, L.D., Luan, F., Larson, L.N., Brown, J.F., Lambson, J., Shimizu, M., 2012. Schwertmannite and Fe oxides formed by biological low-pH FeII oxidation versus abiotic neutralization: impact on trace metal sequestration. Geochem. Cosmochim. Acta 76, 29–44. https://doi.org/10.1016/j.gca.2011.10.015.

Burrows, J.E., Cravotta III, C.A., Peters, S.C., 2017. Enhanced Al and Zn removal from coal-mine drainage during rapid oxidation and precipitation of Fe oxides at near-neutral pH: Appl. Geochem. (Tokyo. 1967) 78, 194–210. https://doi.org/10.1016/j.apgeochem.2016.12.019.

Burté, L., Cravotta III, C.A., Bethencourt, L., Farasin, J., Pédrot, M., Dufrense, Al, Gérard, M.-F., Baranger, C.C., Le Borgne, T., Aquilina, L., 2019. Kinetic study on clogging of a geothermal pumping well triggered by mixing-induced biogeochemical reactions. Environ. Sci. Technol. 53, 5848–5857. https://doi.org/10.1021/acs.est.9b00453.

Charlton, S.R., Parkhurst, D.L., 2011. Modules based on the geochemical model PHREEQC for use in scripting and programming languages. Comput. Geosci. 37, 1653–1663.

Chen, C., Thompson, A., 2018. Ferrous iron oxidation under varying pO_2 levels: the effect of Fe^{III}/Al^{III} oxide minerals and organic matter. Environ. Sci. Technol. 52, 597–606. https://doi.org/10.1021/acs.est.7b05102.

Cole, C.A., Molinski, A.E., Rieg, N., Backus, F., 1977. Oxidation of iron in coal mine drainage. Wat. Pollut. Control Fed. 49, 1616–1620.

Coston, J.A., Fuller, C.C., Davis, J.A., 1995. Pb^{2+} and Zn^{2+} adsorption by a natural aluminum- and iron-bearing surface coating on an aquifer sand. Geochem. Cosmochim. Acta 59, 3535–3547. https://doi.org/10.1016/0016-7037(95)00231-n.

Cravotta III, C.A., 2003. Size and performance of anoxic limestone drains to neutralize acidic mine drainage. J. Environ. Qual. 32, 1277–1289. https://doi.org/10.2134/jeq2003.1277.

Cravotta III, C.A., 2005. Effects of abandoned coal-mine drainage on streamflow and water quality in the mahanoy Creek basin, schuylkill, columbia, and northumberland counties, Pennsylvania, 2001. U.S. Geol. Surv. Sci. Inv. Rep. 2004–5291, 60.

Cravotta III, C.A., 2007. Passive aerobic treatment of net-alkaline, iron-laden drainage from a flooded underground anthracite mine, Pennsylvania, USA. Mine Water Environ. 26, 128–149.

Cravotta III, C.A., 2008a. Dissolved metals and associated constituents in abandoned coal-mine discharges, Pennsylvania, USA – 1. Constituent concentrations and correlations. Appl. Geochem. 23, 166–202.

Cravotta III, C.A., 2008b. Dissolved metals and associated constituents in abandoned coal-mine discharges, Pennsylvania, USA – 2. Geochemical controls on constituent concentrations. Appl. Geochem. 23, 203–226.

Cravotta III, C.A., 2008c. Laboratory and field evaluation of a flushable oxic limestone drain for treatment of net-acidic, metal-laden drainage from a flooded anthracite mine, Pennsylvania, USA. Appl. Geochem. 23, 3404–3422.

Cravotta III, C.A., 2015. Monitoring, field experiments, and geochemical modeling of FeII oxidation kinetics in a stream dominated by net-alkaline coal-mine drainage, Pennsylvania. U.S.A. Appl. Geochem. 62, 96–107.

Cravotta III, C.A., 2020. Interactive PHREEQ-N-AMDTreat Water-Quality Modeling Tools to Evaluate Performance and Design of Treatment Systems for Acid Mine Drainage (Software Download). https://doi.org/10.5066/P9QEE3D5. U.S. Geological Survey Software Release. https://code.usgs.gov/water/phreeq-n-amdtreat/-/archive/v1.44/phreeq-n-amdtreat-v1.44.zip.

Cravotta III, C.A., Trahan, M.K., 1999. Limestone drains to increase pH and remove dissolved metals from acidic mine drainage. Appl. Geochem. 14, 581–606.

Cravotta III, C.A., Ward, S.J., Hammarstrom, J.M, 2008. Downflow limestone beds for treatment of net-acidic, oxic, iron-laden drainage from a flooded anthracite mine, Pennsylvania, USA–Laboratory evaluation. Mine Water Environ. 27, 86–99. https://doi.org/10.1007/s10230-008-0031-y.

Cravotta III, C.A., Watzlaf, G.R., 2003. Design and performance of limestone drains to increase pH and remove metals from acidic mine drainage. In: Naftz, D.L., Morrison, S.J., Fuller, C.C., Davis, J.A. (Eds.), Handbook of Groundwater Remediation Using Permeable Reactive Barriers–Application to Radionuclides, Trace Metals, and Nutrients. Academic Press, San Diego, Ca, pp. 19–66. https://doi.org/10.1016/B978-012513563-4/50006-2.

Cravotta III, C.A., Brightbill, R.A., Langland, M.J., 2010. Abandoned mine drainage in the swatara Creek basin, southern anthracite coalfield, Pennsylvania, USA–1. Streamwater-quality trends coinciding with the return of fish. Mine Water Environ. 29, 176–199. https://doi.org/10.1007/s10230-010-0112-6.

Cravotta III, C.A., Goode, D.J., Bartles, M.D., Risser, D.W., Galeone, D.G., 2014. Surface-water and groundwater interactions in an extensively mined watershed, upper Schuylkill River, Pennsylvania, USA. Hydrol. Process. 28, 3574–3601. https://doi.org/10.1002/hyp.9885.

Cravotta III, C.A., Means, B., Arthur, W., McKenzie, R., Parkhurst, D.L., 2015. AMDTreat 5.0+ with PHREEQC titration module to compute caustic chemical quantity, effluent quality, and sludge volume. Mine Water Environ. 34, 136–152.

Davies, S.H.R., Morgan, J.J., 1989. ManganeseII oxidation kinetics on metal oxide surfaces. J. Colloid Interface Sci. 129, 63–77.

Davison, W., Seed, G., 1983. The kinetics of the oxidation of ferrous iron in synthetic and natural waters. Geochem. Cosmochim. Acta 47, 67–79.

Dempsey, B.A., Roscoe, H.C., Ames, R., Hedin, R., Byong-Hun, J., 2001. Ferrous oxidation chemistry in passive abiotic systems for the treatment of mine drainage. Geochem. Explor. Environ. Anal. 1, 81–88.

Dietz, J.M., Dempsey, B.A., 2017. Heterogeneous oxidation of Fe(II) in AMD. Appl. Geochem. 81, 90–97.

dos Santos Alfonso, M., Stumm, W., 1992. Reductive dissolution of iron(III) (hydr)oxides by hydrogen sulfide. Langmuir 8, 1671–1675.

Dzombak, D.A., Morel, F.M.M., 1990. Surface Complexation Modeling: Hydrous Ferric Oxide. John Wiley and Sons, New York, NY, USA.

Eckert, P., Appelo, C.A.J., 2002. Hydrogeochemical modeling of enhanced benzene, toluene, ethylbenzene, xylene (BTEX) remediation with nitrate. Water Resour. Res. 38 (8) https://doi.org/10.1029/2001WR000692, 1130, 5.1-5.11.

Eggerichs, T., Opel, O., Otte, T., Ruck, W., 2014. Interdependencies between biotic and abiotic ferrous iron oxidation and influence of pH, oxygen and ferric iron deposits. Geomicrobiol. J. 31, 461–472.

Feng, Q., Li, T., Qian, B., Zhou, L., Gao, B., Yuan, T., 2014. Chemical characteristics and utilization of coal mine drainage in China. Mine Water Environ. 33, 276–286. https://doi.org/10.1007/s10230-014-0271-y.

Gammons, C.H., Nimick, D.A., Parker, S.R., 2015. Diel cycling of trace elements in streams draining mineralized areas–A review. Appl. Geochem. 57, 35–44.

Geroni, J.N., Cravotta III, C.A., Sapsford, D.J., 2012. Evolution of the chemistry of Fe bearing waters during CO_2 degassing. Appl. Geochem. 27, 2335–2347.

Gombert, P., Sracek, O., Koukouzas, N., Gzyl, G., Tuñon Valladares, S., Frączek, R., Klinger, C., Bauerek, A., Álvarez Areces, J.E., Chamberlain, S., Paw, K., Pierzchała, L., 2018. An overview of priority pollutants in selected coal mine discharges in Europe. Mine Water Environ. 38, 16–23. https://doi.org/10.1007/s10230-018-0547-8.

Iron and sulfur bacteria. In: Greenberg, A.E., Clesceri, L.S., Eaton, A.D., Franson, M.A.H. (Eds.), 1992. Standard Methods for the Examination of Water and Wastewater (18th). American Public Health Association, Washington, D.C.. Section 9240.

Gustafsson, J.P., 2013. Visual MINTEQ Version 3.1. Stockholm, Sweden. https://vminteq.lwr.kth.se/. December 21, 2013 (accessed January 23, 2019).

Hardwick, T.J., 1957. The rate constant of the reaction between ferrous ions and hydrogen peroxide in acidic solution. Can. J. Chem. 35, 428–436.

Hedin, B.C., Capo, R.C., Stewart, B.W., Hedin, R.S., Lopano, C.L., Stuckman, M.Y., 2019. The evaluation of critical rare earth element (REE) enriched treatment solids from coal mine drainage passive treatment systems. Int. J. Coal Geol. 208, 54–64.

Hedin, R.S., Nairn, R.W., Kleinmann, R.L.P., 1994. Passive Treatment of Coal Mine Drainage, vol. 9389. U.S. Bureau of Mines Information Circular, p. 35.

Henry, Jill E., 2015. Geochemical Factors Controlling the Fate of Fe, Al, and Zn in Coal-Mine Drainage in the Anthracite Coal Region. Ph.D. thesis. Lehigh University, Pennsylvania, USA, p. 195. http://preserve.lehigh.edu/etd/2633.

Hiemstra, T., van Riemsdijk, W.H., 2007. Adsorption and surface oxidation of Fe(II) on metal hydroxides. Geochem. Cosmochim. Acta 71, 5913–5933.

Hoffman, M.R., 1977. Kinetics and mechanism of oxidation of hydrogen sulfide by hydrogen peroxide in acidic solution. Environ. Sci. Technol. 11, 61–66.

Huminicki, D.M.C., Rimstidt, J.D., 2008. Neutralization of sulfuric acid solutions by calcite dissolution and the application to anoxic limestone drain design. Appl. Geochem. 23, 148–165.

Jageman, T.C., Yokley, R.A., Heunisch, H.E., 1988. The Use of Preaeration to Reduce the Cost of Neutralizing Acid Mine Drainage. U.S. Bureau of Mines Information Circular 9183, Pittsburgh, PA, pp. 131–135.

Jones, A.M., Griffin, P.J., Collins, R.N., Waite, T.D., 2014. Ferrous iron oxidation under acidic conditions – the effect of ferric oxide surfaces. Geochem. Cosmochim. Acta 145, 1–12.

Kairies, C.L., Capo, R.C., Watzlaf, G.R., 2005. Chemical and physical properties of iron hydroxide precipitates associated with passive treated coal mine drainage in Bituminous Region of Pennsylvania and Maryland. Appl. Geochem. 20, 1445–1460.

Karamalidis, A.K., Dzombak, D.A., 2010. Surface Complexation Modeling: Gibbsite. John Wiley & Sons, Inc., Hoboken, NJ, USA.

Kirby, C.S., Cravotta III, C.A., 2005. Net alkalinity and net acidity 2: practical considerations. Appl. Geochem. 20, 1941–1964.

Kirby, C.S., Elder-Brady, J.A., 1998. Field determination of Fe^{2+} oxidation rates in acid mine drainage using a continuously-stirred tank reactor. Appl. Geochem. 13, 509–520.

Kirby, C.S., Thomas, H.M., Southam, G., Donald, R., 1999. Relative contributions of abiotic and biological factors in Fe(II) oxidation in mine drainage. Appl. Geochem. 14, 511–530.

Kirby, C.S., Dennis, A., Kahler, A., 2009. Aeration to degas CO_2, increase pH, and increase iron oxidation rates for efficient treatment of net alkaline mine drainage. Appl. Geochem. 24, 1175–1184.

Li, Peiyue, 2018. Mine water problems and solutions in China. Mine Water Environ. 37, 217–221. https://doi.org/10.1007/s10230-018-0543-z.

Liger, E., Charlet, L., Van Cappellen, P.V., 1999. Surface catalysis of uranium(VI) reduction by ironII. Geochem. Cosmochim. Acta 63, 2939–2955.

Lofts, S., Tipping, E., 1998. An assemblage model for cation binding by natural particulate matter. Geochem. Cosmochim. Acta 62, 2609–2625.

Lovley, D.R., Phillips, E.J.P., Lonergan, D.J., 1991. Enzymic versus nonenzymic mechanisms for iron(III) reduction in aquatic sediments. Environ. Sci. Technol. 25, 1062–1067.

Lozano, A., Ayora, C., Fernández-Martínez, A., 2020. Sorption of rare earth elements on schwertmannite and their mobility in acid mine drainage treatments. Appl. Geochem. 113, 104499. https://doi.org/10.1016/j.apgeochem.2019.104499.

McCauley, C.A., O'Sullivan, A.D., Milke, M.W., Weber, P.A., Trumm, D.A., 2009. Sulfate and metal removal in bioreactors treating acid mine drainage dominated with iron and aluminum. Water Res. 43, 961–970.

Means, B., Rose, A.W., 2005. Manganese removal in limestone bed systems. In: Proceedings of the 2005 National Meeting of the American Society of Mining and Reclamation, pp. 702–717.

Means, B., Beam, R., Charlton, D., 2013. Operational and financial studies of hydrogen peroxide versus hydrated lime and hydrogen peroxide versus sodium hydroxide at two Pennsylvania mine drainage treatment sites. In: West Virginia Mine Drainage Task Force, 2013 Symposium. https://wvmdtaskforce.files.wordpress.com/2016/01/13-means-paper.doc.

Means, B., Parker, B., Beam, R., 2015. Decarbonating at the St. Michael Treatment plant: effect on cost, sludge, and sedimentation. In: West Virginia Mine Drainage Task Force, 2013 Symposium. https://wvmdtaskforce.files.wordpress.com/2016/01/15-means-paper.docx.

Millero, F.J., Sotolongo, S., 1989. The oxidation of Fe(II) with H_2O_2 in seawater. Geochem. Cosmochim. Acta 53, 1867–1873.

Millero, F.J., Sotolongo, S., Izaguirre, M., 1987. The oxidation kinetics of Fe(II) in seawater. Geochem. Cosmochim. Acta 51, 793–801.

Morgan, J.J., 2005. Kinetics of reaction between O_2 and Mn(II) species in aqueous solutions. Geochem. Cosmochim. Acta 69, 35–48.

Munk, L., Faure, G., Pride, D.E., Bigham, J.M., 2002. Sorption of trace metals to an aluminum precipitate in a stream receiving acid rock-drainage; Snake River, Summit County, Colorado. Appl. Geochem. 17, 421–430. https://doi.org/10.1016/s0883-2927(01)00098-1.

Neculita, C.M., Yim, G.-J., Lee, G., Ji, S.-W., Jung, J.W., Park, H.-S., Song, H., 2011. Comparative effectiveness of mixed organic substrates to mushroom compost for treatment of mine drainage in passive bioreactors. Chemosphere 83, 76–82.

Nordstrom, D.K., 2011a. Mine waters: acidic to circumneutral. Elements 7, 393–398.

Nordstrom, D.K., 2011b. Hydrogeochemical processes governing the origin, transport and fate of major and trace elements from mine wastes and mineralized rock to surface waters. Appl. Geochem. 26, 1777–1791.

Nordstrom, D.K., 2020. Geochemical modeling of iron and aluminum precipitation during mixing and neutralization of acid mine drainage. Minerals 10, 547. https://doi.org/10.3390/min10060547.

Nordstrom, D.K., Campbell, K.M., 2014. Modeling low-temperature geochemical processes. In: Holland, H.D., Turekian, K.K. (Eds.), Treatise on Geochemistry (2^{nd}) 7. Elsevier, Oxford, pp. 27–68.

Office of Surface Mining Reclamation and Enforcement, 2017. AMDTreat.(last updated 2017). https://amd.osmre.gov/ accessed August 24, 2020.

Palomino-Ore, S.B., Rimstidt, J.D., Chermak, J.A., Schreiber, M.E., Seal II, R.R., 2019. Aluminum hydroxide coatings in limestone drains. Appl. Geochem. 103, 23–30.

Parkhurst, D.L., Appelo, C.A.J., 2013. Description of input and examples for PHREEQC version 3—a computer program for speciation, batch-reaction, one-dimensional transport, and inverse geochemical calculations. U.S. Geol. Surv. Techniques Methods 6-A43, 497. https://pubs.er.usgs.gov/publication/tm6A43 https://www.usgs.gov/software/phreeqc-version-3/.

Peiffer, S., dos Santos Afonso, M., Wehrli, B., Gachter, R., 1992. Kinetics and mechanism of the reaction of H_2S with lepidocrocite. Environ. Sci. Technol. 26, 2408–2412.

Peiffer, S., 2016. Reaction time scales for sulphate reduction in sediments of acidic pit lakes and its relation to in-lake acidity neutralization. Appl. Geochem. 73, 8–12.

Pennsylvania Department of Environmental Protection, 2012. Erosion and Sediment Pollution Control Program Manual: Harrisburg. Pennsylvania Dept. Environmental Protection Bureau of Watershed Management. Document No. 363-2134-008, 563 pp. (tables 6.6 and 6.7).

Pennsylvania Department of Environmental Protection, 2016. Acid Mine Drainage Set-Aside Program Implementation Guidelines. Pennsylvania Department of Environmental Protection, Bureau of Abandoned Mine Reclamation, p. 70. Document 546-5500-001.

Pesic, B., Oliver, D.J., Wichlacz, P., 1989. An electrochemical method of measuring the oxidation rate of ferrous to ferric iron with oxygen in the presence of Thiobacillus ferrooxidans. Biotechnol. Bioeng. 33, 428–439.

Plummer, L.N., Wigley, M.L., Parkhurst, D.L., 1978. The kinetics of calcite dissolution in CO_2-water systems at 5° to 60°C and 0.0 to 1.0 atm CO_2. Am. J. Sci. 278, 179–216.

Postma, D., Appelo, C.A.J., 2000. Reduction of Mn-oxides by ferrous iron in a flow system: column experiment and reactive transport modeling. Geochem. Cosmochim. Acta 64, 1237–1247.

Poulton, S.W., 2003. Sulfide oxidation and iron dissolution kinetics during the reaction of dissolved sulfide with ferrihydrite. Chem. Geol. 202, 79–94.

Rathbun, R.E., 1998. Transport, behavior, and fate of volatile organic compounds in streams. U. S. Geol. Surv. Prof. Pap. 1589, 151.

Reeder, M.D., Branam, T.D., Olyphant, G.A., 2010. Assessment of two field-scale sulfate reducting bioreactors using sulfur isotopes. In: The 2010 National Meeting of the American Society of Mining and Reclamation, pp. 813–827.

Robbins, E.I., Cravotta III, C.A., Savela, C.E., Nord Jr., G.L., 1999a. Hydrobiogeochemical interactions in "anoxic" limestone drains for neutralization of acidic mine drainage. Fuel 78, 259–270.

Robbins, E.I., Brant, D.L., Ziemkiewicz, P.F., 1999b. Microbial, algal, and fungal strategies for manganese oxidation at a Shade Township coal mine, Somerset County, Penna. In: Proceedings American Society of Mining and Reclamation, Scottsdale, AZ, August 13-19, 1999, pp. 634–640. https://doi.org/10.21000/JASMR99010634.

Rose, A.L., Waite, T.D., 2003. Kinetics of iron complexation by dissolved natural organic matter in coastal waters. Mar. Chem. 84, 85–103. https://doi.org/10.1016/S0304-4203(03)00113-0.

Rose, A.W., 1999. Chemistry and kinetics of calcite dissolution in passive treatment systems. In: Proceedings American Society of Mining and Reclamation, Scottsdale, AZ, August 13-19, 1999, pp. 634–640. https://doi.org/10.21000/JASMR99010599.

Rose, A.W., 2004. Vertical flow systems-Effects of time and acidity relations. In: Proceedings American Society of Mining and Reclamation, Morgantown, WV, April 18-24, 2004, pp. 1595–1616. https://doi.org/10.21000/JASMR04011595.

Sánchez-España, J., Usta, I., Gray, J., Burgos, W.D., 2016. Geochemistry of dissolved aluminum at low pH: extent and significance of Al-Fe(III) co-precipitation below pH 4.0. Geochem. Cosmochim. Acta 175, 128–149. https://doi.org/10.1016/j.gca.2015.10.035.

Santelli, C.M., Pfiser, D.H., Lazarus, D., Sun, L., Burgos, W.D., Hansel, C.M., 2010. Promotion of Mn(II) oxidation and remediation of coal mine drainage in passive treatment systems by diverse fungal and bacterial communities. Appl. Environ. Microbiol. 76, 4871–4875. https://doi.org/10.1128/AEM.03029-99.

Santomartino, S., Webb, J.A., 2007. Estimating the longevity of limestone drains in treating acid mine drainage containing high concentrations of iron. Appl. Geochem. 22, 2344–2361.

Sato, M., 1960. Oxidation of sulfide ore bodies 1. Geochemical environments in terms of Eh and pH. Econ. Geol. 55, 928–961.

Skousen, J.G., Zipper, C.E., Rose, A.W., Ziemkiewicz, P.F., Nairn, R., McDonald, L.M., Kleinmann, R.L., 2017. Review of passive systems for acid mine drainage treatment. Mine Water Environ. 36, 133–153.

Skousen, J.G., Ziemkiewicz, P.F., McDonald, L.M., 2019. Acid mine drainage formation, control and treatment: approaches and strategies. The Extractive Industries and Society 6, 241–249.

Stumm, W., Lee, G.F., 1961. Oxygenation of ferrous iron. Ind. Eng. Chem. 53, 143–146.

Stumm, W., Morgan, J.J., 1996. Aquatic Chemistry-Cchemical Equilibria and Rates in Natural Waters, 3rd). Wiley-Interscience, New York, p. 1022.

Sung, W., Morgan, J.J., 1980. Kinetics and product of ferrous iron oxygenation in aqueous systems. Environ. Sci. Technol. 14, 561–568.

Tamura, H., Goto, K., Nagayama, M., 1976. The effect of ferric hydroxide on the oxygenation of ferrous iron in neutral solutions. Corrosion Sci. 16, 197–207.

Tan, H., Zhang, G., Heaney, P.J., Webb, S.M., Burgos, W.D., 2010. Characterization of manganese oxide precipitates from Appalachian coal mine drainage treatment systems. Appl. Geochem. 25, 389–399. https://doi.org/10.1016/j.apgeochem.2009.12.006.

Thomas, R.C., Romanek, C.S., 2002a. Passive treatment of low-pH, ferric dominated acid rock drainage in a vertical flow wetland–I. Acidity neutralization and alkalinity generation. In: Proceedings American Society of Mining and Reclamation, Lexington, Kentucky, June 9-13, 2002, pp. 723–748. https://doi.org/10.21000/JASMR02010723.

Thomas, R.C., Romanek, C.S., 2002b. Passive treatment of low-pH, ferric dominated acid rock drainage in a vertical flow wetland–II. Metal removal. In: Proceedings American Society of Mining and Reclamation, Lexington, Kentucky, June 9-13, 2002, pp. 752–775. https://doi.org/10.21000/JASMR02010752.

Tipping, E., Lofts, S., Sonke, J.E., 2011. Humic ion-binding model VII: a revised parameterisation of cation-binding by humic substances. Environ. Chem. 8 (3), 225–235.

Tonkin, J.W., Balistrieri, L.S., Murray, J.W., 2004. Modeling sorption of divalent metal cations on hydrous manganese oxide using the diffuse double layer model. Appl. Geochem. 19, 29–53.

Vail, W.J., Riley, R.K., 2000. The Pyrolusite Process®: a bioremediation process for the abatement of acid mine drainage. Green Lands. Fall 40–47, 2000.

van Beek, C.G.E.M., Hiemstra, T., Hofs, B., Nederlof, M.M., van Paaassen, J.A.M., Reijnen, G.K., 2012. Homogeneous, heterogeneous and biological oxidation of iron (II) in rapid sand filtration. J. Water Supply Res. Technol. - Aqua 61, 1–10.

Visual Studio, 2019. 16.2.3. Microsoft Visual Studio Community 2019 Version 16.2.3 (Accessed 29 July 2019).

Vries, D., Bertelkamp, C., Schoonenberg Kegel, F., Hofs, B., Dusseldorp, J., Bruins, J.H., de Vet, J.H., van den Akker, B., 2017. Iron and manganese removal: recent advances in modelling treatment efficiency by rapid sand filtration. Water Res. 109, 35–45.

Watzlaf, G.R., Schroeder, K.T., Kairies, C., 2000. Long-term performance of alkalinity-producing passive systems for the treatment of mine drainage. In: Proc. 2000 National Meeting of the American Society for Surface Mining and Reclamation, pp. 262–274.

Watzlaf, G.R., Schroeder, K.T., Kleinmann, R.L.P., Kairies, C.L., Nairn, R.W., 2004. The Passive Treatment of Coal Mine Drainage. U.S. Department of Energy DOE/NETL-2004/1202 (accessed June 15, 2020 at. http://www.bobkleinmann.com/images/2004_DOEPassiveTreatment_of_Coal_Mine_Drainage_NETL-1202.pdf.

Webster, J.G., Swedlund, P.J., Webster, K.S., 1998. Trace metal adsorption onto an acid mine drainage iron(III) oxy hydroxy sulfate. Environ. Sci. Technol. 32 (10), 1361–1368. https://doi.org/10.1021/es9704390.

Winland, R.L., Traina, S.J., Bigham, J.M., 1991. Chemical composition of ochreous precipitates from Ohio coal mine drainage. J. Environ. Qual. 20, 452–460. https://doi.org/10.2134/jeq1991.00472425002000020019x.

Wolfe, N., Hedin, R.S., Weaver, T., 2010. Sustained treatment of AMD containing Al and Fe^{3+} with limestone aggregate. In: International Mine Water Association 2010 Symposium. Nova Scotia, Canada, Sydney, pp. 237–241. https://www.imwa.info/docs/imwa_2010/IMWA2010_Hedin_490.pdf.

Zappa, C.J., Raymond, P.A., Terray, E.A., McGillis, W.R., 2003. Variations in surface turbulence and the gas transfer volocity over a tidal cycle in a macro-tidal estuary. Estuaries 26, 1401–1415.

Supplementary Data:

Interactive PHREEQ-N-AMDTreat Water-Quality Modeling Tools to Evaluate Performance and Design of Treatment Systems for Acid Mine Drainage

Charles A. Cravotta III, Research Hydrologist,
U.S. Geological Survey, Pennsylvania Water Science Center,
215 Limekiln Rd, New Cumberland, PA 17070
cravotta@usgs.gov

This supplementary data file augments the article by the same title (Cravotta, 2020a). It includes 8 tables, 21 figures, expanded explanation of the user interface for the PHREEQ-N-AMDTreat software (Cravotta, 2020b), and additional case-study simulations using the PHREEQ-N-AMDTreat modeling tools that were excluded from the journal article to reduce the paper length.

Supplementary Tables:

Table S1. Expanded description of variables used in PHREEQ-N-AMDTreat modeling tools (Excel file with expanded information from table included in main text).

Table S2. Solubility reactions and equilibrium constants used with PHREEQC database for PHREEQ-N-AMDTreat models (phreeqcAMDTreat.dat). (Excel file)

Table S3. Surface complexation model parameters for hydrous metal oxides (HMeO) used with phreeqcAMDTreat.dat database for PHREEQ-N-AMDTreat models. (Excel file)

Table S4. Surface species for hydrous ferric oxide (HFO), hydrous manganese oxide (HMO), and hydrous aluminum oxide (HAO) in phreeqcAMDTreat.dat database (Excel file)

Table S5. Rate models in phreeqcAMDTreat.dat database coded for use by PHREEQ-N-AMDTreat software. (Excel file)

Table S6. Typical empirical values of rate constants for CO_2 outgassing and O_2 ingassing. (Excel file)

Table S7. Surface area and volume estimates for various coarse aggregates used in limestone beds. (Excel file)

Table S8. Estimated size of passive or active treatment systems for Morea AMD based on retention times used in TreatTrainMix2 and 90th percentile flow (Excel file).

Supplementary Figures:

Figure S1. UI for PHREEQ-N-AMDTreat model exhibiting input values for simulations of caustic titration of Nittanny mine effluent.

Figure S2. Concentration of NaOH added and corresponding pH and solute concentrations indicated for simulated titration of effluent at the Nittanny mine.

Figure S3. Measured and simulated titrant and chemical concentrations as a function of pH during titration of Nittanny mine effluent with NaOH.

Figure S4. UI for PHREEQ-N-AMDTreat parallel model exhibiting input values for simulations of different limestone particle size and sorbent for Orchard oxic limestone drain.

Figure S5. Comparison of measured (symbols) and simulated (curves) values for pH, alkalinity, Ca, Fe, Al, Mn, Pco_2, and calcite saturation index during treatment of AMD at the Orchard oxic limestone drain, 1995-2000.

Figure S6. UI for PHREEQ-N-AMDTreat sequential model exhibiting input values for simulation of water-quality changes through the Pine Forest treatment system, December 2015, which consists of a “biofouled” anoxic limestone drain (ALD), oxidation/settling pond, and three aerobic wetlands, with aeration steps in between.

Figure S7. Comparison of measured (symbols) and simulated (curves) values for pH, Fe^{II}, Mn^{II}, Al, Pco_2, and Po_2 during treatment of AMD at the Pine Forest passive treatment system, December 2015.

Figure S8. UI for PHREEQ-N-AMDTreat model exhibiting input values for simulations of sequential treatment steps at the Silver Creek treatment system, December 2015, which consists of a small sedimentation pond, two large oxidation/settling ponds, and two aerobic wetlands, with aeration cascades in between.

Figure S9. Comparison of measured (symbols) and simulated (curves) values for pH, Fe^{II}, Mn^{II}, Al, Pco_2, and Po_2 during treatment of AMD at the Silver Creek passive treatment system, December 2015.

Figure S10. UI for PHREEQ-N-AMDTreat sequential model exhibiting input values for simulations of sequential steps at the Silver Creek treatment system, August 2016.

Figure S11. Comparison of measured (symbols) and simulated (curves) values for pH, Fe^{II}, Mn^{II}, Al, Pco_2, and Po_2 during treatment of AMD at the Silver Creek passive treatment system, August 2016.

Figure S12. UI for TreatTrainMix2 simulation of passive treatment of net-acidic AMD at Morea Mine through (1) sedimentation pond; (2-4) vertical flow pond (VFP); (6, 8) oxidation/settling ponds; (10) aerobic wetlands; and (11) manganese removal bed with intermediate aeration steps (5 7 9 11).

Figure S13. TreatTrainMix2 simulation results for passive treatment of Morea AMD by (1) VFP (consisting of a 0.61-m (2-ft) deep water layer, 0.61-m (2-ft) thick compost layer composed of 25 % limestone fines and 75% organic matter having 45% porosity, 0.91-m (3-ft) thick limestone layer having 45% porosity), (2) 1.52-m (5-ft) deep aerobic pond, (3) 0.30-m (1-ft) deep wetlands, and (3) 0.30-m (0.5-ft) deep “manganese” removal limestone bed

Figure S14. UI for TreatTrainMix2 simulation of active treatment of net-acidic AMD at Morea Mine through (1) sedimentation pond; (3) lime dosing and sludge recirculation; (4) aerobic pond; and (6) aerobic wetlands with aeration steps (2 5 7).

Figure S15. TreatTrainMix2 input and simulation results for active treatment of AMD at Morea Mine by (1) hydrated lime dosing and recirculation of sludge, including HMeO solids and unreacted lime, (2) 1.52-m (5-ft) deep aerobic pond, and (3) 0.30-m (1-ft) deep wetlands.

Figure S16. UI for PHREEQ-N-AMDTreat model exhibiting input values for simulations of hypothetical treatment using passive aeration after mixing of AMD from the Oak Hill boreholes (Soln#A) and Pine Knot tunnel (Soln#B).

Figure S17. Simulation results for passive treatment of combined Oak Hill boreholes + Pine Knot tunnel AMD by aeration cascades, oxidation+settling pond, aerobic wetlands, and Mn-removal bed.

Figure S18. UI for PHREEQ-N-AMDTreat model exhibiting input values for simulations of hypothetical treatment using aggressive aeration after mixing of AMD from the Oak Hill boreholes (Soln#A) and Pine Knot tunnel (Soln#B).

Figure S19. Simulation results for passive treatment of combined Oak Hill boreholes + Pine Knot tunnel AMD by Maelstrom Oxidizer®, oxidation+settling pond, aerobic wetlands, and Mn-removal bed.

Figure S20. UI for PHREEQ-N-AMDTreat model exhibiting input values for simulations of hypothetical treatment using H_2O_2 after mixing of AMD from the Oak Hill boreholes (Soln#A) and Pine Knot tunnel (Soln#B).

Figure S21. Simulation results for passive treatment of combined Oak Hill boreholes + Pine Knot tunnel AMD by H_2O_2 without sludge recirculation, oxidation+settling pond, aerobic wetlands, and Mn-removal bed.

S1. Access, Installation, and Use of PHREEQ-N-AMDTreat Software

The executable PHREEQ-N-AMDTreat program files including example input and output files are accessible in the U.S. Geological Survey software release (Cravotta, 2020b). Instructions for installation and use of the software are provided in the document, "Instructions_PHREEQ-N-AMDTreatGeochemicalModels.docx," included with the software.

S2. User Interface for PHREEQ-N-AMDTreat

The PHREEQ-N-AMDTreat water-quality modeling tools consider dynamic reactions that take place in AMD treatment systems and other aquatic environments. The CausticTitration and ParallelTreatment tools consider treatment of one or a mixture of two water samples, whereas the TreatTrainMix2 sequential tool may be used for evaluation of progressive changes for the same initial water chemistry over as many as eleven sequential treatment steps, where water chemistry after reactions from the prior step is passed to the next step. Each step can have a different specified reaction (residence) time, temperature, aeration rate, mass of limestone and/or organic matter, and mass and composition of hydrous metal oxide (HMeO) sorbent plus added caustic agent or H_2O_2. Values for variables used in the PHREEQ-N-AMDTreat tools (Tables 1 and S1) are displayed and adjusted in the user interface (UI) that is linked to the PHREEQC code for each of the three tools. After entering or selecting values for each variable in the UI, the input data may be saved to a file "water_quality_input_values.xml" for re-use.

Check boxes on the UI screen permit the activation of selected computations. Specifically, the user can input the values for acidity (hot acidity or net acidity), total inorganic carbon (TIC), and Fe^{II}, or select the relevant option to estimate values for one or more of these parameters from other input dat. Likewise, check boxes are used to activate sequential kinetic steps or addition of caustic agents. Later in this document, the UI for various treatment simulations is displayed with input values. For example, Figure S1 shows the UI for the CausticTitration tool, with radio button activated for direct addition of NaOH without pre-aeration or other pre-treatment steps. The UI for the ParallelTreatment tool (Fig. S4) is identical to that for the TreatTrainMix2 tool (e.g. Figs. S6, S8, S10, S12, S14, S16, S18, and S20). Each step for the ParallelTreatment simulation is

independent of the others, whereas the TreatTrainMix2 simulations use water chemistry results from the prior step at the beginning of the next step.

The mass of precipitated solids is computed as the mass of precipitated minerals plus the adsorbed metals, expressed as the relevant hydroxides. Including the adsorbed metals considers that they could eventually oxidize in situ, with infinite time for reaction. To compute the sludge mass produced by treatment, Fe, Al, Mn, and Mg are assumed to precipitate as $Fe(OH)_3$, $Al(OH)_3$, $Mn(OH)_2$, and $Mg(OH)_2$, respectively, and SO_4 as gypsum ($CaSO_4 \cdot 2H_2O$), which in addition to the unreacted solid chemicals can make up a large fraction of the sludge (e.g. Means and Hilton 2004).

Changes to rate parameters are implemented by changing multiplication factors in the UI, not the actual rate constants. For example, FeOB (iron-oxidizing bacteria) contributions to the Fe^{II} oxidation rate may be changed from 1 (default) to 0 to yield solely abiotic contributions, or the fixed sorbent mass and composition can be specified as 0 to simulate solely autocatalytic oxidation, or to other positive values to reflect measured chemistry (percentage Fe, Mn, Al) of the sorbent.

Net acidity (as mg/L of $CaCO_3$) is computed for “non-purgeable” constituents in AMD; computed net acidity and measured hot acidity exclude CO_2 acidity, because that can be eliminated simply by aeration (Kirby and Cravotta, 2005). The net-acidity computation considers a negative contribution from alkalinity and positive contributions from H^+ (pH) and concentrations of dissolved Fe^{III}, Fe^{II}, Mn, and Al in milligrams per liter (CFe^{III}, CFe^{II}, C_{Mn}, C_{Al}, respectively):

$$\text{Net Acidity} = 50 \cdot (10^{(3-pH)} + 3 \cdot CFe^{III}/55.85 + 2 \cdot CFe^{II}/55.85 + 2 \cdot C_{Mn}/54.94 + 3 \cdot C_{Al}/26.98) - \text{Alkalinity} \quad \text{(S1)}$$

Kirby and Cravotta (2005) showed that if the AMD is net acidic (net acidity > 0; hot-peroxide acidity > 0), the ultimate pH of oxidized samples will be less than 5.0 and additional alkalinity would be needed to maintain pH greater than or equal to 6.0. If the AMD is net alkaline (net acidity < 0; hot-peroxide acidity < 0), the ultimate pH of the oxidized AMD will be greater than or equal to 6.0. Kirby and Cravotta (2005) also showed that the cold acidity or treatment acidity (prior to complete oxidation and atmospheric equilibration) can be larger than the hot acidity because of contributions by dissolved CO_2 that are excluded from the hot acidity or calculated net acidity. Thus, pre-aeration may be conducted to promote the CO_2 outgassing and reduce the caustic chemical requirement for treatment (Jageman et al., 1988; Means and Hilton, 2004).

Some AMD has low pH and no measurable alkalinity, but may still have elevated concentrations of dissolved CO_2 that is included in treatment acidity. Therefore, the model uses the

TIC concentration instead of alkalinity as input to PHREEQC for carbonate speciation calculations. If selected, the initial TIC can be estimated from input values for alkalinity, pH, and temperature, assuming equilibrium among dissolved carbonate species in accordance with the following:

$$\text{TIC (mg/L as C)} = (\text{Alkalinity}/50000)/K_1 \cdot [H^+] \cdot (1 + K_1/[H+] + K_1 \cdot K_2/[H^+]^2) \quad \text{(S2)}$$

where $[H^+] = 10^{-pH}$, and K_1 and K_2 are the temperature-adjusted dissociation constants for carbonate species (Ball and Nordstrom 1991). If alkalinity is 0 and/or pH is less than or equal to 3.9, TIC is assumed to be 0.0001 mol/L (1.2 mg/L), which corresponds to an equilibrium partial pressure of CO_2 (Pco_2) of $10^{-2.5}$ atm. AMD samples from 140 coal mines in Pennsylvania had Pco_2 values from $10^{-2.5}$ to $10^{-0.5}$ atm and were mostly undersaturated with carbonate minerals (Cravotta 2008b).

The initial distribution of Fe^{II} and Fe^{III} species is estimated by PHREEQC using the input values for total dissolved iron (undefined redox state) and Fe^{II}. Thereafter, the PHREEQC titration simulations assume that any Fe^{II} can be oxidized kinetically to consume available DO (without and with pre-aeration, as explained below). However, because data on the initial concentration of Fe^{II} may not be available the initial Fe^{II} concentration can be estimated using the input values for total dissolved Fe and pH:

$$\text{pH} > 2.6 \qquad Fe^{III} = Fe \cdot 10(-1.40844 \cdot pH + 3.675995) \quad \text{(S3a)}$$

$$\text{pH} \leq 2.6 \qquad Fe^{III} = Fe \cdot (0.9999) \quad \text{(S3b)}$$

$$Fe^{II} = Fe - Fe^{III} \quad \text{(S3c)}$$

These computations yield a greater proportion of Fe^{III} to Fe^{II} at progressively lower pH, until pH < 2.6, where 99.99% of the total dissolved Fe is assumed to be Fe^{III}. The computations are based on an approximation of the empirical relation between the ratio of Fe^{III}/total Fe as a function of pH of AMD in Pennsylvania (Cravotta 2008a).

Input values for the sorbent mass and chemistry in the UI are used with the specific surface area and site densities to compute the moles of sorption sites on HFO, HMO, and HAO for adsorption equilibrium computations (Tables S3 and S4). For HFO, the unit mass was estimated as 107 g/mol for $Fe(OH)_3$ instead of using 89 g/mol for FeOOH, otherwise, specific surface area of 600 m^2/g and densities of strong and weak sites of 0.005 mol/mol and 0.2 mol/mol, respectively, were adopted from Dzombak and Morel (1990). For HMO, the unit mass and surface area were specified as 105 g/mol and 746 m^2/g with densities of strong and weak sites of 0.0141 mol/mol and

0.0794 mol/mol, respectively (Tonkin et al., 2004). For HAO, the unit mass and surface area were specified as 78 g/mol and 32 m^2/g, respectively, with only a single site type having a density of 0.033 mol/mol (Karamalidis and Dzombak, 2010). Estimates for Al-HAO and Al-HMO surface species were computed using linear free energy relations with the first-hydrolysis equilibrium constant after Karamalidis and Dzombak (2010) and Tonkin et al. (2004), whereas that for Al-HFO adsorption was taken from Burrows et al. (2017).

S3. Additional Model Validation--Simulations of Observed Changes in Chemistry of AMD

S3.1. Caustic Titration without Pre-Aeration (Nittanny Mine)

The caustic titration tool is used to simulate field acidity titration (cold, no aeration) of Nittanny mine effluent with NaOH (1.6 N = 6.0 wt%). Detailed empirical water chemistry data were collected at points during the field titration in November 2011 and are used for comparison with simulations. The simulation results for titration with NaOH without aeration are consistent with the empirical data on pH and concentrations of major ions, Fe, Al, and Mn (Figs. S1-S3). Additional information about this site and the water-quality evaluation, including the field titration and the active treatment of the effluent, are reported by Cravotta et al. (2015) and Cravotta and Brady (2015).

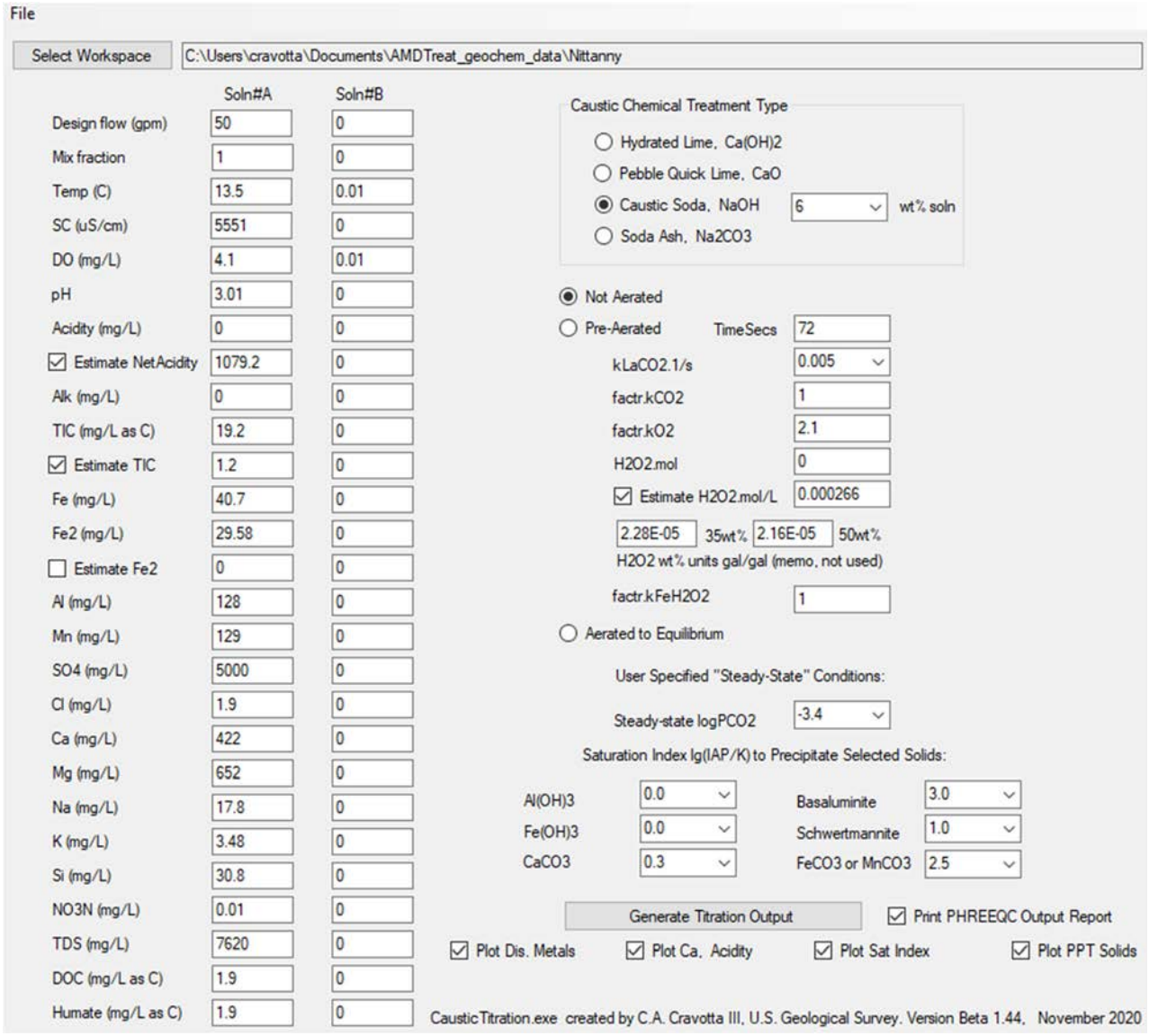

Figure S1. UI for PHREEQ-N-AMDTreat model exhibiting input values for simulations of caustic titration of Nittanny mine effluent. Results of simulations are shown in Figures S2-S3. The value of 1.2 for "Estimate TIC" for solution A or B corresponds to an assumed Pco_2 of $10^{-2.5}$ atm for samples with pH < 3.9 (Eq. S2).

A

pH	Caustic moles	Caustic units	Caustic asCaCO3mg	Fe_mg	Fe2_mg	Al_mg	Mn_mg	Na_mg	Ca_mg	Mg_mg	SO4_mg	Alk_mg	SpCond_uS	TDS_mg	NetAcidity_mg	SolidsPPT_mg	CO2_mg	O2_mg
3.010999	0.000000	0.000000	0.000000	40.963462	29.500570	128.828578	129.835051	17.915224	424.731718	656.220569	5,032.366343	-139.093909	5,381.732596	6,782.110614	1,096.471392	0.000000	4.422939	0.000000
3.010999	0.000000	0.000000	0.000000	40.963479	29.500570	128.828583	129.835062	17.915224	424.731722	656.220569	5,032.366357	-139.093830	5,381.732316	6,782.110746	1,096.471436	0.000000	4.422939	0.000000
4.000000	0.002632	0.001644	131.729299	30.927933	29.499487	128.823854	129.830296	78.427694	423.929334	656.196481	5,030.295835	-16.340967	5,208.996566	6,894.145825	1,016.252790	22.582296	4.400522	0.000000
4.500000	0.002908	0.001817	145.548216	29.676932	29.499393	128.823443	129.829882	84.775487	423.498088	656.194387	5,029.249411	-3.641950	5,198.621912	6,904.236755	1,008.726038	26.822977	4.347788	0.000000
5.000000	0.003079	0.001924	154.091279	29.541372	29.499364	128.823317	129.829754	88.699855	423.149442	656.193741	5,028.409825	4.780329	5,202.110004	6,911.765506	1,002.264595	28.578333	4.189039	0.000000
5.500000	0.014945	0.009336	747.896278	29.512219	29.499739	22.069809	129.831406	361.482400	408.514849	656.202091	4,993.384620	4.529079	5,835.602848	6,824.894963	407.949346	400.172834	3.753572	0.000000
6.000000	0.017254	0.010779	863.450372	29.503809	29.499801	0.965798	129.831677	414.566362	406.034728	656.203458	4,987.448606	2.643948	5,958.340601	6,807.173726	292.238152	471.862082	2.824345	0.000000
6.500000	0.017369	0.010851	869.237714	29.501208	29.499800	0.143455	129.831673	417.224939	405.999566	656.203441	4,987.364231	3.853228	5,965.522307	6,808.046894	286.403850	474.395582	1.581686	0.000000
7.000000	0.017402	0.010871	870.863758	29.500392	29.499797	0.188060	129.831663	417.971879	406.035821	656.203388	4,987.450803	5.726916	5,967.334344	6,810.168680	284.762970	474.112290	0.656795	0.000000
7.500000	0.017432	0.010890	872.388024	29.500134	29.499793	0.526899	129.831645	418.672034	406.069006	656.203296	4,987.529780	9.136713	5,968.658991	6,814.009564	283.233892	472.990332	0.225002	0.000000
8.000000	0.017498	0.010931	875.662622	29.500053	29.499782	1.635557	129.831596	420.176162	406.131010	656.203052	4,987.676895	18.581152	5,970.926733	6,824.606295	279.957437	469.518152	0.067816	0.000000
8.500000	0.017686	0.011049	885.082312	29.500025	29.499745	5.152413	129.831464	424.502940	406.314163	656.202381	4,988.111775	47.572733	5,977.398859	6,857.150958	270.536190	458.561782	0.017282	0.000000
9.000000	0.019022	0.011884	951.956897	7.161506	7.161123	16.292665	129.831198	455.222789	406.377837	656.201041	4,988.256189	136.352837	6,017.228560	6,930.889105	203.655072	462.051008	0.003438	0.000000
9.500000	0.024073	0.015039	1,204.687336	0.785458	0.784729	51.537562	39.647702	571.319656	406.094327	656.198804	4,987.562985	409.548781	6,168.678804	7,153.933034	-49.097383	517.621406	0.000913	0.000000
10.000000	0.044934	0.028071	2,248.687649	0.101922	0.100088	89.624845	4.304857	1,051.239648	250.732682	496.747519	4,840.819347	709.162324	6,677.631397	7,404.052763	-202.378848	1,510.219790	0.000182	0.000000
10.500000	0.084213	0.052609	4,214.335471	0.023208	0.017863	60.901065	0.520543	1,954.969477	123.871022	53.248265	4,700.634506	513.019286	7,872.897102	7,389.928731	-173.114833	3,204.683801	0.000039	0.000000
11.000000	0.089866	0.056141	4,497.233716	0.023228	0.006796	45.935147	0.066962	2,085.261448	58.890600	5.476058	4,627.593805	429.723125	8,061.371739	7,240.294867	-173.919146	3,642.413746	0.000007	0.000000

Display

B

pH	Caustic moles	Caustic units	Caustic asCaCO3mg	Fe_mg	Fe2_mg	Al_mg	Mn_mg	Na_mg	Ca_mg	Mg_mg	SO4_mg	Alk_mg	SpCond_uS	TDS_mg	NetAcidity_mg	SolidsPPT_mg	CO2_mg	O2_mg
3.110592	0.000000	0.000000	0.000000	40.963478	0.763963	128.828627	129.835101	17.915231	424.731880	656.220820	5,032.368252	-164.847370	5,273.793918	6,766.661143	1,110.062723	0.000000	4.422319	0.000000
3.113321	0.000000	0.000000	0.000000	40.963491	0.000006	128.828621	129.835101	17.915229	424.731847	656.220763	5,032.367828	-165.567901	5,271.131100	6,766.272873	1,110.451823	0.000000	0.817309	10.596304
4.000000	0.006088	0.003803	304.664800	1.436339	0.000001	128.823926	63.894837	157.869425	421.173131	656.196845	5,023.691961	-16.433767	5,291.527631	6,800.954609	843.261288	196.417926	0.816936	10.591470
4.500000	0.008456	0.005283	423.179094	0.177923	0.000000	128.822489	6.411334	212.309349	419.105134	656.189524	5,018.690603	-3.775701	5,332.304915	6,760.375843	730.971713	299.714653	0.816904	10.591053
5.000000	0.008833	0.005518	442.015821	0.042017	0.000000	128.822257	0.642033	220.961942	418.607150	656.188342	5,017.489783	4.428532	5,340.808699	6,762.643795	714.348891	311.346959	0.816850	10.590350
5.500000	0.020670	0.012913	1,034.395810	0.012481	0.000000	22.468139	0.066684	493.087885	404.554562	656.196285	4,983.857043	3.919134	5,980.309702	6,677.159336	121.462401	680.210784	0.815568	10.573736
6.000000	0.023009	0.014374	1,151.486648	0.004008	0.000000	0.978835	0.006717	546.877353	402.101674	656.197629	4,977.986164	1.315981	6,106.880154	6,658.589314	4.215240	752.993827	0.815316	10.570474
6.500000	0.023120	0.014443	1,157.005715	0.001408	0.000000	0.143874	0.000672	549.412658	402.061452	656.197617	4,977.889689	2.175655	6,112.779538	6,659.065887	-1.350685	755.595270	0.815304	10.570309
7.000000	0.023184	0.014483	1,160.210309	0.000594	0.000000	0.188078	0.000067	550.884695	402.161564	656.197534	4,978.129131	5.624664	6,116.968019	6,663.072532	-4.570199	755.039698	0.693989	10.570143
7.500000	0.023213	0.014501	1,161.614816	0.000341	0.000000	0.526910	0.000007	551.529828	402.204838	656.197463	4,978.232419	8.914520	6,118.367839	6,666.820759	-5.879448	753.874562	0.244479	10.570067
8.000000	0.023270	0.014537	1,164.500004	0.000271	0.000000	1.635595	0.000001	552.855050	402.291448	656.197275	4,978.438852	17.969617	6,120.720495	6,677.089145	-8.866313	750.296720	0.078935	10.569908
8.500000	0.023439	0.014643	1,172.986733	0.000280	0.000000	5.152584	0.000000	556.753155	402.541665	656.196718	4,979.035164	46.028794	6,127.339865	6,708.874986	-17.354108	739.052015	0.023925	10.569437
9.000000	0.023959	0.014968	1,199.012230	0.000382	0.000000	16.283424	0.000000	568.707196	403.285475	656.195133	4,980.808239	133.996622	6,147.535357	6,808.427943	-43.381516	703.670749	0.006495	10.567982
9.500000	0.025530	0.015949	1,277.633285	0.000729	0.000000	51.539835	0.000000	604.819465	405.199009	656.190747	4,987.461808	406.642463	6,208.975405	7,119.003521	-119.825215	591.932267	0.001103	10.563598
10.000000	0.045079	0.028162	2,255.922109	0.001834	0.000000	89.678781	0.000000	1,054.546167	250.693791	496.858587	4,841.027823	708.741403	6,681.971912	7,400.422109	-209.680858	1,523.174956	0.000182	10.559894
10.500000	0.084231	0.052621	4,215.263473	0.005345	0.000000	60.913266	0.000000	1,955.363524	123.866861	53.247993	4,700.639319	512.916985	7,873.475641	7,389.465396	-173.924908	3,212.032250	0.000039	10.545760
11.000000	0.089869	0.056143	4,497.396164	0.016432	0.000000	45.935330	0.000000	2,085.301685	58.893194	5.476151	4,627.539965	429.701237	8,061.435515	7,240.193553	-174.030432	3,649.133387	0.000007	10.545751

Figure S2. Concentration of NaOH added and corresponding pH and solute concentrations indicated for simulated titration of effluent at the Nittanny mine. Simulations use effluent composition data in Figure S1 for conditions with: A, no gas exchange with atmosphere and B, with equilibrium with atmosphere.

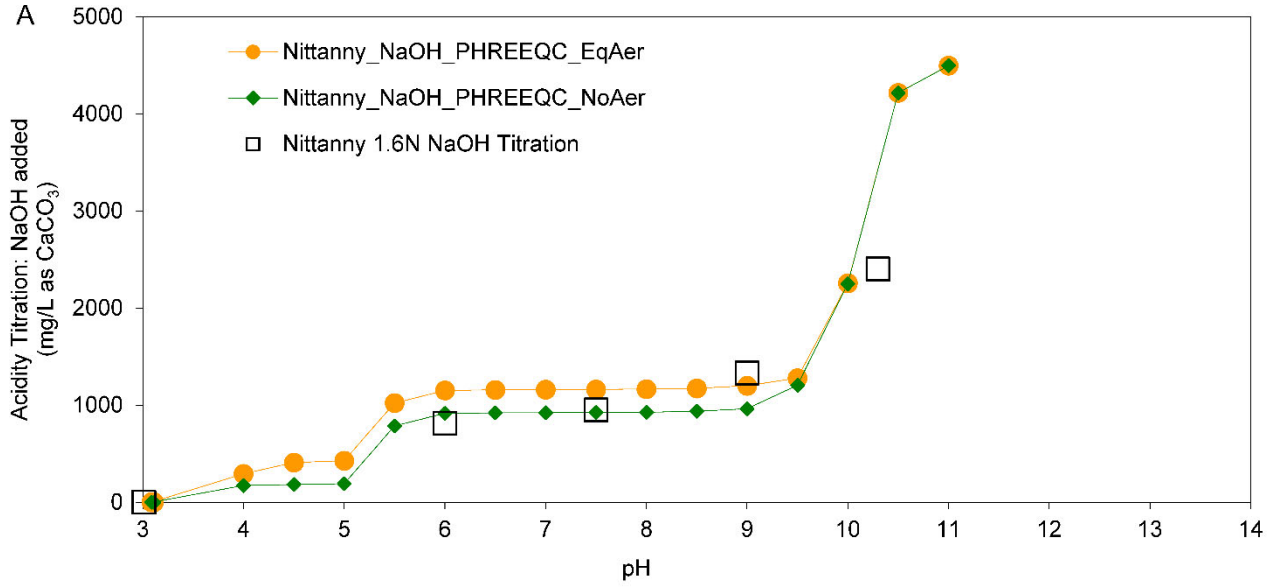

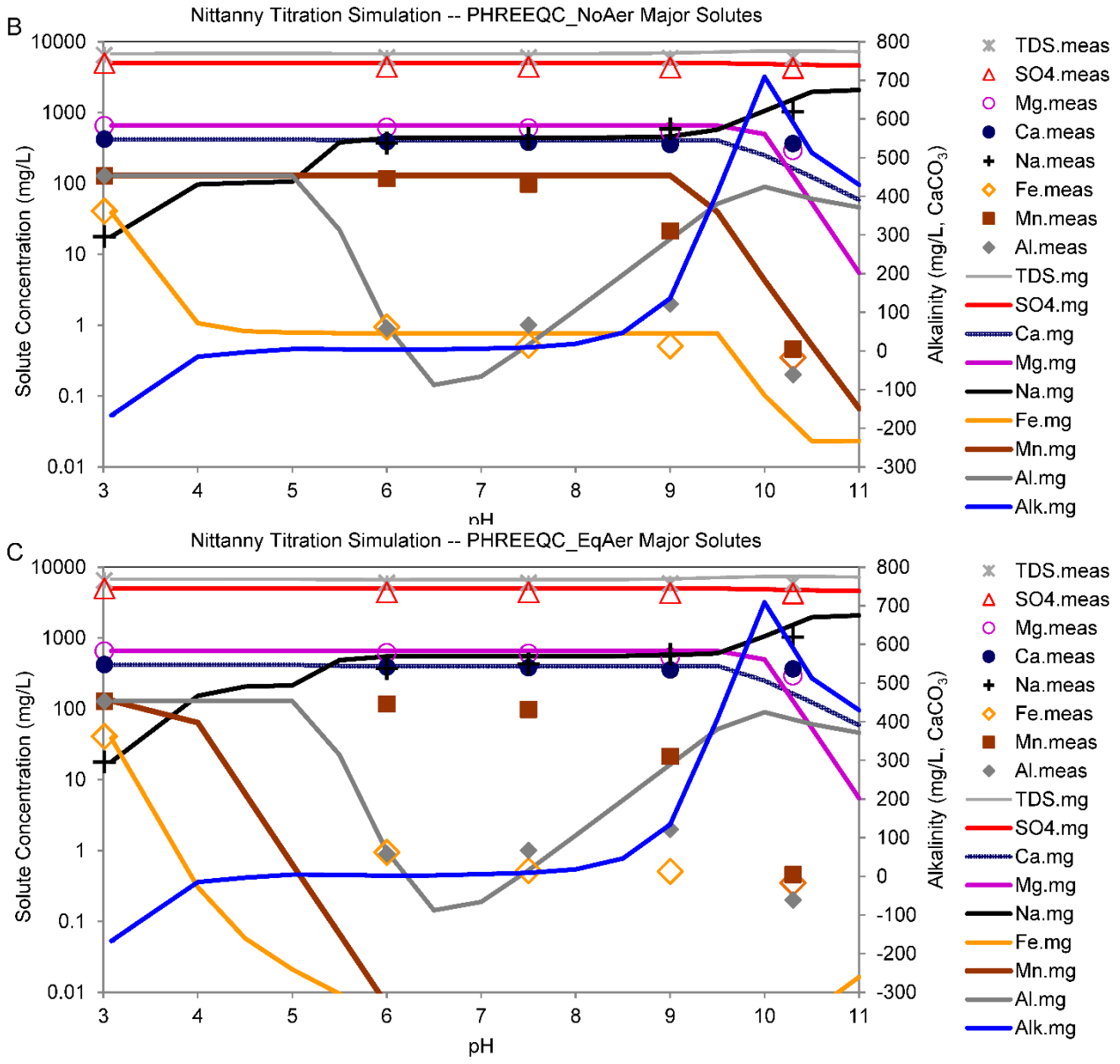

Figure S3. Measured (point symbols) and simulated (lines) titrant and chemical concentrations as a function of pH during titration of Nittanny mine effluent with NaOH. Simulations use effluent composition data shown in Figure S1 for conditions with: B, no gas exchange with atmosphere (PHREEQC_NoAer) and C, with equilibrium with atmosphere (PHREEQC_EqAer). The simulations without atmospheric equilibration are consistent with empirical results where oxidation of Fe^{II} and Mn^{II} are kinetically limited.

S3.2. Parallel Treatment Fragment Size and Coatings (Orchard OLD)

The Orchard limestone drain was constructed in 1995 as a research project to evaluate the efficiency of neutralization of low pH, oxic AMD with relatively low concentrations of dissolved metals (<5 mg/L) by limestone and associated reactions (Figs. S4 and S5). Three parallel “oxic”

limestone drains (OLDs), with access wells at five locations along the length of each drain, were constructed to treat the same influent AMD (Cravotta and Trahan, 1999; Cravotta and Watzlaf, 2003). The untreated AMD (6.9 gal min^{-1}, 0.43 L s^{-1}), sampled during 1995-2000, had median pH 3.5 with DO 2.6 mg/L and dissolved concentrations of Fe, Fe^{II}, Mn^{II}, and Al of 1.8, 0.6, 3.0, and 0.065 mg/L, respectively (Figs. S4 and S5). As reported by Cravotta and Trahan (1999), downgradient trends through the OLDs during the first 6 months of treatment (Fig. S5, Mar95-Aug95) were consistent with those expected for an ALD, with relatively conservative transport of Fe^{II} and Mn^{II}; however, after the first 6 months (Fig. S5, Sep95-May00), the drains began to retain Mn and trace metals consistent with adsorption by HFO and HMO that accumulated in the downstream section of the drains wherein pH was 6-6.5.

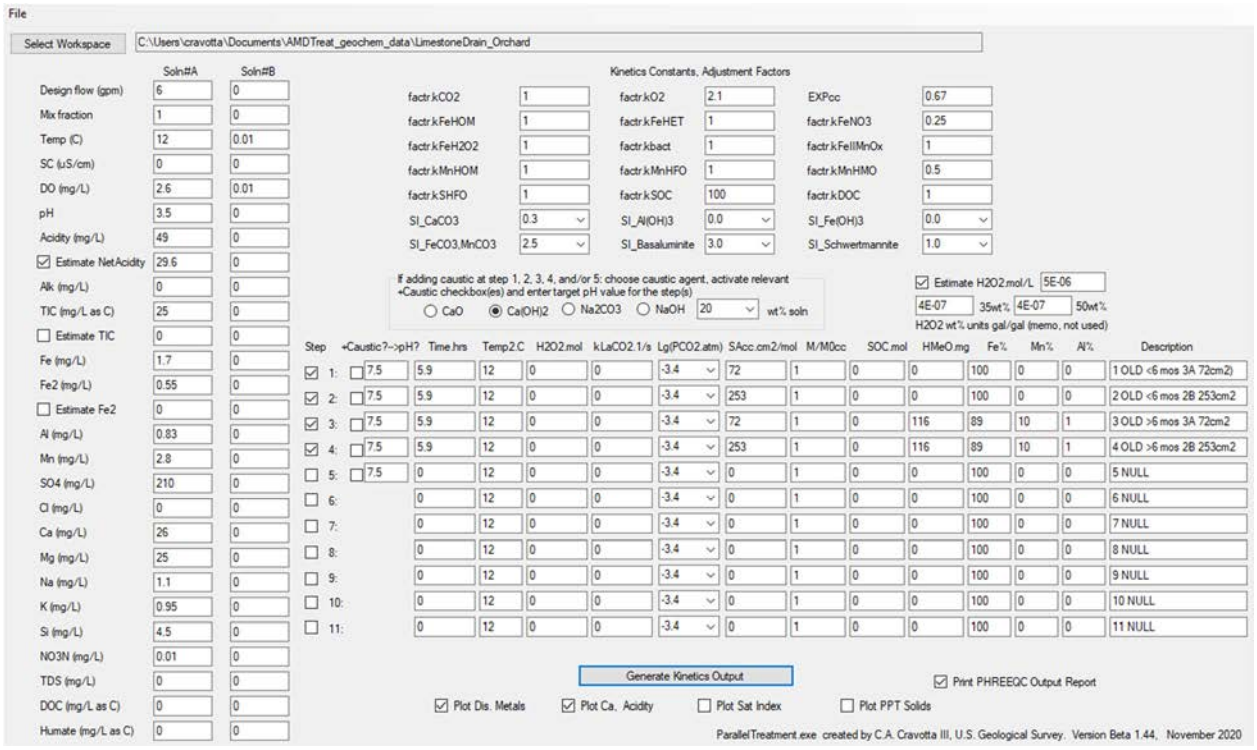

Figure S4. UI for PHREEQ-N-AMDTreat parallel model exhibiting input values for simulations of different limestone particle size and sorbent for Orchard oxic limestone drain. Results are shown in Figure S5

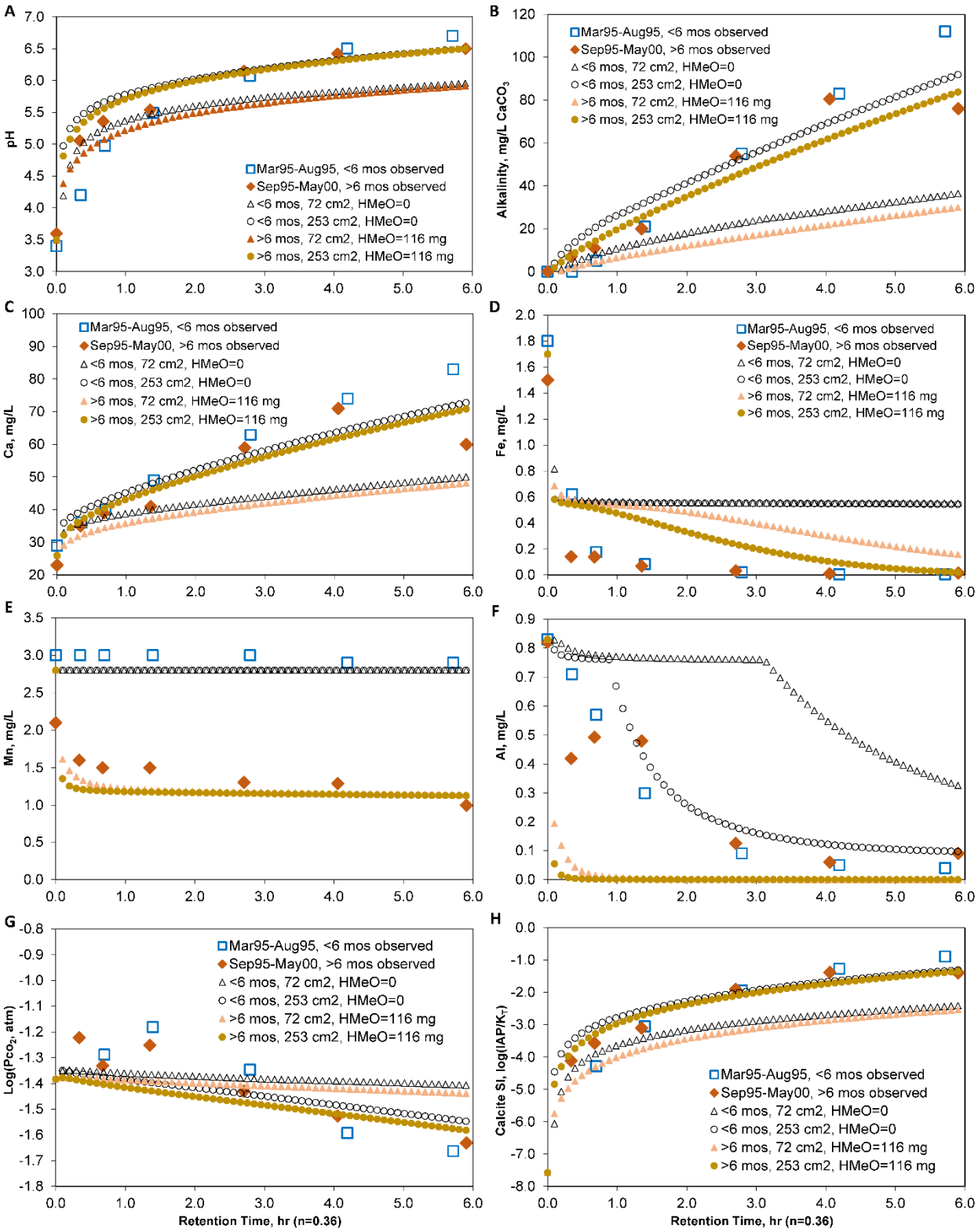

Figure S5. Comparison of measured and simulated values for pH, alkalinity, Ca, Fe, Al, Mn, Pco_2, and calcite saturation index during treatment of AMD at the Orchard oxic limestone drain, 1995-2000.

Travel time through the OLDs increased linearly with distance from the inflow, attaining a total retention time of approximately 6 hrs at the outflow, which assumes a porosity of 35% (Fig. S5). The pH, alkalinity, Ca, and calcite saturation index ($SI_{CALCITE}$) values increased rapidly near the inflow and more gradually toward the outflow (Fig. S5). The asymptotic trends for pH, alkalinity, and Ca with retention time are consistent with rapid rates of limestone dissolution at low pH, and decreasing rates of dissolution as equilibrium with calcite is approached (Plummer et al., 1978).

The simulations consider two different limestone particle sizes consistent with standard aggregate materials (Table S7). The smaller particles correspond to AASHTO 57 or PA 2B size with average axis dimensions of 1.48 cm and estimated surface area of 2.53 cm^2/g (253 cm^2/mol). The larger particles, which correspond to AASHTO 3 or PA 3A size with average axis dimensions of 3.81 cm, have smaller estimated surface area of 0.72 cm^2/g (72 cm^2/mol). The simulated dissolution of the smaller size particles resulted in nearly double the concentrations of Ca and alkalinity (Fig. S5) and matched the observed data values better than simulations with larger particles.

Simulations for the system after 6 months (Sep95-May00) include an accumulated sorbent mass (HMeO.mg) of 116 mg within the OLD that is composed of 89% Fe, 10% Mn, and 1% Al (Fig. S4). This sorbent mass was computed for 0.5-μm thick coating on the limestone particles (72 cm^2/mol) in contact with 1 L water volume, assuming 35% bed porosity and sorbent density of 1.25 g/cm^3 (Table S7). The same mass of sorbent would have a smaller thickness if spread out over the finer particles. The included sorbent in the simulations improved the predictions of Fe and Mn attenuation, but resulted in overestimate of Al attenuation. The simulations do not evaluate potential for HMeO surface coatings to affect the limestone particle dissolution rate. Despite the accumulation of precipitated metals on limestone surfaces in the OLD and elsewhere, Cravotta and Trahan (1999), Cravotta and Watzlaf (2003), Cravotta (2003), and Cravotta et al. (2004, 2008c) showed that limestone theoretically could dissolve throughout the limestone systems they investigated because the water was consistently undersaturated with respect to calcite, attaining $SI_{CALCITE}$ values from -2.4 to -0.3 under the conditions evaluated. Cravotta and Trahan (1999) and Cravotta (2008c) noted etch pits beneath loosely bound surface coatings on limestone as evidence for continued dissolution. Although Palomino-Ore et al. (2019) demonstrated that Al armoring can lower calcite dissolution rates in the lab, Wolfe et al. (2010) demonstrated that automated flushing systems may be designed to effectively remove such solids to sustain the performance of a limestone bed.

S3.3. Sequential Treatment by Anoxic Limestone Drain (ALD), Cascades, Oxidation/Settling Pond, and Aerobic Wetlands

The Pine Forest treatment system consists of an anoxic limestone drain (ALD), oxidation/settling pond, and three aerobic wetlands, in series, with aeration steps in between (Figs. S6 and S7). The untreated AMD (690 gal min^{-1}, 43.5 L s^{-1}), sampled during winter 2015, had pH 5.8 with DO < 0.5 mg/L and dissolved concentrations of Fe^{II}, Mn^{II}, and Al of 14.0, 3.1, and 0.09 mg/L, respectively (Fig. S6). The treated effluent had pH ~7 with Fe and Mn <2 mg/L. After its first year of operation (2006), the ALD began to clog with gelatinous, Fe-rich precipitate. For this "biofouling" scenario, the microbial rate factor was increased from 1 to 2 and a pre-existing (accumulated) sorbent mass (HMeO.mg) of 116 mg was specified for the ALD (Fig. S6). The sorbent mass in the ALD was computed for 0.5-μm thick coating on the limestone particles (72 cm^2/mol) in contact with 1 L water volume, assuming 35% bed porosity and sorbent density of 1.25 g/cm^3 (Table S7). For downstream steps, the specified sorbent mass was only 1 to 3 mg.

The sequential model results for pH, Fe^{II}, Mn^{II}, Al, Pco_2, and Po_2, shown as a function of the retention time (computed as the void volume of the treatment component divided by the flow rate), generally reproduce the longitudinal trends for measured constituent values (Fig. S7). Despite less mass of sorbent indicated for wetlands, progressively increased pH and greater Mn content of sorbent at this stage of the treatment promoted attenuation of dissolved Mn^{II}. Simulation results for a reference scenario are also shown in Figure S7, where the existing sorbent and FeOB rate factor were set to 0, equivalent to the abiotic homogeneous Fe^{II} oxidation rate model. This abiotic reference scenario uses the same aeration coefficients and retention times as the biofouling scenario but underpredicts removal of Fe, Mn, and Al in the upper stages of the system where most chemical changes occur and does not indicate observed Mn^{II} attenuation. Simulation results for additional parameters (alkalinity, net acidity, temperature, specific conductance, accumulated solids, mass of limestone and SOC dissolved, DO, nitrate, DOC, sulfate, and TDS) indicated by the Pine Forest sequential kinetics model are included in the supplementary data (Figs. S6-S7).

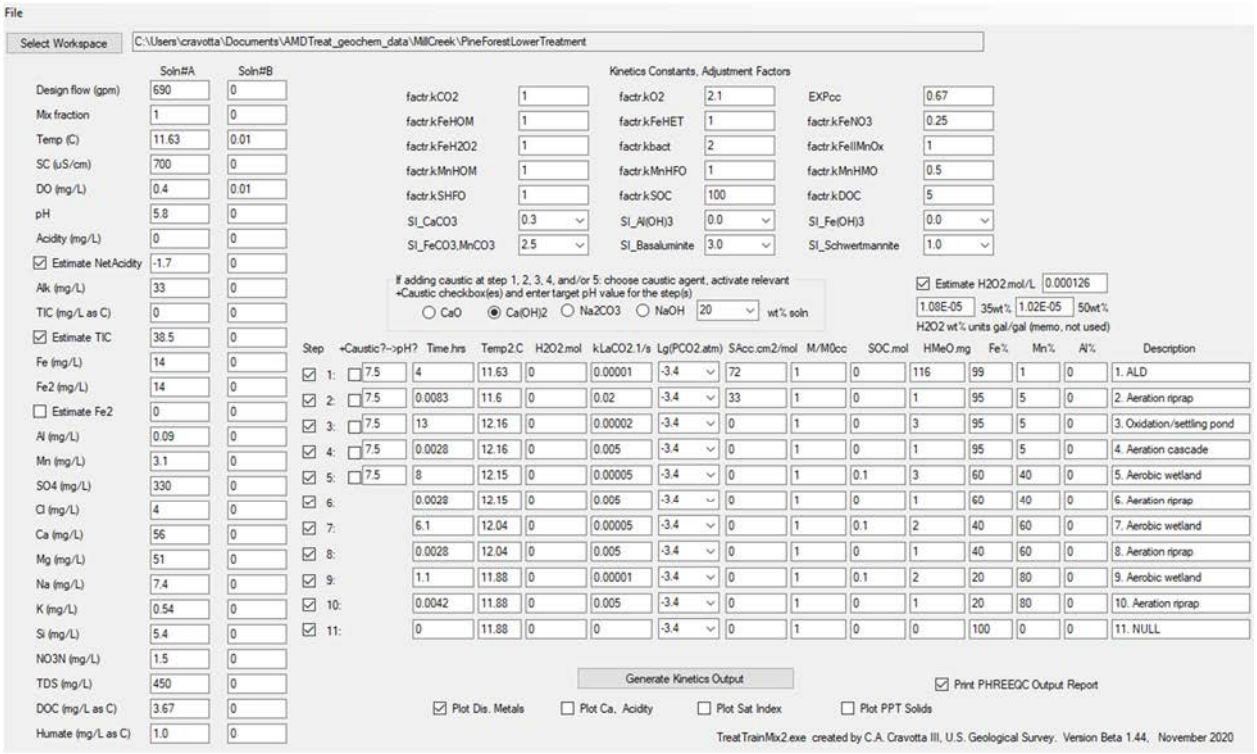

Figure S6. UI for PHREEQ-N-AMDTreat sequential model exhibiting input values for simulation of water-quality changes through the Pine Forest treatment system, December 2015, which consists of a "biofouled" anoxic limestone drain (ALD), oxidation/settling pond, and three aerobic wetlands, with aeration steps in between. The values shown represent enhanced FeOB activity (factr.kbact 2, instead of default value of 1) and a specified sorbent mass of 116 mg in the ALD and smaller sorbent mass with progressively greater Mn content downstream. Results of simulations are shown in Figure S7.

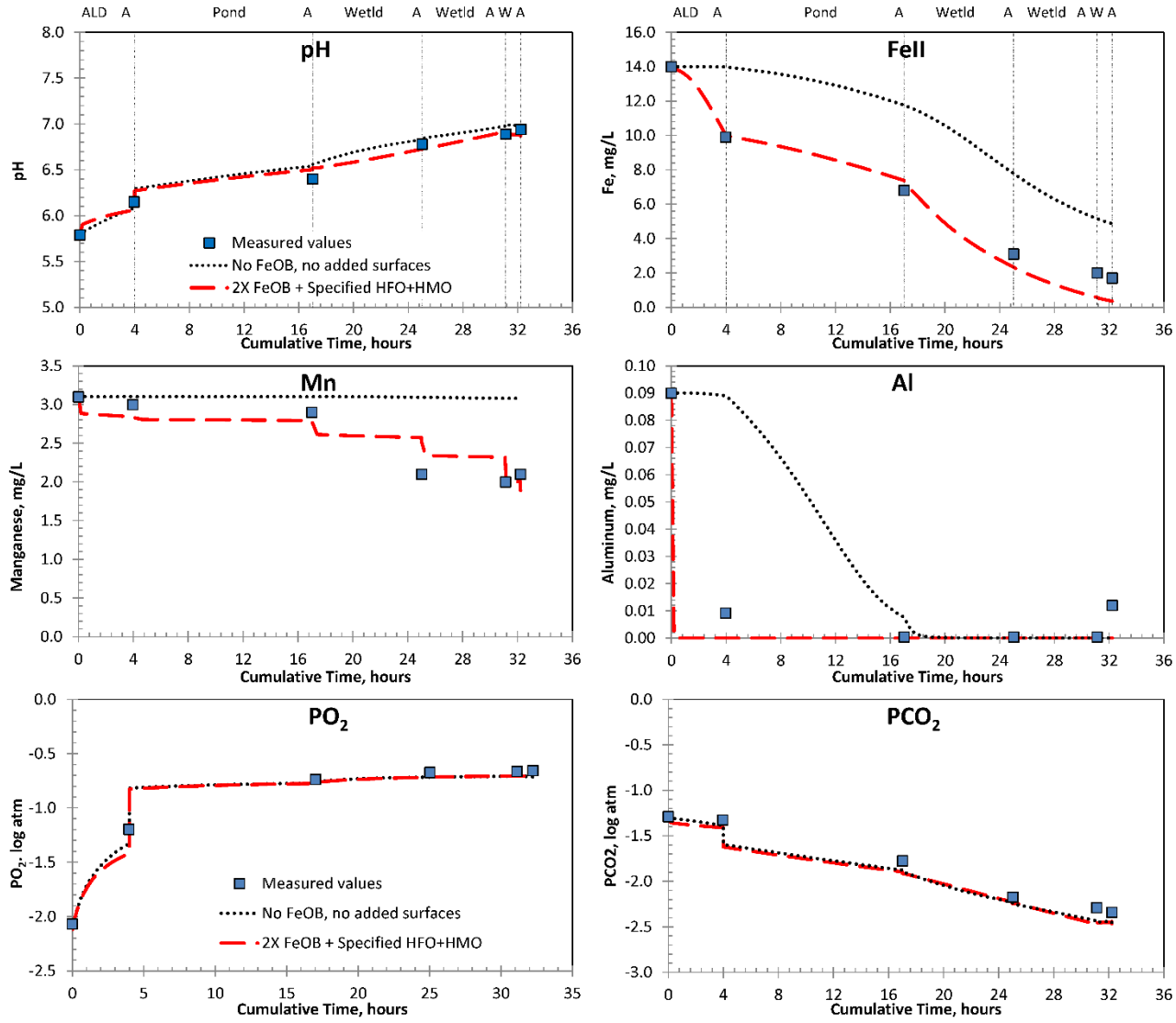

Figure S7. Comparison of measured (symbols) and simulated (curves) values for pH, Fe^{II}, Mn^{II}, Al, Pco_2, and Po_2 during treatment of AMD at the Pine Forest passive treatment system, December 2015. Simulations used the PHREEQ-N-AMDTreat sequential model with initial water chemistry, specified values for $k_{L,CO2}a$, FeOB rate factor, and sorbent mass and composition (Fig. S6). The black dotted curves show results for abiotic conditions without specified sorbent. The red dashed curves show results for enhanced FeOB activity (2X default FeOB rate) and specified sorbent mass in the ALD equivalent to 0.5-μm thick coating on all the limestone particles and smaller sorbent mass with progressively greater Mn content downstream.

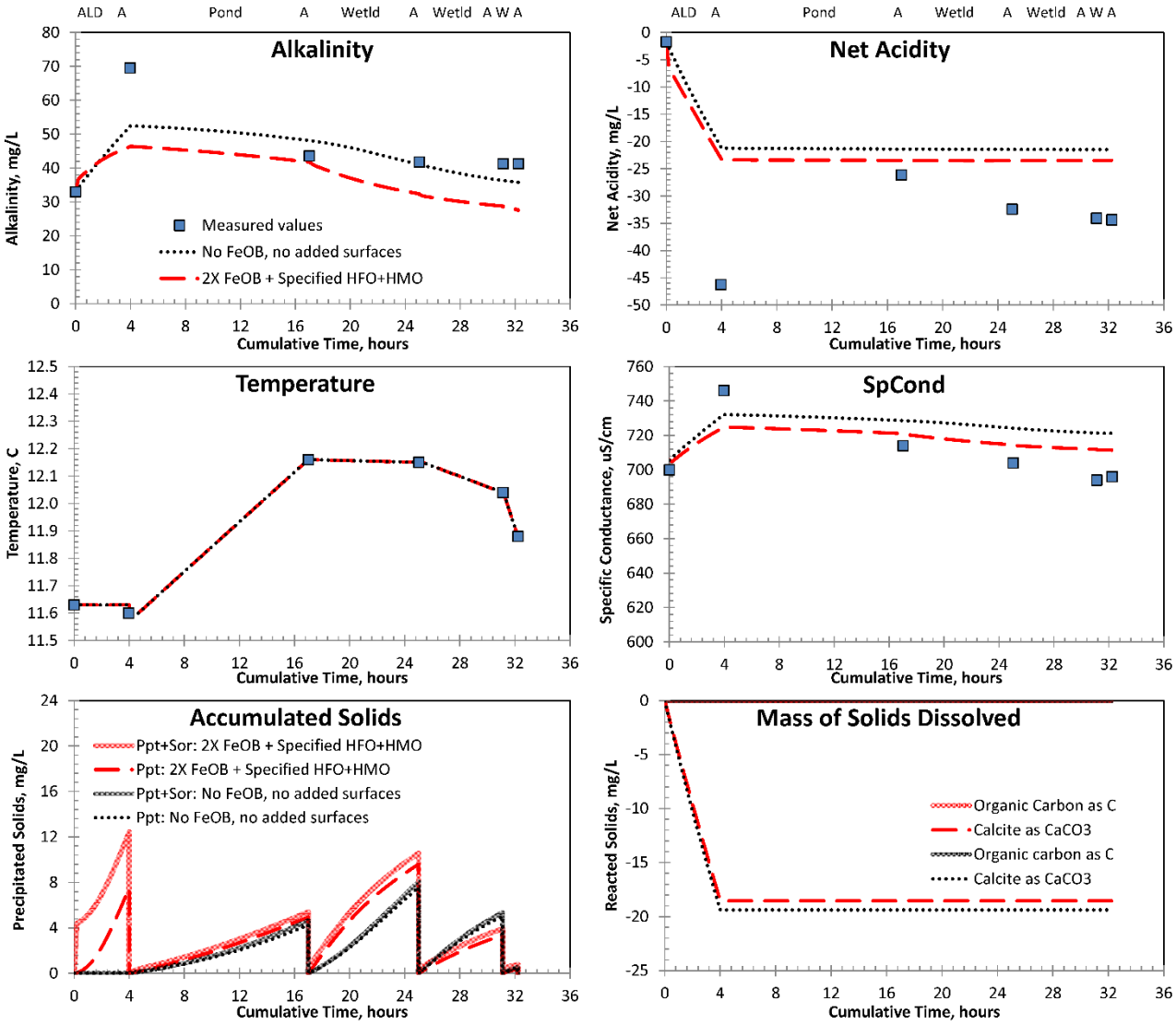

Figure S7 (continued). Comparison of measured (symbols) and simulated (curves) values for pH, Fe^{II}, Mn^{II}, Al, Pco_2, and Po_2 during treatment of AMD at the Pine Forest passive treatment system, December 2015. Simulations used the PHREEQ-N-AMDTreat sequential model with initial water chemistry, specified values for $k_{L,CO2}a$, FeOB rate factor, and sorbent mass and composition (Fig. S6). The black dotted curves show results for abiotic conditions without specified sorbent. The red dashed curves show results for enhanced FeOB activity (2X default FeOB rate) and specified sorbent mass in the ALD equivalent to 0.5-μm thick coating on all the limestone particles and smaller sorbent mass with progressively greater Mn content downstream.

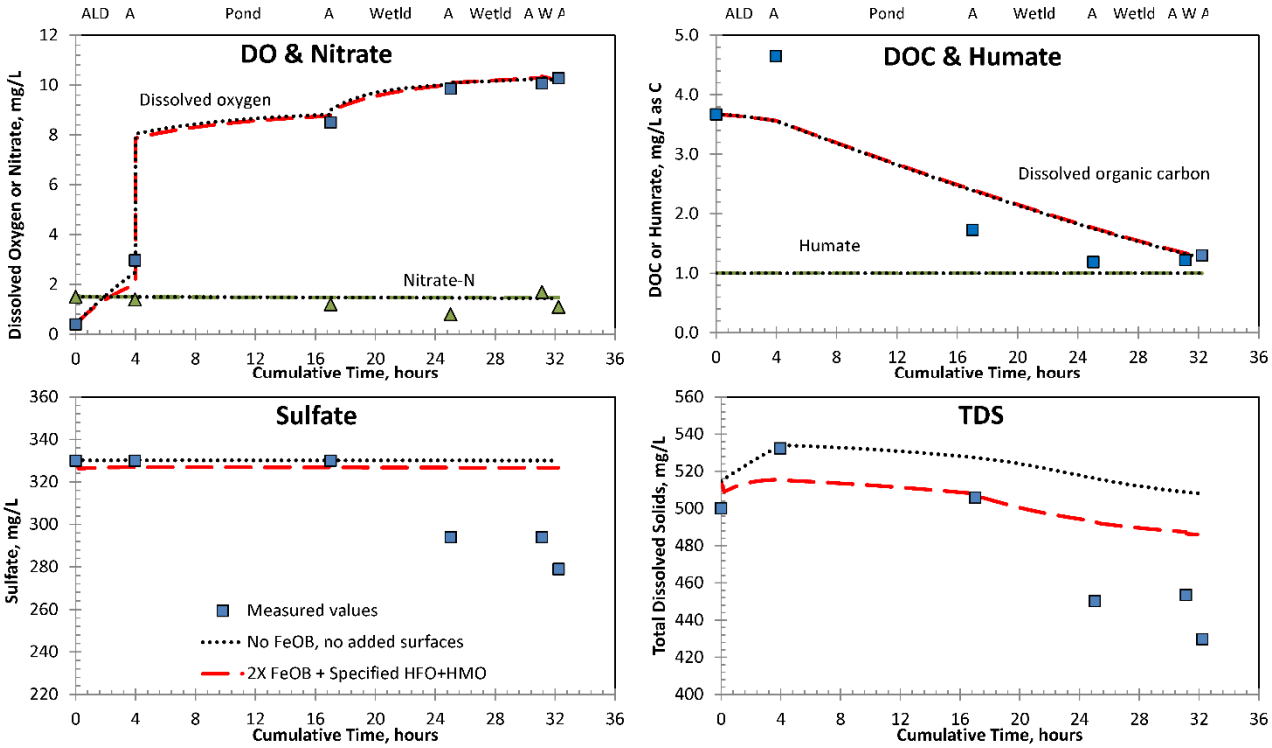

Figure S7 (continued). Comparison of measured (symbols) and simulated (curves) values for pH, Fe^{II}, Mn^{II}, Al, Pco_2, and Po_2 during treatment of AMD at the Pine Forest passive treatment system, December 2015. Simulations used the PHREEQ-N-AMDTreat sequential model with initial water chemistry, specified values for $k_{L,CO2}a$, FeOB rate factor, and sorbent mass and composition (Fig. S6). The black dotted curves show results for abiotic conditions without specified sorbent. The red dashed curves show results for enhanced FeOB activity (2X default FeOB rate) and specified sorbent mass in the ALD equivalent to 0.5-μm thick coating on all the limestone particles and smaller sorbent mass with progressively greater Mn content downstream.

S3.4. Sequential Treatment by Cascades, Oxidation/Settling Ponds, and Aerobic Wetlands

Field and laboratory water quality plus sediment chemistry were measured at points within a passive treatment system for the Silver Creek discharge during winter 2015 and summer 2016 (Ashby, 2017; this paper). The untreated AMD was anoxic with pH 5.9-6.0 and concentrations of Fe^{II}, Mn^{II}, and Al of 17.0-20.0, 2.2-2.9, and 0.12-0.17 mg/L, respectively. This aerobic treatment system, constructed in 2008, consists of a sedimentation pond, two oxidation/settling ponds, and two aerobic wetlands, in series, with aeration cascades in between (Figs. S8-S11). During the winter sampling event, water temperature decreased through the system, whereas during the summer event, water temperature increased. Although influent to the sedimentation pond was clear

each visit, the second and third ponds were turbid orange-brown because of increased pH through the cascades followed by in-situ oxidation of Fe^{II} and slow settling of HFO-rich particles in the ponds. Simulation results where initial sorbent mass was specified with chemical composition of sampled sediments (to simulate suspended particles) and using the default value of 1 for FeOB rate factor (Figs. S8 and S10) resulted in values of pH, Fe^{II}, Mn^{II}, Al, P_{CO_2}, and P_{O_2} that generally reproduced the longitudinal trends for measured values (Figs. S9 and S11). Large changes in pH during the aeration steps resulted from rapid CO_2 outgassing, which affected the rates of Fe^{II} oxidation in subsequent steps. Eventual removal of Mn^{II} in the wetland treatment steps were simulated by the specification of accumulated sorbent having greater HMO content, as measured in the sediment. Higher measured values for Fe (assumed to be Fe^{II}) than simulated values for summer 2018, may reflect a substantial Fe^{III} colloidal fraction in the 0.45-μm filtered sample and/or short circuiting associated with thermal stratification.

In addition to data on the rates of change in water temperature, DO, pH, alkalinity, and solute concentrations used to calibrate these models, sediment chemistry at the outflow of each treatment step at the Silver Creek system were available to estimate the sorbent composition (Ashby, 2017). For the Silver Creek models, the CO_2 outgassing rate (k_{La,CO_2}) and sorbent mass and composition (HMeO.mg, Fe%, Mn%, Al%) at each step were the only kinetics variables adjusted to achieve a reasonable match between empirical and simulated values for dynamic changes in pH, Fe, Mn, Al, and associated solute concentrations. Shallow, wide aeration cascades and long riprap runs were highly effective at facilitating gas exchange and rapid increases in pH, followed by Fe^{II} oxidation in large ponds with long retention times where gas exchange was limited by minimal advection. Greater mass and/or Mn content of sorbent increased Fe^{II} and Mn^{II} attenuation; most Mn was attenuated in wetlands at later treatment steps.

S3.4.1. Sequential Treatment by Cascades, Oxidation/Settling Ponds, and Aerobic Wetlands (Silver Creek, December 2015)

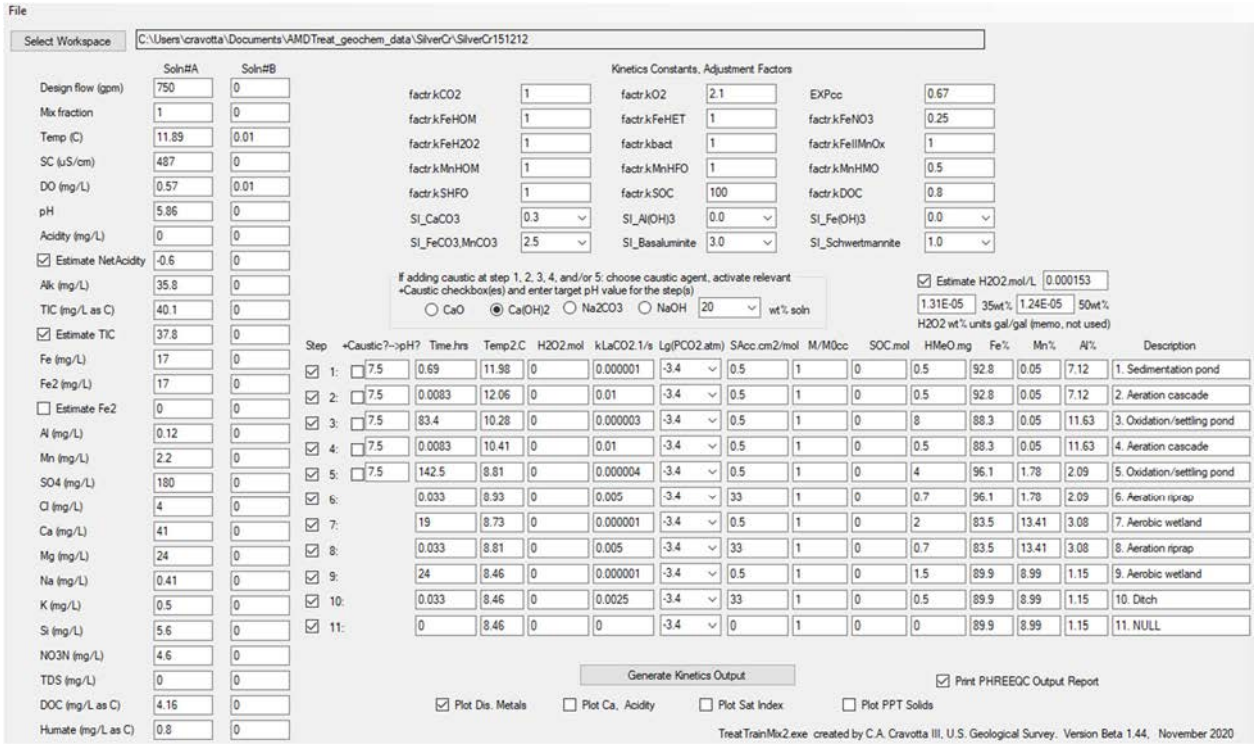

Figure S8. UI for PHREEQ-N-AMDTreat model exhibiting input values for simulations of sequential treatment steps at the Silver Creek treatment system, December 2015, which consists of a small sedimentation pond, two large oxidation/settling ponds, and two aerobic wetlands, with aeration cascades in between. Results of simulations are shown in Figure S9.

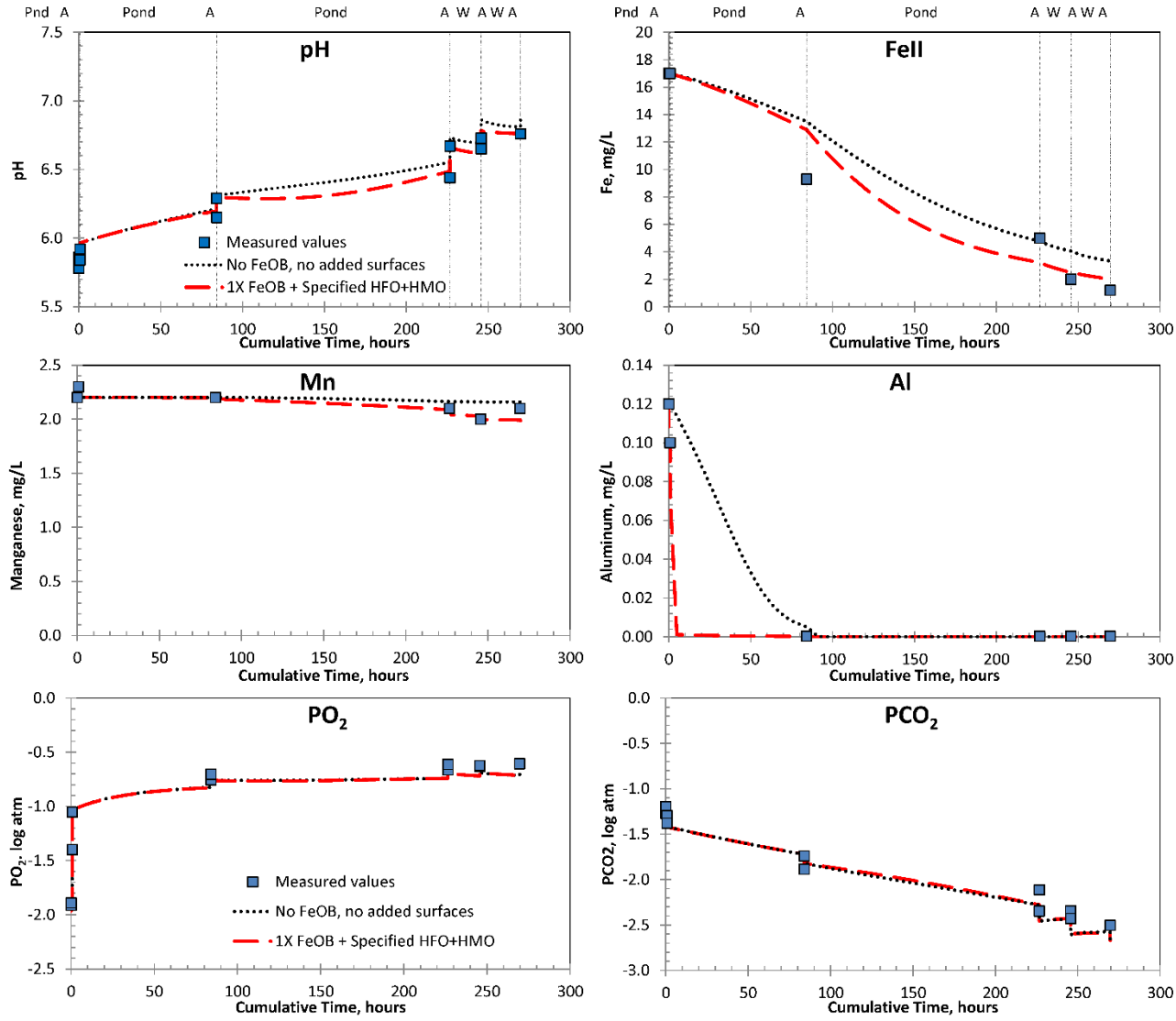

Figure S9. Comparison of measured (symbols) and simulated (curves) values for pH, Fe^{II}, Mn^{II}, Al, Pco_2, and Po_2 during treatment of AMD at the Silver Creek passive treatment system, December 2015. Simulations used the PHREEQ-N-AMDTreat sequential model with initial water chemistry, specified values for $k_{L,CO2}a$, and specified sorbent (Fig. S8). The red dashed curves show results for values in Figure S8, with specified sorbent representative of suspended solids having Fe-Mn-Al composition of sediment samples. The black dotted curves show results for conditions without FeOB catalysis or specified sorbent (values of 0).

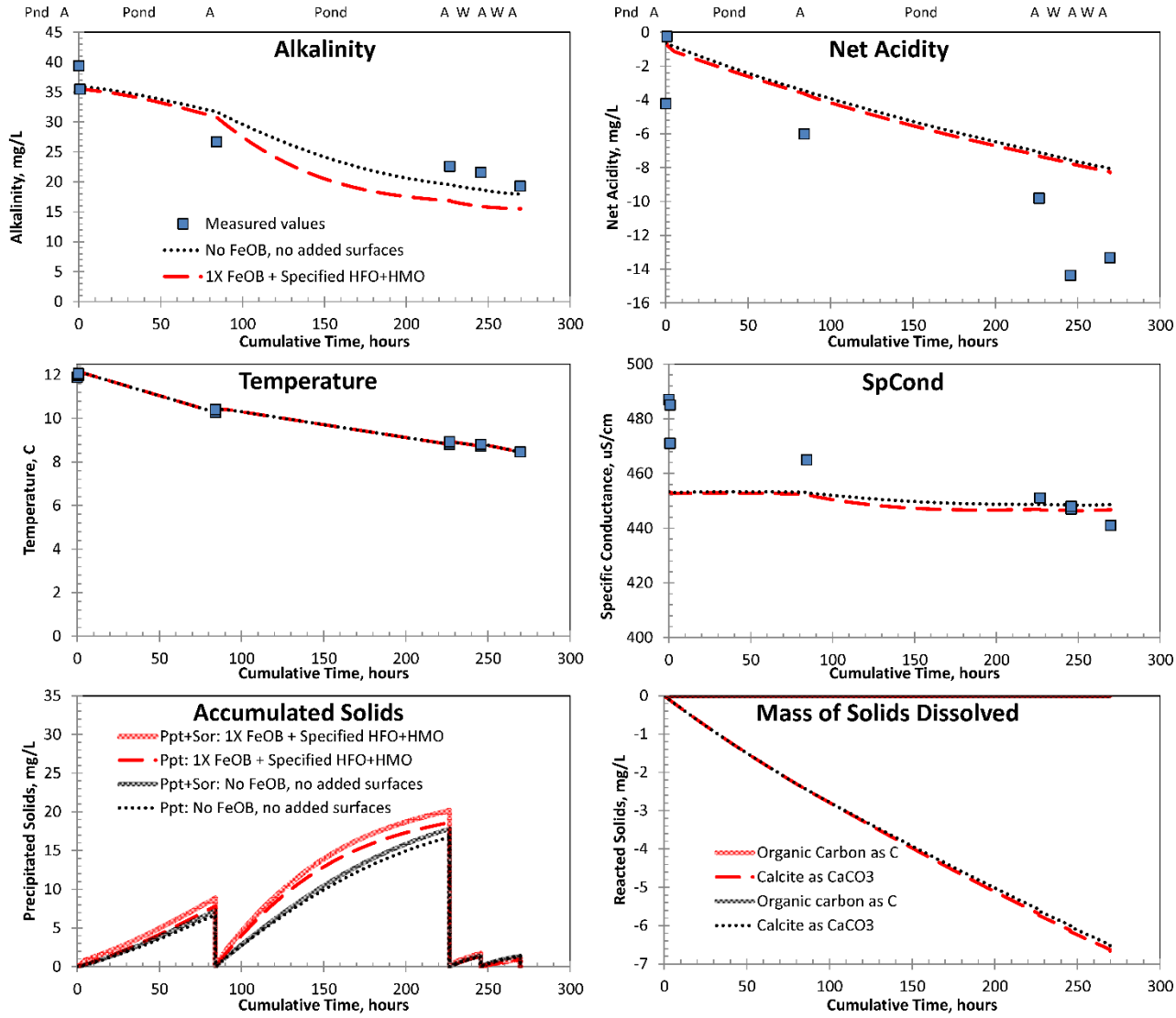

Figure S9 (continued). Comparison of measured (symbols) and simulated (curves) values for pH, Fe^{II}, Mn^{II}, Al, Pco_2, and Po_2 during treatment of AMD at the Silver Creek passive treatment system, December 2015. Simulations used the PHREEQ-N-AMDTreat sequential model with initial water chemistry, specified values for $k_{L,CO2}a$, and specified sorbent (Fig. S8). The red dashed curves show results for values in Figure S8, with specified sorbent representative of suspended solids having Fe-Mn-Al composition of sediment samples. The black dotted curves show results for conditions without FeOB catalysis or specified sorbent (values of 0).

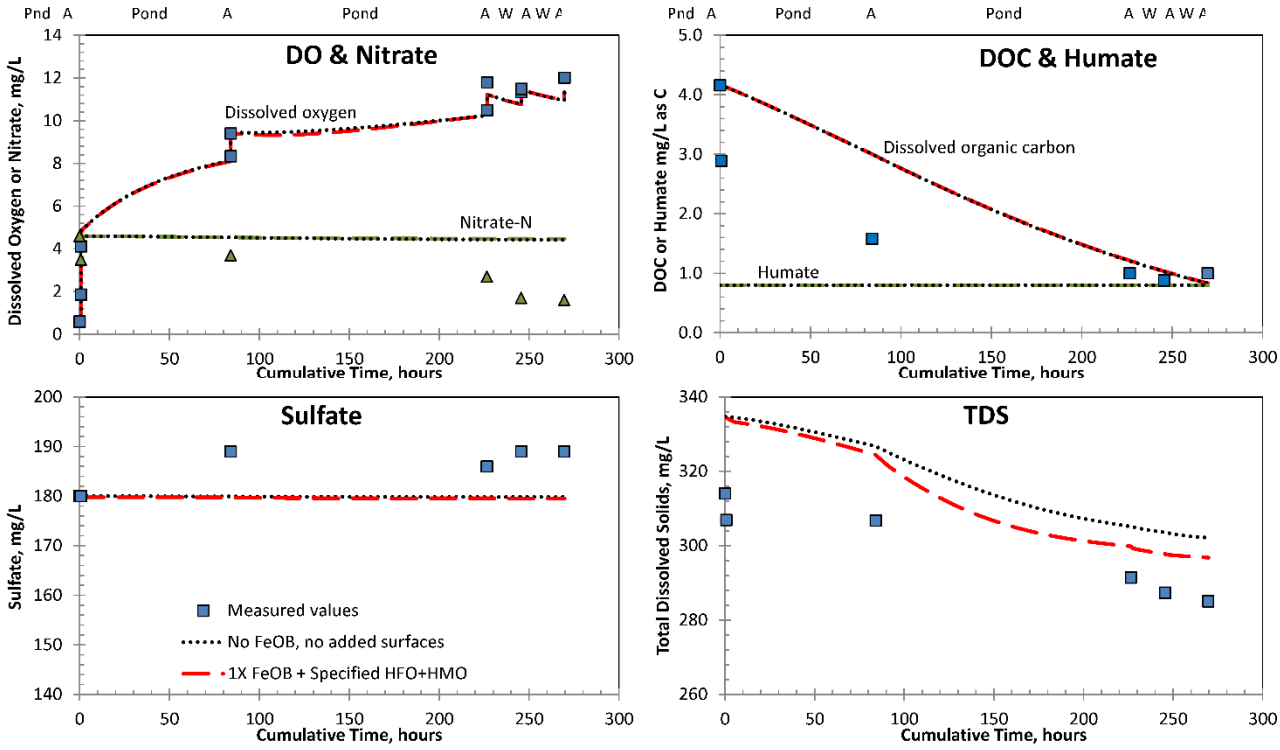

Figure S9 (continued). Comparison of measured (symbols) and simulated (curves) values for pH, Fe^{II}, Mn^{II}, Al, Pco_2, and Po_2 during treatment of AMD at the Silver Creek passive treatment system, December 2015. Simulations used the PHREEQ-N-AMDTreat sequential model with initial water chemistry, specified values for $k_{L,CO2}a$, and specified sorbent (Fig. S8). The red dashed curves show results for values in Figure S8, with specified sorbent representative of suspended solids having Fe-Mn-Al composition of sediment samples. The black dotted curves show results for conditions without FeOB catalysis or specified sorbent (values of 0).

S3.4.2. Sequential Treatment by Cascades, Oxidation/Settling Ponds, and Aerobic Wetlands (Silver Creek, August 2016)

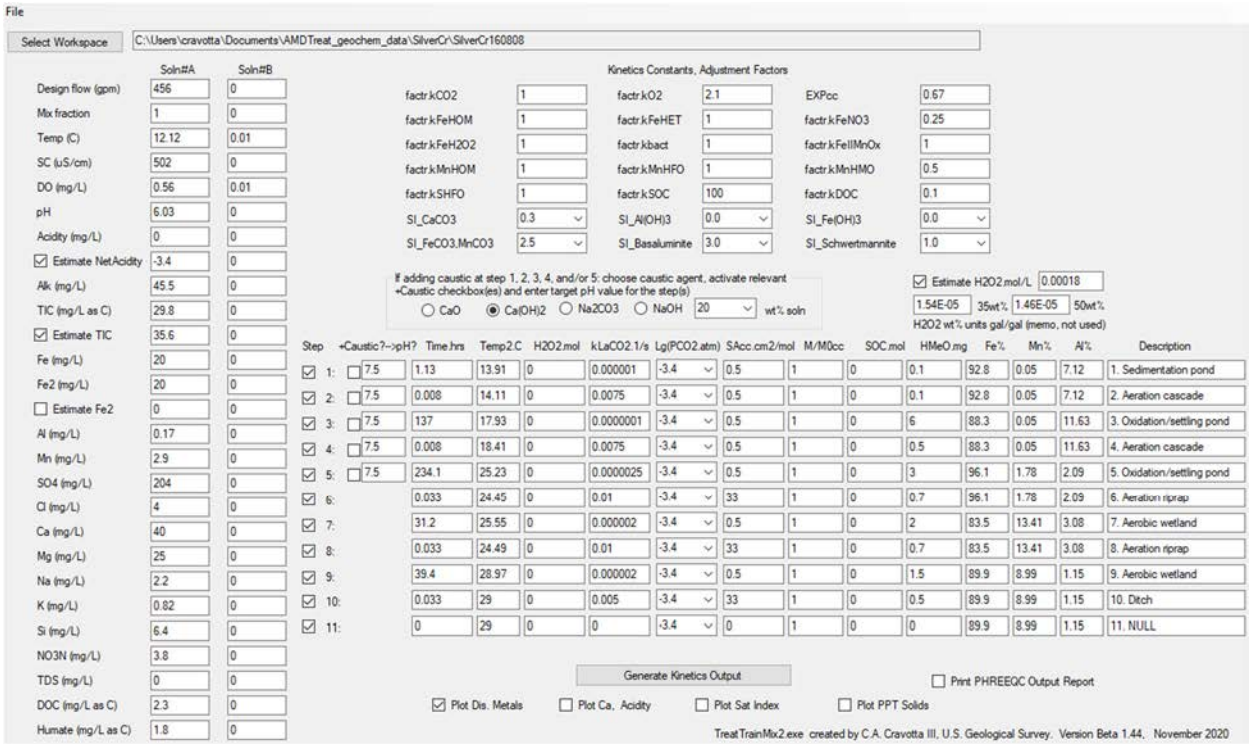

Figure S10. UI for PHREEQ-N-AMDTreat sequential model exhibiting input values for simulations of sequential steps at the Silver Creek treatment system, August 2016. Results are shown in Figure S11.

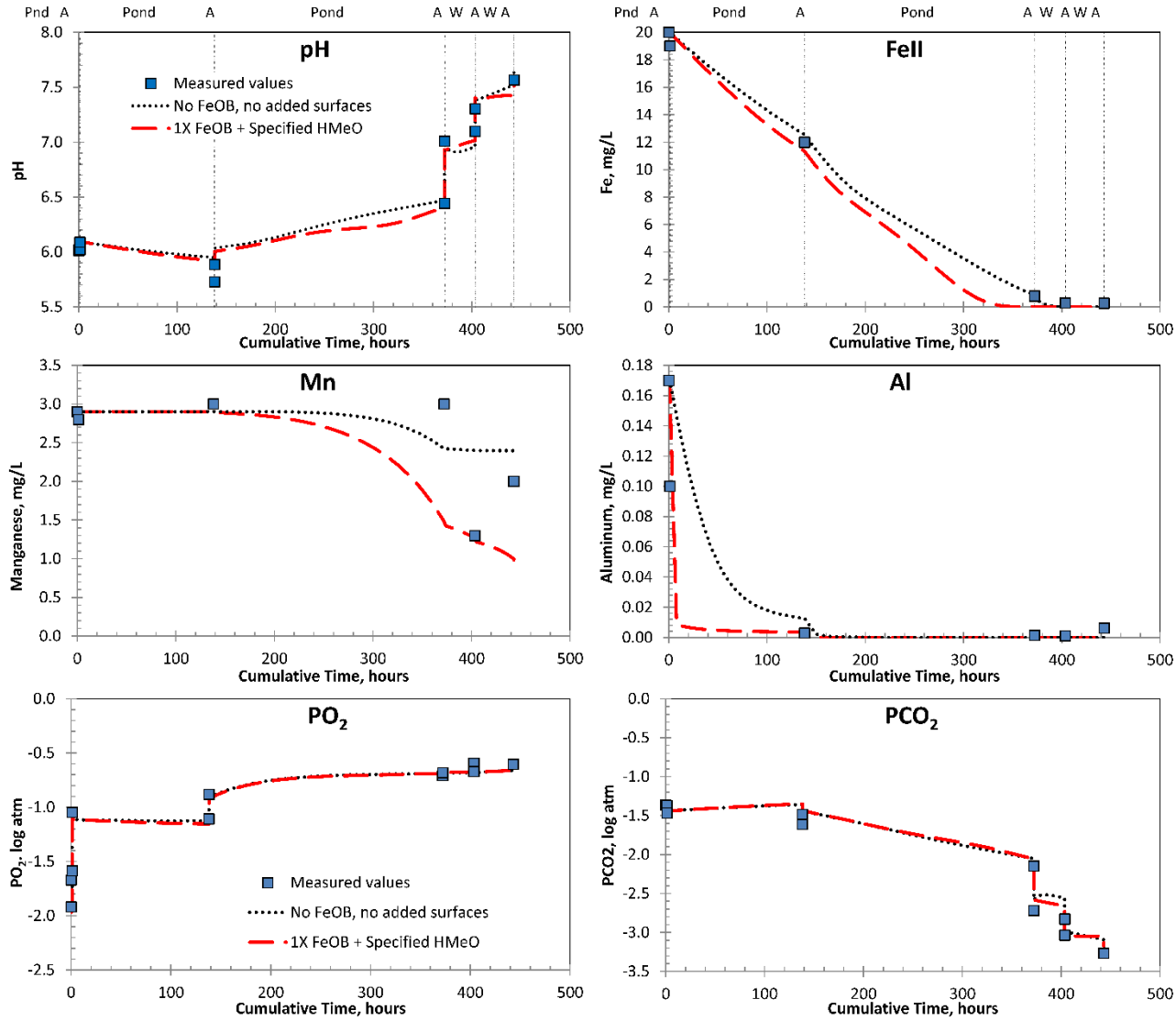

Figure S11. Comparison of measured (symbols) and simulated (curves) values for pH, Fe^{II}, Mn^{II}, Al, Pco_2, and Po_2 during treatment of AMD at the Silver Creek passive treatment system, August 2016. Simulations used the PHREEQ-N-AMDTreat sequential model. The red dashed curves show results for values shown in Figure 8, with specified sorbent representative of suspended solids having Fe-Mn-Al composition of sediment samples. The black dotted curves show results for conditions without FeOB catalysis or specified sorbent (values of 0).

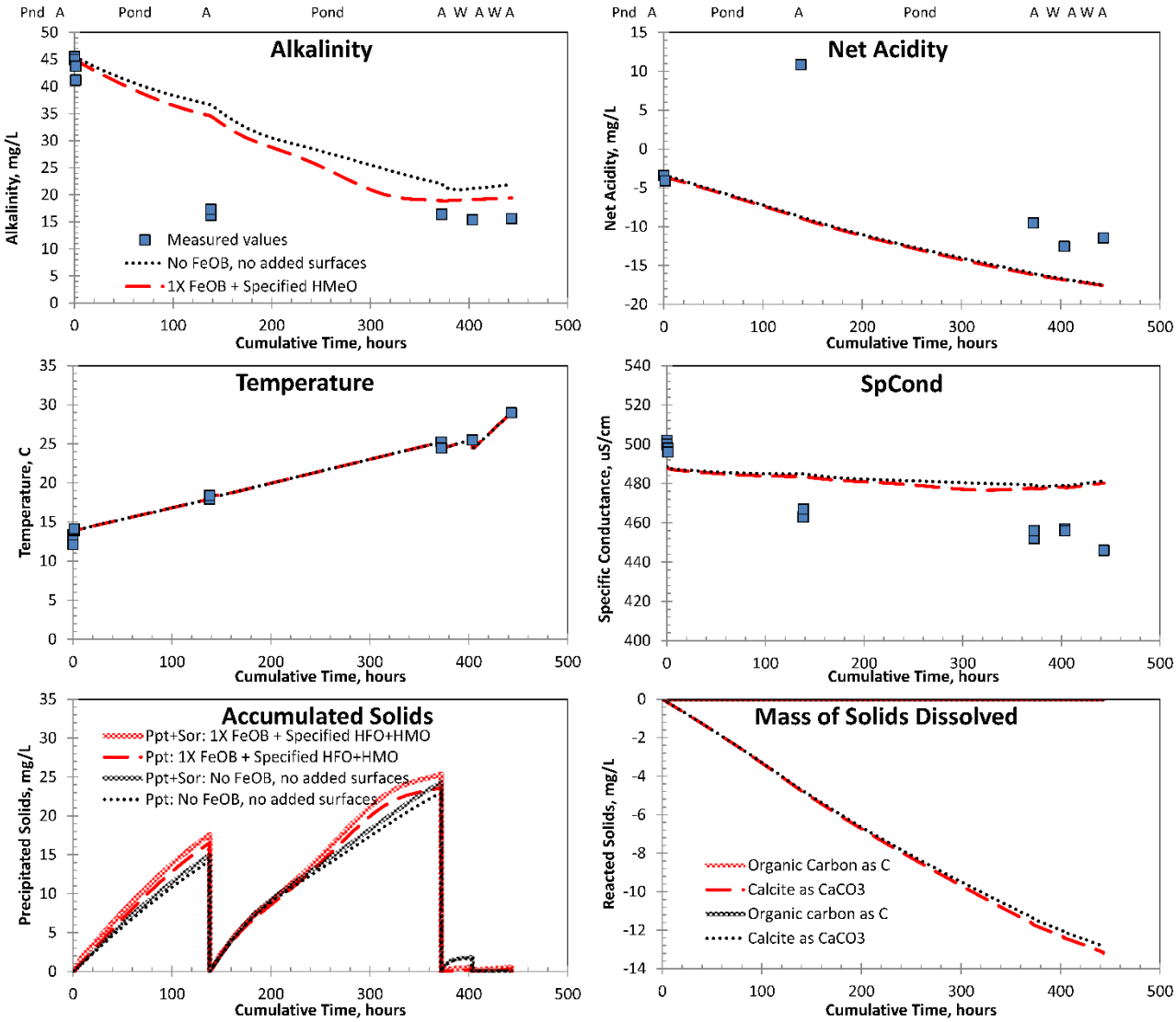

Figure S11 (continued). Comparison of measured (symbols) and simulated (curves) values for pH, Fe^{II}, Mn^{II}, Al, Pco_2, and Po_2 during treatment of AMD at the Silver Creek passive treatment system, August 2016. Simulations used the PHREEQ-N-AMDTreat sequential model. The red dashed curves show results for values shown in Figure 8, with specified sorbent representative of suspended solids having Fe-Mn-Al composition of sediment samples. The black dotted curves show results for conditions without FeOB catalysis or specified sorbent (values of 0).

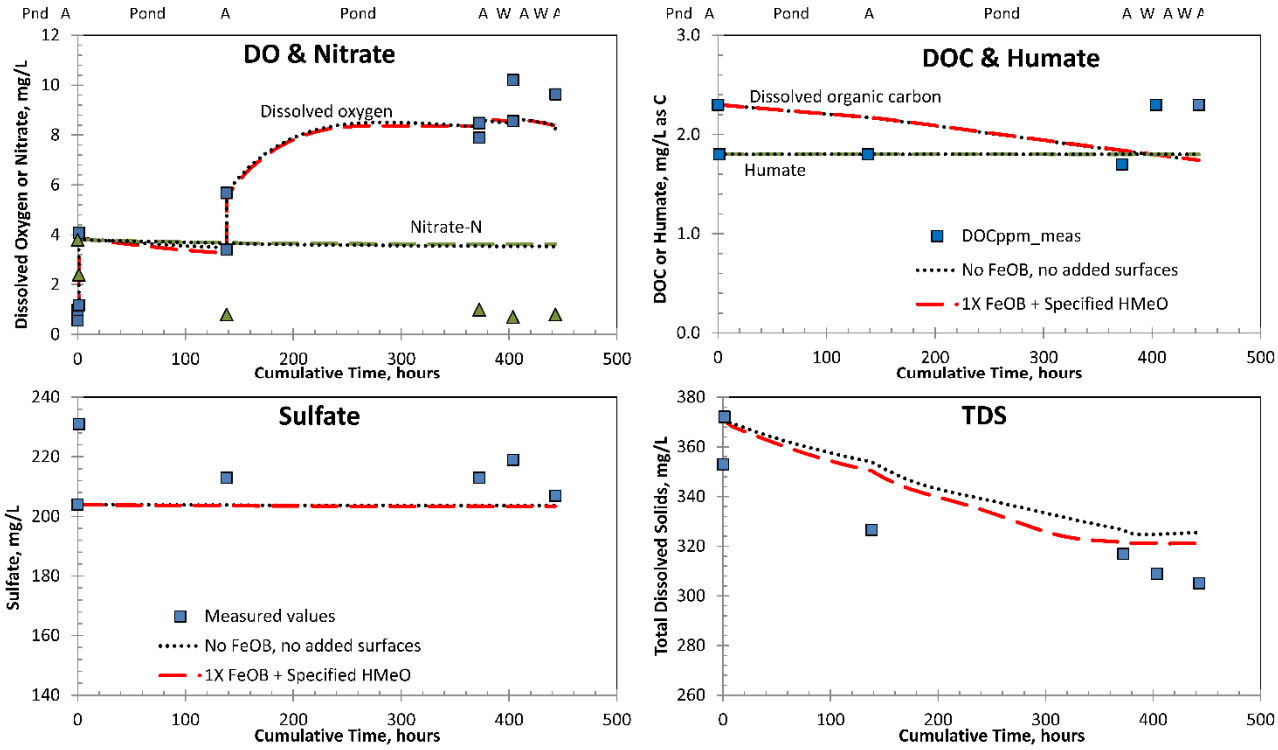

Figure S11 (continued). Comparison of measured (symbols) and simulated (curves) values for pH, Fe^{II}, Mn^{II}, Al, Pco_2, and Po_2 during treatment of AMD at the Silver Creek passive treatment system, August 2016. Simulations used the PHREEQ-N-AMDTreat sequential model. The red dashed curves show results for values shown in Figure 8, with specified sorbent representative of suspended solids having Fe-Mn-Al composition of sediment samples. The black dotted curves show results for conditions without FeOB catalysis or specified sorbent (values of 0).

S4. Hypothetical Scenarios--Assessment of Potential Passive and Active Treatment Strategies

In this section, the TreatTrainMix2 sequential kinetics tool is used to assess hypothetical passive and active treatment strategies that may achieve equivalent effluent quality, with near-neutral pH and dissolved metals concentrations approaching 0. These simulated treatment scenarios demonstrate important effects of neutralization, oxidation-reduction, and precipitation processes during treatment steps. The modeled retention times for the treatment steps are then used to indicate the approximate sizes for comparison of the physical requirements of proposed treatment systems and to estimate generalized costs for installation, operation, and maintenance.

S4.1. Evaluation of Treatment Alternatives for Net-Acidic AMD

For the first case, the TreatTrainMix2 tool was used to evaluate potential chemical changes in the Morea AMD resulting from (1) passive treatment with a VFP followed by two oxidation ponds,

aerobic wetland, and manganese removal bed or (2) active treatment with hydrated lime, settling pond, and wetland. Median water-quality characteristics were considered for the untreated influent (Figs. S12, S13, S14, and S15). System components were simulated as a "treatment train" with retention times and other system properties adjusted to achieve desired water quality for each step.

The Morea mine discharges a large volume (7387 gal min^{-1}, 466 L s^{-1}) of net acidic (pH 3.4 to 3.8; hot acidity 32.6 to 57.8 mg/L as $CaCO_3$) AMD that has elevated concentrations of aluminum (3.1 to 3.8 mg/L), iron (5.0 to 8.7 mg/L), and manganese (1.3 to 1.7 mg/L) that could cause rapid fouling of a limestone bed if introduced directly. For passive treatment of such net-acidic water quality, a VFP, which consists of an organic rich compost layer containing dispersed limestone fines overlying a flushable bed of limestone aggregate, may be effective for the removal of initial Fe^{III} and Al with the addition of alkalinity early in the treatment scheme, followed by oxidation and removal of Fe^{II} and Mn^{II} in aerobic ponds and wetlands, and limestone-filled Mn-removal bed (e.g. Skousen et al., 2017; Watzlaf et al., 2000, 2004). Active lime dosing is an alternative treatment for such water quality (e.g. Cravotta et al., 2015; Skousen et al., 2019), which also requires some sort of settling ponds and/or wetlands to remove the precipitated solids. The active treatment system would require frequent site access for chemical delivery and system maintenance, whereas the passive treatment system would require less frequent access and maintenance and thus could have lower operation and maintenance costs than an active treatment system.

The Morea AMD passive treatment simulation (Fig. S12 and S13) indicates that during the cumulative retention time of 15 hours, pH increases from 3.5 to 7.5 while DO increases to near saturation, with corresponding decreases in dissolved Al, Fe, and Mn. Progressive dissolution of limestone fines within the compost bed of the VFP during 3-hr retention time (step 3) results in pH 6.0 to 6.5 and dissolved Al at a steady-state minimum; most of the initial Al and Fe^{III} accumulate as $Al(OH)_3$ and $Fe(OH)_3$ in the compost layer. Greater retention time in the compost (not shown) leads to more extensive sulfate reduction and the precipitation of a fraction of dissolved Fe^{II} as FeS. Otherwise, dissolved Fe^{II} and Mn concentrations are transported conservatively through the limestone bed of the VFP and are not attenuated until the aerobic ponds (steps 6 and 8), wetland (step 10), and Mn-removal bed (step 11). Aeration between these treatment steps is important for CO_2 outgassing and increasing pH that facilitate oxidation and adsorption processes. Simulations indicate two oxidation ponds with an intermediate aeration step are more efficient for Fe^{II} oxidation and require less space combined than a single, larger pond. After the ponds, remaining dissolved Fe is attenuated in wetlands, which also remove suspended HMeO solids (not modeled) and a small

fraction of dissolved Mn. Attenuation of Mn results mainly from adsorption by HMO-coated limestone surfaces within the Mn removal bed (step 11, HMeO 20 mg consisting of 99 wt% Mn and 1 wt% Fe). The adsorbed Mn is presumed to oxidize in place, aided by microbial activity (e.g. Burté et al., 2019; Means and Rose, 2005; Robbins et al., 1999a, 1999b; Santelli et al., 2010; Tan et al., 2010).

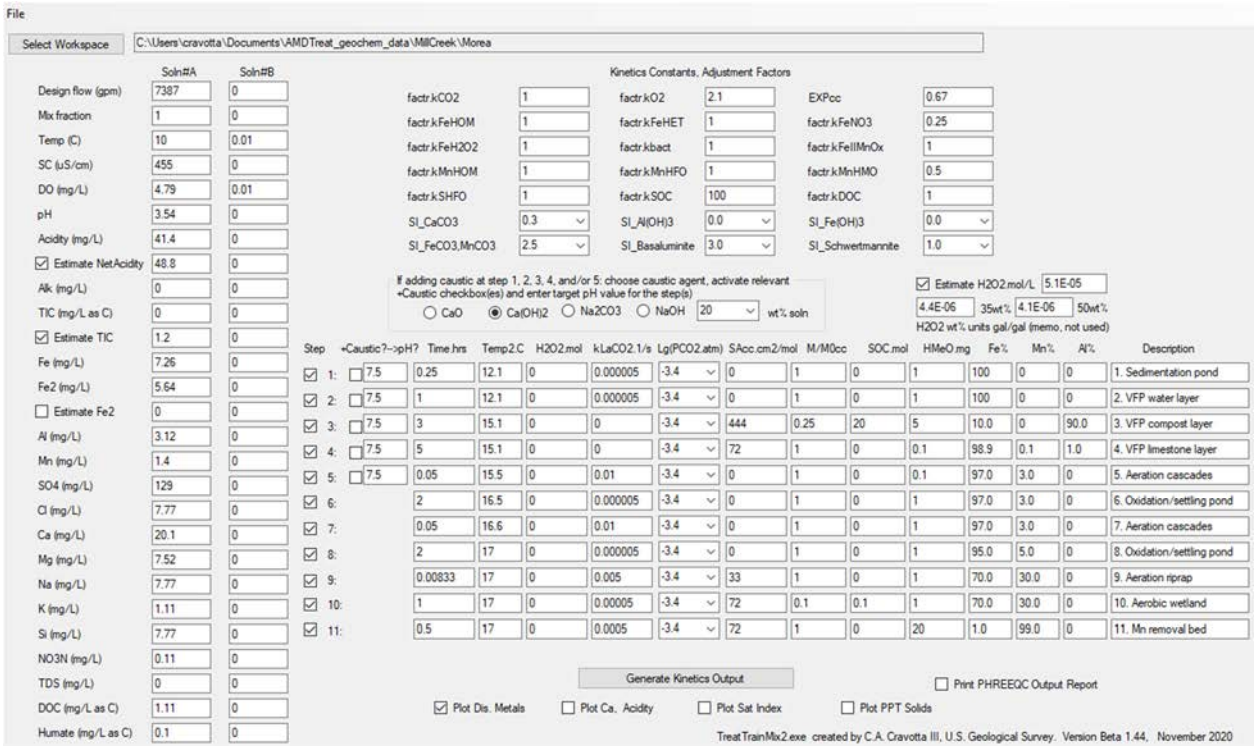

Figure S12. UI showing values of input variables for TreatTrainMix2 simulation of passive treatment of net-acidic AMD at Morea Mine through (1) sedimentation pond; (2-4) vertical flow pond (VFP); (6, 8) oxidation/settling ponds; (10) aerobic wetlands; and (11) manganese removal bed with intermediate aeration steps (5 7 9 11). Results are shown in Figure S13.

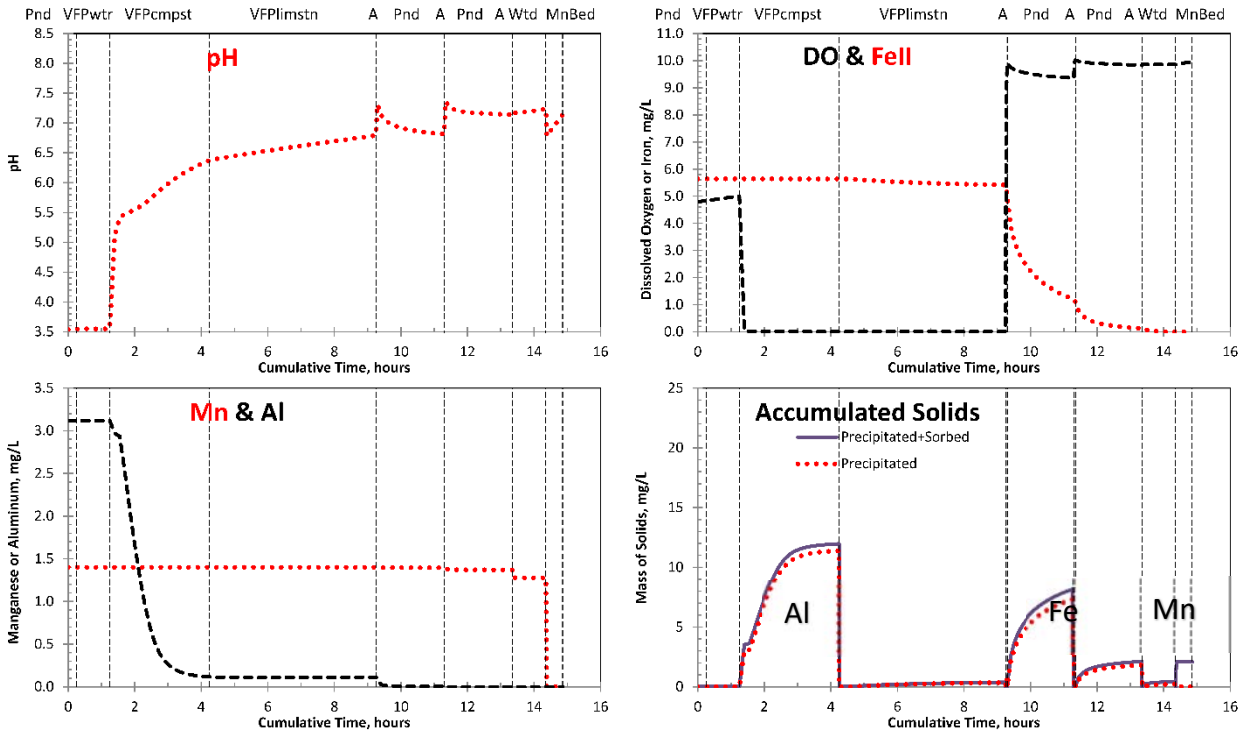

Figure S13. TreatTrainMix2 simulation results for passive treatment of Morea AMD by (1) VFP (consisting of a 0.61-m (2-ft) deep water layer, 0.61-m (2-ft) thick compost layer composed of 25 % limestone fines and 75% organic matter having 45% porosity, 0.91-m (3-ft) thick limestone layer having 45% porosity), (2) 1.52-m (5-ft) deep aerobic pond, (3) 0.30-m (1-ft) deep wetlands, and (3) 0.30-m (0.5-ft) deep "manganese" removal limestone bed. Aeration steps are included between each of the major treatment stages.

The Morea AMD active treatment simulation (Fig. S14 and S15) indicates that during a cumulative retention time of 6.8 hours, the pH increases from 3.5 to 7.6 while DO increases to near saturation, with corresponding decreases in dissolved Al, Fe, and Mn. The Al, Fe, and Mn are indicated to accumulate as amorphous $Al(OH)_3$, $Fe(OH)_3$, and MnOOH in the lime-mixing tank that included 100 mg/L recirculated solids (HMeO of 100 mg consisting of 61 wt% Fe, 12 wt% Mn, and 27 wt% Al). The large sorbent mass combined with high pH (8.5) promoted removal of the metals by adsorption, heterogeneous oxidation, and precipitation from solution. The aerobic pond and wetland that follow are primarily intended for settling of the metal-rich particles. Wetlands are included as "polishing" steps where suspended HMeO particles may be attenuated for both passive and active treatment systems. The PHREEQ-N-AMDTreat simulations do not evaluate particle transport or effects of HMeO accumulation on decreasing the retention times (owing to volume reduction) or limestone dissolution rates (owing to armoring or clogging).

Various sizing adjustments or maintenance may be considered to compensate for potential declines in performance as the systems age (e.g. Cravotta, 2003, 2008c; Hedin et al., 1994; Rose, 2004; Watzlaf et al., 2004; Wolfe et al., 2010).

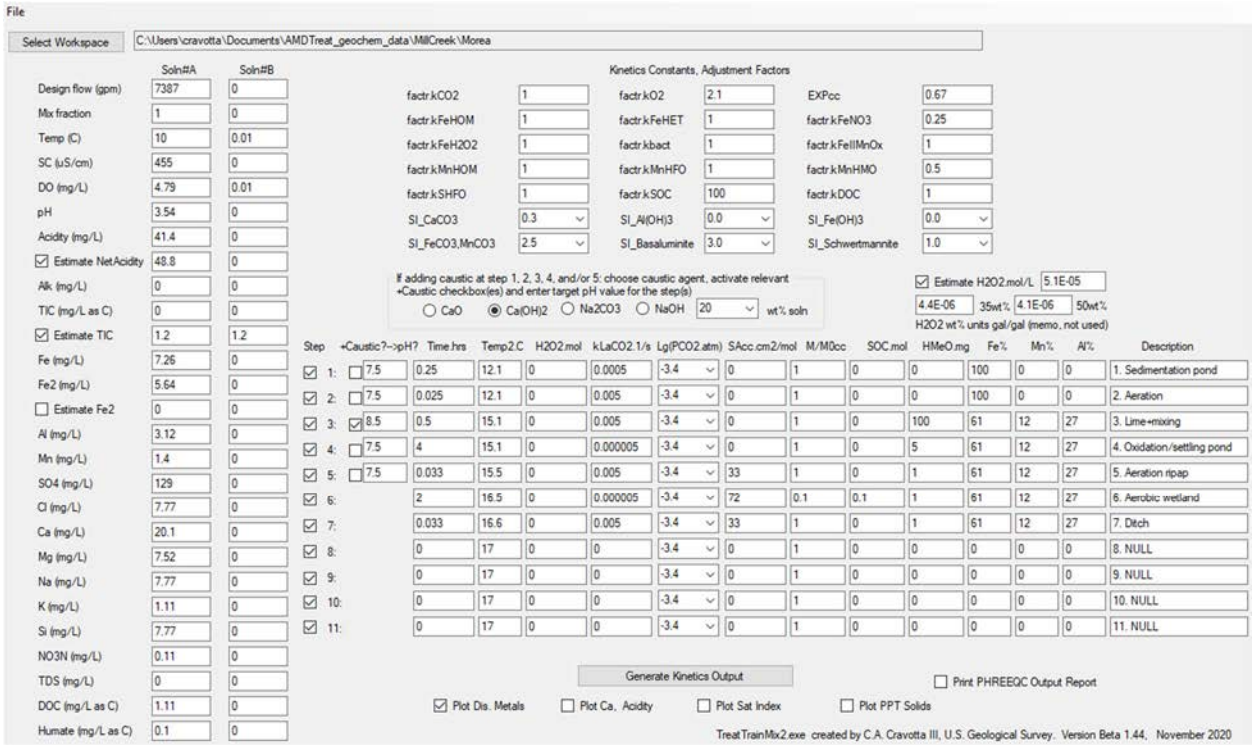

Figure S14. UI showing values of input variables for TreatTrainMix2 simulation of active treatment of net-acidic AMD at Morea Mine through (1) sedimentation pond; (3) lime dosing and sludge recirculation; (4) aerobic pond; and (6) aerobic wetlands with aeration steps (2 5 7). Results are shown in Figure S15.

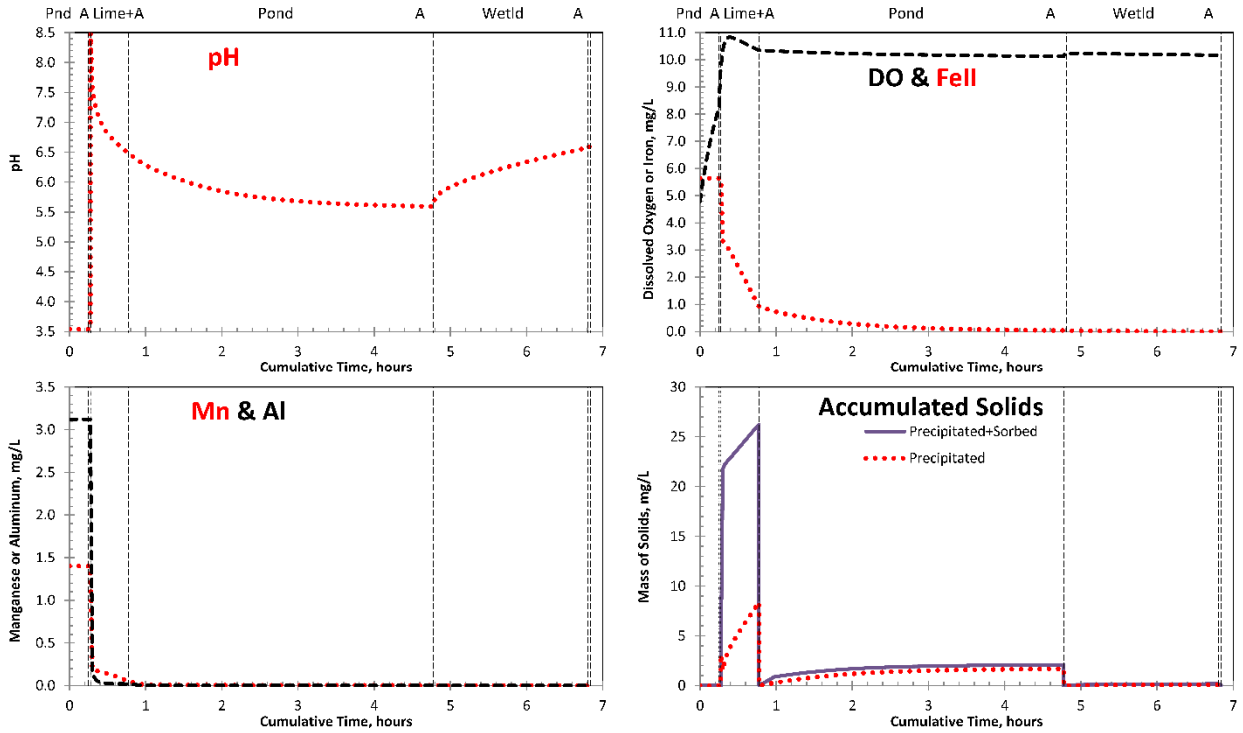

Figure S15. TreatTrainMix2 simulation results for active treatment of AMD at Morea Mine by (1) hydrated lime dosing and recirculation of sludge, including HMeO solids and unreacted lime, (2) 1.52-m (5-ft) deep aerobic pond, and (3) 0.30-m (1-ft) deep wetlands. Aeration steps are included between each of the major treatment stages. Results are shown as a function of the cumulative retention time within the treatment system.

Although the physical site characteristics are not explicitly considered in the PHREEQ-N-AMDTreat modeling tools, the retention time values for a model may be used to compute system sizing (Table S8). The volume for a treatment step in the kinetic model, such as pond or wetland, is computed as the product of flow rate and the retention time; area is computed as the volume divided by depth. For a pond, appropriate depths may be 2 to 4 m, whereas depths for a wetland generally may be 0.5 to 1 m, and less for aeration cascades (e.g. Hedin et al., 1994; Geroni et al., 2013; Skousen et al., 2017). For the VFP, volumes and depths for each of the three overlying layers (steps 2-4 in Table S8) are summed before computing area. Masses of limestone and compost also may be computed as the product of their respective volume and bulk density (Table S8).

Table S8. Estimated size of passive or active treatment systems for Morea AMD based on retention times used in TreatTrainMix2 simulations and 90th percentile flow.

Step	Treatment	flow rate, m^3/s	retention time, sec	retention time, hr	depth, m	porosity	volume, m^3	area of water surface, m^2	area of water surface, hectares	limestone particle size, AASHTO	CaCO3 fraction in bulk, M/M0cc	limestone mass, tonnes	compost organics mass, tonnes
VFP, oxidation+settling pond, aerobic wetlands, and Mn bed													
1	Sedimentation pond	0.466	900	0.25	0.91	1.00	419	459	0.05		1.00	0	0
2	VFP water	0.466	3600	1.00	0.61	1.00	1678				1.00	0	0
3	VFP compost	0.466	10800	3.00	0.91	0.45	11185			8	0.25	4084	8265
4	VFP limestone	0.466	18000	5.00	0.91	0.45	18642	12920	1.29	3	1.00	27230	0
5	Aeration cascades	0.466	180	0.05	0.03	0.45	186	6116	0.61		1.00	272	0
6	Oxidation/settling pond	0.466	7200	2.00	1.52	1.00	3356	2202	0.22		1.00	0	0
7	Aeration cascades	0.466	180	0.05	0.03	0.45	186	6116	0.61		1.00	272	0
8	Oxidation/settling pond	0.466	7200	2.00	1.52	1.00	3356	2202	0.22		1.00	0	0
9	Aeration riprap	0.466	30	0.01	0.03	0.45	31	1019	0.10	R-3	1.00	45	0
10	Aerobic wetland	0.466	3600	1.00	0.30	0.90	1864	6116	0.61	3	0.10	50	272
11	Mn removal bed	0.466	1800	0.50	0.30	0.45	1864	6116	0.61	3	1.00	2723	0
1 to 11	**Total:**			**14.86**	**7.10**			**43266**	**4.33**			**34676**	**8537**
Hydrated lime, oxidation+settling pond, and aerobic wetlands													
1	Sediment pond	0.466	900	0.25	0.91	1.00	419	459	0.05		1.00	0	0
2	Aeration Tank	0.466	90	0.03	1.52	1.00	42	28	0.00		1.00	0	0
3	Lime+recirculated sludge	0.466	1800	0.50	1.52	1.00	839	550	0.06		1.00	0	0
4	Oxidation/settling pond	0.466	14400	4.00	1.52	1.00	6711	4404	0.44		1.00	0	0
5	Aeration riprap	0.466	119	0.03	0.03	0.45	123	4037	0.40	R-3	1.00	180	0
6	Aerobic wetland	0.466	7200	2.00	0.30	0.90	3728	12232	1.22	3	0.10	99	543
7	Ditch	0.466	119	0.03	0.15	0.45	123	807	0.08	R-3	1.00	180	0
8	NULL	0.466	0	0.00	0.00	1.00	0	0	0.00		1.00	0	0
9	NULL	0.466	0	0.00	0.00	1.00	0	0	0.00		1.00	0	0
10	NULL	0.466	0	0.00	0.00	1.00	0	0	0.00		1.00	0	0
11	NULL	0.466	0	0.00	0.00	1.00	0	0	0.00		1.00	0	0
1 to 11	**Total:**			**6.84**	**5.97**			**22516**	**2.25**			**458**	**543**

AASHTO average particle diameter: R-3, 10.16 cm (4 inch); 3, 3.81 cm (1.5 inch); 8, 0.69 cm (0.25 inch). See table S7.

The estimated land area required for construction of the passive VFP and active lime treatment systems for the Morea discharge are given in Table S8. The passive treatment system water surface area is estimated at 4.33 ha, whereas that for the active treatment system is estimated at 2.25 ha. Considering a multiplier of 1.5 for clearing and grubbing, berms, and slopes, the total area increases to 6.5 ha for the passive treatment system and 3.4 ha for the active system. In general, site access, land ownership, and flooding potential would be considered as part of the feasibility analysis. For example, parts of two undeveloped adjoining parcels bordering the drainage channel below the Morea AMD site could be utilized for the construction and operation of the treatment system. Space is adequate to locate a passive or active treatment system outside the mapped flood zone. An existing gravel road could accommodate access for construction, delivery of lime and other chemicals, removal of sludge, and operations and maintenance.

To judge the potential cost-effectiveness of different treatment strategies, the sizing estimates from the PHREEQ-N-AMDTreat models may be considered with corresponding cost estimates for site development and system operations. Using the system sizing estimates given in Table S8 with

AMDTreat 5.0+ (Office of Surface Mining Reclamation and Enforcement, 2017), the approximate costs of construction (capital) plus annual costs of operation (labor, chemicals, sludge disposal) and maintenance (4 % of capital costs) were computed for the Morea AMD. Using default values for unit costs and assuming inflation of 5 % per year over 20 years (Pennsylvania Department of Environmental Protection, 2016), the net present value for the active treatment of Morea AMD is approximately US$2.7 million. Because of greater capital costs and relatively high annual costs based on a percentage of the capital costs, the net present value for the passive system is US$3.9 million using the same net worth factor. Thus, considering equivalent, acceptable effluent quality is predicted for both systems, the active treatment system would be considered the more cost-effective option for the Morea AMD.

S4.2. Evaluation of Treatment Alternatives for Combined AMD from Two Sources

Cravotta et al. (2014) and Cravotta (2015) reported field, laboratory, and modeling results for the headwaters of Schuylkill River, where AMD from the Pine Knot tunnel (PKN) and the Oak Hill boreholes (OAK) accounted for a majority of the streamflow to the West Branch during low-flow conditions. These two AMD sources contribute greater loadings of metals to the Schuylkill River than all the other dozens of AMD sources combined. Both AMD sources are net alkaline with comparable loads of dissolved Fe^{II}; however, the PKN was more dilute with approximately three times the flow volume and one-third the Fe concentration of OAK.

Cravotta (2015) described PHREEQC kinetic models for 1:3 mixtures of the two AMD sources (OAK:PKN) to simulate the observed downstream characteristics in the West Branch based on compositions for low-flow and high-flow end-member samples. Based on these calibrated models, Cravotta proposed a restoration strategy that could involve treatment of OAK and PKN at a single facility constructed on land outside the flood plain using enhanced aeration or H_2O_2 addition to decrease iron concentrations and maintain circumneutral pH of the net-alkaline AMD mixture. Pumping from the Oak Hill mine, which underlies the PKN tunnel outlet, would be conducted at a rate greater than or equal to that of the OAK discharge in order draw down the groundwater level in the Oak Hill mine, thus eliminating the current discharge. The abundant alkalinity of OAK could augment that of PKN, ensuring net-alkaline influent to the treatment plant.

Using the PHREEQ-N-AMDTreat “TreatTrainMix2” model, treatment alternatives were evaluated herein for the median 1:3 OAK:PKN mixtures using multiple treatment steps with variable aeration rates. Each treatment alternative is simulated to produce acceptable water quality

with near-neutral pH and low concentrations dissolved Fe, Al, and Mn. The first scenario considers a passive treatment strategy with aeration cascades (Figs. S16-S17), the second considers active treatment with forced aeration (S18-S19), and the third considers H_2O_2 addition without sludge recirculation (S20-S21). As a modification of the H_2O_2 treatment scenario, sludge recirculation was simulated by the inclusion of HMeO = 50 mg/L consisting of 100% Fe, during the step with H_2O_2 addition (e.g. Fig. S20); the had negligible effect on Mn removal. To attenuate dissolved Mn remaining in effluent after prior steps, a Mn-removal bed (e.g. Means and Rose, 2005) was added as the final step for each of the passive and active treatment models.

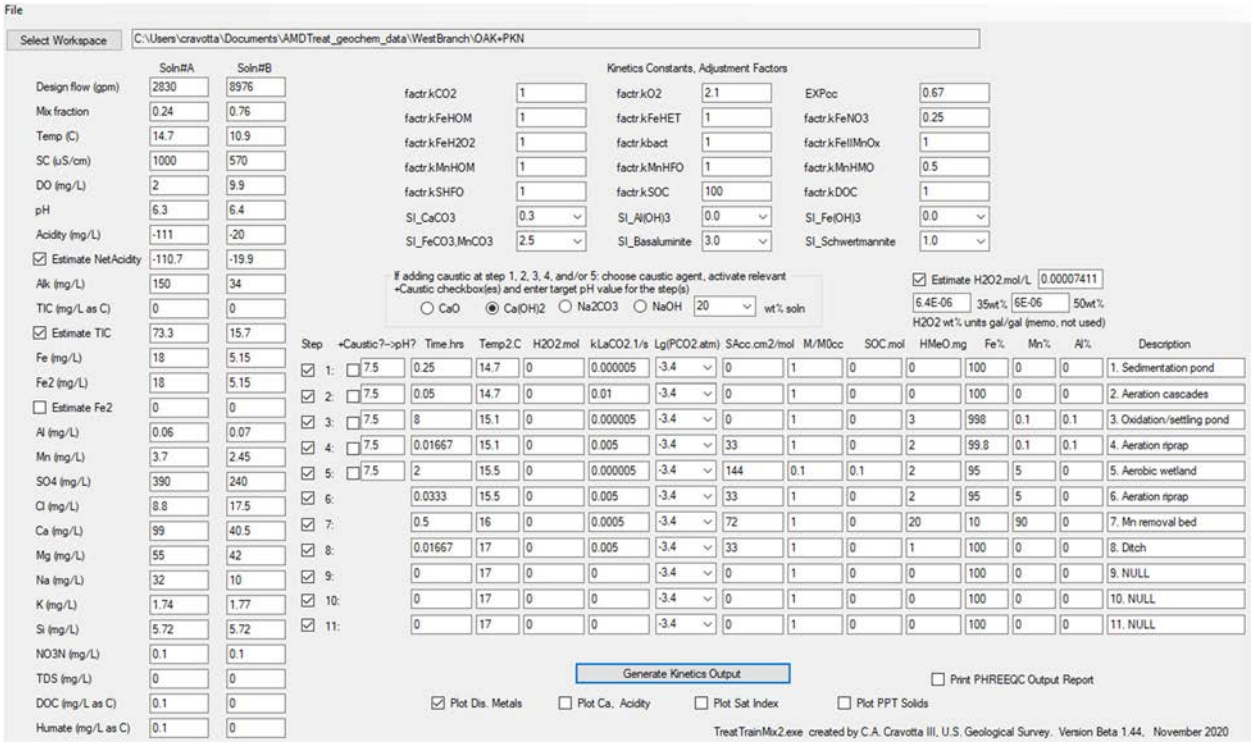

Figure S16. UI for PHREEQ-N-AMDTreat model exhibiting input values for simulations of hypothetical treatment using passive aeration after mixing of AMD from the Oak Hill boreholes (Soln#A) and Pine Knot tunnel (Soln#B). Treatment consists of a small sedimentation pond, aeration cascades, oxidation/settling pond, aerobic wetland, and Mn removal bed with aeration steps in between. Results of simulations are shown in Figure S17.

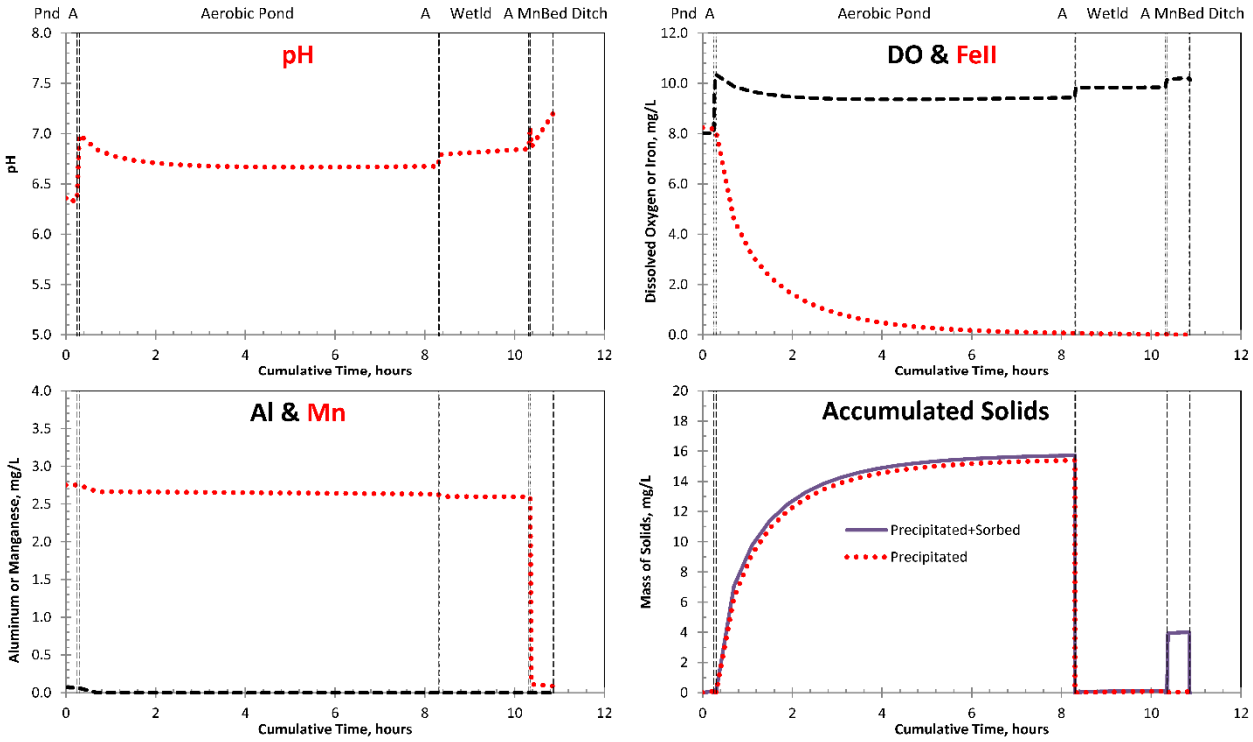

Figure S17. Simulation results for passive treatment of combined Oak Hill boreholes + Pine Knot tunnel AMD by aeration cascades, oxidation+settling pond, aerobic wetlands, and Mn-removal bed.

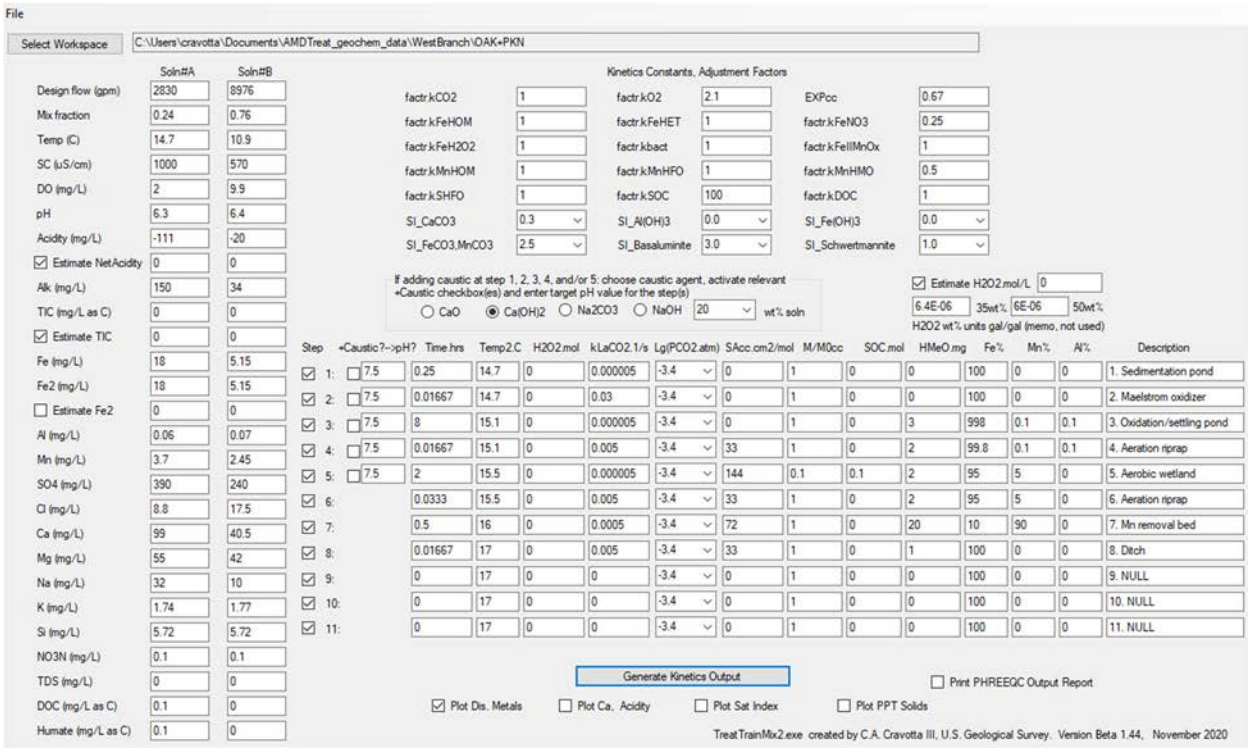

Figure S18. UI for PHREEQ-N-AMDTreat model exhibiting input values for simulations of hypothetical treatment using aggressive aeration after mixing of AMD from the Oak Hill boreholes (Soln#A) and Pine Knot tunnel (Soln#B). Treatment consists of a small sedimentation pond, Maelstrom Oxidizer®, oxidation/settling pond, aerobic wetland, and Mn removal bed with aeration steps in between. Results of simulations are shown in Figure S19.

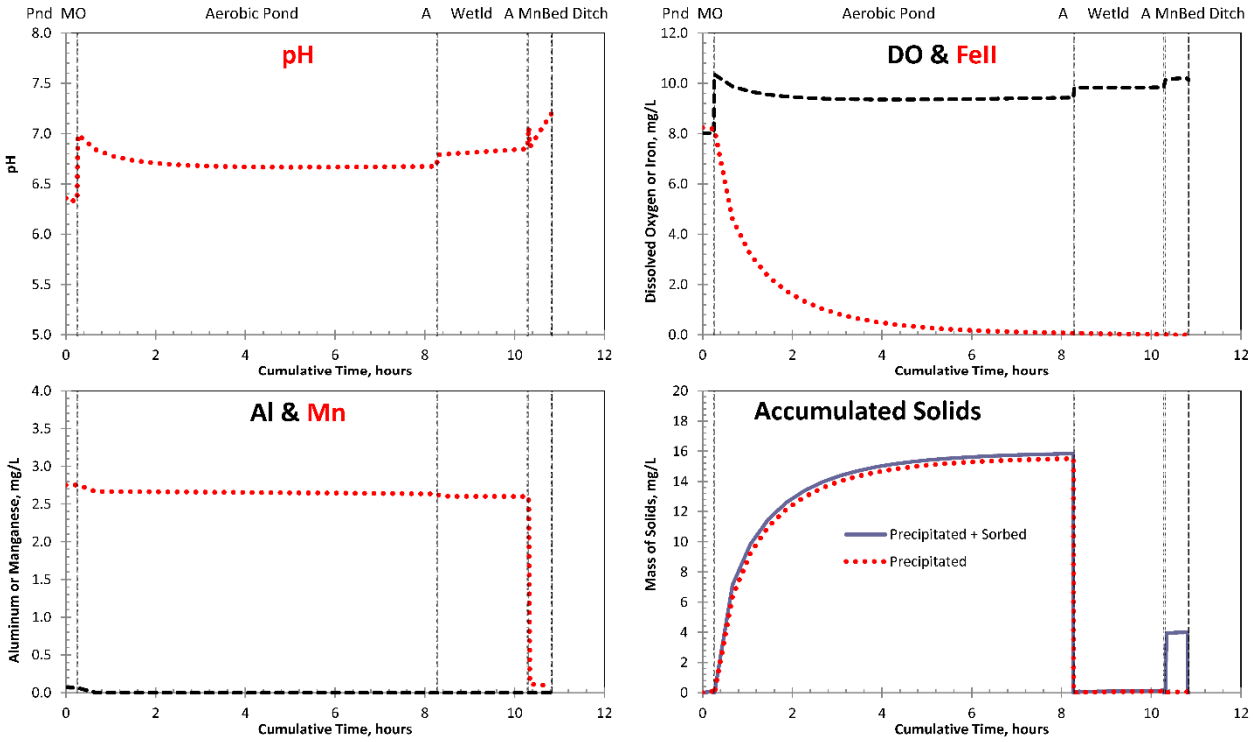

Figure S19. Simulation results for passive treatment of combined Oak Hill boreholes + Pine Knot tunnel AMD by Maelstrom Oxidizer®, oxidation+settling pond, aerobic wetlands, and Mn-removal bed.

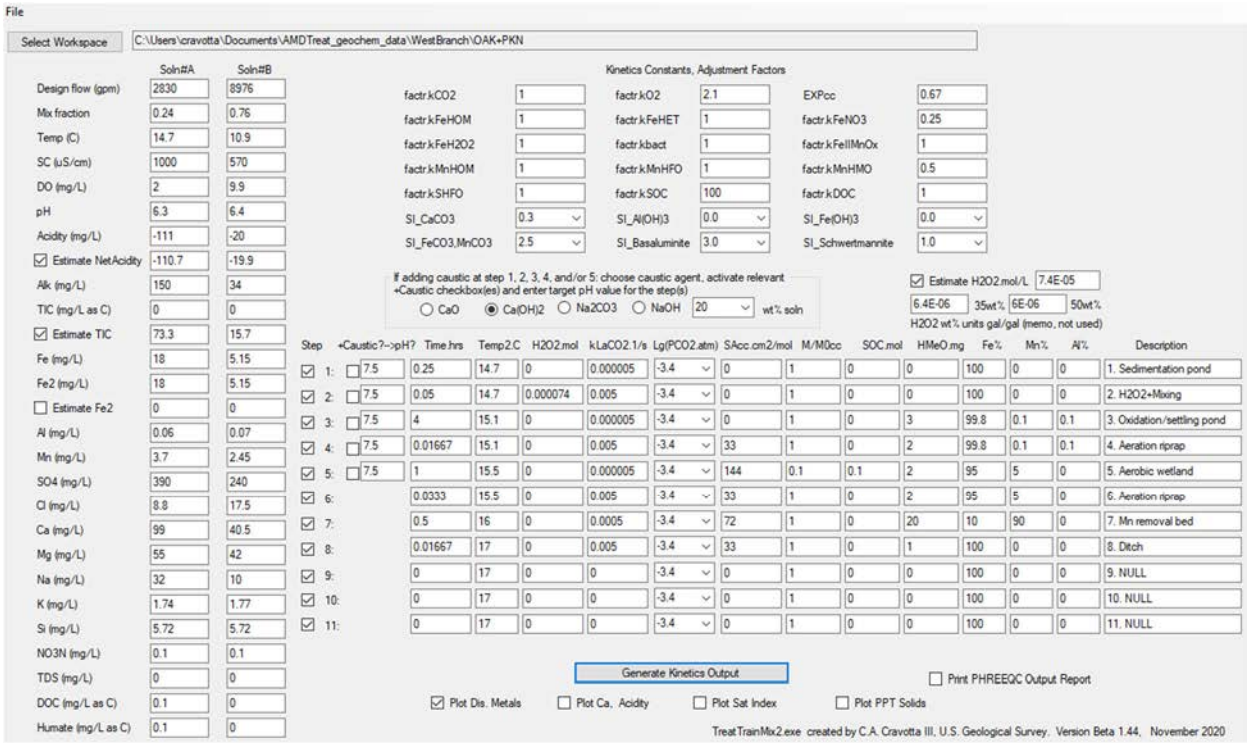

Figure S20. UI for PHREEQ-N-AMDTreat model exhibiting input values for simulations of hypothetical treatment using H_2O_2 after mixing of AMD from the Oak Hill boreholes (Soln#A) and Pine Knot tunnel (Soln#B). Treatment consists of a small sedimentation pond, H_2O_2 without sludge recirculation, oxidation+settling pond, aerobic wetlands, and Mn-removal bed with aeration steps in between. Results of simulations are shown in Figure S21.

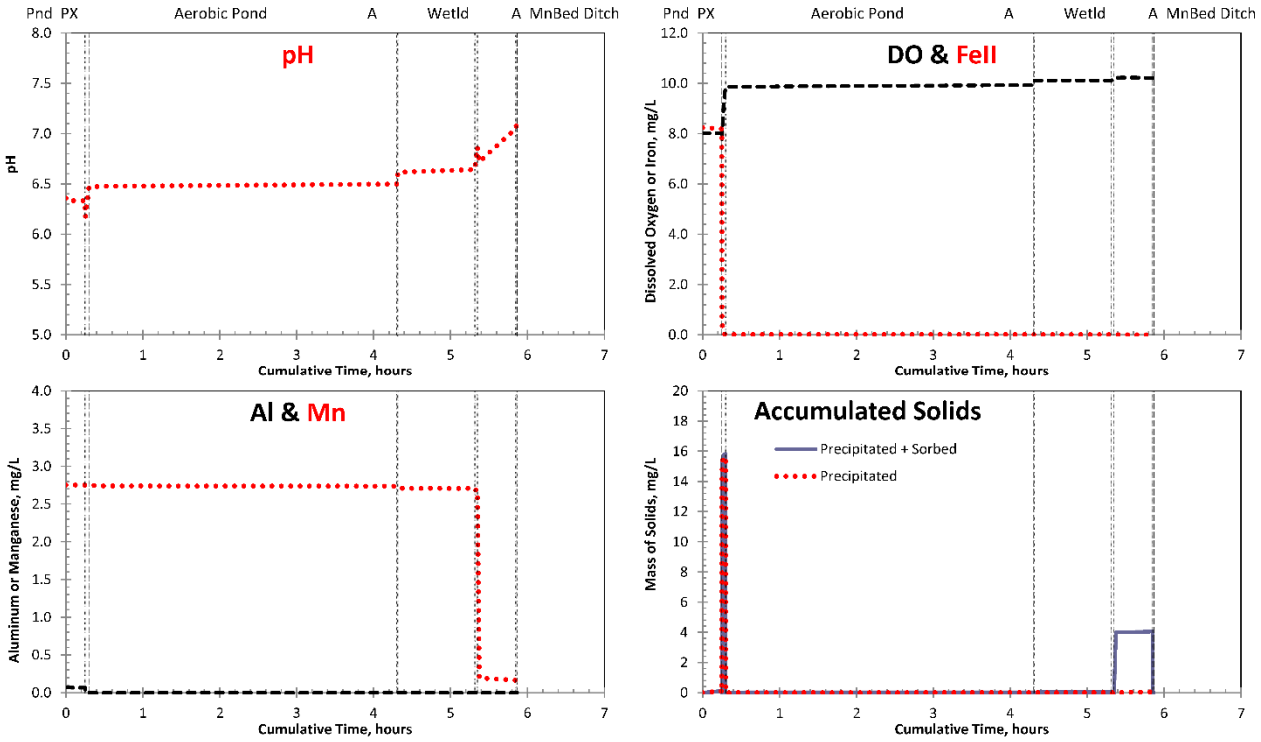

Figure S21. Simulation results for passive treatment of combined Oak Hill boreholes + Pine Knot tunnel AMD by H_2O_2 without sludge recirculation, oxidation+settling pond, aerobic wetlands, and Mn-removal bed. Note that if 100 % HFO sludge concentration of 50 mg/L is recirculated at step 2, almost all the original Mn remains in solution. Increased Mn content of the solids and increased pH as simulated for the Mn removal bed promote Mn attenuation.

Although the amount of retention time and, hence, land area required for treatments decreased for active treatment versus passive treatment, the costs for active treatment increased because of added expenses for electricity and pumping or H_2O_2 for active treatments. The passive aeration treatment system water surface area is estimated at 7.6 ha, whereas the estimates for the Maelstrom Oxidizer® and the H_2O_2 treatment systems are 7.5 ha and 4.8 ha, respectively. A multiplier of 1.5 for clearing and grubbing, berms, and slopes, increases the total acreage required for construction. Using the system sizing estimates given by the PHREEQ-N-AMDTreat TreatTrainMix2 simulations with the AMDTreat 5.0+ software (Cravotta et al., 2015), the approximate capital costs plus annual costs of operation and maintenance (4% of capital costs) for the passive and active treatment systems were computed. Capital costs were estimated to be US$1.2M, US$2.4M, and US$1.9M for the passive aeration, Maelstrom Oxidizer®, and H_2O_2 treatment systems, respectively. The corresponding annual cost for operation and maintenance of the passive aeration,

Maelstrom Oxidizer®, and H_2O_2 treatment systems were estimated to be US$0.014, US$0.019, and US$0.027 per 3785 L (1000 gallons), respectively. Assuming inflation of 5% per year over 20 years, the net present value for the passive treatment of the combined discharges is US$2.7M. Although it has smaller capital costs, H_2O_2 treatment has larger annual costs than the Maelstrom Oxidizer®. The net present value of active treatment with the Maelstrom Oxidizer® is US$4.3 million and that for active treatment with peroxide is US$4.7 million. Such cost estimates are preliminary and imprecise; site-specific information is essential for feasibility analysis and design of the selected treatment system.

S5. References for Supplementary Data

Appelo, C.A.J., Van Der Weiden, M.J.J., Tournassat, C., and Charlet, L., 2002. Surface complexation of ferrous iron and carbonate on ferrihydrite and the mobilization of arsenic. Environ. Sci. Technol. 36, 3096-3103.

Ashby, E.J., 2017. Biogeochemical mechanisms of rare earth element enrichment in mining-affected aqueous environments. University of Ottawa, Canada, M.S. thesis, 133 p.

Ball, J.W., and Nordstrom, D.K., 1991. User's manual for WATEQ4F, with revised thermodynamic data base and test cases for calculating speciation of major, trace, and redox elements in natural waters. U.S. Geol. Surv. Open-File Report 91-183.

Bigham, J.M., Schwertmann, U., Traina, S.J., Winland, R.L., and Wolf, M., 1996. Schwertmannite and the chemical modeling of iron in acid sulfate waters. Geochim. Cosmochim. Acta 60, 2111-2121. DOI: 10.1016/0016-7037(96)00091-9

Burrows, J.E., Cravotta, C.A. III, and Peters, S.C., 2017. Enhanced Al and Zn removal from coal-mine drainage during rapid oxidation and precipitation of Fe oxides at near-neutral pH: Appl. Geochem. 78, 194-210. DOI: 10.1016/j.apgeochem.2016.12.019

Charlton, S.R., and Parkhurst, D.L., 2011. Modules based on the geochemical model PHREEQC for use in scripting and programming languages. Computers & Geosciences 37, 1653-1663.

Cravotta, C.A. III, 2003. Size and performance of anoxic limestone drains to neutralize acidic mine drainage: J. Env. Qual., 32, 1277-1289. (https://doi.org/10.2134/jeq2003.1277)

Cravotta, C.A. III, 2008a. Dissolved metals and associated constituents in abandoned coal-mine discharges, Pennsylvania, USA -- 1. Constituent concentrations and correlations. Appl. Geochem. 23, 166-202.

Cravotta, C.A. III, 2008b. Dissolved metals and associated constituents in abandoned coal-mine discharges, Pennsylvania, USA -- 2. Geochemical controls on constituent concentrations. Appl. Geochem. 23, 203-226.

Cravotta, C.A. III, 2008c. Laboratory and field evaluation of a flushable oxic limestone drain for treatment of net-acidic, metal-laden drainage from a flooded anthracite mine, Pennsylvania, USA. Appl. Geochem. 23, 3404-3422.

Cravotta, C.A. III, 2015. Monitoring, field experiments, and geochemical modeling of FeII oxidation kinetics in a stream dominated by net-alkaline coal-mine drainage, Pennsylvania, U.S.A. Appl. Geochem. 62, 96-107.

Cravotta, C.A. III, 2020a. Interactive PHREEQ-N-AMDTreat water-quality modeling tools to evaluate performance and design of treatment systems for acid mine drainage. Appl. Geoch. https://doi.org/10.1016/j.apgeochem.2020.104845 .

Cravotta, C.A. III, 2020b. Interactive PHREEQ-N-AMDTreat water-quality modeling tools to evaluate performance and design of treatment systems for acid mine drainage (software download). U.S. Geological Survey Software Release https://doi.org/10.5066/P9QEE3D5 https://code.usgs.gov/water/phreeq-n-amdtreat/-/archive/v1.44/phreeq-n-amdtreat-v1.44.zip

Cravotta, C.A. III, and Trahan, M.K., 1999. Limestone drains to increase pH and remove dissolved metals from acidic mine drainage. Appl. Geochem. 14, 581-606.

Cravotta, C.A. III, and Watzlaf, G.R., 2003. Design and performance of limestone drains to increase pH and remove metals from acidic mine drainage, in Naftz, D.L., Morrison, S.J., Fuller, C.C., and Davis, J.A., eds., Handbook of groundwater remediation using permeable reactive barriers--Application to radionuclides, trace metals, and nutrients: San Diego, Ca., Academic Press, p. 19-66. (http://dx.doi.org/10.1016/B978-012513563-4/50006-2)

Cravotta, C.A. III, Means, B., Arthur, W., McKenzie, R., and Parkhurst, D.L., 2015. AMDTreat 5.0+ with PHREEQC titration module to compute caustic chemical quantity, effluent quality, and sludge volume. Mine Water Environ. 34, 136-152.

Cravotta, C.A. III, Ward, S.J., and Hammarstrom, J.M., 2008. Downflow limestone beds for treatment of net-acidic, oxic, iron-laden drainage from a flooded anthracite mine, Pennsylvania, USA--Laboratory evaluation: Mine Water Environ. 27, 86-99. (http://dx.doi.org/10.1007/s10230-008-0031-y).

Dzombak, D.A., and Morel, F.M.M., 1990. Surface complexation modeling: Hydrous ferric oxide. John Wiley and Sons, New York, NY, USA.

Geroni, J.N., Cravotta, C.A. III, and Sapsford, D.J., 2012. Evolution of the chemistry of Fe bearing waters during CO_2 degassing. Appl. Geochem. 27, 2335-2347.

Giffaut, E., Grivé, M., Blanc, P., Vieillard, P., Colàs, E., Gailhanou, H., Gaboreau, S., Marty, N., Madé, B., and Duro, L., 2014. Andra thermodynamic database for performance assessment: ThermoChimie. Appl. Geochem. 49, 225-236. doi.org/10.1016/j.apgeochem.2014.05.007

Hedin, R.S., Nairn, R.W., and Kleinmann, R.L.P., 1994. Passive treatment of coal mine drainage. U.S. Bureau of Mines Information Circular 9389, 35 p.

Jageman, T.C., Yokley, R.A., and Heunisch, H.E., 1988. The use of preaeration to reduce the cost of neutralizing acid mine drainage. U.S. Bureau of Mines Information Circular 9183, Pittsburgh, PA, p 131-135

Karamalidis, A.K., and Dzombak, D.A., 2010. Surface complexation modeling: Gibbsite. John Wiley & Sons, Inc., Hoboken, NJ, USA.

Kirby, C.S., and Cravotta, C.A., III, 2005. Net alkalinity and net acidity 2: Practical considerations. Appl. Geochem. 20, 1941-1964.

Liger, E., Charlet, L., Cappellen, P.V., 1999. Surface catalysis of uranium(VI) reduction by iron(II). Geochim. Cosmochim. Acta 63, 2939-2955.

Lozano, A., Ayora, C., and Fernández-Martínez, A., 2020. Sorption of rare earth elements on schwertmannite and their mobility in acid mine drainage treatments. Appl. Geochem. 113, 104499. doi.org/10.1016/j.apgeochem.2019.104499

Majzlan, J., Navrotsky, A., and Schwertmann, U., 2004. Thermodynamics of iron oxides. Part III. Enthalpies of formation and stability of ferrihydrite ($\sim Fe(OH)_3$), schwertmannite ($\sim FeO(OH)_{3/4}(SO_4)_{1/8}$), and e-$Fe_2O_3$. Geochim. Cosmochim. Acta 68, 1049-1059.

Means, B., and Hilton, T., 2004. Comparison of three methods to measure acidity of coal-mine drainage. Proceedings of the 2004 National Meeting of the American Society of Mining and Reclamation and the 25th West Virginia Surface Mine Drainage Task Force, p. 1249-1277.

Means, B., and Rose, A.W., 2005. Manganese removal in limestone bed systems. Proceedings of the 2005 National Meeting of the American Society of Mining and Reclamation, p. 702-717.

Means, B., Beam, R., and Charlton, D., 2013. Operational and financial studies of hydrogen peroxide versus hydrated lime and hydrogen peroxide versus sodium hydroxide at two

Pennsylvania mine drainage treatment sites. West Virginia Mine Drainage Task Force, 2013 Symposium https://wvmdtaskforce.files.wordpress.com/2016/01/13-means-paper.doc

Means, B., Parker, B., and Beam, R., 2015. Decarbonating at the St. Michael Treatment plant: Effect on cost, sludge, and sedimentation. West Virginia Mine Drainage Task Force, 2013 Symposium https://wvmdtaskforce.files.wordpress.com/2016/01/15-means-paper.docx

Myneni, S.C.B., Traina, S.J., and Logan, T.J., 1998. Ettringite solubility and geochemistry of the $Ca(OH)_2$-$Al_2(SO_4)_3$-H_2O system at 1 atm pressure and 298K. Chem. Geol. 148, 1-19.

Office of Surface Mining Reclamation and Enforcement, 2017. AMDTreat.(last updated 2017). https://amd.osmre.gov/ accessed August 24, 2020.

Parkhurst, D.L., and Appelo, C.A.J., 2013. Description of input and examples for PHREEQC version 3—A computer program for speciation, batch-reaction, one-dimensional transport, and inverse geochemical calculations. U.S. Geol. Surv. Techniques Methods 6-A43, 497 p. https://pubs.er.usgs.gov/publication/tm6A43 https://www.usgs.gov/software/phreeqc-version-3/

Peiffer, S., dos Santos Afonso, M., Wehrli, B., and Gachter, R., 1992. Kinetics and mechanism of the reaction of H_2S with lepidocrocite. Environ. Sci. Technol. 26, 2408-2412.

Robbins, E.I., Cravotta, C.A. III, Savela, C.E., and Nord, G.L. Jr., 1999a. Hydrobiogeochemical interactions in “anoxic” limestone drains for neutralization of acidic mine drainage. Fuel 78, 259-270.

Robbins, E.I., Brant, D.L., and Ziemkiewicz, P.F., 1999b. Microbial, algal, and fungal strategies for manganese oxidation at a Shade Township coal mine, Somerset County, Penna, in Proceedings American Society of Mining and Reclamation, Scottsdale, AZ, August 13-19, 1999, p. 634-640. DOI: 10.21000/JASMR99010634.

Rose, A.W., 1999. Chemistry and kinetics of calcite dissolution in passive treatment systems, in Proceedings American Society of Mining and Reclamation, Scottsdale, AZ, August 13-19, 1999, p. 634-640. DOI: 10.21000/JASMR99010599.

Rose, A.W., 2004. Vertical flow systems-Effects of time and acidity relations, in Proceedings American Society of Mining and Reclamation, Morgantown, WV, April 18-24, 2004, p 1595-1616. DOI: 10.21000/JASMR04011595.

Sajih, M., Bryan, N., Livens, F., Vaughan, D., Descostes, M., Phrommavanh, V., Nos, J., and Morris, K., 2014. Adsorption of radium and barium on goethite and ferrihydrite: A kinetic and surface complexation modelling study. Geochim. Cosmochim. Acta, 146: 150-163.

Skousen, J.G., Zipper, C.E., Rose, A.W., Ziemkiewicz, P.F., Nairn, R., McDonald, L.M., and Kleinmann, R.L., 2017. Review of passive systems for acid mine drainage treatment. Mine Water Environ. 36, 133-153.

Swedlund, P.J., and Webster, J.G., 1999. Adsorption and polymerisation of silicic acid on ferrihydrite, and its effect on arsenic adsorption. Water Research 33 3413-3422.

Tan, H., Zhang, G., Heaney, P.J., Webb, S.M., Burgos, W.D., 2010. Characterization of manganese oxide precipitates from Appalachian coal mine drainage treatment systems. Appl. Geochem. 25, 389-399. DOI: 10.1016/j.apgeochem.2009.12.006

Thomas, R.C., and Romanek, C.S., 2002a. Passive treatment of low-pH, ferric dominated acid rock drainage in a vertical flow wetland--I. Acidity neutralization and alkalinity generation, in Proceedings American Society of Mining and Reclamation, Lexington, Kentucky, June 9-13, 2002, p. 723-748. DOI: 10.21000/JASMR02010723

Thomas, R.C., and Romanek, C.S., 2002b. Passive treatment of low-pH, ferric dominated acid rock drainage in a vertical flow wetland--II. Metal removal, in Proceedings American Society of Mining and Reclamation, Lexington, Kentucky, June 9-13, 2002, p. 752-775. DOI: 10.21000/JASMR02010752

Tonkin, J.W., Balistrieri, L.S., and Murray, J.W., 2004. Modeling sorption of divalent metal cations on hydrous manganese oxide using the diffuse double layer model. Appl. Geochem. 19, 29-53.

Van Geen, A., Robertson, A.P., and Leckie, J.O., 1994. Complexation of carbonate species at the goethite surface: Implications for adsorption of metal ions in natural waters. Geochim. Cosmochim. Acta 58, 2073-2086.

Watzlaf, G.R., Schroeder, K.T., Kleinmann, R.L.P., Kairies, C.L., and Nairn, R.W., 2004. The passive treatment of coal mine drainage. U.S. Department of Energy DOE/NETL-2004/1202 (accessed June 15, 2020 at http://www.bobkleinmann.com/images/2004_DOEPassiveTreatment_of_Coal_Mine_Drainage_NETL-1202.pdf)

Wolfe, N., Hedin, R.S., and Weaver, T., 2010. Sustained treatment of AMD containing Al and Fe^{3+} with limestone aggregate, in International Mine Water Association 2010 Symposium, Sydney, Nova Scotia, Canada, p. 237-241. https://www.imwa.info/docs/imwa_2010/IMWA2010_Hedin_490.pdf

Additional relevant references used for the model development are included in the main paper by Cravotta (2020a).